Aus dem Zentrum für Innere Medizin der Universität zu Köln

Klinik I für Innere Medizin

Direktor: Universitätsprofessor Dr. med. M. Hallek

Molekulare Charakterisierung der mit Zellteilungsarretierung assoziierten antigenspezifischen $CD8^+$ T-Zell Anergie vor dem Hintergrund der adoptiven T-Zell Therapie

Inaugural-Dissertation zur Erlangung der Doktorwürde
der Hohen Medizinischen Fakultät
der Universität zu Köln

vorgelegt von

Michael Rudolf Mallmann

aus Bonn

promoviert am 14. Juli 2010

Gedruckt mit Genehmigung der
Medizinischen Fakultät der Universität zu Köln, 2010

Druck: AV Druck, Bonn

Dekan: Universitätsprofessor Dr. med. J. Klosterkötter

1. Berichterstatter: Universitätsprofessor Dr. med. J. L. Schultze
2. Berichterstatter: Universitätsprofessor Dr. med. M. Krönke

Erklärung:

Ich erkläre hiermit, dass ich die vorliegende Arbeit ohne unzulässige Hilfe Dritter und ohne Benutzung anderer als der angegebenen Hilfsmittel angefertigt habe; die aus fremden Quellen direkt oder indirekt übernommenen Gedanken sind als solche kenntlich gemacht.

Bei der Auswahl und Auswertung des Materials sowie der Herstellung des Manuskriptes habe ich Unterstützungsleistungen von folgenden Personen erhalten:

Herrn Universitätsprofessor Dr. med. Joachim L. Schultze

Herrn Dr. med. Marc Beyer

Herrn Dr. med. Thomas Zander

Frau Dr. rer. nat. Daniela Eggle

Frau Dr. rer. nat. Svenja Debey-Pascher

Weitere Personen waren an der geistigen Herstellung der vorliegenden Arbeit nicht beteiligt. Insbesondere habe ich nicht die Hilfe einer Promotionsberaterin/ eines Promotionsberaters in Anspruch genommen. Dritte haben von mit weder unmittelbar noch mittelbar geldwerte Leistungen für Arbeiten erhalten, die im Zusammenhang mit dem Inhalt der vorgelegten Dissertationsschrift stehen.
Die Dissertationsschrift wurde von mir bisher weder im Inland noch im Ausland in gleicher oder ähnlicher Form einer anderen Prüfungsbehörde vorgelegt.

Köln, den 15.12.2009 Michael Rudolf Mallmann

Die der vorliegenden Arbeit zugrunde liegenden zellbiologischen und molekularbiologischen Untersuchungen sind von mir im Labor für Molekulare Tumorbiologie und Tumorimmunologie der Klinik I für Innere Medizin der Universität zu Köln in der Arbeitsgruppe von Herrn Professor Dr. med. Joachim L. Schultze, Kerpener Strasse 62, 50924 Köln durchgeführt worden.

Die in der vorliegenden Arbeit genutzten T Zell- und Melanom-Zelllinien sowie die Krankheitsverläufe der Patienten wurden durch Frau Professorin Dr. med. Elke Jäger und Frau Julia Karbach im Forschungslabor der „Krebsforschung Rhein-Main e.V." an der Klinik für Onkologie und Hämatologie am Krankenhaus Nordwest GmbH, Steinbacher Hohl 2-26, 60488 Frankfurt, generiert bzw. erarbeitet.

Die in der vorliegenden Arbeit genutzten PCR und RT-PCR Versuche sind von mir selbst nach entsprechender Anleitung durch Herrn Dr. med. Thomas Zander und Herrn Dr. med. Marc Beyer durchgeführt worden.

Die dieser Arbeit zugrunde liegenden FACS-Experimente sind nach entsprechender Anleitung durch Herrn Dr. med. Marc Beyer von mir selbst ausgeführt werden.

Die der vorliegenden Arbeit zugrunde liegenden Microarray-Experimente sind von Frau Dr. rer. nat. Svenja Debey-Pascher und Herrn Dr. med. Thomas Zander durchgeführt worden. Die Auswertung der generierten Daten ist von mir zusammen mit Frau Dr. rer. nat. Daniela Eggle, Herrn Dr. med. Thomas Zander und Herrn Dr. med. Marc Beyer durchgeführt worden.

Die in der vorliegenden Arbeit durchgeführte Reverse-Phase HPLC und Massenspektroskopie sind durch Herrn Prof. Dr. rer. nat. Michael Famulok am LIMES Institute, Program Unit Chemical Biology & Medicinal Chemistry im Laboratory of Chemical Biology, Bonn, durchgeführt worden.

Acknowledgments

I would like to express my deepest gratitude and appreciation to all who have contributed to the successful completion of the present work. I wish to extend my heartiest thanks to:

- Professor Dr. med. Joachim L. Schultze, Head of the Laboratory for Molecular Tumor Biology and Tumor Immunology, Clinic for Hematology & Oncology at the Department of Internal Medicine I, University of Cologne, for his valuable instructions, never ending support and the constructive guidance during the period of this work. In addition for his remarkable encouragement to obtain further research experience in the Laboratory of Immunology of Prof. Dr. med. Kai W. Wucherpfenning, Boston.
- Prof. Dr. med. Kai W. Wucherpfenning, Head of the Laboratory of Immunology, Dana Farber Cancer Institute at Harvard University in Boston, USA, for his offer to study the structural aspects of autoimmune T-cell receptors in the setting of autoimmune thyroiditis and autoimmune encephalopathy in his laboratory.
- Dr. med. Marc Beyer for his help and guidance in the work concerned with FACS analysis, RT-PCR and Microarray analysis.
- Dr. med. Thomas Zander for his help and guidance in the work concerned with PCR, microarray analysis and cell culture.
- Dr. rer. nat. Svenja Debey-Pascher and Dr. rer. nat. Daniela Eggle for help and guidance in the work concerned with microarray analysis.
- All members of the Laboratory of Molecular Tumor Biology and Tumor Immunology, Cologne and the Laboratory for Genomics and Immunoregulation, LIMES-Institute, Bonn who have contributed to the successful accomplishment of this work.
- The numerous patients who despite their severe illness in the course of their disease incessantly were willing to donate blood samples for experiments.

This work has been supported by scholarships of the Bayer Studienstiftung, the Boehringer Ingelheim Foundation and the DAAD – German academic exchange service.

Dedicated to my parents

whose continual and unflagging patience and support have made possible

whatever success I have experienced in my professional and personal career.

Table of contents

Glossary

Amp	Ampicillin
APC	Allophycocyanin
APS	Ammonium persulfate
Bp	Base pair
BSA	Bovine serum albumine
CD	Cluster of differentiation
CDR	Complementary determining region
Cy5	Indodicarbocyanin
DMEM	Dulbecco's modified Eagle's medium
dNTP	Desoxyribonukleotide
DTT	Dithiothreitol
EDTA	Ethylenediaminetetraacetic acid
FACS	Fluorescence activated cell sorting
FCS	Fetal calf serum
Fig.	Figure
FITC	Fluorescein isothiocyanate
HPLC	High performance liquid chromatography
IFN	Interferon
Ig	Immunoglobulin
IL	Interleukin
K_D	Molar concentration at which the ligand half-occupies the receptor
LCMV	Lymphocytic choriomeningitis virus
LPS	Lipopolysaccharide
MHC	Major histocompatibility complex
ml	Milliliter

µg	Microgram
µl	Microliter
ng	Nanogram
OD	Optical density
PBMC	Peripheral blood mononuclear cells
PBS	Phosphat buffered saline
PCR	Polymerase chain reaction
PE	R-phycoerythrin
PerCP	Peridin-chlorophyll
pMHC	Peptide-MHC-complex
PMA	Phorbol 12-myristate 13-acetate
PMSF	Phenylmethylsulfonylfluorid
rIL-2	Recombinant IL-2
RNA	Ribonucleic acid
RT-PCR	Real-time polymerase chain reaction
SDS	Sodiumdodecylsulfate
SDS-PAGE	SDS-Polyacrylamidgelelectrophoresis
TCR	T-cell receptor
TFA	Trifluoroacetic acid
TEMED	N,N,N',N′-tetramethyl-ethane-1,2-diamine
TNF	Tumor necrosis factor
TNFR	Tumor necrosis factor receptor
WHO	World health organization
ZAP-70	Zeta associated protein

1. Introduction

1.1. Malignant melanoma

Cancer is the leading cause of death in the age from 40 years to 70 years both in the United States and Germany (144, 349). Malignant melanoma herewith in accounts for about 4% of all cancers in the United States. With an increase of 4% to 7% annually, it is the most rapidly growing cancer. Particularly aggressive local invasion and metastatic spread at the time of diagnosis are responsible for high morbidity and mortality in malignant melanoma and result in 2% of all deaths from neoplasia and approximately 80% of deaths from skin cancer (143, 215).

In the progression of malignant melanoma, distinct molecular changes in the tumor cells occur combined leading to continuous loss of cell growth suppressing proteins and increase in growth and metastasis promoting factors (215). Five steps of progression have been defined in malignant melanoma, starting with the common melanocytic benign nevus, which does not show any architectural or cytologic atypia. Step two, a dysplastic nevus shows both architectural and cytological atypia. These two lesions can be considered as precursor lesions of malignant melanoma. Step three of progression is represented by the radial-growth phase primary malignant melanoma, which shows a strong tendency for invasion of neighboring tissue, but not for metastasis. In the radial-growth phase (step four), focal lesions may arise to form the vertical growth phase primary malignant melanoma, which has acquired competence for metastasis, the incidence of which being related in linear fashion to the thickness of the vertical growth phase. Finally, the development of metastases represents the fifth step of tumor progression (127, 215).

As with other tumors, progression or regression of tumor load has been attributed to the interaction between tumor and host environment. Up to today, in the setting of malignant melanoma surgery offers the best chance for cure in the early stages of disease (313). In the advanced AJCC (American Joint Committee on Cancer) stages IIb, IIc and III, the 5-year risk of relapse and death exceeds 40%, requiring additional adjuvant systemic therapy (17, 18).

The highly fatal nature of disseminated disease is due to the overall poor response of malignant melanoma patients to conventional chemotherapy or radiation therapy (127, 215). Consequently, the urge in finding new therapeutic options in cases of metastatic malignant melanoma has led to adjuvant therapies which take advantage of non-specific immunoactivation (such as interferon-alpha or Interleukin-2) alone or in addition to conventional chemotherapy. These regimens have been shown to yield positive effects on both progression-free as well as overall survival (92, 104, 121, 158-160), but induce elevated liver enzymes, myelosuppression, neurologic and psychiatric disorders (e.g. depression), nausea and constitutional symptoms requiring discontinuation of therapy in up to 50% (160, 243).

In this context, a more tumor specific and side effect low therapy is needed, and observations allocating the observed clinical responses of immunoactivation to the involvement of the adaptive immune system have prepared the basis for the concept of immunotherapy, not only in malignant melanoma, but in a variety of neoplasic diseases (177, 269). This concept is guided by precise activation of the adaptive immune system by targeting defined tumor specific antigens rather than simply attacking tumor cell growth or evoking tumor-cell-unspecific immunoactivation. In this setting, cancer vaccines are an attractive approach as the immune system is capable of mounting productive immune responses leading to tumor regression (31).

1.2. Innate and adaptive immunity

The immune system of each individual continuously is exposed to a myriad of challenges. These consist in general of non-self, self, and mutated self antigens. The immunological integrity is protected by passive and active immunological mechanisms. Integrity of skin and mucosa passively assures defense towards the majority of potential pathogens. If penetration of this barrier has occurred, innate and adaptive immunity become activated to clear the pathogen. The innate immune system ensures rapid clearance of pathogens which have penetrated the defense mechanisms of skin or mucosa by recognizing pathogens by their conserved molecular patterns such as LPS, mannans or glycans. Receptors of the innate immune system are genome fixed such that rearrangement is unnecessary and self-non-self-discrimination is selected over evolutionary time. These germline-encoded recognition receptors are employed by macrophages, dendritic cells, mast cells, neutrophils, eosinophils and the so-called natural killer cells. During an inflammatory response, cells of the innate immune system rapidly differentiate into short-lived effector cells to clear the infectious agent. This mainly succeeds without recourse to adaptive immunity (142). However, if the innate immune system is unable to deal with the infection, activation of an adaptive immune response becomes necessary. It is now generally accepted that in such cases, the innate immune system can instruct the adaptive immune system about the nature of the pathogenic challenge by expression of co-stimulatory molecules, secretion of cytokines such as IL-1β and IL-6, and secretion of chemokines such as IL-8 (142).

The extremely specific adaptive immunity, in chief B and T cells, guarantees the clearances of remaining and/or intracellular pathogens and arising tumor cells. To recognize the tremendous amount of different antigens, adaptive immunity has evolved a system of recombination, assembling discontinuous gene segments to a diverse set of functional B-cell receptors and T-cell receptors (TCR) guaranteeing maximal diversity of the estimated 10^{12} T cells in the human body. Taking into account the extensive diversity of both an α-and β-chain by recombination of their different V- (variable), D- (diversity), J- (joining), and C- (constant) segments already, diversification is once more

increased by pairing of an α-chain to a β-chain to form the T-cell receptor heterodimer. α/β-T-cell receptor diversity theoretically reaches 10^{15} by random rearrangement and nucleotide addition/ excision (40, 69). Since the process of positive and negative selection, diversity lies in the range of $2.5x10^7$ different T-cell receptors in the subset of naïve T cells (10^6 different β-chains each pairing with at least 25 different α-chains) and $1\text{-}2x10^5$ different T-cell receptors in the T-cell memory subset ($1\text{-}2x10^5$ β-chains each pairing with a single α-chain) (13). The human body generates about 10^8 naïve T cells per day, roughly estimated from recovery rates after T-cell depletion (56) and a 0.1% T-cell turnover in the pool of 10^{11} naïve T cells (213). Upon specific stimulus, the adaptive immune response reacts by clonal expansion or clonal anergy depending on strength and circumstances of stimulation. Mechanisms include effector cytokine release, in particular IL-4 and IFN-γ, and cell lysis by perforine granula.

1.3. T-cell receptor-peptide-MHC interaction

T-cell recognition of cognate antigen is initiated by binding of the T-cell receptor to a cognate pMHC. When encountering an antigen-loaded MHC, T-cell receptor, the cognate pMHC and surrounding co-stimulatory molecules form a specialized structure known as immunological synapse or supramolecular activation cluster resulting in T-cell activation.

As outlined above, the theoretical T-cell receptor diversity covers about 10^{15} different T-cell receptors. Mature T cells express highly selected T-cell receptors in that they exhibit tolerance to self-antigenic peptides and are restricted by self-MHC molecules. This mainly results from positive and negative selection, two reciprocal processes taking place in the thymus.

Positive selection induces the differentiation of $CD4^+CD8^+$ immature thymocytes into $CD4^-CD8^+$ or $CD4^+CD8^-$ mature thymocytes if their T-cell receptors recognize self-MHC class I or II, respectively, with sufficient affinity, and ensures that T-cell receptors are directed towards antigenic peptides presented by self-MHC molecules (99). By means of negative selection, TCR-pMHC affinities are hold in a narrow range (278), allowing T cells to recognize pathogens while remaining tolerant to self-antigens.

The central factor defining the amount of T-cell receptor activation is the interaction of T-cell receptor with the pMHC complex. For $CD4^+$ T cells, differences in the half-live of this interaction which allow each pMHC-complex to be engaged by many T-cell receptors are an important influencing factor (320). Thus, only a “sophisticated” TCR-pMHC interaction characterized by an optimal combination of high affinity and high/low off-rate guarantees enough triggering events for the T cell in order to be activated (333). Whether $CD8^+$ T-cell activation relies on both TCR-pMHC affinity and off-rate, or whether off-rate has any influence at all, is still under intense debate. There is evidence to link cytotoxicity and IFN-γ release of $CD8^+$ T cells mainly to the affinity of the TCR-pMHC-complex arguing that a defined affinity threshold has to be overcome in order to provoke full T-cell effector function (308). Data from transgenic mice taking into account the participation of CD8 co-stimulation has substantiated this apparent affinity threshold for full T-cell activation in MHC class-I restricted TCR to a constant of $\sim K_d \leq 6$ µM (220). Interestingly, this affinity lies in the

range of negative-selecting ligands (68). Experiments with MHC class-I restricted T-cell receptors with affinities near the threshold affinity between positive and negative selection define the threshold affinity that results in negative selection at a dissociation constant K_D of 6 µM and a half-life of 1–3 seconds (220). As consequence of the interaction between positive and negative selection, low affinity self-peptides no longer provoke a response, whereas foreign peptides 'incidentally' being high affinity ligands are potent T-cell stimulators.

Additional factors influencing the amount of T-cell receptor activation by stabilizing the TCR-pMHC interaction and finetuning the resulting T-cell activation are (a) TCR-MHC-interaction, (b) peptide-MHC interaction, and (c) CD8 participation.

Contacts between T-cell receptor and MHC helices are important in determining the overall architecture of the T-cell receptor-pMHC interaction (106, 107, 176, 200). Engagement of MHC helices by CDR1 and CDR2 loops of the T-cell receptor provides MHC restriction, a conclusion that can be drawn from crystallographic studies where the CDR2 loops of Vα and Vβ are positioned almost exclusively over the MHC helices and show only marginal contact with the peptide. The CDR1 loop mainly interacts with the MHC-molecule. Although residues of CDR1α and CDR1β might interact with the N-Terminus and the C-Terminus of the peptide, respectively (105, 106), CDR1 and CDR2 contribute approximately 2/3 of the binding free energy of the TCR-pMHC-interaction and reflect the on-rate of the TCR-pMHC interaction (176, 200, 354).

Peptide-MHC-affinity has been shown to be one of the crucial factors influencing T-cell activation, particular in negative selection. Peptide-MHC affinity influences peripheral T-cell activation as peptides with high affinity to the T-cell receptor and long half-life that would group them with the strong agonists are only partial agonists if they exert low affinity binding to the MHC (134). Consequently, amino acid substitution at a MHC anchor residue of an immunogenic peptide results in an unstable interaction between peptide and MHC attenuating the peptide-specific T-cell response and inducing T-cell anergy (340).

As outlined below, the α/β T-cell receptor exists as part of a complex containing CD3$\gamma\varepsilon$, CD3$\delta\varepsilon$-heterodimer and TCR$\zeta\zeta$-homodimer. An important role in modulating and stabilizing the TCR-pMHC interaction is observed for the co-receptors CD4 and CD8. CD4 determines MHC II restriction and is expressed on T_{Helper} cells, whereas CD8 determines MHC I restriction and is expressed on the $T_{Effector}$ cell subset. CD4 and CD8 molecules, primarily identified as cell adhesion molecules (230), are believed to bind MHC molecules enhancing T-cell responses and facilitating TCR-MHC complex formation (194, 363, 364). Additionally, variations in the level of co-receptors can change positive to negative selection during thymocyte selection (174, 264). Importantly, CD8 participation in the complex formation increases the bimolecular affinity of the TCR-pMHC complex to a trimolecular binding characterized as “apparent affinity” by 10-15 fold (220).

1.4. T-cell activation

Extent and focus of the adaptive immune response to antigens are controlled by human T cells. T cells become activated by interaction of their cell surface T-cell receptor with a cognate antigen presented by a major histocompatibility complex. In addition to activation of their T-cell receptor, T cells require activating signals from one or more co-stimulatory receptors to become fully activated. The T-cell antigen receptor/ CD3 complex on the cell surface of T cells comprises variant chains of T-cell receptor α- and β-subunits non-covalently associated with invariant T-cell receptor ζ-chains and CD3 γ-, δ- and ε-chains.

In unstimulated condition, the TCRα/β-heterodimer and non-covalently associated CD3$\gamma\varepsilon$, CD3$\delta\varepsilon$-heterodimer and TCR$\zeta\zeta$-homodimer are expressed on the cell surface. Upon engagement of the T-cell receptor by cognate pMHC, CD3$\gamma\varepsilon$, CD3$\delta\varepsilon$-heterodimer and TCR$\zeta\zeta$-homodimer associate with the T-cell receptor in the cell membrane through conserved transmembrane residues (42). These signaling subunits contain immunoreceptor tyrosine-based activation motifs (ITAMs) inserted into the hydrophobic core of the lipid bilayer of the plasma membrane (356). The earliest biochemical response elicited by T-cell receptor triggering is the dissociation of the ITAM from the cell membrane rendering the tyrosine accessible to rapid phosphorylation by the Src family tyrosine kinases Lck or Fyn (275). The protein tyrosine kinase ZAP-70 (ζ-chain-associated protein kinase of 70 kd) is recruited by dually phosphorylated ITAMs and activated upon phosphorylation of tyrosine 319 by Lck (225), the number of ZAP-70 molecules that are recruited being dictated by the affinity of the T-cell receptor for its peptide ligand (199, 290). Consequently, the number of recruited ZAP-70 molecules is limited in case of low-affinity interactions, increases with increase of TCR-pMHC affinity and the resulting stoichiometry of ITAM phosphorylation can serve as signaling amplification mechanism (192, 225). Activated Lck, Fyn, and ZAP-70 then phosphorylate downstream components of the T-cell receptor signaling pathway including linker for activation of T cells (LAT) and Pyk2 (proline-rich tyrosine kinase 2) (136, 234, 275). Pyk2 controls actin cytoskeletal rearrangements critical for T-cell activation (234). LAT is phosphorylated on five conserved tyrosine residues that bind to several SH2

domain-containing proteins, such as the adaptor proteins Grb2 (growth factor receptor-bound protein), Grap (Grp2-related adaptor protein), and Gads (Grb2-related adaptor downstream of Shc), as well as phospholipase C (PLC-γ1) (275). Once recruited to LAT, PLC-γ1 is activated by a Tec kinase recruited by SLP-76 (SH2 domain–containing leukocyte protein of 76 kd), and cleaves phosphatidylinositol (4,5) biphosphate into inositol (1,4,5) triphosphate (Ip3), which releases Ca^{2+} from endoplasmic reticulum sites, and diacylglycerol, which mediates protein kinase C (PKCθ) activation (225, 252).

Ca^{2+} release predominantly leads to the activation of the Ca^{2+}-dependent NFAT pathway. Once intracellular Ca^{2+} stores are depleted, store-operated Ca^{2+} channels in the plasma membrane allow influx of extracellular Ca^{2+} (225). Ca^{2+} activates the calcium-calmodulin-dependent serine phosphatase calcineurin, which dephosphorylates the nuclear factor of activated T cells (NFAT), leading to intranuclear translocation of NFAT and binding to NFAT binding sites as can be seen in Figure 1 (16, 256).

The connection of the nuclear factor kappa-light-chain-enhancer of activated B cells (NF-κB) pathway to T-cell receptor induced T-cell activation is established by the interaction of Vav with PKCθ (64, 332). Activation of the NF-κB complex results in degradation of inhibitory proteins IκBα and IκBβ, release of NF-κB transcription factors c-Rel, RelA, p65 and p50 and consecutive gene activation with a key gene target being the CD28 response element (CD28RE) in the IL-2 promotor (76, 156, 188).

The MAPK pathway is another important pathway involved in T-cell receptor signaling. Upon T-cell receptor ligation, Grb2 gets recruited to LAT and SOS (Son of Sevenless) resulting in Ras activation. Once activated, Ras itself activates a cascade involving Raf, a Mitogen-activated protein 3 kinase (MAP3K), MEK 1 and MEK 2, which are Mitogen-activated protein 2 kinases (MAP2K), and the extracellular signal-regulated kinase (ERK) that plays an important role in the expression of the activator protein 1 (AP-1) transcription factor c-fos (225, 260). C-fos gets involved in transcriptional regulation of AP-1 response elements in the IL-2 promoter (141, 225).

The p38 MAPK and JNK cascades play another important role in T-cell receptor signaling. Activation of JNK (N-terminal c-Jun kinase) is CD28

dependent and JNK deviates T-cell fate towards a T_H1 response. This is accomplished by interference with T_H2 development through the JNK1 isoform and activation of the IFN-γ gene through the JNK2 isoform (83, 358). Similarly, the p38 MAPK cascade regulates the expression of IFN-γ gene expression in T_H1 cells without affecting T_H2 cytokines (260).

These events in T-cell receptor engagement lead to a series of biochemical changes evolving over different times of engagement: expression of cytokine receptors occurs in about 2 hours, secretion of cytokines in about 6 hours, initiation of DNA replication after about 24 hours, cell division after about 48 hours and altered differentiation over a period of days (65). Not every interaction with ligand triggers a full T-cell response. Full T-cell activation requires T-cell receptor engagement by cognate antigen presented by MHC and formation of a highly organized spatially encompassed network of T cell receptor, co-receptors and signaling molecules, known as the “Immunological Synapse” (217). The formation of this terminally stabilized synapse is accompanied by an extensive lateral movement of plasma membrane proteins organizing the contact area of the T cell with the corresponding pMHC presenting cell. The synapse is organized into two supramolecular activation clusters, rings consisting of different surface molecules. After T-cell receptor engagement, co-stimulatory molecules CD28 and CD8 move centrifugally into the center of the immunological synapse, setting up the central supramolecular activation cluster, cSMAC. The surrounding peripheral supramolecular activation cluster pSMAC has stabilizing function containing adhesion molecules and the cytoskeleton, LFA-1, ICAM and talin (117, 217, 248). By this activation-induced segregation, co-stimulatory molecules are brought into narrow contact with the activated T-cell receptor-CD3 complex. Upon CD28 engagement for example, Lck is recruited into CD28-signaling rafts in the immunological synapse. Subsequently, CD8 and CD28 are thought to cooperate to induce autophosphorylation of Lck at position (Y394) and recruite Lck to the T cell-APC interface (133, 305). Upon engagement, Lck is dephosphorylated at its inhibitory residue tyrosine 505, activated and phosphorylates the mentioned downstream targets, resulting in gene activation and cell proliferation.

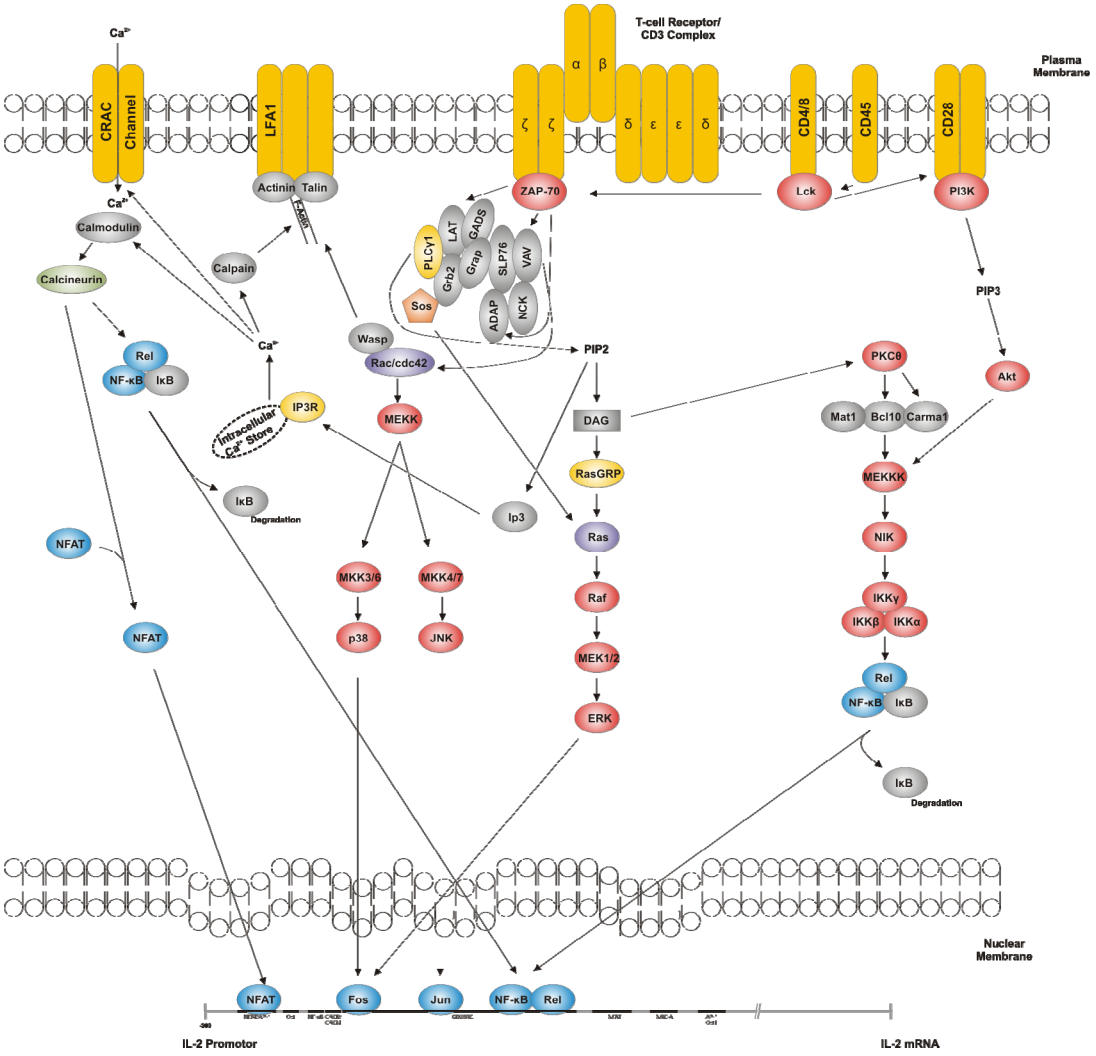

Figure 1 | Current Model of T-cell Activation

Model of T-cell activation taking into account the different pathways involved in T-cell activation and full effector function. Model adapted from Cell Signaling Technologies (Beverly, MA, USA), Doreen Cantrell (43), and Andre E. Nel (225).

1.5. T-cell tolerance

As described above, T-cell receptor engagement by pMHC cannot only lead to T-cell activation but might also result in T-cell tolerance. As T-cell tolerance generally can be based on different mechanisms, a division into central and peripheral T-cell tolerance is generally accepted.

Central tolerance relies on a sufficient negative and positive selection in the thymus. As mature $CD4^+CD8^-$ or $CD4^-CD8^+$ thymocytes are generated by positive selection, self-reactive T cells are eliminated as a result of high reactivity towards self antigens which is known as negative selection. Interestingly, it has been shown for a variety of diseases that self reactivity is not fully eliminated by central tolerance, the sense of what has not been fully evident so far. Consequently, the necessity of peripheral mechanisms to regulate auto-reactivity and maintain peripheral immune homeostasis results from T cells with intermediate auto-reactive affinity that leave the thymus and - in an inflammatory setting - are capable of exerting damage to self-tissue.

Three important mechanisms by which the immune system controls peripheral T-cell reactivity are (1) $T_{effector}$ cell extrinsic mechanisms such as regulation by means of regulatory T cells and other subsets of immune regulative cells, (2) intrinsic regulation of each peripheral $T_{effector}$ cell by means of the particular avidity of its T-cell receptor to the pMHC complex and/or the amount of co-stimulatory or co-inhibitory molecules, and (3) peripheral ignorance as naïve T cells are not activated by pMHC antigen presented by cells if not activated before by professional antigen presenting cells, mainly dendritic cells.

The importance of extrinsic control is provided by experiments with $Foxp3^{-/-}$ mice lacking the $CD4^+CD25^+$ $T_{regulatory}$ subset that show an overt autoreactive T-cell attack against surrounding host tissue. Nonetheless, extrinsic control is not sufficient as has been shown by more physiological experiments where the generation of a small T-cell receptor transgenic proportion of the peripheral T-cell repertoire was sufficient to elude a self-reactive immune response.

Peripheral immunocompetent T cells, a hallmark of the adaptive immune system, are the result of an ingenious system of positive and negative selection. Despite the variety of peptides which are generated during the processing of a

given protein by means of the antigen processing machinery, the T-cell response towards this protein is characteristically directed against single immunodominant epitopes. The epitope towards which the immune response is predominantly directed is selected by its immunogenic properties.

In the case of foreign proteins, the immunodominant epitopes usually (a) show the highest affinity for the MHC molecule (2), (b) form stable complexes with the MHC molecule due to their high affinity and (c) are present in sufficient amounts (185). In this case competition for empty MHC molecules does not regulate immunodominance, albeit it might play a role (190). This does not apply for immunodominant epitopes from self-peptides. Here, avidity of the T-cell receptor for the peptide-MHC-complex is instrumental in exerting T-cell activation. T cells with low affinity for self-peptides are positively selected, whereas T cells with high affinity for self-peptides are deleted during negative selection in the thymus (151). In this model, negative selection deletes T cells with high affinity for self peptides.

Negative selection for a given epitope can be missing, if (1) the affinity of the T-cell receptor for the peptide-MHC complex is low, if (2) despite high affinity of the T-cell receptor for the peptide, the binding of the peptide to the MHC is unconstrained, and, if (3) epitopes that are generated in the periphery are not presented in the thymus, e.g. cryptic epitopes. Hence, these mechanisms ensure a specific T-cell response to foreign antigens.

In general, T-cell tolerance as a non-lytic $CD8^+$ T-cell phenotype can be applied to T-cell subsets with distinct functions as for example $CD8^+CD28^-$ suppressor T cells, adoptively tolerant T cells, clonally anergic T cells and finally, T cells with a ‘division arrest’ phenotype all of which are unified by the fact that they show impaired or absent cell lysis.

Characteristic for $CD8^+CD28^-$ suppressor T cells is their indirect inhibition of immune responses. Instead of inhibiting other T cells directly, $CD8^+CD28^-$ suppressor T cells recognize peptides on antigen-presenting cells (APC) and downregulate costimulatory molecules on the APC-surface. They neither induce apoptosis via granzyme B nor do they kill other cells via perforin (189), typically proliferate well upon stimulation and produce IFN-γ and IL-2 (55). This T-cell subset is defined by the absence of CD28, CD45RO, CD27 and CCR7 on the

cell surface (95), though they express CD45RA and GITR upon stimulation. They gain FOXP3 expression a few days after stimulation and show low expression of CD25. CD62L is expressed variably without influence on suppressive function. Furthermore, they have been characterized by expression of OX40, 41BB, CD103, TNFR2, CD158K and CD158B2 (282).

Adaptive T-cell tolerance or "*in vivo* tolerance" describes a T-cell phenotype that is characterized by three phenomena: these cells show (a) downregulation of multiple effector cytokines such as IL-4, IFN-γ and most importantly IL-2, (b) dependence on antigen-persistence for maintenance of the anergic state, and (c) failure of exogenous IL-2 to reverse the tolerant state, as the IL-2α chain is consistently downregulated in this tolerant T-cell subset (53). Adaptively tolerant T cells have normal levels of surface T-cell receptor. The predominant T-cell receptor signaling block is located at the level of ZAP-70 kinase activity thus impacting mostly on the calcium/NFAT and the NFκB-pathway (53, 304). ERK phosphorylation, another downstream target of T-cell receptor signaling is predominantly not or only minimally inhibited in adaptive tolerance as it is in most T-cell anergy models, most likely because usually more than one T-cell receptor downstream cascade activates Ras through GRB2/ SOS (53). In summary, adaptive tolerance involves a primary impairment in early T-cell receptor activation leading to profound impairment in the activation of the NF-κB pathway and hence impaired intracellular calcium mobilization.

Adaptive tolerance is contrasted with T-cell clonal anergy. T-cell clonal anergy is characterized by a profound block in cell proliferation, whereas cytotoxicity is only slightly diminished. This state is generated by suboptimal stimulation represented by either strong T-cell receptor signal without costimulation or weak T-cell receptor signal with costimulation. Clonal anergic T cells show specific features. During the initial stimulation, these cells respond by increasing their activation markers, CD25 and CD69, but produce no detectable cytokines. Proliferation upon antigen stimulation is diminished, and effector cytokines such as IL-4, IFN-γ and IL-2 are downregulated (254). The primary signaling pathway that is inhibited in clonal anergy has been shown to be the RAS/MAPK pathway (53, 94, 184). The block occurs at the level of RAS activation and affects the ERK and JNK as well as the p38 pathway (53, 75),

whereas the complete calcium/NFAT activation pathway was found to be intact or reactively activated (102).

A newly described and in $CD4^+$ T cells well characterized T-cell anergic phenotype is the T-cell division arrest phenotype. Designative for division arrest T cells is their disability to proliferate strongly even upon optimal T-cell receptor stimulation and supply of IL-2 (112). Pathognomonic for this type of T-cell anergy is the constant expression of $p27^{kip1}$. This T-cell subset shows high expression of T-cell activation markers CD25 and CD69, but production of IFN-γ is massively impaired. A defect in T-cell signaling has been proposed, but not been found to this date.

A seldomly discussed but important other mechanism to change sensitivity of T-cell responsiveness towards antigens is T-cell maturation. As discussed above, the affinity threshold for positive and negative selection is hold in narrow range during clonal deletion (220). T cells that respond with high affinity towards antigens presented by the thymus are negatively selected and T cells that have no affinity for self die by neglect. Consequently, T cells that undergo positive selection show low affinity for self-antigens and potentially can lead to autoimmunity in the periphery. However responsiveness of these T cells seems to change during development and prevents autoreactivity of the mature T-cell population. As a result mature peripheral lymphocytes are less responsive to low-affinity ligands than are maturing lymphocytes in the thymus (173). Recently, this mechanism has been attributed to the function of the microRNA miR-181a. High expression of miR-181a in thymic thymocytes enhances both the sensitivity to low-affinity as well as high-affinity pMHC-complexes. Downregulation of miR-181a is observed in peripheral lymphocytes as compared to immature $CD4^+CD8^+$ T cells thus allowing positive selection in the thymus but unresponsiveness in the periphery (183). Furthermore T cells seem to modulate their immune properties towards given antigens. Naïve T cell populations that are stimulated with different amounts of antigen are able to give rise to both high- and low-avidity effector T cells thus extending T cell responsiveness modulation to the postthymal maturation (167). Whether there exist tumor-reactive T cells that are capable of intrinsically modulating their response towards the tumor is yet unclear.

1.6. Bias in T-cell receptor repertoire selection upon antigenic stimulus

In general, a rather small frequency of $CD8^+$ T cells of variable avidity for any given antigen – self or foreign – exists in the T-cell repertoire in the absence of an antigenic stimulation (Figure 2a). In response to an antigenic stimulus, only a relatively small number of naïve T cells is activated that comprises T cells bearing high avidity T-cell receptors resulting in a few clonotypes differing from each other in T-cell receptor sequence yet recognizing the same pMHC complex (73, 293). Dependent on the antigen, T-cell responses can be characterized as polyclonal or oligoclonal resulting in the preferential usage of particular α/β-T-cell-receptor combinations.

Following stimulation with a foreign antigen, strong activation and expansion of T cells occur that are characterized by high avidity T-cell receptors for the target antigen (Figure 2b). Under these circumstances, expansion of T cells that display high avidity T-cell receptors is favored, and T cells with low avidity T-cell receptors undergo cell death. Similarly, to strong binding avidity of the T-cell receptor results in activation induced cell death (221). Most of the productive anti-viral immune responses provide *in vivo* evidence for this model, as they are characterized by the expansion of a small number of T cells with very high avidity T-cell receptors (5, 103, 251, 289). T cells carrying intermediate or low avidity T-cell receptors are not expanded. Similarly, vaccination against infectious diseases and selected tumor antigens is accompanied by an oligoclonal expansion of antigen-specific T cells with high avidity TCR (324).

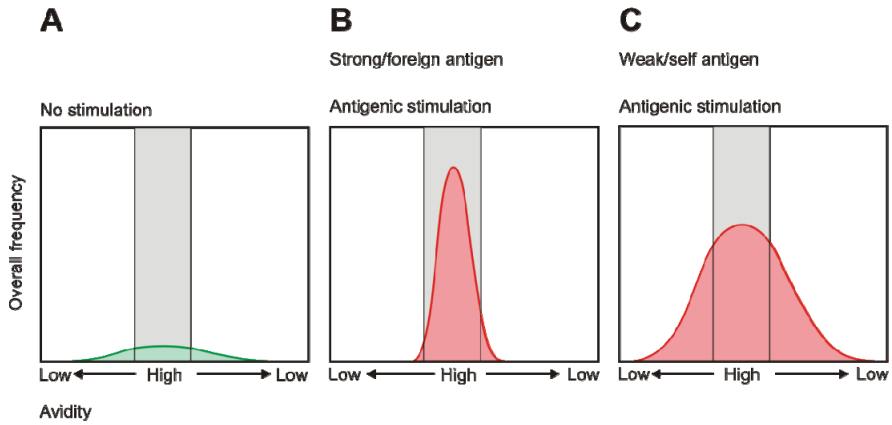

Figure 2 | Current model for the outcome after antigenic stimulation of CD8$^+$ T cells
(A) Under homeostatic conditions, only a small frequency of CD8$^+$ T cells of variable avidity exists in the T-cell repertoire in the absence of antigenic stimulation
(B) Stimulation with a foreign antigen induces strong activation and results in an oligoclonal expansion of T cells with high avidity T-cell receptors for the target antigen.
(C) In the context of tumor-antigens, the immune response results in a broader repertoire of antigen-specific T cells each with lower avidity for the target antigen. Grey, area of optimal T-cell receptor avidity for a given antigen.

Nonetheless, viral infections and other antigenic challenges are often characterized by substantial activation and expansion of T cells that does not only result from antigen-driven expansion but also from other mechanisms such as stimulation of cell division by cross-reactive antigens or cytokine-mediated bystander activation (24, 207, 310, 311, 317).

As many self-antigens are expressed in the thymus, negative selection of T cells expressing specific T-cell receptors might explain why self/tumor antigen-specific T-cell receptors are of lower avidity opposed to pathogen-specific T-cell receptors (327). Based on low avidity T-cell receptors, the immune response towards self/tumor antigens additionally presents with higher degrees of T-cell receptor heterogeneity (77) resulting in a broader repertoire of antigen-specific T cells each with lower avidity for the target antigen (Figure 2c). Among self/tumor antigens, NY-ESO-1 is an antigen of high immunogenicity leading to spontaneous immune responses in a large proportion of patients with NY-ESO-1 expressing cancer. HLA-A2$^+$ patients are capable of strong CD8$^+$ T-cell responses towards the NY-ESO-1 157-165 peptide. Comparable to a stimulus with foreign antigen, a small number of precursor T cells is selected in response to an antigenic stimulus with NY-ESO-1 peptide and comprises T cells bearing

several T-cell receptors resulting in ~10-50 clonotypes differing from each other in T-cell receptor sequence yet recognizing the same pMHC complex (73).

1.7. Tumor immunosurveillance

In the paradigm of self and non-self immunity, cancer occupies a field between classical exogenous pathogens and host tissue, as it arises from normal host cells but differs from these by a tumor-specific set of distinct genome alterations. The term “altered self” implicating a change in the “genomic configuration” of the particular tumor cell describes these fundamental differences in antigenic composition and biological behavior of tumor cells, the molecular hallmark of carcinogenesis being genetic instability (241). The major pathophysiologic characteristics of malignant cancer responsible for morbidity and mortality are the ability of malignant cells to invade across natural tissue barriers and to metastasize. This is associated with a dramatic disruption of tissue architecture, causing elaboration of proinflammatory signals that are the basis for initiation of both innate and adaptive immune responses towards cancer (241).

The concept of the immune surveillance hypothesis, initially proposed 1959 by Thomas (307) and then Burnet (38), picks up the idea that frequently arising tumors are constantly recognized, confronted with inflammatory immune responses and eliminated on the basis of expression of tumor-associated antigens (241). The assumption that the term “altered self” reflects the tumor-intrinsic expression of novel antigenic structures that are amenable to therapeutic approaches comprising the autologous immune system of the tumor host bases on the finding that induced tumors in animal models were frequently rejected when transplanted into syngeneic hosts, whereas transplants of normal tissue between syngeneic hosts were accepted (19, 96, 97, 122, 250). Based on the concept of tumor immune surveillance, a variety of novel antigenic peptides has been described whose immunogenicity can generally be generated by (1) mutations or (2) antigens normally only expressed in immune privileged sides (e.g. eye, testis, etc.) and therefore not presented to T cells under homeostatic circumstances, e.g. cancer/testis antigens.

Mutations with immunodominant properties usually lie within exons of protooncogenes or tumor suppressor genes and result in altered peptide presentation towards T cells at the cell surface (85, 196).

Depending on the pathogenesis of the type of cancer, immunogenicity might be minimal or absent (1) if loss of expression of tumor suppressor genes by methylation of nucleotides in promoter regions from healthy tissue is the reason of tumor growth, (2) if amplification of non-mutated growth supporting genes is the reason for tumor growth, (3) if tumor cells escape immune recognition by means of MHC downregulation (35) or lack of β_2-microglobulin synthesis (93), (4) if mutations that generate a non-immunodominant epitope in the context of epitope selection are presented on the cell surface and (5) because of peptide-MHC instability (362). Interestingly, the absence of costimulatory molecules on the surface of tumor cells has long been viewed as one of the reasons for low immunogenicity, yet by means of recognition by NK cells these tumors show higher rejection numbers.

1.8. Tumor immune evasion

Murine tumor models elicited with potent carcinogens in short time barely reflect natural tumor development in humans characterized by discrete mutations accumulating over time (135). Whereas it is widely accepted that immunosurveillance protects against cancers with viral etiology, disagreement exists whether spontaneously arising tumors are cleared by the immune system in a similar manner (161). Prototypes of highly immunogenic tumor subsets are Non-Hodgkin-lymphoma, Kaposi sarcoma and HPV-associated tumors of the genitourinary tract that contain variable amounts of viral proteins marking them as 'foreign'. Spontaneously arising tumors in mice, likely to be more representative for most human tumors than strongly immunogenic mutagen-induced tumors, show weak immunogenicity as do most human tumors (129). These tumors are only seldomly rejected spontaneously, yet the possibility of tumor-specific T cell-mediated tumor rejection exists if these T cells are generated by special immunization strategies (135, 237). In general, tumors are believed to have evolved numerous mechanisms to evade both innate and adaptive immunity and to induce an immune inhibitory microenvironment (100, 101, 371). These include at first a poor immunogenicity accomplished by (a) the modulation of MHC antigens (203, 222, 223) and (b) downregulation of co-stimulatory molecules. Additionally, tumor cells express (c) Fas ligand or other proapoptotic molecules on the cell surface (228, 292) and secrete (d) immune inhibitory factors. Among these mainly soluble immune inhibitory factors targeting the adaptive immune system are transforming growth factor β (226, 227), IL-10 (300, 338), and vascular endothelial growth factor (VEGF) (157, 359, 371). Recently identified mechanisms of immune modulation are (e) constitutive expression of tryptophan-depleting enzyme, indoleamine 2,3-dioxygenase (IDO) (319) and (f) recruitment of regulatory T cells (Tregs) (177).

1.9. Cancer immunotherapy and NY-ESO-1 antigen

As depicted above, the cancer immunosurveillance hypothesis predicts that cancers express substances in which they differ from healthy tissue and by which they may be detected by the immune system. The discovery that malignant melanoma cells indeed express antigens in which they differ from melanocytes, with the malignant melanoma antigen MAGE being the first tumor associated antigen to be reported, led to clinical trials using these tumor specific proteins as a target of cellular immunotherapy (326). By now many such genes encoding malignant melanoma specific antigens have been cloned and HLA restricted peptide epitopes have been identified that are recognized by cytotoxic T cells (52, 231). MHC I-restricted malignant melanoma associated antigens (Table 1) generally can be grouped into three main groups: (a) Cancer/ testis antigens such as BAGE, GAGE, MAGE, NY-ESO-1 and PRAME, (b) melanocyte differentiation antigens such as gp100, Melan-A/ MART-1, Tyrosinase, TRP-1, TRP-2 and (c) mutated or aberrantly expressed antigens as CDK4 and MUM-1 (31, 34, 271).

Melanocyte differentiation antigens are not unique to malignant melanoma cells (11) and during malignant melanoma immunotherapy using melanocyte differentiation antigens as target, malignant melanoma- as well as melanocyte-directed T-cell responses occur (30, 361).

In contrast to melanocyte differentiation antigens, which are expressed in both malignant melanoma cells and normal melanocytes, cancer/testis antigens are immunogenic protein antigens naturally expressed selectively in immune previleged tissues such as the testis and various human cancer types. NY-ESO-1 is a cancer/testis antigen of high immunogenicity leading to spontaneous immune responses in a large proportion of patients with NY-ESO-1 expressing cancer (22, 113, 140, 295, 297, 323, 339) and has attractive properties as therapeutic target for immunotherapy in patients with different malignancies. In particular, three peptides corresponding to overlapping sequences located between positions 155 und 167 of the NY-ESO-1 protein have been shown to be recognized by tumor-reactive HLA-A2 restricted T cells from malignant melanoma patients (137, 323).

Gene	Frequency of expression in metastatic malignant melanoma	Presenting HLA	Peptide sequence	Position in the protein
MAGE-A1	46%	A2	KVLEYVIKV	278–286
		A3	SLFRAVITK	96–104
MAGE-A3	74%	A1	EVDPIGHLY	168–176
		DP4	KKLLTQHFVQENYLEY	243–258
MAGE-A4	28%	A2	GVYDGREHTV	230–239
MAGE-A10	47%	A2	GLYDGMEHL	254–262
MAGE-A12	62%	Cw7	VRIGHLYIL	170–178
MAGE-C2	59%	A2	ALKDVEERV	336–344
NY-ESO-1/ LAGE-2	28%	A2	SLLMWITQ(A,I,L,V)	157–165 (C165A,I,L,V)
Tyrosinase	>90%	A2	YMDGTMSQV	369–377
Melan-A/ MART-1	>90%	A2	ELAGIGILTV	26–35 (A27L)
gp100	>90%	A2	IMDQVPFSV	209–217 (T210M)

Table 1 | Main antigenic peptides used to vaccinate melanoma patients

Table adapted from the database of T-cell epitopes and cancer peptides at cancerimmunity.org and from Thierry Boon et al. (31).

Consequently, therapeutic regimens with different NY-ESO-1 peptides and a varying composition of additional immune stimulating cytokines have been carried out to evaluate immunogenicity, safety and clinical response in HLA-A2 positive patients with NY-ESO-1 expressing malignant melanoma.

Different schedules of vaccination with HLA-A2 restricted NY-ESO-1 peptides p157-167 and p157-165 have been explored in Phase I clinical trials to study their efficacy on NY-ESO-1 peptide-specific $CD8^+$ T-cell responses. In the LUD97-009 trial, NY-ESO-1 peptides were administered intradermally at a dose of 100 µg/injection weekly for 4 weeks followed by a 4-week treatment-free interval. In the present Phase I study LUD00-009, intensive-course immunization was carried out with NY-ESO-1 peptides on 5 consecutive days every 3 weeks for 6 cycles (22). In the later phase of both studies, 75 µg GM-CSF starting with the third cycle of vaccination was used as a systemic adjuvant (46, 139, 181). Comparison of both studies showed that epitope-specific T-cell responses were induced in the majority of seronegative and all antibody-positive patients in both studies. However in the intensive-course study LUD00-009, NY-ESO-1 specific T-cell responses were detectable earlier and at a

higher frequency. Patients with detectable NY-ESO-1 immune responses showed better survival than patients with no or pre-existing immune responses (138, 152).

The current pilot study LUD02-007 analyzes the effect of the adjuvants Montanide ISA-51 and CpG 7909 on immunogenicity and clinical response. In this study, NY-ESO-1 peptide p157-165 is mixed with CpG 7909 and Montanide ISA-51, also known as incomplete Freund's adjuvant, and administered subcutaneously every 3 weeks for a total of 4 injections (152). Basis for this regimen is the observation that motifs present in the bacterial genomes serve as strong immunostimulatory agents in mice and humans. Particularly unmethylated CpG dinucleotide motifs are present in bacterial DNA and are strong stimulators of immune responses in mammalian hosts. CpG mediated stimulation of TLR9 (toll like receptor) predominantly expressed in B cells and plasmacytoid dendritic cells (164, 165) causes activation of monocytes, macrophages and dendritic cells with consecutive higher degree of protective immunity upon vaccination (171).

Although nowadays, relapse-free intervals and overall survival, reliable clinical endpoints used to compare therapeutic regimens, can markedly be improved by immunotherapy (148), most clinical trials still show only limited efficacy in terms of survival (84). Integrating 4 studies with a total of 111 patients, only 8 patients have shown an objective clinical response with some evidence of tumor regression being observed in additional 12 patients (31, 169, 201, 202, 325). The underlying causes for the differences in observed success rates are widely unknown and need to be determined.

2. Aim of this study

As outlined above, cancer vaccines are an attractive approach to treat malignant disease as the immune system is capable of mounting productive immune responses leading to tumor regression (31). Despite a variety of clinical trials, clinical efficiency of cancer vaccination is under intense debate as substantial advantage in overall survival has rarely been induced. This fact has so far mainly been attributed to mechanisms exerted by tumor cells within the tumor microenvironment (253). Intrinsic defects of tumor-responding immune cells have only recently been considered as well (124). Heterogenicity of the antigen-specific $CD8^+$ T-cell repertoire responding to NY-ESO-1 peptide 157-165 has been described (28) and peptide-specific but non-tumor-reactive $CD8^+$ T cells have been identified (62, 152, 360). Lack of tumor reactivity of antigen-specific $CD8^+$ T cells might be due to different intrinsic T-cell defects, differential antigen presentation, differences in functional avidity of T cells, or induction of antigen-specific T-cell tolerance. Although numerous mechanisms of T-cell tolerance have been described, their role in the clinical setting and their influence on clinical outcome are still unknown. As outlined above, there has been considerable interest in determining the phenotype and functional characteristics of antigen-specific $CD8^+$ T cells that are expanded during antigenic stimulus (31). Concerning this question, it is unclear whether tetramer staining of peptide-specific T cells, a practice that is used to quantify immune responses to peptide vaccination in cancer settings, adequately emulates the immune response towards a tumor-related antigen, or if important subsets of peptide-specific T cells with binding affinities below tetramer-sensitivity are missed and can explain the so far insufficient antitumor efficacy.

Aim of this study thus was to characterize this subset of T cells by means of their molecular markers. Antigen-unresponsiveness was explored by revealing the molecular profile related to this distinct T-cell phenotype. Finally, this T-cell subset was detected in cancer patients *in vivo*, and patient survival was set in context with the existence of these non-tumor-reactive T cells.

3. Materials and Methods

3.1. Patients and studies

Twenty NY-ESO-1$^+$ HLA-A2$^+$ cancer patients were enrolled in this study following institutional review board approval and informed written consent. Patients were enrolled either in LUD97-008 (138), LUD00-009 (22), a Phase I study of intensive-course immunization with HLA-A2 restricted NY-ESO-1 peptides combined with GM-CSF, LUD00-026, a study of immunization with HLA-A2 restricted NY-ESO-1 peptides alone or combined with polyarginine, and LUD02-007, a pilot study of NY-ESO-1 p157-165 peptide combined with CpG7909 and Montanide ISA-51. From 17 patients, peripheral blood mononuclear cells could be isolated before and after completion of the trial. For flow cytometric assessment of prevalence of CD8$^+$CD69$^+$CD25$^+$CD7$^+$ T cells, sufficient material from 7 patients was available.

Patients NW1045, NW1789 and NW2608 that had been diagnosed with metastatic malignant melanoma and whose metastatic lesions showed strong expression of NY-ESO-1 (152) could be assessed in further detail. Patients NW1045 and NW1789 were enrolled in the LUD00-009 study, patient NW2608 was enrolled in the LUD02-007 study.

3.2. Cell culture

Cultivation of eukaryotic cells requires strict sterile conditions. All procedures were performed using a sterile working bench with laminar air flow. Cells were cultured in 5% CO_2, 100% humidity and the appropriate medium.

$CD8^+$ T-cell clones, T2 cells and malignant melanoma cell lines were cultivated in the respective medium as described below. Growth of cultures was controlled continuously. Media contained pH-Indicator indicating acidification by metabolites. If acidification of media was detected in T-cell cultures, half of the volume of media was exchanged against fresh media.

Medium exchange differed in the setting of T2- and malignant melanoma cell lines as these cell lines grow adherently. If acidification of media was detected here or cells reached a certain degree of confluency (>80%) acidulated media was removed and a solution of 1% Trypsin and 0.02% EDTA was added. Cells were detached by tapping the flask and washed 2 times with 15 ml 1 x PBS (for 1 liter of 1x PBS, 8 g NaCl, 0.2 g KCl, 1.44 g Na_2HPO_4 and 0.24 g KH_2PO_4 were mixed, filled up with H_2O to 1 Liter and adjusted to pH 7.4 with HCl). Cells were resuspended in fresh media and allowed to grow again.

3.2.1. Malignant melanoma cell lines

Malignant melanoma cells were cultured in DMEM (Invitrogen, Karlsruhe, Germany) supplemented with 10% FCS, 1% Glucose, 10 IU/ml Penicillin, 100 mg/ml Streptomycin and 300 mg/l L-Glutamine further referred to as ‘Malignant Melanoma Cell Line Medium’. Expression of NY-ESO-1 in malignant melanoma cells was assessed by RT-PCR or immunhistochemistry as described before (149). The malignant melanoma cell line SK-Mel-37 has been established at Memorial Sloan-Kettering Cancer Institute, New York, USA. Malignant melanoma cell lines NW-Mel-1045, NW-Mel-1789, NW-Mel-2608 and NW-Mel-145 have all been established at Krankenhaus Nordwest, Frankfurt, Germany (all cell lines were kind gifts of Elke Jäger, Frankfurt, Germany).

3.2.2. Generation of NY-ESO-1 p157-165 pulsed T2 cells

T2 cells are defective in the presentation of endogenously synthesized antigens to cytotoxic T cells due to a deletion of MHC class II-encoded genes

for transporters associated with antigen presentation (TAP1/TAP2). Delivering exogenous peptides consisting of 9-11 amino-acids causes presentation on empty MHC class-I molecules (HLA-A2) leading to recognition and cell lysis by peptide specific MHC class-I restricted T cells.

T2 cells were cultured in DMEM (Invitrogen, Karlsruhe) supplemented with 10% FCS, 1% Glucose, 10 IU/ml Penicillin, 100 mg/ml Streptomycin and 300 mg/ml Glutamine further referred to as 'T2 Cell Line Medium'. Lyophilized NY-ESO-1 p157-165 peptide was solubilized in DMSO to a concentration of 10 mg/ml. The solution was diluted with 1 x PBS to a final concentration of 1 mg NY-ESO-1 peptide/ml. To generate T2 cells presenting NY-ESO-1 p157-165 peptide, T2 cells were pulsed with NY-ESO-1 peptide. For that purpose $5x10^6$ T2 cells were washed with 10 ml X-Vivo 15 media and resuspended in 1 ml X-Vivo 15. NY-ESO-1 peptide in DMSO/1xPBS solution was added to a final concentration of 10 µg/ml and incubated at room temperature for 1 hour. Hereafter cells were washed once with 10 ml X-Vivo 15 and used in T cell assays.

3.2.3. Generation of $CD8^+$ T-cell clones

Tumor-reactive and non-tumor-reactive $CD8^+$ T-cell clones were established at Krankenhaus Nordwest, Frankfurt, Germany. As the frequency of vaccine responding T cells is often lower than the detection limit of tetramer or ELISPOT assays (31), limiting dilution with restimulation and cloning of lytic microcultures were performed. During the restimulation, the precursor lymphocytes that recognize the antigen are multiplied by several hundredfold. Cloning is followed by lysis assays on T2 cells presenting the NY-ESO-1 p157-165 antigen and autologous malignant melanoma cell lines. Using this method, tumor-reactive as well as non-tumor-reactive $CD8^+$ T-cell clones are generated.

T-cell experiments were performed using RPMI 1640 medium containing 10 mM Hepes buffer, 300 mg/l L-Glutamine, 10 IU/ml Penicillin, 100 mg/ml Streptomycin, 1% of nonessential amino acids and 100 U/ml of IL-2 further referred to as 'T-Cell Medium'.

For generation of $CD8^+$ T-cell clones, $CD8^+$ T cells were first presensitized in vitro by mixed lymphocyte peptide culture (MLPC) and mixed lymphocyte tumor cell culture (MLTC). For MLPC, $CD8^+$ and $CD4^+$ T-cell depleted PBMC

were irradiated (3000 rad) and pulsed with 10 µg/ml NY-ESO-1 p157-165 peptide (SLLMWITQC, Multiple Peptide Systems, San Diego, USA) for 1 hour. For MLTC, irradiated (10.000 rad) autologous tumor cells were used as antigen presenting cells and pulsed with 10 µg/ml NY-ESO-1 p157-165 peptide for 1 hour as well. $CD8^+$ T cells from *in vitro* prestimulated T cells from MLPC or MLTC cultures were cloned by limiting dilution in 96 U-bottom plates by using irradiated (10.000 rad) NY-ESO-1-peptide-pulsed T2 cells or irradiated autologous tumor cells as antigen presenting cells ($3x10^3$ cells/well) and irradiated EBV-transformed B cells as feeder cells ($4x10^4$ cells/well).

After 2 weeks, with one restimulation on day 7, aliquots of proliferating clones were tested for NY-ESO-1 specific reactivity in ^{51}Cr-release assays against autologous tumor cells as well as NY-ESO-1 p157-165 peptide-pulsed T2 cells. NY-ESO-1 specific clones were restimulated weekly as described above and used for further experiments.

Patient	#clone	Tumor reactivity	Designation in text
NW1789	W10	non-tumor-reactive	W10-NTR
NW1789	W26	tumor-reactive	W26-TR
NW1045	F19	non-tumor-reactive	F19-NTR
NW1045	F40	tumor-reactive	F40-TR
NW2608	B21	non-tumor-reactive	B21-NTR
NW2608	B4	tumor-reactive	B4-TR

Table 2 | Tumor-reactive and non-tumor-reactive $CD8^+$ T-cell clones

$CD8^+$ T-cell clones from three patients NW1789, NW1045 and NW2608 were examined in detail. $CD8^+$ T-cell clones were generated as described and designated according to their lytic activity towards peptide-pulsed T2 cells and autologous melanoma cells.

3.2.4. Mixed lymphocyte peptide culture

Experiments that demonstrate specific lysis of target cells by cytotoxic $CD8^+$ T cells are usually done with a ^{51}Cr-release-assay. In this assay, viable target cells are incubated with $Na^{51}CrO_4$, which binds tightly to intracellular proteins. After a washing step, target cells are incubated with target-cell-specific $CD8^+$ T cells, releasing labeled proteins into the culture supernatant due to

plasma-membrane damage after cell lysis. Consecutive radioactivity in the supernatant is determined with a gamma counter.

$CD8^+$ T-cell reactivity post peptide vaccination was tested in ^{51}Cr-release-assays against a NY-ESO-1 expressing tumor cell line and peptide-pulsed T2 cells (232). For ^{51}Cr-release-assays, peptide pulsed T2 cells or autologous malignant melanoma cells were labeled with 100 µCi of $Na^{51}CrO_4$ (DuPont, Wilmington, USA). Then, $CD8^+$ T cells were incubated with peptide pulsed T2 cells or autologous malignant melanoma cells for 4 hours with 5% CO_2 at 37°C. The percentage of specific ^{51}Cr release was determined as follows: percent specific ^{51}Cr release = (experimental ^{51}Cr release − spontaneous ^{51}Cr release) × 100/(maximum ^{51}Cr release − spontaneous ^{51}Cr release). Maximum ^{51}Cr release was obtained by adding 100 µl of 1% Nonidet P-40 (Sigma, Steinheim, Germany) to labeled target cells. Overall reactivity was calculated as the percentage of reactive cultures per patient. No reactivity was defined as ≥20% lysis of T2 cells or tumor cells in ≤12.5% of wells analyzed. No tumor-reactivity was defined as ≥75% of reactive wells with ≥20% lysis of only peptide-pulsed T2 cells. Tumor-reactivity was defined as ≥20% tumor cells lysis in ≥25% of reactive wells. At least 24 individual $CD8^+$ T-cell cultures per patient were performed. Individuals were classified according to the named criteria.

To confirm that non-tumor-reactivity was not based upon recognition of a potential contaminant or degradation product, the NY-ESO-1 p157-165 peptide was separated by reverse-phase HPLC on a MultoHigh-Bio 300 RP4 5 µm column (CS-Chromatographie-Service, Langerwehe, Germany) using a 35-min linear gradient of acetonitrile in water (35-45%) containing 0.1% TFA. The purified SLLMWITQC monomer peak was subsequently reanalyzed by reverse-phase HPLC and mass spectroscopy and routinely revealed purities >99%. Subfractions were obtained by reverse-phase HPLC and reactivity against these subfractions was measured. Additionally, T-cell reactivity against irrelevant NY-ESO-1 p159-167 peptide-pulsed T2 cells, IFN-γ pretreated tumor cells and NY-ESO-1 p157-165 peptide pulsed tumor cells was measured.

3.2.5. Purification of $CD8^+$ T cells from fresh blood

For purification of $CD8^+$ T cells, blood samples from healthy blood donors at the Center for Transfusion Medicine (University of Cologne, Germany) were

collected after informed written consent had been obtained. $CD8^+$ T cells were purified using the RosetteSep Human $CD8^+$ T-cell Enrichment Kit (StemCell Technologies, Cologne, Germany). 500 µl of RosetteSep Human $CD8^+$ T-cell Enrichment Cocktail were added to 10 ml of leukocyte-enriched blood derived from buffy coat and mixed well. The mixture was incubated for 20 minutes at room temperature and gently shaken every 5 minutes. The sample was diluted with an equal volume of 1 x PBS, mixed gently, layered on the top of 15 ml cold Ficoll-Paque PLUS (GE Healthcare, Munich, Germany) and centrifuged for 25 minutes at 1200 x g at room temperature. The $CD8^+$ T cells enriched at the plasma interface were carefully collected and washed twice with 20 ml 1 x PBS. The enriched $CD8^+$ T cells were counted and used for further experiments. Purity of $CD8^+$ T cells was assured by FACS staining using antibodies against CD3, CD4 and CD8 as described below. Purified T cells routinely showed purity of >90% $CD8^+$ T cells.

3.3. Flow cytometry

3.3.1. Detection of surface protein-expression by flow cytometry

For quantification of cell surface molecules and intracellular cytokine expression, cell cycle determination and Cytometric bead array, a BD FACSCanto™ flow cytometer was used. With two excitation lasers and 6 fluorescence channels, up to six different fluorescences can be detected. By use of the blue Argon laser with an excitation wavelength of 488 nm, FITC (Absorption maximum at 495 nm; Emission maximum at 520 nm), PE (Absorption maximum at 564 nm; Emission maximum at 578 nm), PerCP (Absorption maximum at 482 nm; Emission maximum at 678 nm), Pe-Cy5 (Absorption maximum at 496 nm; Emission maximum at 667 nm) and Pe-Cy7 (Absorption maximum at 488 nm; Emission maximum at 785 nm) were detected. By use of a red helium-neon laser with an excitation wavelength of 633 nm, APC (Absorption maximum at 650 nm; Emission maximum at 660 nm) and APC-Cy7 (Absorption maximum at 650 nm; Emission maximum at 785 nm) were detected.

The particular fluorochrome-conjugated antibodies were purchased from BD PharMingen (Heidelberg, Germany), BD Biosciences (Heidelberg, Germany), R&D Systems (Minneapolis, MN, USA) and MorphoSys UK Ltd (Oxford, UK) (see supplemental Tables 3 and 4). To detect specific binding of $CD8^+$ T cells to the NY-ESO-1 157-165 peptide, NY-ESO-1 tetramer staining was performed. For this purpose $CD8^+$ T-cell clones were stained with an HLA-A*0201-tetramer loaded with the NY-ESO-1 157-165 peptide (Peptide sequence: SLLMWITQC; C, cysteine; I, Isoleucine; L, leucine; M, methionine; Q, glutamine; S, serine; T, threonine; W, tryptophan) conjugated to Phycoerythrin. As negative control, an HLA-A*0201-tetramer loaded with the HIV polRT 476-484 peptide (Peptide sequence: ILKEPVHGV; E, glutamic acid; G, glycine; H, histidine; K, lysine; P, proline; V, valine) conjugated to Phycoerythrin was used (both kind gifts of Elke Jäger, Frankfurt, Germany).

To determine the phenotype of $CD8^+$ T-cell clones by flow cytometry, expression of surface molecules on tumor-reactive and non-tumor-reactive $CD8^+$ T-cell clones was assessed. For that purpose, 4×10^5 $CD8^+$ T-cell clones

were washed twice with 2 ml 1 x PBS and centrifuged at 200 x g for 5 minutes. 5 x 10^4 T cells per $CD8^+$ T-cell clone were stained with the respective fluorescence labeled antibody in 200 µl 1x PBS. After staining for 15 minutes at 4°C, $CD8^+$ T cells were centrifuged as before, washed once with BD Cellwash (BD Biosciences, Heidelberg, Germany) and surface protein expression was determined on a BD FACSCanto™ flow cytometer using the BD FACS DiVa 4.0 software (BD Biosciences, Heidelberg, Germany).

3.3.2. Detection of intracellular protein-phosphorylation by flow cytometry

To assess the intracellular T-cell receptor signaling cascade and to unveil changes in the T-cell receptor downstream signaling, phosphorylation of T-cell receptor downstream targets was measured using antibodies against phosphorylation sites of the T-cell receptor downstream targets CD3ζ, ZAP-70, lck^{p505}, ERK, p38 and NF-κB. This experiment was performed using T cells seven days post antigen stimulation. To avoid unspecific activation before measuring intracellular downstream signaling, T cells were allowed to rest in X-Vivo 15 medium at 37°C for at least 6 hours before start of the experiment. To assure that T-cell activation was started at the same time point and to avoid altered phosphorylation, the complete assay was performed on ice. First, T cells were washed twice with ice cold 1 x PBS. For each molecule, phosphorylation of 1 x 10^5 non-tumor-reactive or tumor-reactive $CD8^+$ T-cell clones was analysed. $CD8^+$ T-cell clones were stimulated with 0.1 µg anti-CD3 (clone OKT3) and 0.1 µg anti-CD28 (clone 9.3) antibodies per 1 x 10^5 $CD8^+$ T cells. Antibodies were allowed to bind for 20 minutes on ice. T cells were washed once with 5 ml ice cold 1x PBS and centrifuged at 200 x g for 6 minutes at 4° C. To crosslink CD3 and CD28, T cells were incubated afterwards for 20 minutes with an secondary anti-mouse-IgG specific antibody (Goat anti-Mouse Ig(H+L), Beckman Coulter Inc., Fullerton, CA, USA) at 4° C followed by a washing step with ice cold 1x PBS. A polyclonal antibody directed against calcitonin was used as negative control. 10 ng/ml Phorbol myristate acetate (Sigma-Aldrich Chemie GmbH, Taufkirchen, Germany), a T-cell mitogen, was used as positive control. After crosslinking with secondary antibody, $CD8^+$ T-cell clones were resuspended in 100 µl ice cold 1x PBS and exposed to 37°C in a pre-warmed water bath for the optimal time point established for each T-cell receptor

signaling molecule. The time points needed to allow optimal phosphorylation had been established in previous experiments using $CD8^+$ T cells isolated from peripheral blood.

T-cell Signaling Molecule	Time of Stimulation of the T-cell receptor/ CD3-complex
TCR ξ-chain	1 minute
ZAP-70	1 minute
Lck p505	4 minutes
ERK	4 minutes
p38	4 minutes
NF-κB	10 minutes

Table 3 | Assessment of Phosphorylation

Timepoints used to determine phosphorylation of T-cell receptor downstream signaling. Timepoints were choosen according to published literature. Additionally, timepoints of T-cell receptor/ CD3-complex stimulation were validated in advance using Jurkat T cells.

At designated time points of T-cell activation, phosphorylation status of T-cell receptor signaling molecules was fixed by adding 2 ml 1x BD™ Phosflow Lyse/Fix Buffer (BD Biosciences Pharmingen, San Diego, USA) and incubation for 10 minutes at 37°C. After centrifugation for 6 minutes at room temperature at 200 x g, T-cell pellets were resuspended with 1 ml 1x BD™ Phosflow Perm/Wash Buffer (BD Biosciences Pharmingen, San Diego, USA), incubated for 10 minutes at room temperature and centrifuged as before. This wash step was repeated once. T-cell pellets were resuspended in 150 µl 1x BD™ Phosflow Perm/Wash Buffer and the particular phosphorylation specific antibody was added (see supplemental Tables 5 and 6). After incubation for 30 minutes in the dark at room temperature, T cells were washed twice with 2 ml 1x PBS. Finally, $CD8^+$ T cells were resuspended in 200 µl 1x PBS and applied to flow cytometry.

3.3.3. Detection of cytokine production by cytometric bead array

Cytometric Bead Array (CBA) permits simultaneous quantification of up to six cytokines in a single sample. Particles discrete in size and color coated with antibody to the particular antigens and capturing the antigen with a second fluorescence labeled antibody allow sensitive and efficient capturing of analytes. The CBA Human Th1/Th2 Cytokine Kit (BD Biosciences, Heidelberg, Germany)

was used to measure cytokines related to distinct $CD8^+$ T-cell phenotypes as IL-2, IL-4, IL-5, IL-10, TNF and IFN-γ.

For that purpose, $5x10^5$ non-tumor-reactive and tumor-reactive $CD8^+$ T-cell clones were either rested or incubated with the corresponding malignant melanoma cell lines or NY-ESO-1 peptide pulsed T2 cells at a 1:10 ratio (T cell: target cells) for 24 hours in a x-bottom 96-well plate. To exclude that malignant melanoma or T2 cells might be the source of the cytokine profile measured, they were cultured alone for 24 hours and their supernatants were quantified for cytokines as well. To show that non-tumor-reactive $CD8^+$ T-cell clones are – as postulated – negatively regulated by means of low avidity T-cell receptor-pMHC interaction in response to malignant melanoma cells, but that an optimal T-cell receptor-stimulus can restore T-cell cytokine production and overcome division arrest anergy, cytokine response of each clone towards the “virtual” cognate stimulus of CD3/CD28/MHC-I magnetic beads was quantified after 24 hours as well.

Preparation of standard curves

A standard curve was established by serial dilution for each of the six cytokines. Human Th1/Th2 Cytokine Standards were reconstituted with 2 ml Assay Diluent for 15 minutes and reconstituted proteins were mixed. The standard curve ranged from 5000 pg/ml for each cytokine in the initially reconstituted standard tube to 20 pg/ml in the 1:256 diluted tube.

Preparation of Mixed Human Th1/Th2 Cytokine Capture Beads

Each capture bead suspension was vortexed and 10 µl of capture beads for each assay tube to be analyzed was mixed to prepare a stock tube of mixed capture beads.

Assay procedure

50 µl of mixed capture beads, 50 µl of Human Th1/Th2 PE detection reagent and 50 µl of the particular test sample were mixed in this order in test assay tubes. The standard curve was created likewise in standard curve assay tubes. Tubes were incubated for 3 hours at room temperature protected from light. 1 ml of wash buffer was added to each tube and tubes were centrifuged for 5 minutes at 200 x g. The supernatant was removed from each tube and 300

µl wash buffer was used to resuspend the bead pellet. Samples were analyzed on a FACSCanto cytometer using FACSDiva 4.0 Software .

Cytometer Setup

Three tubes A, B, C, were set up with 50 µl of cytometer setup beads. 50 µl of FITC-positive and 50 µl of PE-positive control detector were added to tube B and C, respectively. Tubes A, B, C were incubated for 30 minutes at room temperature in the dark, and 450 µl 1x PBS to tube A and 400 µl to tube B and C were added. The forward and side scatter were adjusted as recommended and gates set as described by the manufacturer.

Data Acquisition and Analysis of Sample Data

The reporter PE as parameter for cytokine concentration was assessed in the FL2 channel. The clustering parameter APC was assessed in the FL3 channel. Data was recorded as recommended and FCAP Array™ Software (BD Biosciences, Heidelberg, Germany) was used to plot standard curves and to calculate sample concentrations.

3.3.4. Detection of XCL1 production by ELISA

ELISA (Enzyme Linked ImmunoSorbent Assay) is a highly sensitive method to detect proteins in supernatants of cell cultures. XCL1 in cell supernatants from $CD8^+$ T-cell clones was measured using the XCL-1 ELISA kit (Antigenix America Inc., New York, USA). Prior to assay run, 50 µg of lyophilized capture antibody was reconstituted in 0.5 ml sterile H_2O to a concentration of 0.1 mg/ml. 25 µg antigen-affinity purified and biotin labeled detection antibody was reconstituted in 500 µl of sterile water containing 0.1% BSA. Standard solution was prepared using 5 µg of recombinant human XCL1 (lymphotactin) that were reconstituted in 100 µl of sterile H_2O (pH 7.2). Stock solutions were kept frozen at -80°C until further use.

Plate preparation

100 µl of capture antibody were diluted with 1x PBS to a final concentration of 1.0 µg/ml. 100 µl of the 1.0 µg/ml capture antibody were added to each ELISA well of Nunc Maxisorp™ 96 well plates (Nunc GmbH & Co. KG, Langenselbold, Germany). Plates were sealed and incubated overnight at room temperature. On the following day, wells were aspirated to remove all liquid and

were washed four times using 300 µl of wash buffer (0.05% Tween in 1x PBS) per well. After the last wash, 200 µl of blocking buffer (1% BSA in 1x PBS) were added to each well. After incubation for 60 minutes at room temperature, wells were washed four times using 300 µl of wash buffer and plates were taped dry.

Preparation of standard curves

10 ng/ml of XCL1-standard was diluted in serial dilution to zero (10 ng/ml; 5 ng/ml; 2.5 ng/ml; 1.25 ng/ml; 0.625 ng/ml; 0.3125 ng/ml; 0.15625 ng/ml; 0 ng/ml).

Assay procedure

100 µl of standard or sample were added to each well in duplicate. The assay was incubated at room temperature for 2 hours, fluid was aspirated and plates were washed four times with 300 µl of wash buffer. A portion of the detection antibody stock solution was diluted to a concentration of 0.25 µg/ml. 100 µl of 0.25 µg/ml detection antibody solution were added to each well and incubated at room temperature for 2 hours. Subsequently, fluid was aspirated from each well and plates were washed again four times using 300 µl of wash buffer. Horseradish Peroxidase conjugated streptavidin stock solution (Streptavidin-HRP, Antigenix America Inc., New York, USA) was diluted 1:500 with 1x PBS, 100 µl were added per well and incubated for 30 minutes at room temperature. Again, fluid was aspirated from each well and plate was washed for four times with 300 µl of wash buffer. 3,3´,5,5´-tetramethylbenzidine (TMB Substrate, Antigenix America Inc., New York, USA) was used as subtrate. TMB is a chromogen that yields a blue color when oxidized with hydrogen peroxide catalyzed by Horseradish Peroxidase with major absorbances at 370 nm and 652 nm. After addition of phosphoric acid, the reaction is stopped and a color change to yellow occurs that results in a maximum absorbance of 450 nm (147). 100 µl of TMB substrate solution were added to each well and incubated for color development at room temperature. Reaction was stopped with phosphoric acid at approximately 30 minutes after plate had been monitored every 5 minutes. Monitoring and measurement were performed on an ELISA microplate reader (Dynatech Microplate Reader MR5000, DYNEX Technologies, Virginia, USA). All samples were analyzed at least in triplicates.

3.4. T-cell activation

3.4.1. Nonspecific T-cell receptor-mediated activation of T cells

3.4.1.1. Generation of CD3/CD28/MHC-I beads

The Bead stimulation assay is a possibility to activate $CD8^+$ T Cells by mean of crosslinking their T-cell receptor and the CD3/CD28 complex (48). For that purpose artificial antigen presenting cells (aAPC) are used comprised of polyurethane-coated tosyl-activated magnetic beads coated with anti-CD3 (5%), anti-CD28 (14%) and anti-MHC-I (81%) antibodies, each in suboptimal doses to prevent overstimulation.

To coat magnetic beads with different amounts of anti-CD3, anti-CD28 and anti-MHC-I antibodies, 1 ml of magnetic beads (Dynal Biotech, Oslo, Norway) was incubated with 7.5 µg anti-CD3 (clone OKT3, Janssen-Cilag, Neuss, Germany), 20.3 µg anti-CD28 (clone 9.3, a kind gift of Drs. Carl June and Jim Riley, Abramson Cancer Research Center, University of Pennsylvania, Philadelphia, USA) and 122.2 µg anti-MHC-1 antibody (clone W6/32, Abcam, Cambridge, United Kingdom). For that purpose the corresponding amounts of antibodies were solubilized in 750 µl borate solution (0.1 M Boric acid pH 9.5, containing 1,236 g Boric Acid in 200 ml H_2O, sterile filtered using a 0,22 µm filter and adjusted to pH 9.5). In the mean time, beads were vortexed and resuspended several times with a 10 ml pipette. The bead storage liquid was removed against a magnet and beads resuspended in 100 µl borate solution. The antibodies solubilized in borate solution were added and the tube was mixed on a wheel at 37°C over night. After 15 hours borate solution was removed using a magnet and beads were washed three times for 10 minutes each with Bead wash media (250 mg BSA and 50 mg NaN_3 added to 250 ml 1x PBS, pH 7,4) at room temperature. Following a fourth wash step for 30 minutes with Bead wash media at room temperature, beads were washed at 4°C over night on a wheel as before. Again, bead wash media was removed against a magnet und beads were resuspended in 7.5 ml Bead wash media. Beads were counted on an improved Neubauer hemacytometer and stored upon use at 4°C.

3.4.1.2. Unspecific T-cell receptor stimulation

Prior to use, beads stored in Bead wash media were washed three times with RPMI/10% FCS using a magnetic tube rack. To ascertain T-cell stimulation, cells were stimulated at 37°C by mixing with beads at a ratio of 1:3 (T cell to beads). $1x10^6$ $CD8^+$ T-cell clones per well were incubated for 24 hours with $3x10^6$ Beads. Cells were washed twice with 1x PBS and subsequently used for western blotting. Supernatant of stimulated and unstimulated $CD8^+$ T-cell clones was stored at -80°C and applied to Cytometric Bead Array for cytokine secreting analysis as described above.

3.4.2. Antigen-specific T-cell receptor stimulation

3.4.2.1. CFSE labeling

CFSE, a protein fluorescing in the FITC channel, binds to intracellular molecules and consecutively is captured in these cells after intake. The particular number of T2 or malignant melanoma cells was washed twice with 10 ml 1x PBS at 300g for 10 minutes and resuspended in 500 ml of 1x PBS. 0.5 µl of a 0.5 mM CFSE stock solution was added to a final concentration of 0.5 µM. Cells were vortexed and incubated at room temperature for 8 minutes with occasionally carefully shaking the vial to allow equal distribution of CFSE to the cells. After incubation, cells were vortexed once and washed with 10 ml of RPMI/10% FCS. Cells were washed twice with RPMI/10% FCS and used for the following T-cell stimulation assay.

3.4.2.2. Stimulation using autologous malignant melanoma cells/ peptide pulsed T2 cells

To test for cell cycle associated molecules in T cells responding towards malignant melanoma cells and peptide pulsed T2 cells, tumor-reactive and non-tumor-reactive $CD8^+$ T-cell clones were incubated at a ratio of 10:1 with the particular malignant melanoma cell line or NY-ESO-1 157-165 peptide-pulsed T2 cells, respectively, for 24 hours in DMEM. $2x10^6$ W10-NTR $CD8^+$ T-cell clones were incubated either alone, with $2x10^5$ peptide-pulsed T2 cells or with $2x10^5$ cells of the NY-ESO-1 expressing malignant melanoma cell line generated from patient NW1789. The same was performed for tumor-reactive W26-TR $CD8^+$ T-cell clones. Due to insufficient amounts of $CD8^+$ T-cell clones,

this experiment could not be performed with T cells from patients NW1045 and NW2549. Supernatant of stimulated and unstimulated $CD8^+$ T-cell clones was stored at -80°C and applied to Cytometric Bead Array for cytokine secreting analysis. T cells were separated from T2 cells and malignant melanoma cells using FACS (fluorescence activated cell sorting) and applied to western blotting.

3.4.2.3. FACS – Fluorescence activated cell sorting

Fluorescence activated cell sorting enables isolation of different cells by use of cell specific fluorescence, being introduced by methods such as antibody labeling or cell organelle staining. To isolate T2 cells and malignant melanoma cell lines from responding non-tumor-reactive and tumor-reactive $CD8^+$ T-cell clones, respectively, $CD8^+$ T-cell clones were specifically labeled with a PE-Cy-5 labeled antibody against CD8, whereas cellular proteins in the cytosol of T2 cells and malignant melanoma cells were labeled prior to the stimulation assay with CFSE as described above.

In contrast to T2 cells and malignant melanoma cells, which were all labeled prior to stimulation due to the non-specific incorporation of CFSE in all cells exposed to CFSE, T cells were specifically labeled using antibodies against CD8. After incubation of non-tumor-reactive or tumor-reactive $CD8^+$ T-cell clones for 24 hours with either T2 cells or malignant melanoma cells, the cell mixture was washed twice with ice cold 1x PBS and incubated for 30 minutes at room temperature with PE-Cy-5 labeled antibodies against CD8. Afterwards, cells were washed twice with ice cold 1x PBS, resuspended in 1x PBS to $1x10^6$ cells/ml and separated at 4°C on a BD FACSVantage SE System at the Institute of Genetics, University of Cologne.

After separation of $CD8^+$ T-cell clones from malignant melanoma cells, equivalent amounts of T cells from each $CD8^+$ T-cell clone were lysed with lysis buffer and used for subsequent western blotting as described below.

3.5. Protein chemistry

3.5.1. Cell lysis

After the particular stimulation assay, cells were centrifuged at 4°C and lysed with lysis buffer. For 6.11 ml of cell lysis buffer, the following reagents were used: 5 ml of Triton X 1%, 750 µl of 150 mM NaCl, 250 µl of 50 mM Tris-HCl and 10 µl of 1M PMSF. 50 µl of both Phosphatase Inhibitor Cocktail I and II as well as 1 tablet of Protease inhibitor Complet Mini were added freshly to the lysis buffer at 1:100 dilution.

3.5.2. Protein quantification

Protein concentration was determined using the BCA (Bicinchoninic acid) Protein assay reagent kit (Thermo Fisher Scientific, Rockford, IL, USA). In alkaline conditions, proteins form complexes with Cu^{2+} followed by reduction of Cu^{2+} to Cu^{1+}. The amount of reduction is proportional to the amount of protein present in the sample. Two molecules of BCA chelate with one molecule of Cu^{1+} to form a purple-blue complex that can be monitored at its absorbance maximum of 562 nm.

A standard curve was established by serial dilution. 2 µl of protein lysates were used and diluted with 98 µl of lysis buffer. To prepare a standard curve, 0 µg, 5 µg, 10 µg, 15 µg and 20 µg of bovine serum albumin (BSA; Sigma, Steinheim, Germany) were diluted in lysis buffer to a final volume of 100 µl. BCA reagent mixture were prepared freshly by mixing reagent A and reagent B from the BCA-assay kit in a 1:50 (v/v) ratio. The protein samples were diluted with 900 µl of reagent mixture and mixed by serial pipetting. The reaction tubes were incubated at 65°C for 5 minutes followed by 10 minutes on ice. Then, absorbance was measured at 562 nm using a spectrophotometer (Ultraspec 2100pro). A standard curve of absorbance versus protein concentration was plotted and protein concentration in each sample was determined by linear regression.

3.5.3. SDS-Polyacrylamide gel electrophoresis (SDS-PAGE)

SDS-Polyacrylamide Gel Electrophoresis bases upon the separation of proteins on the basis of their molecular weight. Two sequential gels are cast:

the top “stacking” gel with a low polyacrylamide concentration is slightly acidic (pH 6.8), separates proteins only poorly, but forms thin and sharply defined protein bands. The lower “resolving” gel with a higher polyacrylamide concentration (10% polyacrylamide concentration in my experiments) is basic (pH 8.8) and separates proteins according to their molecular weight with smaller proteins traveling faster through the gel than larger proteins. The gel contains (a) sodium dodecyl sulfate (SDS), an anionic detergent which denaturates proteins and imparts a negative charge, and (b) Tris(2-carboxyethyl)phosphine (TCEP), a reducing compound that breaks disulfide bonds in proteins. In an electric field, negatively charged proteins are attracted towards the anode and resolved by the pores of the polyacrylamide gel solely on the basis of their size.

A mini protean II system (Bio-Rad, Hercules, California, USA) was used for electrophoresis. First, the 10% resolving gel was prepared by mixing 2.01 ml sterile H_2O, 1.25 ml 1.5 M Tris-HCl (pH 8.8), 1.67 ml 30% Acrylamide, 50 µl 10% SDS, 16.65 µl 10% APS and 7 µl TEMED. The mixture was applied between two glass slides producing a gel of 1.0 mm thickness, of approximately 8.3 cm width and of 6.0 cm height. The stacking gel was prepared by mixing 1.83 ml sterile H_2O, 0.83 ml 1 M Tris (pH 6.8), 0.42 ml 30% Acrylamide, 25 µl 10% SDS, 17 µl 10% APS and 3.3 µl TEMED. The mixture was layered upon the polymerized resolving gel and a comb was applied on the top until polymerization. The chamber was filled with 1x electrophoresis buffer (0.025 M Tris, 0.192 M Glycine, 0.5% SDS filled up to 1000 ml with sterile H_2O).

Protein samples were prepared to contain the same amount of total protein/ µl. For electrophoresis 1 µl of 4x Laemli-Buffer (125 mM Tris pH 6.8, 40% Glycerol, 6% SDS and 0.02% Bromphenolblue) was added to equal amounts of lysed protein to a final volumen of 4 µl and incubated for 5 minutes at 95°C. After cooling down on ice and centrifugation for 30 seconds at 12.000 x g, the mixture was applied onto a 10% SDS-Polyacrylamide Gel. A standard protein ladder ran parallel to check for protein size on Western blot. Gels were run at 100 V for 15 minutes followed by 180 V for 45-60 minutes.

3.5.4. Protein transfer

Blotting equipment for the protein transfer onto nitrocellulose-membranes, such as sponges, filters and the nitrocellulose-membrane were incubated for 10

minutes with 1x transfer buffer (250 mM Tris, 200 mM Glycine and 20% methanol). Then, the SDS-Gel was applied onto a nitrocellulose-membrane (Amersham, Buckinghamshire, UK) avoiding the existence of air bubbles in-between the SDS-Gel and the nitrocellulose-membrane. The inner blotting chamber was filled up with 1x transfer buffer, the outer chamber with H_2O. A cooling block was inserted into the chamber to dissipate the heat and avoid degradation of proteins during the transfer. Transfer was carried out at 100 V for 1 hour.

3.5.5. Western blot

Western blotting involves the detection of specific proteins on membranes using specific antibodies. First, the nitrocellulose-membrane was blocked for 1 hour with 5% milk (10 g milk powder filled up to a final volume of 200 ml with 1x TBS) to prevent non-specific binding of antibodies. The membrane was then probed over night at 4°C with 2 µl of primary antibody against $p27^{kip1}$ (clone F-8, Santa Cruz Biotechnology, Santa Cruz, CA, USA) in 3 ml 5% milk. On the following day, membranes were washed 3 times for 10 minutes with Tween buffer (for 2 liters of Tween buffer, 1 ml Tween (Merck, Darmstadt, Germany) was added to 2 liters of 1x TBS buffer (6.05 g Tris-Base and 8.76 g NaCl dissolved in 800 ml H_2O, adjusted to pH 7.5 with HCl and filled up with H²O to 1 liter) to remove excess antibody and then incubated with 1.5 µl of secondary antibody (polyclonal goat anti-mouse HRP conjugate purchased from DakoCytomation, Glostrup, Denmark) in 3 ml 5% milk for 1 hour at room temperature. Membranes were washed again 3 times for 10 minutes with Tween buffer and were exposed for 1 minute to a 1:1 mixture of ECL™ Western Blot detection Reagents 1 and 2 (Amersham, Buckinghamshire, UK). Membranes were carefully dried, exposed to Hyperfilm® ECL (Amersham, Buckinghamshire, UK) and processed on a Cronex CX-130 (DuPont, Neu-Isenburg, Germany). Densitometry was performed using ImageJ software (National Institutes of Health, http://rsb.info.nih.gov/ij/index.html).

3.5.6. Membrane stripping

For reuse of membranes, blots were stripped using ReBlot™ Plus Kit according to the manufacturers protocol (Chemicon, Temecula, CA, USA), blocked twice with 3 ml 5% milk for 10 minutes and reprobed with primary

antibodies against β-actin (clone C4, Chemicon, Chandlers Ford, UK). Expression of β-actin was used as control to assure equal sample loading in all analyses.

3.6. DNA and RNA chemistry

3.6.1. TRIzol® cell lysis

To obtain DNA, RNA and protein from cell culture samples, the respective number of cells was centrifuged at 12.000 x g and the supernatant was removed. The cells were lysed by repetitive pipetting using 1 ml TRIzol® (Invitrogen, Karlsruhe, Germany) per 1x 10^7 cells and the homogenized sample was incubated for 5 minutes at room temperature to permit complete dissociation of nucleoprotein complexes. 0.2 ml Chloroform per ml TRIzol® was added, the tube shaked vigorously by hand for 15 seconds and incubated for 3 minutes at room temperature. Subsequently, the mixture was centrifuged at 12.000 x g at 4°C for 10 minutes resulting in an aqueous phase containing RNA, a solid phase containing DNA, and an organic phase containing protein top down. All three phases were carefully isolated and stored at -80°C for later use.

3.6.2. RNA isolation

The aqueous phase from TRIzol® cell lysis contains RNA. 0.5 volumes of isopropanol (Carl Roth GmbH + Co. KG, Karlsruhe, Germany) per ml TRIzol® used for the initial homogenization was added and the mixture incubated at room temperature for 10 minutes. Following a centrifugation step at 12.000 x g, 4°C for 30 minutes, supernatant was removed and the RNA pellet was washed twice with 1 ml 80% Ethanol per ml TRIzol®. The sample was mixed by vortexing and centrifuged at 12.000 x g, 4°C for 5 minutes. The supernatant was removed and the RNA pellet dried. Finally, the RNA was dissolved in 50 µl RNase-free water and incubated for 5 minutes at 55°C to facilitate solving. RNA concentration and purity were measured as described below.

3.6.3. RNA cleanup

Depending on the purity of the RNA, the sample was applied to another RNA Cleanup step using the RNeasy Mini Kit (Quiagen, Hilden, Germany). The volume was adjusted to 100 µl using RNase-free water and 350 µl RLT buffer was added. 250 µl Ethanol was added and the sample was applied to an RNeasy column placed in a 2 ml collection tube. After centrifugation for 15

seconds at 12.000 x g, 500 µl RPE buffer was applied to the column and the tube centrifuged for 15 seconds at 12.000 x g to wash the sample. This step was repeated once. To remove residual ethanol, the column was centrifuged at 13.000 x g for 1 minute. For elution, the membrane was transferred to a new 1.5 ml Eppendorf tube, 50 µl H_2O was applied directly onto the membrane, incubated for 1 minute and centrifuged at 12.000 x g for 1 minute to elute RNA. RNA concentration was measured as described and RNA integrity, purity and size distribution were checked by agarose gel electrophoresis and ethidium bromide staining.

3.6.4. cDNA synthesis

For cDNA synthesis, 200-300 ng RNA per reaction was used to synthesize cDNA using the Superscript™ II Reverse Transcriptase Kit (Invitrogen, Karlsruhe, Germany). Per reaction (20 µl), 1 µl Oligo(dT)^{18} Primer (Fermentas, St. Leon-Rot, Germany), 1 µl 10 mM dNTP Mix (Fermentas, St. Leon-Rot, Germany) and 200-300 ng RNA were filled up with H_2O to a volume of 12 µl and incubated at 65°C for 5 minutes. Then, 4 µl of 5 x First strand Buffer (250 mM Tris-HCl, pH 8.3 at room temperature, 375 mM KCl and 15 mM MgCl2), 2 µl 0.1 M DTT and 1 µl H_2O were added. The mixture was incubated at 42°C for 2 minutes followed by addition of 1 µl Superscript II RT and another incubation period for 50 minutes at 42°C. The mixture was finally heated to 70°C for 15 minutes to assure degradation of reverse transcriptase and stored at -20°C upon further use.

3.6.5. DNA preparation

300 µl of 100% Ethanol per 1 ml TRIzol® initially used were added to the remaining interphase/organic phase. The sample was vortexed gently, incubated at room temperature for 2-3 minutes and centrifuged at 12.000 x g for 5 minutes. To obtain DNA, the protein containing supernatant was removed, and the DNA pellet was washed two times in 1 ml of 0.1 M sodium citrate solution. The sample was incubated at room temperature for 30 minutes, centrifuged at 12.000 x g for 5 minutes and washed once again. The resulting DNA pellet was resuspended in 1 ml 75% Ethanol, incubated for 10-20 minutes at room temperature and centrifuged at 12.000 x g for 5 minutes. Supernatant

was removed, the pellet was dried briefly, resuspended in 100 µl RNase free H_2O and concentration was measured as described below.

3.7. Gel electrophoresis

3.7.1. Determination of nucleic acid concentration

DNA and RNA (single and double stranded) have an absorbance maximum at a wave length of 260 nm. To measure concentration in a given sample, the OD (optic density) was determined at 260 nm in a photometer (Eppendorf, Hamburg, Germany). Background correction was performed using OD320. OD320 was subtracted from OD260 before multiplying the OD with the appropriate factor. As 1 OD corresponds to a defined amount of nucleic acid concentration (40 µg/ml (RNA), 50 µg/ml (dsDNA)) nucleic acid concentration was calculated using the following algorithm:

c(dsDNA) [µg/ ml] = OD260 x 50 x dilution

c(RNA) [µg/ ml] = OD260 x 40 x dilution

Contamination with protein was assessed by measuring OD at a wavelength of 280 nm. The OD260/OD280-quotient was taken as parameter for purity. In the case for DNA, A_{260}/A_{280} ≥1.8 and <2 indicates pure DNA, whereas A_{260}/A_{280} < 1.8 indicates contamination with proteins or aromatic substances and an A_{260}/A_{280} > 2 contamination with RNA. Pure RNA has an A_{260}/A_{280} ratio of 1.9-2.1.

Integrity of total RNA was assessed by agarose gel electrophoresis and ethidium bromide staining. Integrity was assumed if the respective ribosomal bands appeared as sharp bands on the stained gel. 28S ribosomal RNA bands (~5 kb) should be present with an intensity approximately twice that of the 18S ribosomal RNA (~2 kb). If ribosomal bands are not sharp but appear as a smear of smaller sized RNA, the RNA sample is likely to have suffered from major degradation during preparation.

3.7.2. Agarose gel

For a 2% Agarose gel, 150 ml 1x TBE buffer (for 1 liter of 1x TBE-Buffer 10.78 g Tris Base, 5.5 g Boric Acid and 0.93 g Na_2-EDTA were mixed and filled up to 1 liter with sterile H_2O) and 3 g Agarose (Sigma, Steinheim, Germany) were mixed and heated in a microwave for 4 minutes. After cooling to ~40°C, 8

µl Ethidium Bromide (Invitrogen, Karlsruhe, Germany) were added and the fluid was given in a PCR chamber to cool down.

3.7.3. DNA ladder

To determine the length of the particular PCR-product, 10 µl of each PCR-reaction mixed with 2 µl of 6x MassRuler Loading Dye Solution™ (Fermentas, St. Leon-Rot, Germany) were applied in parallel into the slots of the agarose gel. 10 µl of the particular Gene Fragment ladder (depending on the anticipated length of the PCR-product: 1 kb, 100 bp or 50 bp, each purchased from Fermentas, St. Leon-Rot, Germany) were applied into one slot of the Agarose gel to indicate the correct length of the PCR-product. After a runtime of 60-90 minutes at 100 V, bands were made visible at a UV-Transilluminator.

3.8. T-cell receptor specific PCR

TCR V-regions determine the antigen specifity of T cells. After V-D-J-recombination in the thymus, each T cell expresses a unique T-cell receptor corresponding to the recombinant genomic T-cell specific T-cell receptor. Human Vα and Vβ gene segments have been classified into 29 and 24 subfamilies, respectively, according to a sequence similarity >75%. Remaining nucleotide differences have been documented offering TCR V-subfamily specific PCR. Primers specific for the C β-chain and the respective TCR β-chain (see supplemental Table 2) were obtained from Sigma-Aldrich Chemie GmbH (Taufkirchen, Germany) as previously published (108).

100-200 ng RNA from each $CD8^+$ T-cell clone was reversely transcribed as described above. 20-100 ng of cDNA from each clone was used in a standardized PCR to detect the affiliation to one of the Vβ-subfamilies and to sequence the expressed T-cell receptor. 2.5 µl of 10x PCR Buffer (100 mM Trizma®-HCl, pH 8.3 and 500 mM KCl), 1.5 µl 25mM $MgCl_2$ (both purchased from Sigma, Steinheim, Germany), 2.5 µl of 2mM dNTP Mix (Fermentas, St. Leon-Rot, Germany) and 12.5 nmol of both forward and reverse primer were filled up with H_2O to a final volume of 24 µl. The mixture was layered by 1-2 drops of silicone oil (Sigma, Steinheim, Germany) and PCR performed on a TRIO-Thermoblock TB-1 (Biometra, Goettingen, Germany). The following thermal profile was used: The reaction was denaturated for 5 minutes at 95°C. Two units of Taq DNA Polymerase (Sigma, Steinheim, Germany) were added in a second step for 3 minutes at 68°C. 15-40 cycles of PCR were performed with each including a denaturating step for 30 seconds at 95°C, an annealing step for 30 seconds at 59°C and an elongation step for 1 minute at 72°C. After a final elongation step for 7 minutes at 72°C the reaction was applied to a 2% Agarose gel as described above and DNA was extracted for sequencing.

3.8.1. Agarose gel DNA extraction

For DNA-extraction from Agarose, the JETsorb Gel extraction kit (Genomed GmbH, Bad Oeynhausen, Germany) according to the manufacturer's protocol was used. DNA-bands were cut from the gel, its weight was determined and for each 100 mg gel slice, 300 µl buffer A1 and 10 µl

JETSORB suspension were added. To dissolve the agarose the assay was incubated at 50°C for 15 minutes, mixed every 3 minutes and then centrifuged for 30 seconds at 13.000 x g. The supernatant was removed and the resulting pellet washed twice with 300 µl high salt buffer A2. After the subsequent washing step that was repeated twice using 300 µl low salt buffer A2 the pellet was dried by air, resuspended with 30 µl H_2O and incubated 5 minutes at 50°C. It was centrifuged as before and the supernatant containing the DNA was used for further applications or stored at -80°C.

3.8.2. Sequencing

For sequencing the BigDye® Terminator v3.1 Cycle Sequencing Kit (Applied Biosystems, Warrington, UK) was used. 5-20 ng of DNA purified from Agarose was mixed with 8 µl of Terminator Ready Reaction Mix®, 3.2 pmol of the particular primer and filled up to 20 µl with deionized sterile H_2O. The mixture was applied to cycle sequencing, starting with an initial denaturation step at 96°C for 1 minute, followed by 25 cycles of 96°C for 10 seconds, 50°C for 5 seconds and 60°C for 4 minutes. Afterwards the reaction was stopped by cooling down to 4°C and sequenced at the Institute for Genetics of the University of Cologne.

3.8.3. Sequence analysis

Analysis of sequences was performed using the Chromas 2 software (Technelysium Pty Ltd, Tewantin QLD, Australia). Because of the infidelity of Taq polymerase, sequences that were likely to present polymerase chain reaction mistakes, defined as sequences differing from the replicate sequence and the IMGT database sequence (http://imgt.cines.fr/) by a single nucleotide, were excluded from analysis (111). To assure correct sequences especially for the CDR3 region which cannot be compared to an universal sequence (13), at least one replicate PCR and subsequent sequencing was performed for each clone to assure sequence validity.

3.9. Gene expression profiling

3.9.1. Microarray

The subset of genes that is expressed confers unique properties to each cell type. Gene expression is tightly regulated and allows a cell to dynamically respond to environmental stimuli. Manipulations in T-cell activation or inhibition result in a massive remodeling of the T-cell molecular signature through gene activation and silencing resulting in a T-cell phenotype associated with a distinct T-cell function. A microarray exploits the ability of a mRNA molecule to bind specifically to the DNA template from which it originated. On a microarray, thousands of DNA samples are arranged on a glass slide in a regular pattern. The amount of mRNA bound to each spot on the microarray can precisely be measured and generates a profile of gene expression in the respective cell.

3.9.1.1. Cell preparation and RNA purification

The molecules initially involved and the pathway terminally used to induce and maintain this T-cell phenotype, respectively, can perish in the genetic “background noise” measured short time after the induction preceding a phenotypic change due to cell remodeling. To assess the gene expression profile related to the observed phenotype, gene expression profiling was performed at day 7 of culture after stimulation with malignant melanoma cells. All cells were lyzed in TRIzol® as described above and stored at 1x 10^7 cells/ml at -80°C until further use. Total RNA was purified using the RNeasy MiniElute Cleanup Kit as described above. Integrity of RNA was assessed by agarose gel electrophoresis and RNA quantity measured by UV spectroscopy at 260 nm.

3.9.1.2. Two-cycle cDNA synthesis

Preparation of poly-A RNA spike-in controls

To monitor the target labeling process, a set of *in vitro* synthesized poly-A RNA controls (Eukaryotic Poly-A RNA Control Kit, Affymetrix, Santa Clara, CA, USA) from Bacillus subtilis genes lys, phe, thr and dap were used as exogenous positive controls. Each Affymetrix GeneChip probe array contains probe sets for these Bacillus subtilis genes lys, phe, thr and dap that are absent in eukaryotic samples. The concentrated Poly-A control stocks were diluted with

the Poly-A Control Dil Buffer and spiked into the RNA samples to achieve final concentrations (ratios of copy numbers) of 1:100,000 (lys), 1:50,000 (phe), 1:25,000 (thr) and 1:7,500 (dap). To prepare Poly-A RNA dilutions for 10 ng of total RNA, 2 µl of the Poly-A Control stock were diluted in serial dilutions 1:20 (first dilution), 1:50 (second dilution), 1:50 (third dilution) and 1:10 (fourth dilution) as recommended by Affymetrix. Subsequently, "T7-Oligo(dT) Primer/ Poly-A Control Mix" (Affymetrix, Santa Clara, CA, USA) was prepared by mixing 2 µl of 50 µM T7-Oligo(dT) Primer, 2 µl of the fourth dilution of Poly-A control stocks and 16 µl of RNase-free H_2O to a final volume of 20 µl. Controls were amplified and labeled together with the RNA samples and hybridization intensities of these controls were used to monitor the labeling process.

First-cycle, first-strand cDNA synthesis

For this step, the Two-Cycle cDNA Synthesis Kit (Affymetrix, Santa Clara, CA, USA) was used. First, the "First-Cycle, First-Strand Master Mix" was prepared by mixing 2 µl of 5x First-Strand Reaction Mix, 1 µl of 0.1 M DTT, 0.5 µl of RNase Inhibitor, 0.5 µl of 10 mM dNTP and 1 µl of SuperScript II to a final volume of 5 µl. Then, Total RNA sample was placed in a separate 0.5 ml PCR tube, 2 µl of the T7-Oligo/Poly-A Controls Mix were added and filled up to a final volume of 5 µl by RNase-free H_2O. The tube was flicked gently to mix, centrifuged briefly for 5 seconds to collect the solution at the bottom of the tube and incubated for 6 minutes at 70°C. The sample was subsequently cooled to 4°C for at least 2 minutes and again centrifuged briefly for 2 seconds to collect the sample at the bottom of the tube. 5 µl of First-Cycle, First-Strand Master Mix were added to each total RNA sample/ T7-Oligo(dT) Primer/Poly-A Controls Mix to a final volume of 10 µl. The tube was mixed by flicking the tube and centrifuged briefly for 5 seconds to collect the reaction at the bottom of the tube. The tubes were then immediately incubated at 42°C for 1 hour, heated for 10 minutes at 70°C to inactivate the reverse transcriptase and cooled at 4°C for at least 2 minutes. Finally, the tube was centrifuged briefly for 5 seconds to collect the reaction at the bottom of the tube.

First-cycle, second-strand cDNA synthesis

First, the "First-Cycle, Second-Strand Master Mix" was prepared by mixing 4.8 µl of RNase free H_2O, 4 µl of freshly diluted 17.5 mM $MgCl_2$, 0.4 µl of

10 mM dNTP, 0.6 µl of *E. coli* DNA Polymerase I and 0.2 µl of RNase H to a final volume of 10 µl. 10 µl of the First-Cycle, Second-Strand Master Mix were added to each sample from the First-Cycle, First-Strand reaction to a total volume of 20 µl, flicked gently a few times to mix the reaction and centrifuged briefly for 5 seconds to collect the reaction at the bottom of the tube. The reaction was the incubated for 2 hours at 16°C, 10 minutes at 75° and cooled down to 4°C for at least 2 minutes. After 2 minutes of incubation at 4°C, tubes were again centrifuged briefly for 5 seconds.

3.9.1.3. First-cycle, IVT amplification of cRNA

For this step, MEGAscript® T7 Kit (Ambion Inc., Austin, TX, USA) was used. 30 µl of "First-Cycle, IVT Master Mix" for each cDNA sample was prepared by mixing 5 µl of 10x reaction buffer, 5 µl of ATP solution, 5 µl of CTP solution, 5 µl of UTP solution, 5 µl of GTP solution and 5 µl of enzyme mix. The solution was mixed by gentle flicking and briefly centrifuged for 5 seconds to collect the solution at the bottom of the tube. Subsequently, 30 µl of First-Cycle, IVT Master Mix were transferred to each 20 µl of cDNA sample from the "First-Cycle, Second-Strand cDNA Synthesis" step for a final volume of 50 µl. The tube was gently flicked to mix the reaction, centrifuged briefly for 5 seconds to collect the reaction at the bottom of the tube and incubated for 16 hours at 37°C. After incubation for 16 hours at 37°C, the tube was centrifuged briefly for 5 seconds to again collect the *in vitro* transcription reaction at the bottom of the tube. The reaction was then applied to cRNA cleanup.

3.9.1.4. cRNA cleanup

For cRNA cleanup, the Sample Cleanup Module (Affymetrix, Santa Clara, CA, USA) was used. Before using for the first time, 20 ml of 100% Ethanol were added to the "ICT cRNA Wash Buffer" concentrate to obtain the usable working solution. First, 50 µl of RNase-free H_2O were added to the *in vitro* transcription reaction and mixed by vortexing for 3 seconds. 350 µl of IVT cRNA Binding Buffer were added to the sample and mixed by vortexing for 3 seconds. 250 µl of 100% ethanol were added and mixed by pipetting. The sample was then applied to the IVT cRNA Cleanup Spin Column sitting in a 2 ml collection tube. The system was centrifuged for 15 seconds at ≥8,000 x g and the flow-through as well as the collection tube were discarded. The spin column was transferred

into a new 2 ml collection tube. 500 µl of IVT cRNA Wash Buffer were pipetted onto the spin column, centrifuged for 15 seconds at ≥8,000 x g and the flow-through was discarded. 500 µl of 80% ethanol were pipetted on to the spin column, centrifuged for 15 seconds at ≥8,000 x g and the flow-through was discarded. The cap of the spin column was opened and the spin column was centrifuged for 5 minutes at maximum speed. Again the flow-through as well as the collection tube were discarded. The spin column was transferred into a new 1.5 ml Collection Tube and 13 µl of RNase-free H_2O were pipette directly onto the spin column membrane. The spin column was centrifuged for 1 minute at maximum speed for elution of an average of 11 µl volume. cRNA yield was determined by mixing 2 µl of the eluted cRNA with 68 µl of RNase-free H_2O. Absorbance was measured at 260 nm as described. If not used directly, samples were stored at -20°C for later use.

3.9.1.5. Second-cycle, cDNA synthesis

Second-cycle, first-strand cDNA synthesis

For Second-Cycle, cDNA Synthesis, the “Two-Cycle cDNA Synthesis Kit” (Affymetrix, Santa Clara, CA, USA) was used. First, a fresh solution of Random Primers was prepared by mixing 2 µl of 3 µg/µl Random Primers with 28 µl of RNase-free H_2O to a final volume of 30 µl. 2 µl of these 0.2 µg/µl diluted random primers were added to 600 ng of cRNA from the cRNA cleanup step. The mixture was then filled up with RNase-free H_2O to a final volume of 11 µl and incubated for 10 minutes at 70°C. The sample was cooled at 4°C for at least 2 minutes und centrifuged briefly for 5 seconds to collect the reaction at the bottom of the tube. In parallel, the “Second-Cycle, First-Strand Master Mix” was prepared by mixing 4 µl of 5x First-Strand Reaction Mix, 2 µl of 0.1 M DTT, 1 µl of RNase Inhibitor, 1 µl of 10 mM dNTP and 1 µl of SuperScript II to a final volume of 9 µl. 9 µl of the Second-Cycle, First-Strand Master Mix were transferred to each cRNA/random primer sample to a final volume of 20 µl. The reaction was mixed thoroughly by gently flicking the tube a few times, centrifuged briefly for 5 seconds to collect the reaction at the bottom of the tube, incubated for 1 hour at 42°C and cooled down to 4°C for at least 2 minutes. 1 µl of RNase H was added to each sample for a final volume of 21 µl, mixed thoroughly by gently flicking the tube a few times and centrifuged briefly for 5

seconds to collect the reaction at the bottom of the tube. The reaction was then incubated for 20 minutes at 37°C, heated for 5 minutes at 95°C and cooled down to 4°C for at least 2 minutes.

Second-cycle, second-strand cDNA synthesis

2 µl of 50 µM T7-Oligo(dT) Primer were mixed with 18 µl of RNase-free H_2O to a final concentration of 5 µM. 4 µl of diluted 5 µM T7-Oligo(dT) Primer were added to 20 µl of the Second-Cycle, First-Strand cDNA Synthesis Reaction to a final volume of 25 µl. The mixture was gently flicked a few times, centrifuged briefly for 5 seconds to collect the reaction at the bottom of the tube and incubated at 70°C for 6 minutes. The reaction was then cooled down to 4°C for at least 2 minutes, again centrifuged briefly for 5 seconds to collect the reaction at the bottom of the tube and mixed with 125 µl of “Second-Cycle, Second-Strand Master Mix” that had been prepared freshly by mixing 88 µl of RNase-free H_2O, 30 µl of 5x Second-Strand Reaction Mix, 3 µl of 10 mM dNTP and 4 µl of *E.coli* DNA Polymerase I. The total volume of 150 µl was mixed by gently flicking the tube a few times, centrifuged briefly for 5 seconds to collect the reaction at the bottom of the tube and incubated for 2 hours at 16°C. 2 µl of T4 DNA Polymerase were added to the sample for a final volume of 152 µl, the tube was again flicked gently, centrifuged briefly for 5 seconds, incubated at 4°C and again centrifuged briefly for 5 seconds to collect the reaction at the bottom of the tube.

3.9.1.6. Cleanup of double stranded cDNA

For cleanup of double stranded cDNA, the sample cleanup module (Affymetrix, Santa Clara, CA, USA) was used. Before using for the first time, 24 ml of 100% ethanol were added to the cDNA Wash Buffer Concentrate to obtain the cDNA Wash Buffer Working Solution. 600 µl of cDNA Binding Buffer were added to the final double-stranded cDNA synthesis preparation. The reaction was mixed by vortexing for 3 seconds. Color of the mixture was checked to be yellow indicating acidic pH. If the color of the mixture was orange or violet, 10 µl of 3 M sodium acetate pH 5.0 were added. 500 µl of the sample were then applied onto the cDNA Cleanup Spin Column sitting in a 2 ml collection tube and centrifuged for 1 minute at 8,000 x g. Flow-through and collection tube were discarded. The spin column was transferred into a new 2 ml collection tube. 750

µl cDNA wash buffer were pipetted onto the spin column, the spin column was centrifuged for 1 minute at 8,000 x g and flow-through was discarded. The cap of the spin column was opened and the spin column was centrifuged again for 5 minutes at 12,000 x g. Flow-through and collection tube were discarded. The spin columns were again transferred into a 1.5 ml collection tube, 14 µl of cDNA Elution Buffer were pipetted directly onto the spin column membrane, incubated for 1 minute at room temperature and centrifuged 1 minute at 12,000 x g for elution of an average of 12 µl volume.

3.9.1.7. Synthesis of biotin-labeled cRNA

For this step, “Gene Chip IVT Labeling Kit” (Affymetrix, Santa Clara, CA, USA) was used. After cleanup, template cDNA was mixed with 4 µl of 10x IVT Labeling Buffer, 12 µl of IVT Labeling NTP Mix, 4 µl of IVT Labeling Enzyme Mix and a variable amount of RNase-free H_2O to a final volume of 40 µl. In parallel, 1 µg of a 3’-Labeling Control was used in place of the template cDNA sample as a positive control for the ICT components in the kit. The mixture was mixed carefully and collected at the bottom of the tube by brief microcentrifugation. The mixture was then incubated at 37°C for 16 hours in a thermal cycler.

3.9.1.8. Clean up and quantification of biotin-labeled cRNA

For this step, “Sample Cleanup Module” (Affymetrix, Santa Clara, CA, USA) was used. 60 µl of RNase-free H_2O and 350 µl of IVT cRNA Bindung Buffer were added to labeled cRNA and mixed by vortexing for 3 seconds. 250 µl of 100% ethanol were added to the lysate and mixed well by pipetting. The sample was applied to the ICT cRNA Cleanup Spin Column sitting in a 2 ml collection tube, and centrifuged for 15 seconds at 10,000 x g. Flow-through and collection tube were discarded. The spin column was transferred into a new 2 ml collection tube. 500 µl of IVT cRNA Wash Buffer were pipetted onto the spin column, the spin column was centrifuged for 15 seconds at 10,000 x g and flow-through was discarded. 500 µl of 80% ethanol were pipetted onto the spin column, the spin column was centrifuged for 15 seconds at 10,000 x g and flow-through was discarded again. The cap of the spin column was opened and the spin column was centrifuged again for 5 minutes at 12,000 x g. Flow-through and collection tube were discarded. The spin columns were transferred into a

new 1.5 ml collection tube, 11 µl of RNase-free H_2O were pipetted directly onto the spin column membrane and centrifuged for 1 minute at 12,000 x g for elution. Again, 10 µl of RNase-free H_2O were pipetted directly onto the spin column membrane and eluted by centrifugation for 1 minute at 12,000 x g.

Spectrophotometric analysis was used to determine the cRNA yield. cRNA was diluted 1:100 fold and 1:200 fold and the absorbance at 260 nm and 280 nm was checked to determine sample concentration and purity. The convention was applied that 1 absorbance unit at 260 nm equals 40 µg/ml RNA. RNA was taken as pure if the A260/A280 ratio was close to 2.0 (ratios between 1.9 and 2.3 were accepted)

3.9.1.9. Fragmentation of cRNA for target preparation

cRNA with a minimal concentration of 0.6 µg/µl was used for fragmentation to maintain a small volume during the procedure and to minimize the amount of magnesium in the final hybridization cocktail. To 20 µg of cleaned cRNA, 2 µl of 5x Fragmentation Buffer for every 8 µl of cRNA plus H_2O were added. Fragmentation Buffer breaks down full length cRNA to 35-200 bases fragments by metal-induced hydrolysis. The mixture was incubated at 94°C for 35 minutes, put on ice and stored undiluted at -20°C until performing of hybridization.

3.9.1.10. Microarray hybridization and quality control

Gel electrophoresis was performed to estimate the yield and size distribution of labeled transcripts. 1 µg of cRNA was mixed with 2 x loading dye and 1x TE buffer to a final volume of 10 µl, heated to 65°C for 5 minutes and applied to Agarose gel electrophoresis and ethidium bromide staining. The standard fragmentation procedure produced a distribution of RNA fragment sizes from approximately 35 to 200 bases. Array hybridization were performed as described previously (71).

3.9.1.11. Microarray data analysis

For data assessment and normalization, dCHIP 1.3 was used. Selection of differentially expressed genes was performed using the following filter criteria: fold change ≥1.5, absolute difference in signal intensity between group means ≥50 and p-value ≤0.05. For visualization and gene ontology assessment,

GenMAPP® and MAPPfinder® were used. All heatmaps were visualized using MAYDAY. All microarray data can be accessed under GSE11188 at the National Center for Biotechnology Information (NCBI) Gene Expression Omnibus (GEO) repository (20).

3.9.2. Quantitative RT-PCR

To validate the Microarray gene expression data, gene expression was determined by quantitative RT-PCR for 14 genes. Primer pairs (see supplemental Table 1) were generated using the Primer3 software provided by the Massachussets Institute of Technology, Boston, USA (http://frodo.wi.mit.edu/). To check for specificity of the chosen primer pairs, each primer pair was blasted against the human genome using the NCBI blast software (http://blast.ncbi.nlm.nih.gov/Blast.cgi).

To 2 µl of LightCycler Fast Start DNA Master SYBR Green I (Roche Diagnostics, Penzberg, Germany), forward and reverse primer for the particular gene to be analyzed were added to a final concentration of 0.5 µM each. $MgCl_2$ was added to a final concentration of 4 mM. The solution was filled up to 18 µl with H_2O, given into a Roche capillary and 2 µl of the cDNA to be analyzed or H_2O as negative control were added. The capillary was centrifuged at 200 x g for 1 minute and run on a LightCycler 1.3 instrument (Roche Diagnostics, Penzberg, Germany).

The following thermal profile was used: The reaction was denaturated for 10 minutes at 95°C. 15-40 cycles (depending on gene expression) of amplification were performed with a denaturating step at 95°C for 10 seconds, an annealing step at 60°C for 30 seconds and an elongation step for one second at 72°C (temperature transition rates were 20°C/s between each step). A melting curve was generated for each gene by data acquisition starting at 65°C with a temperature transition rate of 0.1°C/s ending at 95°C. After the run had finished, the reaction was applied to a 2% agarose gel as described above and product size was compared to a standardized ladder. All products run on the predicted height. For each gene 5 replicate reactions were performed. All data were normalized to expression of the housekeeping gene GAPDH.

3.10. Taqman quantitative RT-PCR

To assess the frequency of defined CD8$^+$ T-cell clones *in vivo,* primers specific for the corresponding genomic CDR3 region were designed. The CDR3-sequence had prior been defined by sequencing the TCR-genomic region of *in vitro* analyzed CD8$^+$ T-cell clones. *In vivo* detection of a tumor-reactive and a non-tumor-reactive CD8$^+$ T-cell clone from patient NW1789 was feasible with Taqman quantitative PCR using the Universal ProbeLibrary Assay (Roche Diagnostics, Penzberg, Germany). For patients NW1045 and NW2608 the assessment of CD8$^+$ T-cell clones was technically unfeasible as no primer specific for the respective CDR3 regions could be designed.

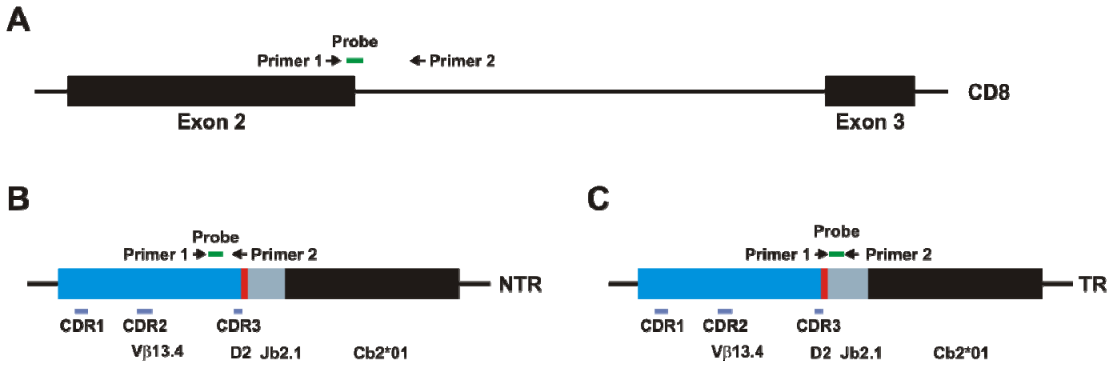

Figure 3 | Strategy to detect CD8$^+$ T-cell clones using Taqman quantitative RT-PCR

(A) Design of primers for the specific amplification of genomic CD8 DNA as well as **(B)** genomic TCR DNA derived from the non-tumor-reactive W10-NTR and **(C)** the tumor-reactive W26-TR CD8$^+$ T-cell clone from patient NW1789. Primers were chosen to span exon-intron boundaries in order to assure PCR specific for genomic DNA. CDR, complementarity-determining region.

Genomic DNA was isolated from purified total CD8$^+$ T cells from blood samples of patient NW1789 before and in the course of adoptive immunotherapy. For absolute quantification of non-tumor-reactive (*CDR3 W10-NTR*) and tumor-reactive (*CDR3 W26-TR*) CD8$^+$ T-cell clones (Figures 3b and 3c, respectively), the results were normalized to CD8 DNA (Figure 3a). A known CDR3 sequence of a CD8$^+$ T-cell clone from a HLA-A2 positive patient recognizing a mycobacterial heat-shock-protein 60-derived peptide (*CDR3 M-HSP60*) was used as negative control (115). The following primers (Sigma-Aldrich Chemie GmbH, Taufkirchen, Germany) and human probe libraries (Roche Diagnostics, Mannheim, Germany) were used: *CDR3 W10-NTR* forward: 5'-CCG CTC AGG CTG CTG TC-3', *CDR3 W10-NTR* reverse: 5'-CGG CCC GAA GTA CTG CTC-3', Universal Probe Library probe: #32 (CTG CTC

CC); *CDR3 W26-TR* forward: 5'-CTG TGC CAG CAG TTA CTT GG-3', *CDR3 W26-TR* reverse: 5'-CGG TCA GCC TAG AGC CTT C-3', Universal Probe Library probe: #24 (CAG CTC CC); *CD8* forward: 5'-CAT GTA CTT CAG CCA CTT CGT G-3', *CD8* reverse: 5'-TTG AGG TGA ACC CCA AGC-3', Universal Probe Library probe: #4 (CTT CCT GC); *CDR3 M-HSP60* forward: 5'-CGT CTC CAC TCT GAC GAT CC-3', *CDR3 M-HSP60* reverse: 5'-TCA TTA CCC TGC CGT TGA CT-3', Universal Probe Library probe: #18 (TCC TGC TG).

Real-time PCR was performed as previously described (29). To 4 µl of LightCycler® TaqMan Master (Roche Diagnostics, Penzberg, Germany), forward and reverse primer CDR3 W10-NTR or CDR3 W26-TR for the respective $CD8^+$ T-cell clones and CD8 or CDR3 M-HSP60 were added to a final concentration of 0.2 µM each. 0,2 µl of UPL probe #4 (detection of CD8), UPL probe #18 (detection of CDR3 M-HSP60), UPL probe #24 (detection of CDR3 W26-TR) or UPL probe #32 (detection of CDR3 W10-NTR) were added and the solution was filled up to 15 µl with H_2O and pipetted into a Roche glass capillary. 5 µl of DNA prepared from blood samples from patient NW1789 to be analyzed or H_2O as negative control were added. The capillary was centrifuged at 200 x g for 1 minute and run on a LightCycler 1.3 instrument.

The following thermal profile was used: 60 cycles of amplification were performed with a denaturating step at 95°C for 10 seconds, an annealing step at 60°C for 30 seconds and an elongation step for one second at 72°C (temperature transition rates were 20°C/s between each step). Data was acquired at the end of amplification. After the run had finished, the reaction was applied to a 2% Agarose gel as described above and product size was compared to a standardized ladder. All products run on the predicted height.

3.11. Statistical analysis

All statistical analysis was performed using SPSS 15.0 and SigmaPlot 2001 software (both from SPSS GmbH Software, Munich, Germany). P values were determined by two-tailed t-test assuming equal variance. Significance of differences between groups was considered if $p < 0.05$. Overall patients survival was defined was the interval between diagnosis and death. Data were censored at the last follow-up for patients who were alive at the time of the analysis of this work. Median survival times were visualized using Kaplan-Meier-Analysis. Differences in survival function were assessed using the log-rank test.

4. Results

4.1. Vaccination generates non-tumor-reactive but peptide-specific CD8$^+$ T cells

4.1.1. Distinct lytic activity of tumor-reactive and non-tumor-reactive CD8$^+$ T-cell clones

In patients NW1045, NW1789 and NW2608, two distinct types of NY-ESO-1 p157-165 specific CD8$^+$ T-cell clones were detectable after peptide vaccination (Figure 4): (1) tumor-reactive T-cell clones that lysed both NY-ESO-1 peptide-pulsed T2 cells as well as the NY-ESO-1 expressing malignant melanoma cell line SK-Mel-37 (clones W26-TR, F40-TR and B4-TR) and (2) non-tumor-reactive CD8$^+$ T-cell clones that showed lytic reactivity towards NY-ESO-1 peptide-pulsed T2 cells but were unable to kill SK-Mel-37 or autologous NY-ESO-1$^+$ malignant melanoma cell lines (clones W10-NTR, F19-NTR and B21-NTR).

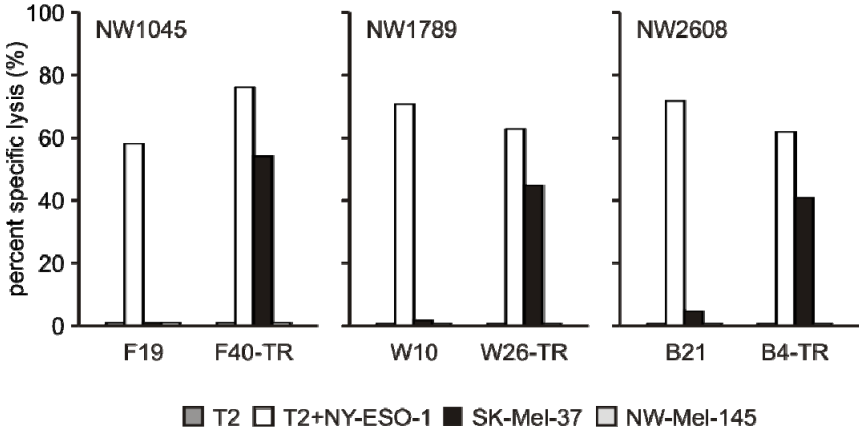

Figure 4 | Tumor-reactive and non-tumor-reactive CD8$^+$ T-cell clones show distinct lytic activity

CD8$^+$ T-cell clones from patients NW 1045 (left, F19 and F40-TR), NW1789 (middle, W10, W26-TR), and NW2608 (right, B21, B4-TR) were cocultured with NY-ESO-1 p157-165 peptide-pulsed T2 cells (white bars), the NY-ESO-1 expressing melanoma cell line SK-MEL-37 (black bars), unpulsed T2 cells (dark grey bars) and NY-ESO-1 negative melanoma cell line NW-Mel-145 (light grey bars). Lytic activity was assessed by ^{51}Cr-release assay. Mean of at least two independent experiments with at least duplicates for each condition is shown. TR = tumor-reactive CD8$^+$ T-cell clone.

4.1.2. No lytic activity of non-tumor-reactive CD8$^+$ T-cell clones towards irrelevant p159-167 NY-ESO-1 peptide

To demonstrate that non-tumor-reactive CD8$^+$ T-cell clones are not simply recognizing autologous HLA-A2 (or potential differences in minor suballele expression) on the surface of peptide-loaded T2 cells, which express more HLA than the non-peptide-pulsed T2 cells, but are truly NY-ESO-1 specific, additional experiments were performed comparing lysis of T2 pulsed with p157-165 NY-ESO-1/HLA-A2 binding peptide in comparison to the irrelevant NY-ESO-1/HLA-A2 binding peptide L9L (p159-167).

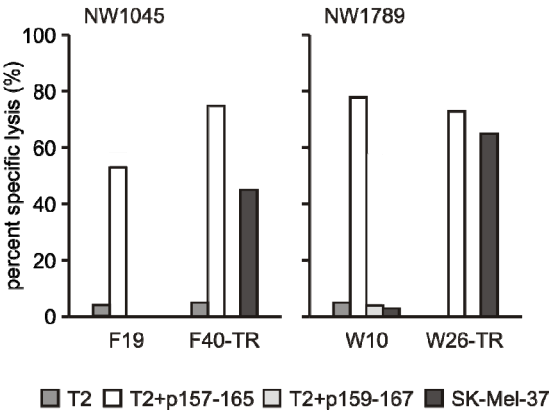

Figure 5 | Reactivity of tumor-reactive and non-tumor-reactive CD8$^+$ T-cell clones against irrelevant p159-167 NY-ESO-1 peptide

CD8$^+$ T-cell clones from patient NW 1045 (left, F19 and F40-TR) and NW1789 (middle, W10, W26-TR), were cocultured with unpulsed T2 cells (dark grey bars), NY-ESO-1 p157-165 peptide-pulsed T2 cells (white bars), p159-167 peptide-pulsed T2 cells (light grey bars), and NY-ESO-1 expressing melanoma cell line SK-MEL-37 (black bars). Lytic activity was assessed by ^{51}Cr-release assay. CD8$^+$ T-cell clones from patient NW2608 (B21, B4-TR) were not available for this experiment. TR = tumor-reactive CD8$^+$ T-cell clone.

As can be seen in Figure 5, tumor-reactive as well as non-tumor-reactive CD8$^+$ T-cell clones from patients NW1045 and NW1789 show only minimal lysis of unpulsed T2 cells. All CD8$^+$ T-cell clones show no lysis of T2 cells pulsed with an irrelevant p159-167 peptide from NY-ESO-1. All CD8$^+$ T-cell clones show clear reactivity towards T2 cells pulsed with p157-165 NY-ESO-1 peptide. As expected, only tumor-reactive CD8$^+$ T-cell clones show lysis against NY-ESO-1 expressing malignant melanoma cell line SK-MEL-37. These results clearly demonstrate that the non-tumor-reactive CD8$^+$ T-cell clones are specific for the p157-165 NY-ESO-1 peptide as they do not recognize T2 cells pulsed with an irrelevant peptide from NY-ESO-1.

4.1.3. Lytic activity of non-tumor-reactive CD8$^+$ T-cell clones towards highly purified p157-165 NY-ESO-1 peptide

It has been postulated that both tumor-reactive and non-tumor-reactive CD8$^+$ T-cell clones recognize the same peptide, namely the NY-ESO-1 157-165 peptide. However, a possible trivial explanation of the results in Figure 5 is that the tumor-reactive CD8$^+$ T-cell clones recognize SLLMWITQC (the NY-ESO-1 157-165 peptide), whereas the non-tumor-reactive CD8$^+$ T-cell clones recognize a contaminant in the peptide batch used to pulse T2 cells. That would explain, why non-tumor-reactive CD8$^+$ T-cell clones do not recognize the tumor cells and are not labeled by NY-ESO-1 157-165 peptide-tetramers (as demonstrated below in Figure 8), because one tetramer would very unlikely contain several contaminant peptides. To exclude this possibility and to demonstrate that indeed both tumor-reactive and non-tumor-reactive CD8$^+$ T-cell clones recognize SLLMWITQC (the NY-ESO-1 157-165 peptide), the NY-ESO-1 peptide batch was purified by HPLC. This fraction was then again used for stimulation of CD8$^+$ T-cell clones.

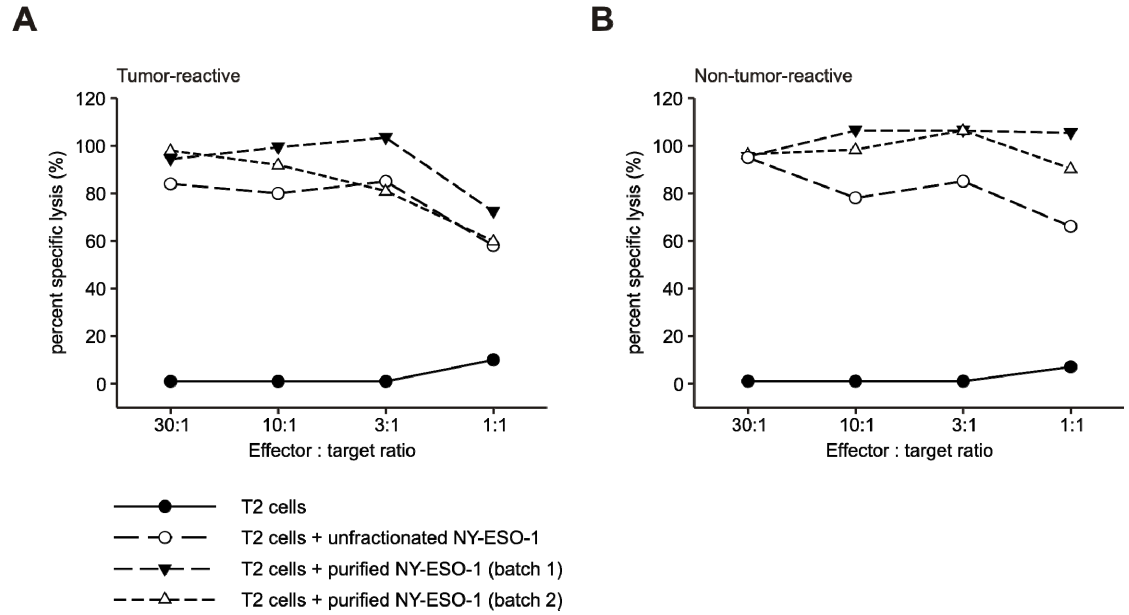

Figure 6 | Reactivity of tumor-reactive and non-tumor-reactive CD8$^+$ T-cell clones against highly purified SLLMWITQC (p157-165) NY-ESO-1 peptide

(A) Tumor-reactive and **(B)** non-tumor-reactive CD8$^+$ T-cell clones were cocultured with NY-ESO-1 peptide-pulsed T2 cells. To functionally assess, if tumor-reactive and non-tumor-reactive CD8$^+$ T-cell clones recognize the same peptide, their ability to lyse T2 cells pulsed with different fractions of NY-ESO-1 p157-165 peptide was tested in ^{51}Cr-release assays. ^{51}Cr-release assays at different effector:target ratios were performed with either unpulsed T2 cells (●), T2 cells pulsed with the unfractionated NY-ESO-1 peptide (○), T2 cells pulsed with NY-ESO-1 peptide (batch 1)(▼), and T2 cells pulsed with NY-ESO-1 peptide (batch2)(△).

As demonstrated in Figure 6a, tumor-reactive $CD8^+$ T-cell clones lyse nearly no unpulsed T2 cells, whereas high lysis of peptide pulsed T2 cells is observed with purified NY-ESO-1 as expected. Non-tumor-reactive $CD8^+$ T-cell clones show strong lysis of T2 cells pulsed with purified NY-ESO-1, with diminished cytotoxicity against T2 cells pulsed with unfractionated NY-ESO-1 (Figure 6b). Consequently, both tumor-reactive and non-tumor-reactive $CD8^+$ T-cell clones recognize the purified NY-ESO-1 157-165 peptide, and not a concomitant within the peptide batch.

4.1.4. Tumor-reactive and non-tumor-reactive $CD8^+$ T-cell clones differ in their functional avidity

As can be seen in Figure 7, tumor-reactive as well as non-tumor-reactive $CD8^+$ T-cell clones are capable of lysing NY-ESO-1 pulsed T2 cells. T-cell mediated target cell lysis depends on the interaction of T-cell receptor with its counterpart on the target cells, the peptide-loaded MHC I complex. As outlined above, this T-cell receptor-peptide-MHC-interaction is characterized by the summation of TCR-pMHC-affinity and serial triggering of T-cell receptor by peptide-MHC-complexes (308, 320, 333). A strong TCR-pMHC-interaction enables a T cell to lyse target cells even at low concentrations of NY-ESO-1-MHC-complexes, as affinity and serial triggering are high. On the other hand, low concentrations of antigen and a weak TCR-pMHC-interaction are insufficient for target cell lysis, whereas increase in antigen concentration might at least partially restore this failure. We thus assessed the functional avidity of tumor-reactive and non-tumor-reactive $CD8^+$ T-cell clones with increasing amounts of NY-ESO-1 peptide.

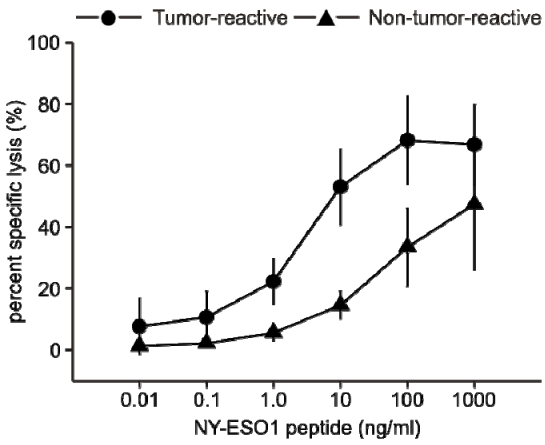

Figure 7 | Tumor-reactive and non-tumor-reactive $CD8^+$ T-cell clones differ in their functional avidity

Tumor-reactive (●) and non-tumor-reactive (▲) $CD8^+$ T-cell clones were assessed for their ability to lyse T2 cells pulsed with different concentrations of NY-ESO-1 peptide p157-165 ranging from 0.01 ng/ml to 1 µg/ml in ^{51}Cr-release assays at a effector:target ratio of 10:1. Functional avidity was tested for >8 individual clones each. Values represent percent of specific lysis.

A strong TCR-pMHC-interaction - as can be seen for the interaction of T-cell receptors of tumor-reactive T cells with NY-ESO-1 loaded MHC on the target cell - enables the T cell to lyse target cells even at low concentrations of NY-ESO-1-MHC-complexes. At a concentration of only 0.01 ng/ml NY-ESO-1 peptide, tumor-reactive $CD8^+$ T-cell clones already show 15% specific lysis with up to 70% lysis at a concentration of 100 ng/ml. In contrast, non-tumor-reactive $CD8^+$ T-cell clones show a weak TCR-pMHC-interaction with no observed target cell lysis at low concentrations of NY-ESO-1 peptide (e.g. 0.01 ng/ml) and only suboptimal target cell lysis at high concentrations (e.g. 100 ng/ml) of antigen. Using this peptide titration assay, it can be shown that tumor-reactive $CD8^+$ T-cell clones exhibit a higher functional avidity for NY-ESO-1 p157-165 peptide than non-tumor-reactive $CD8^+$ T-cell clones.

4.1.5. Tumor-reactive and non-tumor-reactive $CD8^+$ T-cell clones differ in NY-ESO-1-tetramer binding

In peptide titration assays, tumor-reactive $CD8^+$ T-cell clones exhibited a significantly higher avidity for the NY-ESO-1 p157-165 peptide than non-tumor-reactive $CD8^+$ T-cell clones (152). To confirm these findings in $CD8^+$ T-cell clones generated from patients NW1045, NW1789 and NW2608, tetramer staining with NY-ESO-1 p157-165 peptide bound to PE-labeled HLA-A*0201-Tetramer was performed.

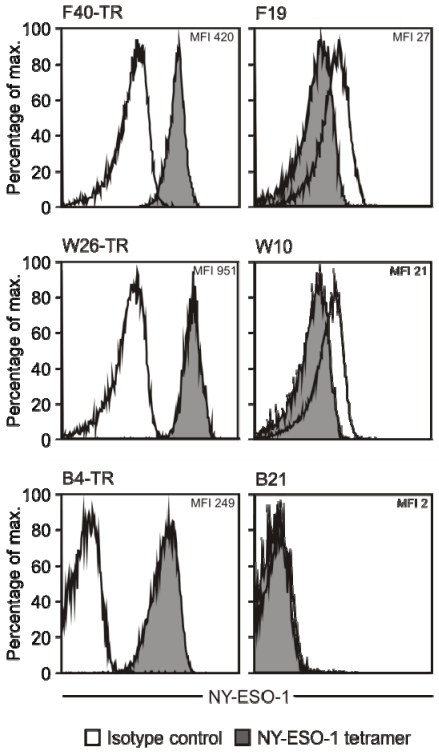

Figure 8 | HLA-A2 NY-ESO-1 p157-165 tetramer staining

Flow cytometric analysis of tetramer binding of tumor-reactive and non-tumor-reactive T-cell clones.

Histogram plots depict staining with isotype control (bold black lines) and staining with NY-ESO-1 loaded HLA-A2-tetramer (gray filled plots). Y-axis represents cell counts referring to 100%, X-axis represents fluorescent activity. Mean fluorescence intensity (MFI) values are presented in the upper right corner. All experiments were done at least four times.

Figure 8 shows that tumor-reactive $CD8^+$ T-cell clones F40-TR, W26-TR and B4-TR bind the pMHC with high avidity. Non-tumor-reactive $CD8^+$ T-cell clones show no staining with NY-ESO-1 p157-165 tetramers in line with similar observations made for low affinity TCR-pMHC interactions (355) and in experiments using agonistic, weakly agonistic and antagonistic pMHC-tetramers illustrating that a decrease in TCR-pMHC avidity aggravates T-cell labeling with peptide-loaded-tetramer and determines high peptide-concentrations for staining (134).

4.2. Tumor-reactive and non-tumor-reactive $CD8^+$ T-cell clones are from different origin

4.2.1. V-D-J recombination

The T-cell receptor plays the central role in the recognition of peptide antigens presented by MHC molecules. The T-cell receptor consists of two subunits, the T-cell receptor α-chain and the T-cell receptor β-chain. Both are comprised of a variable (V), a diversity (D), a joining (J) and a constant (C) amino acidic region. The juxtaposition of these segments called V-D-J recombination takes place in the thymus (240). The juxtaposition of these segments, the lack of precision during the V-D-J-gene rearrangement and the removal and/or addition of non-template encoded nucleotides at the V-D-J-junctions create a unique T-cell receptor β-chain (40, 240) with three loci of hypervariability known as complementary-determining regions (CDR). V-D-J-recombination thus results in a T-cell receptor β-chain unique for the particular T cell after exit from the thymus. By sequencing the TCR β-chain, clonality of tumor-reactive and non-tumor-reactive $CD8^+$ T-cell clones can be analyzed.

As can be seen in Table 4, for patient NW1789 identical Vβ, joining and constant domains in tumor-reactive and non-tumor-reactive $CD8^+$ T-cell clones are found (W10 and W26-TR, both Vβ-13.4-chain and Jβ-2.1-chain), whereas in patient NW2608, both $CD8^+$ T-cell clones show different Vβ, joining and constant domains (B21: Vβ-8.1-chain and Jβ-1.1-chain, and B4-TR: Vβ-4.1-chain and Jβ-2.1-chain). In patient NW1045, both $CD8^+$ T-cell clones show identical Vβ (both Vβ-8.1-chain) and constant domains, but differed in the joining-chain used (F19: Jβ-1.1-chain, F40-TR: Jβ-2.1-chain). This clearly

indicates that non-tumor-reactive and tumor-reactive T cells clones are from different origin as they are not generated from the same progenitor cell during vaccination.

4.2.2. Complementary-determining region 1/2/3 (CDR1/ CDR2/CDR3)

MHC restriction is provided by engagement of MHC helices by CDR1 and CDR2 loops of the T-cell receptor. This conclusion can be drawn from crystallographic studies where the CDR2 loops of Vα and Vβ are positioned almost exclusively over the MHC helices and show only marginal contact with the peptide. The CDR1 loop mainly interacts with the MHC-molecule although residues of CDR1α and CDR1β might interact with the N-Terminus and the C-Terminus of the peptide, respectively (105, 106). They are therefore thought to be mainly involved in the binding to MHC. In this model, CDR1 and CDR2 contribute approximately 2/3 of the binding free energy of the TCR-pMHC-interaction (174, 200). In a phage display based approach, CDR2-only mutations in native T-cell receptors specific for the NY-ESO-1 p157-165 peptide displayed by HLA-A*0201, as in the context of our experiments, have been shown to have an influence on affinity.

CDR3 is the hypervariable region of each TCR thought to be the antigen recognizing region and is accountable for a large part in the physical and energetic interaction of the particular TCR with the peptide presented by the MHC (106, 174). In the setting of NY-ESO-1, two residues, Methionine-160 and Tryptophan-161, located in the middle region of the NY-ESO-1 157-165 peptide, are critical for recognition by most of T-cell clonotypes examined (51, 72) and amino acid substitutions in the T-cell receptor CDR3 recognizing these residues strongly alter the antigen-specific T-cell response (262). The distribution of CDR3 lengths follows a Gaussian distribution (116). As the CDR3 region determines the binding avidity of the TCR-pMHC complex (32), the sequence of the CDR3 region was determined according to the IMGT database (178).

As outlined above, the current model of V-D-J-recombination predicts that the sequence of a T-cell receptor β-chain is unique to the $CD8^+$ T-cell clone analyzed. Consequently, sequence comparison of the specific T-cell receptor β-chains enables determination of the relationship of non-tumor-reactive and tumor-reactive $CD8^+$ T-cell clones. To exclude that non-tumor-reactive and

tumor-reactive CD8$^+$ T-cell clones were of the same origin, CDR3 sequences of non-tumor-reactive CD8$^+$ T-cell clones were compared to those of tumor-reactive CD8$^+$ T-cell clones.

Clone	Vβ	CDR1	CDR2	CDR3	Jβ	Cβ
F19	8.1	n.d.	FNNNVP	FSGGATEA	1.1	2
F40-TR	8.1	n.d.	FNNNVP	SLGSNEQ	2.1	2
W10	13.4	MNHEY	SVGAGI	SSGGPSEQ	2.1	2
W26-TR	13.4	MNHNY	SVGAGI	SYLFANTGEL	2.1	2
B21	8.1	n.d.	FNNNVP	NKPGQENTGA	1.1	1
B4-TR	4.1	n.d.	n.d.	GIPVW	2.1	2

Table 4: TCR β-chain usage and CDR sequences of CD8$^+$ T-cell clones

T-cell receptor sequences of the respective CD8$^+$ T-cell clones were amplified by PCR using Cβ- and Vβ-chain-specific primer pairs. The PCR-product was applied onto an agarose gel and purified as described. Sequencing was carried out at the Institute for Genetics of the University of Cologne. Analysis of sequences was performed using the Chromas 2 software. Sequences were compared with TCR sequences in the IMGT database. Vβ and Jβ were attributed according to the nomenclature available at http://imgt.cines.fr. Experiments were carried out at least twice. A, alanine; E, glutamic acid; F, phenylalanine; G, glycine; H, histidine; I, isoleucine; K, lysine; L, leucine; M, methionine; N, asparagine; P, proline; Q, glutamine; S, Serine; T, threonine; V, valine; W, tryptophan; Y, tyrosine; n.d., not determined.

As can be seen in Table 4, the particular tumor-reactive and non-tumor-reactive CD8$^+$ T-cell clones differ considerably in their CDR3 base sequence stressing that these T cells are from different origin.

4.3. Different surface molecule expression of CD8$^+$ T-cell clones

4.3.1. CD3 and α/β T-cell receptor expression

In T cells, the TCR/CD3 complex is constitutively expressed on the cell surface, internalized and recycled. Triggering of TCR/CD3 complexes by cognate pMHC is rapidly followed by downregulation from the cell surface by internalization and degradation in the lysosomal compartement self-limitating the TCR-pMHC interaction (322, 350). As can be seen in Figure 9, the time course of TCR downregulation independently from peptide concentration is characterized by an exponential model and reaches a plateau after ~5 hours (41, 320).

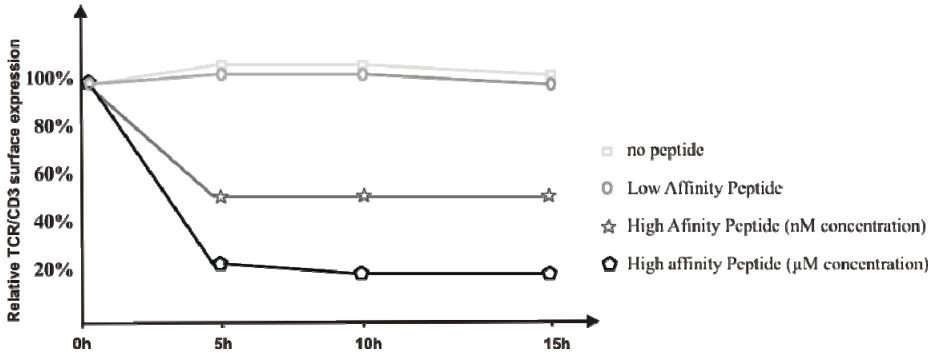

Figure 9 | Time course of T-cell receptor-downregulation after T-cell stimulation

Stimulation with antigen leads to rapid downregulation of the TCR-CD3-complex on the cell surface of naïve CD8$^+$ T-cells leading to consecutive unresponsiveness of the respective T cell towards stimulus. Unstimulated T cells and T cells stimulated with low affinity peptides both show no or only minimal downregulation of TCR-CD3-complex on the cell surface. In contrast, stimulation with high affinity peptides result in an exponential decrease of T-cell receptor on the cell surface with consecutive decreased T-cell function. Time course generated by use of data from Cai et al. (41) and Valitutti et al. (320).

Measuring TCR/CD3 complex after stimulation with antigen on the cell surface of tumor-reactive and non-tumor-reactive CD8$^+$ T-cell clones therefore (a) allows estimation of the quality/affinity of the T-cell receptor signal preceding the time of measurement, as strong affinity should have led to a more potent downregulation of the T-cell receptor/CD3-complex (41), (b) it enables to answer the question whether T-cell unresponsiveness of non-tumor-reactive CD8$^+$ T-cell clones might be caused by TCR/CD3 complex downregulation resulting in an insufficient antigenic stimulation by malignant melanoma cells (321), and (c) concordantly might show that T-cell intrinsic upregulation of

TCR/CD3 complex on the T-cell surface has occurred to enhance T-cell responsiveness after preceding insufficient signaling (242). To furthermore exclude that impaired effector function was due to internalization of the TCR-CD3-complex after repeated antigen stimulation, extracellular TCR α/β-chain expression was assessed.

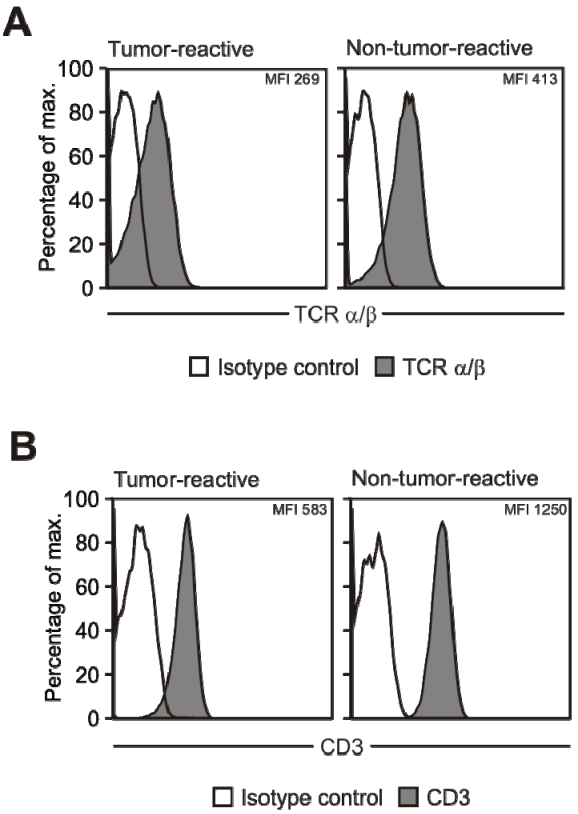

Figure 10 | Extracellular TCR α/β and CD3 protein expression

(A) Representative flow-cytometric analysis of TCR α/β expression (grey fill) on the T-cell surface of tumor-reactive (left) and non-tumor-reactive (right) T-cell clones. All experiments were performed at least four times. Isotype control (bold black lines).

(B) Representative flow-cytometric analysis of CD3 protein expression (grey fill) on the T-cell surface of tumor-reactive (left) and non-tumor-reactive (right) T-cell clones. All experiments were performed at least four times. Isotype control (bold black lines).

Interestingly, TCR α/β expression (Figure 10a) on the cell surface was higher in non-tumor-reactive $CD8^+$ T-cell clones (MFI 413) than in tumor-reactive $CD8^+$ T-cell clones (MFI 269). As can be seen in Figure 10b, also expression of the CD3 protein is enhanced on the surface of non-tumor-reactive $CD8^+$ T-cell clones (MFI 1250) compared to that of tumor-reactive $CD8^+$ T-cell clones (MFI 583), suggesting that neither strong affinity has led to downregulation of the T-cell receptor/CD3-complex nor that T-cell unresponsiveness is caused by TCR/CD3 complex downregulation but that T-cell intrinsic upregulation of TCR/CD3 complex has occurred due to preceding insufficient signaling

4.4. Different surface molecule expression of $CD8^+$ T-cell clones

4.4.1. $CD62L^-CCR7^-$ expression reveals central memory $CD8^+$ T-cell phenotype

Differentiation from a naïve towards an effector-memory $CD8^+$ T-cell phenotype is required for effective immune response against malignant melanoma. On the basis of the surface expression of activation molecules (CD45RO, CD45RA) and lymph node homing receptors (CD62L, CCR7), different stages of T lymphocyte maturation can be defined. Naïve $CD8^+$ T cells (T_N) express both CD45RA and CCR7 ($CD8^+CD45RA^+CCR7^+$ T cells). Additional phenotypic analysis has identified at least three subsets of antigen-experienced $CD45RA^-$ $CD8^+$ T cells termed central memory T cells (T_{CM}), effector memory T cells (T_{EM}) and effector T cells (T_E).

Central memory $CD8^+$ T_{CM} cells lack CD45RA expression, express lymph node homing markers such as CCR7 and CD62L, preferentially reside in secondary lymphoid organs, and can be found in the blood and in the spleen ($CD8^+CD45RA^-CD62L^+CCR7^+$ T cells). Effector memory T_{EM} cells lack CD45RA, are devoid of lymph node homing markers and preferentially localize into peripheral tissue, but as well can be found in the blood and in the spleen ($CD8^+CD45RA^-CD62L^-CCR7^-$T cells). Terminally differentiated cytotoxic effector T_E cells regain expression of CD45RA ($CD8^+CD45RA^+CCR7^-$ T cells) (47, 272, 316).

To exclude that incomplete or terminal differentiation accounted for the cytotoxic impairment of non-tumor-reactive $CD8^+$ T-cell clones as compared to tumor-reactive $CD8^+$ T-cell clones, surface expression of differentiation markers CD45RA, CCR7 and CD62L was assessed.

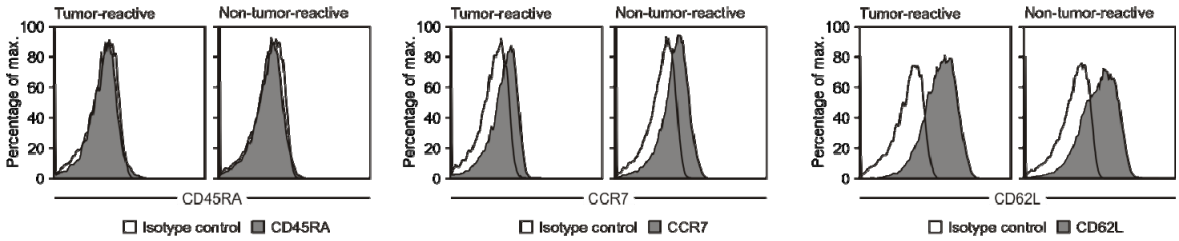

Figure 11 | Expression of differentiation markers

(A) Representative flow-cytometric analysis of CD45RA protein expression (grey fill) on the T-cell surface of tumor-reactive (left) and non-tumor-reactive (right) T-cell clones. All experiments were performed at least four times. Isotype control (bold black lines).

(B) Representative flow-cytometric analysis of CCR7 protein expression (grey fill) on the T-cell surface of tumor-reactive (left) and non-tumor-reactive (right) T-cell clones. All experiments were performed at least four times. Isotype control (bold black lines).

(C) Representative flow-cytometric analysis of CD62L protein expression (grey fill) on the T-cell surface of tumor-reactive (left) and non-tumor-reactive (right) T-cell clones. All experiments were performed at least four times. Isotype control (bold black lines).

As can be seen in Figure 11, both non-tumor-reactive as well as tumor-reactive $CD8^+$ T-cell clones do not show surface expression of CD45RA, arguing against a naïve T-cell phenotype but as expected indicating antigen experience. Both T-cell subsets belong to the T_{CM}-cell compartment as displayed by surface expression of both lymph node homing markers CCR7 and CD62L.

4.4.2. CD7 expression indicates advanced differentiation of tumor-reactive CD8$^+$ T-cell clones

As expected, both tumor-reactive and non-tumor-reactive CD8$^+$ T-cell clones show a central memory phenotype, reflecting suboptimal stimulation nevertheless sufficient for partial activation and differentiation into central memory T cells. Another level of complexity regarding T-cell effector function in the memory T-cell subset has been introduced by expression of CD7. *Aandahl and colleagues* identified T-cell subsets by means of their CD7 expression with low or absent expression of CD7 being associated with full and high CD7 expression inversely associated with insufficient effector function (1). Consequently, CD7 expression was assessed for tumor-reactive as well as non-tumor-reactive CD8$^+$ T-cell clones.

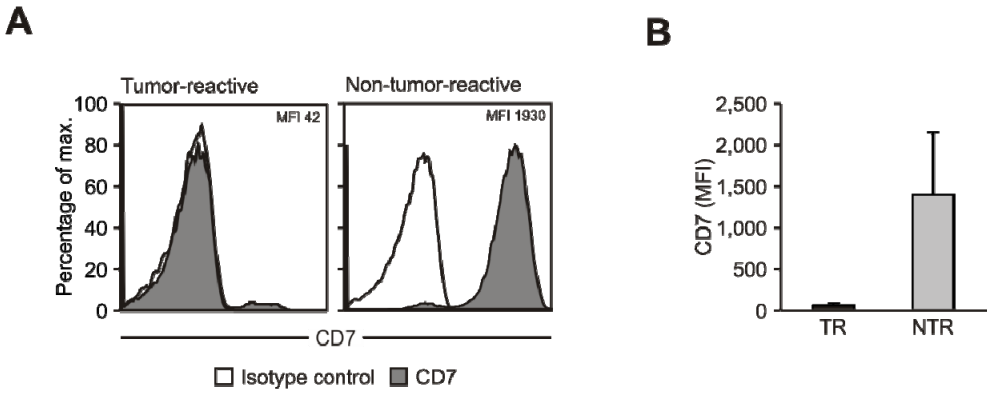

Figure 12 | Surface expression of CD7

(A) Representative flow-cytometric analysis of CD7 expression (grey fill) on the T-cell surface of tumor-reactive (left) and non-tumor-reactive (right) CD8$^+$ T-cell clones. All experiments were performed at least four times. Isotype control (bold black lines). Top right, mean fluorescence intensities (MFI) values.

(B) Mean ± standard deviation of CD7 surface expression of tumor-reactive (left) and non-tumor-reactive (right) CD8$^+$ T-cell clones. Result from at least 4 independent experiments .

As examplified in Figures 12a and 12b, non-tumor-reactive CD8$^+$ T-cell clones highly express CD7, whereas expression of CD7 is significantly reduced or completely absent in tumor-reactive CD8$^+$ T-cell clones.

4.4.3. Expression of co-stimulatory molecules

$CD8^+$ T-cell co-stimulatory molecules are cell-surface molecules that cannot activate T cells on their own, but upon their engagement counteract or multiply signals provided by the TCR-complex (166). The minority of co-stimulatory molecules has positive amplifying effects and is constitutively expressed, whereas the majority of co-stimulatory molecules is expressed upon engagement of TCR by pMHC only and can be either positive or negative regulative (Table 5).

Expression	Signal	Receptor	Ligand
Constitutive	Positive	CD28	B7-1 (CD80)
		CD28	B7-2 (CD86)
Inducible	Positive	OX40 (CD134)	OX40-L
		4-1BB (CD137)	4-1BB-L
	Negative	CTLA-4 (CD152)	B7-1 (CD80)
		CTLA-4 (CD152)	B7-2 (CD86)

Table 5 | Co-stimulatory molecules on $CD8^+$ T cells

$CD8^+$ T cells posses a variety of co-stimulatory molecules that enables antigen-presenting cells to fine-tune the T-cell response. CD28, is a co-stimulatory molecule that is engaged by CD80 and CD86 on antigen-presenting cells thus ensuring full T-cell activation. Among the inducible co-stimulatory molecules, both positive regulatory (OX40 and 4-1BB) and negative regulatory (CTLA-4) molecules on $CD8^+$ T cells have been explored. Adapted from Kroczek et al. (166).

Expression of co-stimulatory CD28

The constitutively expressed co-stimulatory molecule CD28 is involved in very early T-cell activation and T-cell receptor engagement. Absence of CD28 co-stimulation results in T-cell anergy (280).

A second model for human T-cell differentiation adds the co-stimulatory molecule CD28 to the definition of T-cell subsets. Undergoing differentiation, co-stimulatory molecules CD28 and CD27 are progressively downregulated, defining three subsets of naïve T cells ($CD45RA^+CD28^+$), memory T cells ($CD45RA^-CD28^+$) and effector T cells ($CD45RA^+CD28^-$) (14, 123, 343, 351).

Thus, absent or diminished CD28 expression would point towards insufficient co-stimulation as a factor causing the unresponsiveness of non-tumor-reactive $CD8^+$ T-cell clones. To exclude that differences in CD28 surface expression cause tumor-unresponsiveness of non-tumor-reactive $CD8^+$ T-cell clones and to define more precisely the differentiation status of both tumor-

reactive and non-tumor-reactive CD8$^+$ T-cell clones, CD28 expression of tumor-reactive and non-tumor-reactive CD8$^+$ T-cell clones was assessed (Figure 13).

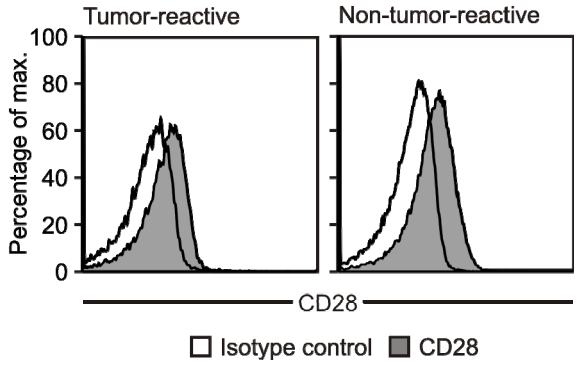

Figure 13 | Expression of CD28 on the cell surface

Representative flow-cytometric analysis of CD28 expression (grey fill) on the cell surface of tumor-reactive (T-cell clone W26-TR) (left) and non-tumor-reactive (T-cell clone W10-NTR) (right) CD8$^+$ T-cell clones. All experiments were performed at least four times with each tumor-reactive and non-tumor-reactive CD8$^+$ T-cell clones from patients NW1045, NW1789 and NW2608. Isotype control (bold black lines).

Expression of co-stimulatory molecules OX40 and 4-1BB

OX40 is a co-stimulatory molecule of the tumor necrosis factor receptor family. OX40 is not expressed on resting T cells, and expression is restricted to T cells activated by TCR/CD3 signals. OX40 has been visualized *in vivo* in T-cell zones of spleen or lymph nodes several days after immunization with protein antigen, directly coinciding with the peak of the primary T-cell response (67, 118, 296). It appears 12-24 hours after stimulation of naïve T cells (114, 119) with a peak expression seen after 2-3 days and consecutive downregulation. OX40 expression is not dependent on CD28 signals, but CD28 can augment the level of OX40 expressed on T cells suggesting that both molecules co-operate together in a sequential manner. In this model, OX40 signals act in a temporal manner after CD28 signals. OX40 signals allow effector T cells to survive and continue proliferating late in response, predominantly by transmitting anti-apoptotic signals BCL-xL and BCL-2 that prevent excessive T-cell death (67). To exclude that differences in OX40 expression on the cell surface, as observed for other cell surface signaling molecules, contribute to different phenotypes demonstrated for tumor-reactive and non-tumor-reactive CD8$^+$ T-cell clones, expression of the OX40 molecule on the T-cell surface was measured (Figure 14).

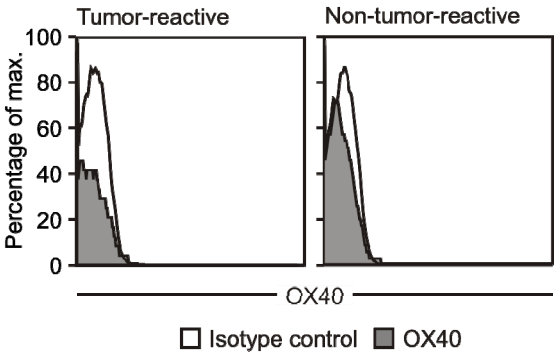

Figure 14 | Expression of OX40 (CD134) on the CD8$^+$ T-cell surface

Representative flow-cytometric analysis of OX40 expression (grey fill) on the cell surface of tumor-reactive (T-cell clone B4-TR) (left) and non-tumor-reactive (T-cell clone B21-NTR) (right) CD8$^+$ T-cell clones. Isotype control (bold black lines).

4-1BB (CD137) is another inducible T cell signaling molecule belonging to the tumor necrosis factor receptor superfamily. Both the molecular and cellular studies of OX40 and 4-1BB show similar effects on CD4$^+$ and CD8$^+$ T cells (67). 4-1BB particularly influences the number of antigen-reactive CD8$^+$ T cells generated in immune responses towards a specific antigen, as 4-1BBL-deficient mice responding to the viruses LCMV and influenza generate 2-10 fold fewer antigen-reactive CD8$^+$ T cells (70, 302, 303), and conversely agonist anti-4-1BB antibodies result in increased numbers of antigen-specific T cells (212). To exclude that differences in 4-1BB expression on the cell surface contribute to different phenotypes demonstrated for tumor-reactive and non-tumor-reactive CD8$^+$ T-cell clones, expression of the 4-1BB molecule on the T-cell surface was measured (Figure 15).

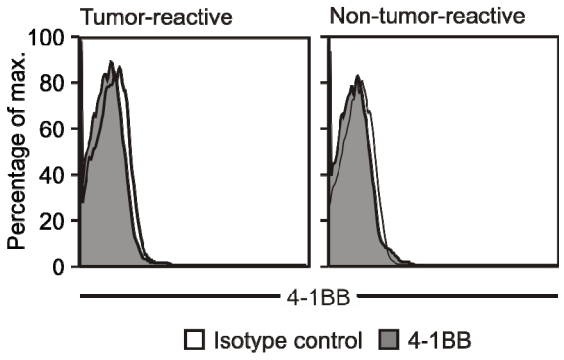

Figure 15 | Expression of 4-1BB (CD137) on the CD8$^+$ T-cell surface

Representative flow-cytometric analysis of 4-1BB expression (grey fill) on the cell surface of tumor-reactive (T-cell clone B4-TR) (left) and non-tumor-reactive (T-cell clone B21-NTR) (right) CD8$^+$ T-cell clones. Isotype control (bold black lines).

As can be seen in Figures 14 and 15, both OX40 and 4-1BB are not expressed on tumor-reactive or non-tumor-reactive CD8$^+$ T-cell clones 7 days after antigen exposure. This argues against substantial differences in expression of OX40 or 4-1BB to contribute to the observed functional differences in tumor reactivity.

Expression of co-inhibitory molecule CTLA-4

CTLA-4, an inhibitory molecule in terms of T-cell activation, was assessed to exclude that non-tumor-reactive $CD8^+$ T-cell clones are actively inhibited by cell surface engagement of CTLA-4. This consideration bases on the fact that activation of CTLA-4 sustains T-cell anergy (279) by blocking IL-2 production, cell cycle progression and T-cell differentiation. Further experiments indicate that CTLA-4 is required to maintain the unresponsive state of tolerized T cells, and consequently CTLA-4 blocking antibodies have been described to reverse the anergic T-cell phenotype in several model systems (90, 280, 334).

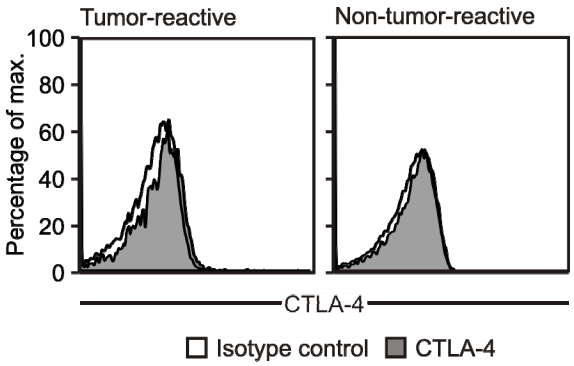

Figure 16 | Expression of CTLA-4 on the $CD8^+$ T-cell surface

Representative flow-cytometric analysis of CTLA-4 expression (grey fill) on the cell surface of tumor-reactive (T-cell clone W26-TR) (left) and non-tumor-reactive (T-cell clone W10-NTR) (right) $CD8^+$ T-cell clones. All experiments were performed at least four times with each tumor-reactive and non-tumor-reactive $CD8^+$ T-cell clones from patients NW1045, NW1789 and NW2608. Isotype control (bold black lines).

As can be seen in Figure 16, tumor-reactive and non-tumor-reactive $CD8^+$ T-cell clones express similar amounts of CTLA-4 on the cell surface. $CD8^+$ T-cell clones rarely express any CTLA-4 in both tumor-reactive and non-tumor-reactive $CD8^+$ T-cell clones.

4.4.4. CD5 modulation of T-cell receptor responsiveness

T-cell receptor co-stimulatory molecules are modulated upon strong T-cell receptor signals resulting in CD8 downregulation. Downregulation of CD8 from the cell surface is accompanied by an inverse regulation of CD5 leading to increased CD5 expression on the cell surface (242). To assess whether this regulation is intact in tumor-reactive and non-tumor-reactive $CD8^+$ T-cell clones, $CD8^+$ T-cell clones were stained for CD5 and CD8 surface expression.

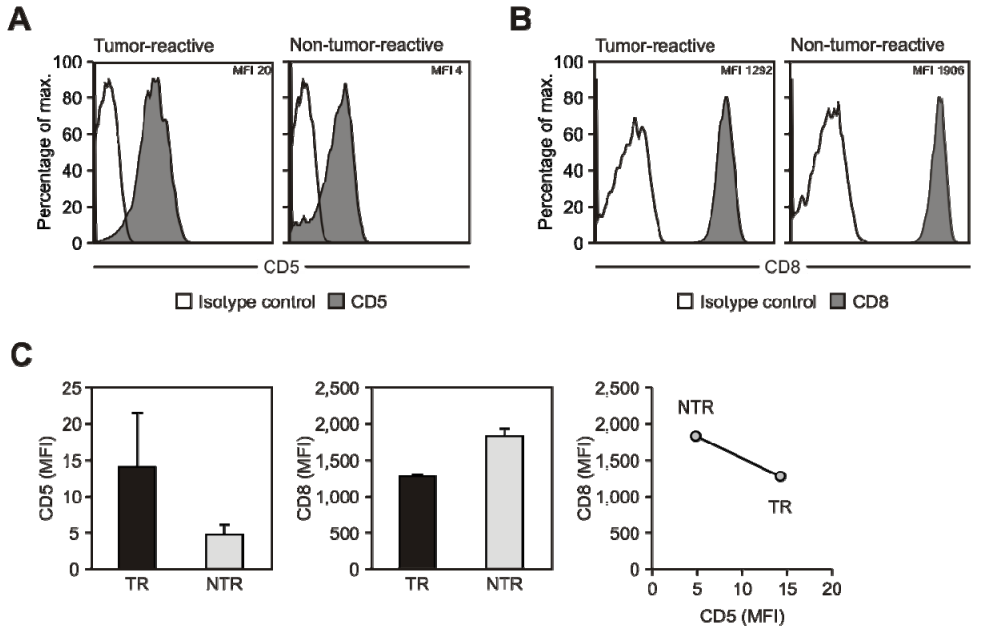

Figure 17 | Inverse correlation of CD5 and CD8 expression

(A) Representative flow-cytometric analysis of CD5 expression (grey fill) on the T-cell surface of tumor-reactive (left) and non-tumor-reactive (right) T-cell clones. All experiments were performed at least two times. Isotype control (bold black lines).

(B) Expression of the CD8 co-receptor expression (grey fill) on the T-cell surface of tumor-reactive (left) and non-tumor-reactive (right) T-cell clones. All experiments were performed at least two times. Isotype control (bold black lines).

(C) Expression of CD5 (left) and CD8 (middle) on the surface of tumor-reactive (black filled) and non-tumor-reactive (grey filled) $CD8^+$ T cells. Right, CD8 versus CD5 expression on tumor-reactive (TR) and non-tumor-reactive (NTR) $CD8^+$ T cells. MFI, mean fluorescence intensity. Data are representative of two experiments.

As can be seen in Figure 17a, CD5 expression in tumor-reactive $CD8^+$ T-cell clones is increased as compared to non-tumor-reactive $CD8^+$ T-cell clones. CD8 is higher expressed on non-tumor-reactive $CD8^+$ T-cell clones (Figure 17b). This is in accordance with a proposed stronger T-cell receptor signaling upon NY-ESO-1 recognition and hence higher CD5 expression. Expression of CD8 is comparable lower in tumor-reactive $CD8^+$ T-cell clones. This inverse correlation of both co-receptors reflects the strength of the antigenic stimulus

and supports lower affinity of the non-tumor-reactive T-cell receptors towards the NY-ESO-1/HLA-A2 complex (Figure 17c).

4.4.5. Concordant expression of activation markers HLA-DR and GITR

Glucocorticoid-induced TNFR family related gene (GITR), first identified as a dexamethasone-inducible molecule on a murine T-cell hybridoma (229), is expressed only at low levels on resting human T cells, but is upregulated upon activation of $CD8^+$ T cells with greater induction in the presence of CD28. There is evidence for a co-stimulatory role for GITR on $CD4^+$ and $CD8^+$ T cells (150, 162, 268, 286, 309, 330, 341). In addition, GITR ligation in the presence of a T-cell receptor signal upregulates IL-2Rα, IFN-γ, IL-2, IL-4, and IL-10 and enhances killing in T-cell lysis assays (150, 268, 341). A regulative role of GITR could be drawn from $GITR^{-/-}$ mice that showed hyperresponsiveness to anti-CD3 (267), but subsequent analysis of $GITR^{+/+}$ with $GITR^{-/-}$ T-cell responses to anti-CD3 plus GITR-ligand showed a co-stimulatory role for GITR-GITR-ligand interaction (268).

Another molecule on the surface of T cells indicating T-cell activation is the HLA-DR molecule. To assure that both non-tumor-reactive and tumor-reactive $CD8^+$ T-cell clones are equally activated by means of expression of activation markers, cell surface molecule expression of GITR and HLA-DR indicating activation of T cells after T-cell receptor signaling was assessed.

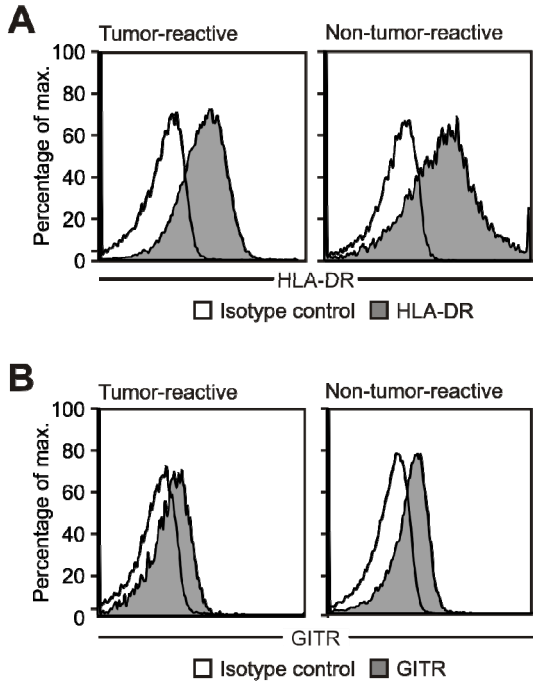

Figure 18 | Cell surface expression of activation markers HLA-DR and GITR

(A) Representative flow-cytometric analysis of HLA-DR expression (grey fill) on the T-cell surface of tumor-reactive (left) and non-tumor-reactive (right) T-cell clones. All experiments were performed at least four times. Isotype control (bold black lines).

(B) Representative flow-cytometric analysis of GITR protein expression (grey fill) on the T-cell surface of tumor-reactive (left) and non-tumor-reactive (right) T-cell clones. All experiments were performed at least four times. Isotype control (bold black lines).

As demonstrated by Figures 18a and 18b, both tumor-reactive as well as non-tumor-reactive $CD8^+$ T-cell clones show concordantly high expression of the activation markers HLA-DR and GITR, implying an activated status of both T-cell subsets.

4.4.6. Discordant expression of early activation markers CD69 and CD25

Proteins that are expressed on the surface of T cells can be categorized in proteins that are part in the T-cell activation pathway after antigen stimulation and molecules that are expressed upon T-cell receptor engagement but are regulative in that they augment or diminish the T-cell response. Interestingly, surface molecules that have been linked with regulative function and have been shown to be expressed on anergic T cells are CD25 and CD69 (112, 130).

CD69 is a molecule selectively expressed on the cell surface of activated T cells. Its exact function in T-cell activation has not been defined, but experimental data suggest a regulative role in T-cell homeostasis. Forced expression of CD69 after T-cell receptor engagement might reflect a regulatory feedback circuit important for $CD8^+$ T-cell homeostasis as discussed below. CD69 expression is furthermore in line with a partial activation phenotype as suggested by low affinity pMHC stimulation (336).

CD25 is the α-chain of the IL-2 receptor. Its expression has been reported to be upregulated in activated T cells but upregulation of CD25 has also been reported as characteristic for anergic T cells as well. In this context, it greatly enhances IL-2 intake by T cells suggesting a compensatory mechanism to bypass the IL-2 gene blockade often seen in anergic T cells and in non-tumor-reactive $CD8^+$ T-cell clones perpetuated by different mechanisms. In line with a putative influence on the outcome of T-cell activation, to unknown reasons the activation threshold for the induction of CD25 as well as CD69 in response to stimulation is lowered in anergic T cells (318). Characteristic defects of proximal T-cell receptor signaling seen in $CD4^+CD25^+$ T cells are reduced activities of phospholipase C, calcium mobilization, NFAT, NF-κB and ERK, resulting in the observed hyporesponsive state reported for this subset of T cells with the exact mechanism remaining unsolved (130).

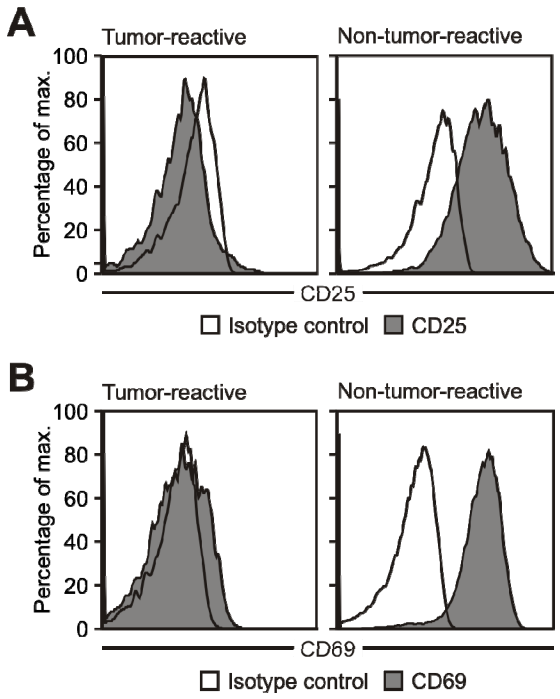

Figure 19 | Expression of early activation markers CD25 and CD69

(A) Representative flow-cytometric analysis of CD25 expression (grey fill) on the T-cell surface of W26-TR tumor-reactive (left) and W10-NTR non-tumor-reactive (right) T-cell clones. All experiments were performed at least four times. Isotype control (bold black lines).

(B) Representative flow-cytometric analysis of CD69 protein expression (grey fill) on the T-cell surface of W26-TR tumor-reactive (left) and W10-NTR non-tumor-reactive (right) T-cell clones. All experiments were performed at least four times. Isotype control (bold black lines).

As can be seen in Figure 19a, tumor-reactive $CD8^+$ T-cell clones do not show expression of CD25 while non-tumor-reactive $CD8^+$ T-cell clones show partial to strong expression of CD25 on the cell surface. CD69 is barely expressed or negative on tumor-reactive $CD8^+$ T-cell clones, whereas non-tumor-reactive $CD8^+$ T-cell clones show high expression of this cell surface molecule (Figure 19b). This is in line with a partial activation phenotype of non-tumor-reactive $CD8^+$ T-cell clones (276, 336).

4.4.7. Expression of chemokine receptors

Chemokine receptors define distinct subsets of T cells and regulate homing of T cells to different sites of action (273). In general, they determine homing of T cells into either lymphoid-tissue or inflamed extralymphoid tissue. As outlined above, particularly CCR7 has been implicated in the homing to lymph nodes and CCR7 expression defines two subsets in the T-cell memory population, central memory ($CCR7^+$) and effector memory ($CCR7^-$) T cells with distinct functions (272). CCR2 is a inflammation-related cytokine receptor which has been implicated to allow homing to inflammatory sites (60), and CCR4 together with other chemokine receptors determines skin homing of T lymphocytes (10, 291). CCR4 expressing of skin-homing T cells is generated during priming in skin-draining peripheral lymph nodes, thus CCR4 expression may suggest that priming of naïve tumor-reactive T cells as well as non-tumor-reactive T cells has occurred in draining lymph nodes at either the tumor site or the injection site of NY-ESO-1 peptide in the skin. Importantly, CCR4 is also up-regulated on T cells at the peak of expansion (day 6) after immunization followed by a fast down-regulation between day 6 and 8 (86). Consequently, CCR4 should be considered to be not only an exclusive skin-homing marker, but might also be used as marker of successful immunization as well.

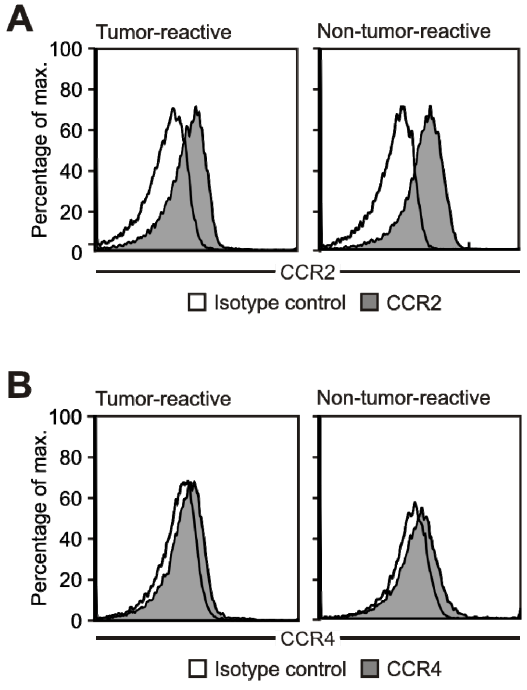

Figure 20 | Expression of chemokine receptors CCR2 and CCR4

(A) Representative flow-cytometric analysis of CCR2 expression (grey fill) on the T-cell surface of tumor-reactive (left) and non-tumor-reactive (right) T-cell clones. All experiments were performed at least four times. Isotype control (bold black lines).

(B) Representative flow-cytometric analysis of CCR4 protein expression (grey fill) on the T-cell surface of tumor-reactive (left) and non-tumor-reactive (right) T-cell clones. All experiments were performed at least four times. Isotype control (bold black lines).

As can be seen in Figure 11 and Figure 20, both tumor-reactive and non-tumor-reactive T-cell subsets express CCR7, CCR2 as well as CCR4. This not only supports the central memory T-cell phenotype as compared to an effector memory phenotype as already outlined above but also suggests that adequate priming of both subsets in tumor filtrating lymph nodes has taken place and that both subsets have the possibility to invade inflammatory sides as well as skin tissues. Both are very important characteristics to allow efficient accumulation at the tumor side.

4.5. T-cell receptor signaling pathway

Altered phosphorylation of molecules involved in T-cell signaling has been shown to induce different types of T-cell anergy, an intrinsic functional inactivation following antigen encounter (280). To assess whether a partial activation phenotype of non-tumor-reactive T cells is linked to altered T-cell receptor signaling and is reversible upon strong T-cell receptor stimulation as would be suggested by an inhibitory T-cell model, phosphorylation of key signaling molecules of non-tumor-reactive and tumor-reactive $CD8^+$ T-cell clones was analyzed.

4.5.1. Lck is inactive in non-tumor-reactive $CD8^+$ T-cell clones upon stimulation

Phosphorylation of the ITAM motifs in the T-cell receptor by the Src family tyrosine kinase Lck is the earliest event during T-cell activation (328). Lck, as other Src family members, contains a negative regulatory site of tyrosine phosphorylation at the COOH-terminal tyrosine Y505 that, when phosphorylated, decreases kinase activity (284). In the unstimulated state, the distribution of Lck-phosphorylation at positions tyrosine 505 and 394 is shifted towards high phosphorylation of inhibitory tyrosine 505. T-cell receptor activation induces dephosphorylation of Lck p505 and increased phosphorylation at tyrosine 394 resulting in increased activity of Lck and phosphorylation of ZAP-70. As discussed below, phosphorylation of Lck at tyrosine 505 has been linked with altered T-cell activation and T-cell unresponsiveness by means of T-cell receptor signal attenuation and cell cycle alteration. Resting T cells contain high levels of Lck phosphorylated at tyrosine 505. Upon stimulation, Lck p505 is dephosphorylated as expected in tumor-reactive $CD8^+$ T-cell clones. Phosphorylation was measured in resting tumor-reactive and non-tumor-reactive $CD8^+$ T-cell clones after 1 minute and after 4 minutes of CD3/CD28 crosslinking.

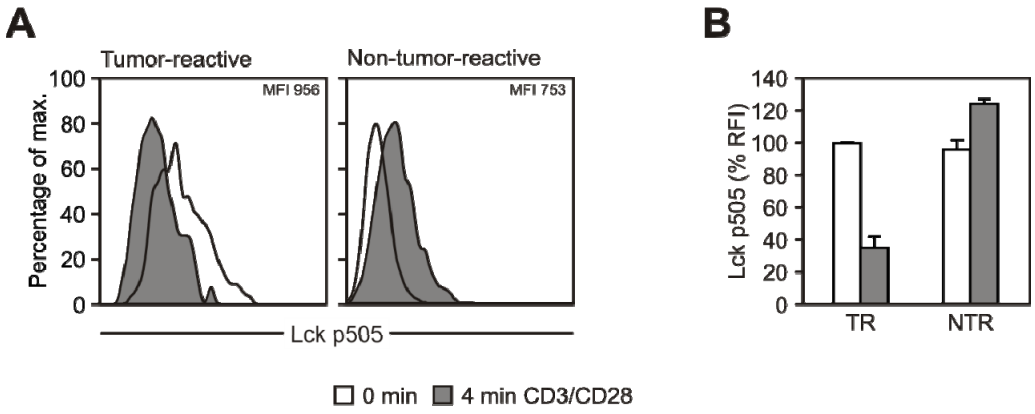

Figure 21 | Phosphorylation of lck^{p505}

(A) Phosphorylation of lck^{p505} was assessed in tumor-reactive (left) and non-tumor-reactive (right) CD8$^+$ T-cell clones 4 minutes after cross-linking of CD3 and CD28. Baseline steady-stae phosphorylation of lck^{p505} at the 0 minute time point is depicted as black line. Phosphorylation of lck^{p505} upon cross-linking is depicted as grey fill. One representative experiment is shown as histogram plot.

(B) Phosphorylation before stimulation was set as 100% and phosphorylation after stimulation was normalized to that before stimulation. Phosphorylation is presented as relative fluorescence intensity (RFI). Mean ± standard deviation.

As can be seen in Figures 21a and 21b, Lck p505 is actively dephosphorylated in tumor-reactive CD8$^+$ T-cell clones upon stimulation with a peak of dephosphorylation after 4 minutes. In contrast, phosphorylation at Lck tyrosine 505 remains active and is even increased in non-tumor-reactive CD8$^+$ T-cell clones after stimulation with cross-linked CD3/CD28 antibodies.

4.5.2. Intact early T-cell receptor signaling

Initial substrates for lck kinase in T-cell signaling are ITAM motifs in the cytoplasmic tails of CD3γ, CD3δ, CD3ε and CD3ζ. Phosphorylation of these early signaling molecules is indispensable for successful T-cell receptor signaling. As outlined above, the protein tyrosine kinase ZAP-70 is recruited by dually phosphorylated ITAMs, activated upon phosphorylation of tyrosine 319 by Lck, and fulfills an important function in further downstream molecule activation. Moreover, defective activation of these early T-cell receptor signaling molecules has been linked to T-cell anergy. Consequently, phosphorylation of CD3ζ and ZAP-70 as early T-cell receptor signaling proteins was assessed by flow cytometry.

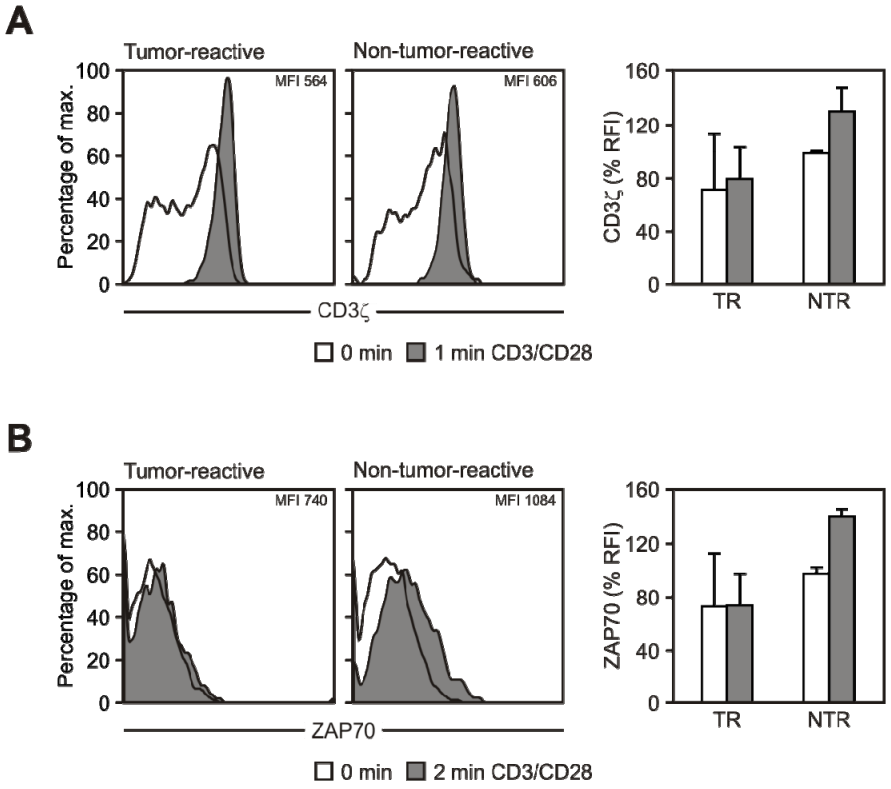

Figure 22 | Intact phosphorylation of CD3ζ and ZAP-70

Flow-cytometric analysis of **(A)** CD3ζ-phosphorylation (grey fill) and **(B)** ZAP-70 (grey fill) of tumor-reactive (left) and non-tumor-reactive (right) $CD8^+$ T-cell clones. $CD8^+$ T-cell clones were stimulated by ligation of CD3 and CD28. Both phosphorylation and dephosphorylation were stopped after one minute resp. two minutes of stimulation. Phosphorylation was assessed using specific antibodies against phosphorylated CD3ζ and ZAP-70. Baseline steady-state phosphorylation (bold black lines). Histograms in (A) and (B) display one representative experiment each. Phosphorylation after stimulation was normalized to that before stimulation (set as 100%) and is presented as relative fluorescence intensity (RFI).

As can be seen in Figure 22A and B, both CD3ζ and ZAP-70 are successfully phosphorylated upon unspecific stimulation with CD3/ CD28 ligation. Interestingly, phosphorylation is even enhanced in non-tumor-reactive as compared to tumor-reactive $CD8^+$ T-cell clones.

4.5.3. Intact T-cell receptor downstream signaling

Once ERK is phosphorylated, it forms dimers which are transported into the nucleus and subsequently phosphorylate the Ets family of transcription factors. By this mechanism, the signal from the cell surface is transported into the nucleus and translated into transcription.

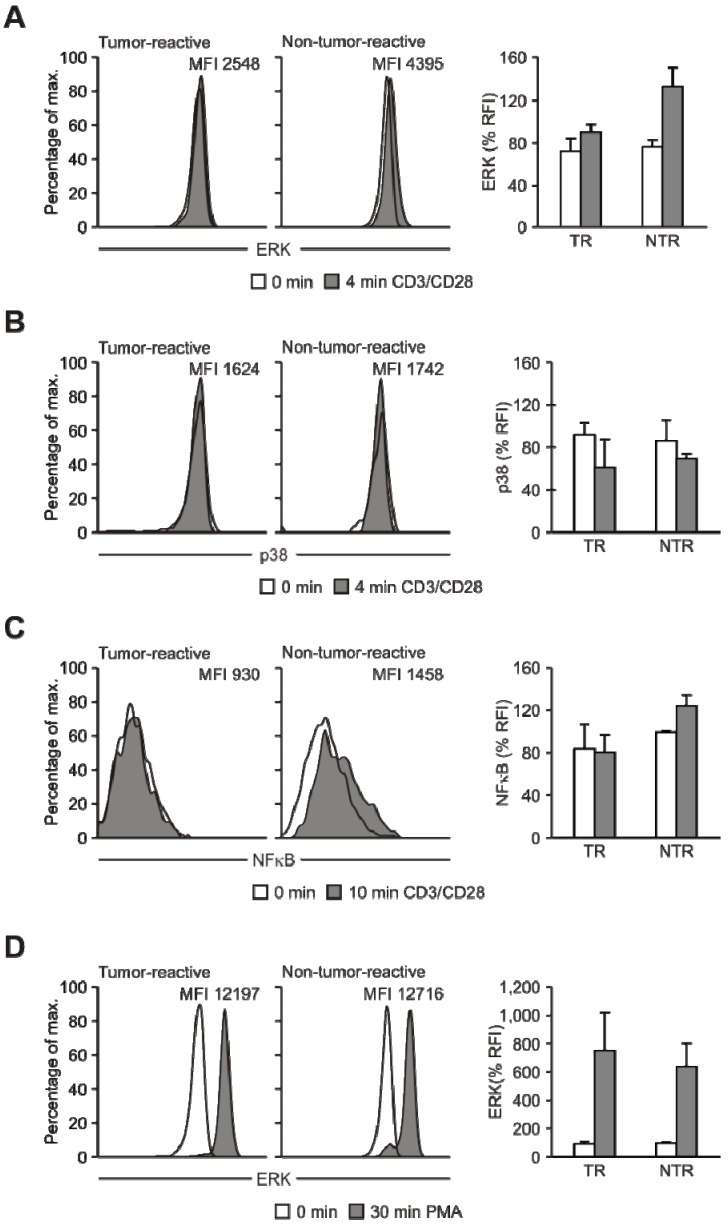

Figure 23 | Intact T-cell receptor downstream signaling

Flow-cytometric analysis of phosphorylation of T-cell receptor downstream signaling molecules (grey fill) in tumor-reactive (left) and non-tumor-reactive (right) $CD8^+$ T-cell clones. $CD8^+$ T-cell clones were stimulated by ligation of CD3 and CD28, both phosphorylation and dephosphorylation were stopped after **(A)** 4 minutes, **(B)** 4 minutes, **(C)** 10 minutes, and **(D)** 30 minutes of stimulation, and phosphorylation was assessed using specific antibodies against the phosphorylated status of the particular signaling molecule. Baseline steady-state phosphorylation (bold black lines). Histograms display one representative experiment each. Phosphorylation after stimulation was normalized to that before stimulation (set as 100%) and is presented as relative fluorescence intensity (RFI).

Interestingly non-tumor-reactive $CD8^+$ T-cell clones showed an increase in phosphorylation of ERK upon optimal stimulation, which could also be observed for NF-κB , albeit to a lesser extent. Phosphorylation of p38 was comparable.

4.6. Functional differences

4.6.1. Cytokine production upon specific and polyclonal T-cell receptor stimulation

Cytokine profiles of $CD8^+$ T cells correlate with T-cell receptor avidity. One mechanism by which $CD8^+$ effector T cells exert their function in response to antigens, foreign or altered-self, is the production of cytokines, in particular INF-γ. Additionally, distinct cytokine profiles of tumor-associated $CD8^+$ T cells are correlated with superior defense against tumor cells than other cytokine profiles (80, 155).

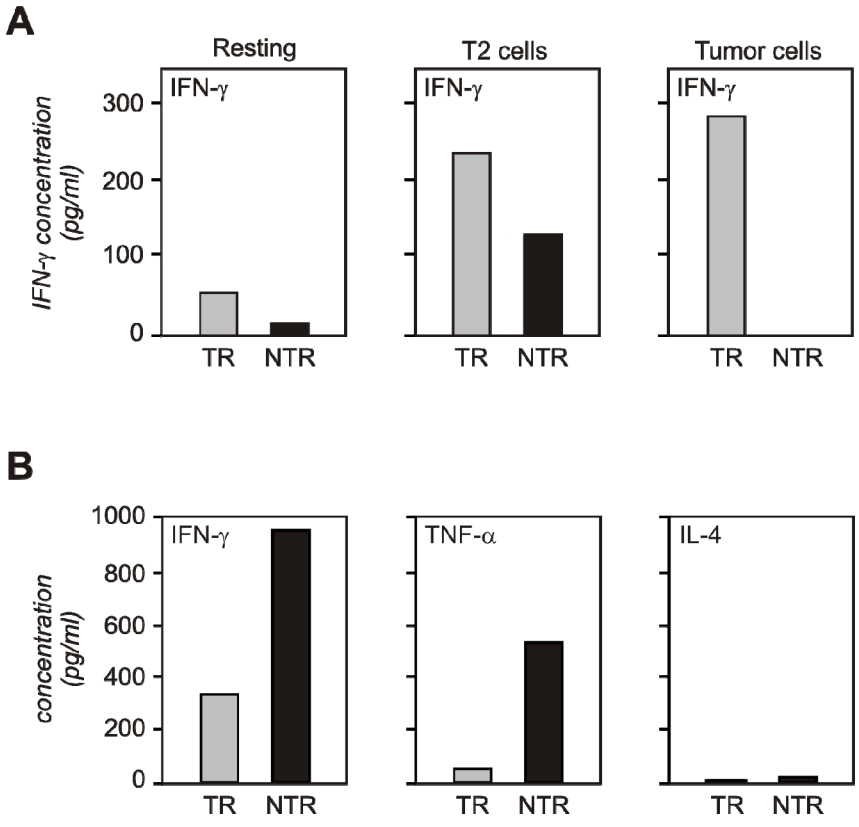

Figure 24 | Cytokine production of $CD8^+$ T-cell clones

(A) Cytokine production upon specific T-cell receptor activation. To test for NY-ESO-1 specific cytokine production of tumor-reactive (TR) and non-tumor-reactive (NTR) T-cell clones, $CD8^+$ T-cell clones were incubated with either NY-ESO-1 157-165 peptide-pulsed-T2 cells or melanoma cells at a ratio of 1:10 for 24 hours. Supernatants of stimulated and unstimulated $CD8^+$ T-cell clones were subsequently assessed by cytometric bead arrays for secretion of effector cytokines. One exemplary experiment of four is shown.

(B) Cytokine production upon polyclonal T-cell receptor activation. Cytokine production of tumor-reactive (TR) and non-tumor-reactive (NTR) $CD8^+$ T-cell clones was compared. $1x10^6$ T cells were incubated for 24 hours with CD3/CD28/MHC-I coated beads in a ratio of 1:3 (T cell to beads). Supernatants of stimulated and unstimulated $CD8^+$ T-cell clones were subsequently assessed by cytometric bead arrays for secretion of effector cytokines. One exemplary experiment of four is shown.

Cytokine production of tumor-reactive and non-tumor-reactive $CD8^+$ T-cell clones (Figure 24) clearly shows that non-tumor-reactive $CD8^+$ T-cell clones are impaired in their ability to produce the cytokine IFN-γ. Basal rate of IFN-γ secretion as well as production of IFN-γ in response to peptide-pulsed T2 cells is impaired. Strikingly, these cells do not show any production of IFN-γ in response to HLA-A2 expressing cognate malignant melanoma cell lines, extending the non-tumor-reactive $CD8^+$ T-cell phenotype to cytokine production as well. Interestingly, when stimulated with a strong agonist such as anti-CD3 and anti-CD28 stimulation, these cells produce significant more IFN-γ and TNF-α than tumor-reactive $CD8^+$ T-cell clones but no IL-4 suggesting that these cells reside in a state that is potential hyper-responsive to cognate stimulus with a bias towards classical effector cytokines like IFN-γ and TNF-α.

4.7. Cell cycle inhibition

4.7.1. Upregulation of $p27^{kip1}$ in non-tumor-reactive $CD8^+$ T-cell clones

Phosphorylation of lck at the inhibitory tyrosine residue 505 has been associated with induction of anergy in $CD4^+$ T cells by induction of $p27^{kip1}$ resulting in T-cell anergy (48, 98). As lck^{p505} is highly phosphorylated in the non-tumor-reactive $CD8^+$ T-cell clones, expression of $p27^{kip1}$ in tumor-reactive and non-tumor-reactive $CD8^+$ T-cell clones was assessed. Cell cycle molecules as $p27^{kip1}$ are differentially expressed in T2 and malignant melanoma cells. To specifically check for these molecules in T cells after exposure to NY-ESO-1 presenting T2 cells or corresponding malignant melanoma cell lines, FACS was used to guarantee separation of T cells from malignant melanoma/ T2 cells in a cell mixture by the use of fluorescence labeled antibodies against distinct surface molecules.

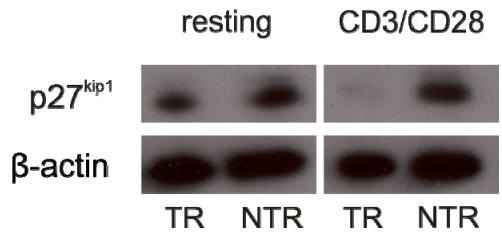

Figure 25 | $p27^{kip1}$ expression upon polyclonal T-cell receptor stimulation

To analyze $p27^{kip1}$-expression of tumor-reactive (TR) and non-tumor-reactive (NTR) $CD8^+$ T-cell clones, T cells were incubated for 24 hours at 37°C with CD3, CD28 and MHC-I coated beads. Cells were lysed and proteins applied to SDS-PAGE and Western blotting. Expression of $p27^{kip1}$ was assessed using a primary antibody against $p27^{kip1}$. Expression of β-actin was assessed to control for equal loading.

As can be seen in Figure 25, both tumor-reactive as well as non-tumor-reactive $CD8^+$ T-cell clones express $p27^{kip1}$ prior to stimulation, although the level of $p27^{kip1}$-expression is lower in tumor-reactive than in non-tumor-reactive $CD8^+$ T-cell clones. Upon stimulation with CD3/CD28/MHC-I coated beads, tumor-reactive $CD8^+$ T-cell clones almost completely downregulate $p27^{kip1}$. In contrast, expression of $p27^{kip1}$ in non-tumor-reactive $CD8^+$ T-cell clones remains high. This result is similar to observations in $CD4^+$ T cells where $p27^{kip1}$ has been associated with T-cell anergy (33, 170, 344), suggesting that similar mechanisms merging T-cell effector status and cell division exist in both $CD4^+$ and $CD8^+$ T cells.

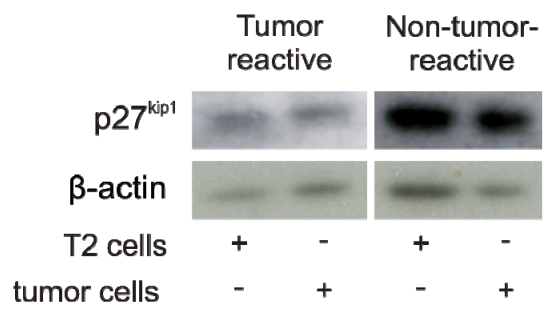

Figure 26 | p27kip1 expression upon specific T-cell stimulation

To assess $p27^{kip1}$-expression of tumor-reactive and non-tumor-reactive $CD8^+$ T-cell clones upon NY-ESO-1-specific stimulation, T cells were incubated with either NY-ESO-1 157-165 peptide-pulsed-T2 cells or autologous melanoma cells at a ratio of 10:1 for 24 hours. Cells were lysed and proteins applied to SDS-PAGE and Western blotting. Expression of $p27^{kip1}$ was assessed using a primary antibody against $p27^{kip1}$. Expression of β-actin was assessed to control for equal loading.

Next, we assessed if non-tumor-reactive $CD8^+$ T-cell clones show differential regulation of $p27^{kip1}$ after polyclonal stimulation, i.d. in response to NY-ESO-1 pulsed T2 cells or autologous malignant melanoma cell lines (Figure 26). As expected, tumor-reactive $CD8^+$ T-cell clones respond to both NY-ESO-1 pulsed T2 cells and malignant melanoma cell lines with down-regulation of $p27^{kip1}$. In contrast, non-tumor-reactive $CD8^+$ T-cell clones show high levels of $p27^{kip1}$ to both stimulation with NY-ESO-1 pulsed T2 cells and autologous malignant melanoma cell lines. The fact that high $p27^{kip1}$ levels are maintained upon stimulation with NY-ESO-1 pulsed T2 cells and autologous malignant melanoma cell lines is interesting in so far that previous reports of $p27^{kip1}$ associated T-cell anergy have suggested that $p27^{kip1}$ expression in functional T cells is downregulated even if the function was massively impaired.

These observations extend the phenotype proposed for $p27^{kip1}$ associated T cell anergy. It seems that even upon strong stimulation and despite induction of full effector function as assessed by cytokine levels and cytotoxicity against T2 cells, $p27^{kip1}$ level remain high, at least upon first strong stimulation with cognate antigen presented in physiological context after tolerance induction.

4.8. Molecular fingerprint

4.8.1. Microarray analysis to detect global differences in gene expression between tumor-reactive and non-tumor-reactive CD8$^+$ T-cell clones and confirmation of gene expression by RT-PCR

Gene expression profiles distinguish T-cell phenotypes with distinct functional properties and allow identification of signaling pathways specifically activated in these subsets. So far, expression profiles have been reported for a variety of CD8$^+$ T-cell anergic subsets, e.g. conventional CD8$^+$ T-cell anergy (197), partial versus full activation of CD8$^+$ T cells (331), and CD8$^+$ $T_{regulatory}$ cells (154). Expression profiling of CD8$^+$ T-cell responses towards viruses show distinct molecular programs, starting from naïve T cells towards differentiation into effector and memory T cells (12, 204). Also terminal exhaustion of CD8$^+$ T cells during chronic viral infection is associated with a unique gene expression profile (347). In the setting of anergy, comparison of the unique gene expression signature of non-tumor-reactive CD8$^+$ T-cell clones with published gene profiles of CD8$^+$ T-cell subsets may allow allocation and comparison of the non-tumor-reactive CD8$^+$ T-cell clones to T-cell subsets with well determined phenotypes. In the context of malignant melanoma, comparison with published gene expression profiles of CD8$^+$ T cells from malignant melanoma patients enables further insight into the immune response towards this tumor (50, 66, 238, 239, 357).

To identify genes which are important for non-tumor-reactivity or characterize signaling pathway contributing to the functional differences between non-tumor-reactive and tumor-reactive CD8$^+$ T-cell clones, we performed whole genome microarrays. Therefore, CD8$^+$ T cells were stimulated with peptide-pulsed T2 cells on day -7, then rested for 6 days and activated with CD3/CD28 beads 24 hours prior to analysis. Wells were harvested on day 0 and CD8$^+$ T cells lyzed in Trizol reagent. After RNA isolation and clean-up, cDNA was generated using a double-IVT reaction. After cRNA generation and fluorescent labeling, cRNA was fragmented and hybridized to U133A arrays from Affymetrix.

After primary data analysis to ensure data quality, differentially expressed genes were determined using dCHIP software according to the following

criteria: fold-change ≥ 1.5, p ≤ 0.05, Diff. ≥ 50. Overall 25 differentially expressed genes with twelve up and 13 downregulated in non-tumor-reactive $CD8^+$ T-cell clones were observed (Table 6). EGR1, TIMP1, KLF2, BCL3, SLC27A2, GZMB, VDR, CEBPB, IFITM2, ADAM19, HPGD and ENO1 were upregulated in non-tumor-reactive $CD8^+$ T-cell clones, whereas CHES1, ZNF160, GOLGA8B, SYNE2, RBPSUH, RORA, ASAH1, GNPTAB, TRIM22, XIST, XCL1 and XCL2 were downregulated in non-tumor-reactive $CD8^+$ T-cell clones (Figure 27a, Table 6 and supplemental Tables 7 and 8). To validate the microarray results, quantitative RT-PCR was performed as described for 14 of the differentially expressed genes (BCL3, CEBPB, EGR1, GZMB, IFITM2, TIMP1, VDR, ASAH1, CHES1, RORA, SYNE2, XCL1, XCL2, ZNF160) and confirmed the differential expression for all 14 genes (Figure 27b).

Among the genes upregulated in non-tumor-reactive $CD8^+$ T-cell clones, Krüppel-like factor 2 (KLF2) is a member of zinc-finger transcription factors and KLF2 is postulated to regulate T cell homeostasis by promoting cell quiescence via upregulation of cyclin-dependent kinase inhibitor p21WAF1/CIP1 while being at the same time essential for T cell trafficking (15, 37, 45, 353). EGR1 is upregulated after TCR engagement independent of MHC-antigen recognition and promotes activation and expansion of antigen-specific $CD8^+$ T cells (23, 287). The Vitamin D receptor (VDR) is known to block T-cell responses by inhibiting NFAT complex formation and by direct repression of the IL-2 promoter and IFN-γ production (7, 26, 206, 301). The upregulation of the transcription factor BCL3 by mitogenic stimuli represses tumor necrosis factor (TNF)-induced NF-κB transactivation, and hence, IL-2 transcription and T-cell activation (27, 233, 259). CEBPβ gene encodes a member of the basic leucine zipper family of transcription factors known to exert anti-proliferative effects on multiple cell types (36, 74, 368). A potential role of TIMP-1 (tissue inhibitor of metalloproteinases-1) on the IL-2 network has recently been suggested by a mathematical model (61), while little is known about the interferon induced transmembrane protein IFITM2. Elevated expression of Granzyme B might be a compensatory mechanism, however, so far, we were unable to determine, whether this correlates with differential function of granzyme B in non-tumor-reactive T cells.

Among the genes expressed at lower levels in non-tumor-reactive T-cell clones, at least three genes have been previously associated with T-cell activation or effector function. Upregulation of XCL1 (lymphotactin) has been described in $CD8^+$ T-cell clones stimulated with agonist peptide while no significant expression could be observed in unstimulated $CD8^+$ T cells or cells stimulated with irrelevant ligand (238, 239). The retinoid acid-related orphan receptor alpha (RORα) was previously shown to elevate cytotoxicity during activation (88). The forkhead protein CHES1/FOXN3 has been introduced as a regulator of the cell cycle directly interacting with the C-terminus of SKIP, a nuclear protein involved in regulating cell growth and differentiation through the TGF-β pathway (39, 281). Overall, genes associated with T-cell activation show a reduced expression in non-tumor-reactive $CD8^+$ T-cell clones while genes associated with T-cell inhibition are increased.

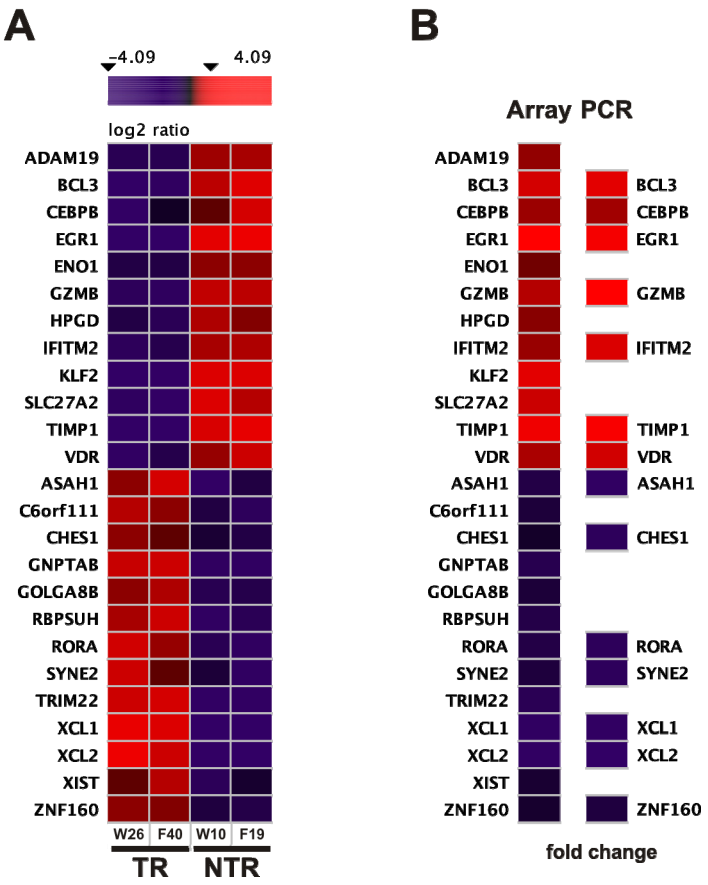

Figure 27 | Heatmap of genes differentially expressed in tumor-reactive and non-tumor-reactive T cells

Visualization of differentially expressed genes between non-tumor-reactive versus tumor-reactive $CD8^+$ T-cell clones as assessed by **(A)** microarray analysis and verified by **(B)** RT-PCR with a subset of genes. Genes with increased expression (fold change (FC) > 1.5, $p < 0.05$) are highlighted in red, genes with a decreased expression (FC < -1.5, $p < 0.05$) are highlighted in blue. Mean expression values from 2 tumor-reactive and 2 non-tumor-reactive $CD8^+$ T-cell clones are shown (W26-TR, W10-NTR; F40-TR, F19-NTR).

Cross-annotation of gene expression data of non-tumor-reactive $CD8^+$ T-cell clones was performed comparing the gene expression profile of this T-cell subset with published gene expression profiles of naïve, partial and full activated $CD8^+$ T cells as well as with gene expression profiles of T-cell

differentiation such as $CD8^+$ $T_{regulatory}$ cells, conventional $CD8^+$ T-cell anergy, memory T cells and T cells from chronic viral infection. The observed phenotype of non-tumor-reactive $CD8^+$ T cells did not correspond to any of these gene expression profiles (data not shown) implicating that the observed gene expression profile corresponds to another yet undescribed T-cell gene expression profile.

Probe Set ID	Gene Symbol	Gene Title	Fold Change	P value
Genes upregulated in non-tumor-reactive CD8+ T-cell clones				
201694_s_at	*EGR1*	*Early growth response factor 1*	17.98	0.034318
201666_at	*TIMP1*	*TIMP metallopeptidase inhibitor 1*	7.26	0.020906
219371_s_at	*KLF2*	*Kruppel-Like Factor 2*	5.17	0.04204
204908_s_at	*BCL3*	*B-cell CLL/lymphoma 3*	3.84	0.033404
205769_at	*SLC27A2*	*Solute carrier family 27 (fatty acid transporter), member 2*	3.46	0.048569
210164_at	*GZMB*	*Granzyme B (granzyme 2, cytotoxic T-lymphocyte-associated serine esterase 1)*	2.66	0.036333
204254_s_at	*VDR*	*Vitamin D (1,25-dihydroxyvitamin D3) receptor*	2.46	0.049616
212501_at	*CEBPB*	*CCAAT/enhancer binding protein (C/EBP), beta*	2.21	0.042375
201315_x_at	*IFITM2*	*Interferon induced transmembrane protein 2*	2.17	0.034248
209765_at	*ADAM19*	*ADAM metallopeptidase domain 19*	2.03	0.020424
211548_s_at	*HPGD*	*Hydroxyprostaglandin dehydrogenase 15-(NAD)*	1.91	0.045606
217294_s_at	*ENO1*	*Enolase 1*	1.69	0.020415
Genes downregulated in non-tumor-reactive CD8+ T-cell clones				
205022_s_at	*CHES1*	*Forkhead box N3*	-1.55	0.0464
214715_x_at	*ZNF160*	*Zinc finger protein 160*	-1.65	0.047555
214218_s_at	*XIST*	*X (inactive)-specific transcript*	-1.75	0.04904
213650_at	*GOLGA8B*	*Golgi autoantigen, golgin subfamily a, 8B*	-1.94	0.046437
212177_at	*C6orf111*	*Splicing factor, arginine/serine-rich 18*	-2.01	0.048566
202761_s_at	*SYNE2*	*Spectrin repeat containing, nuclear envelope 2*	-2.09	0.040098
211974_x_at	*RBPSUH*	*Recombining binding protein suppressor of hairless*	-2.69	0.049027
210426_x_at	*RORA*	*RAR-related orphan receptor A*	-2.54	0.049176
213702_x_at	*ASAH1*	*N-acylsphingosine amidohydrolase (acid ceramidase) 1*	-2.53	0.023795
212959_s_at	*GNPTAB*	*N-acetylglucosamine-1-phosphate transferase, alpha and beta subunits*	-3.18	0.044094
213293_s_at	*TRIM22*	*Tripartite motif-containing 22*	-3.75	0.03398
206366_x_at	*XCL1*	*Chemokine (C motif) ligand 1*	-8.4	0.041017
214567_s_at	*XCL2*	*Chemokine (C motif) ligand 2*	-8.74	0.049122

Table 6 | Genes differentially expressed in non-tumor-reactive $CD8^+$ T-cell clones

Gene expression profiles of non-tumor-reactive $CD8^+$ T-cell clones and tumor-reactive $CD8^+$ T-cell clones were assessed 7 days post stimulation with autologous melanoma cell lines. Gene expression profiles of non-tumor-reactive $CD8^+$ T-cell clones were compared to profiles of tumor-reactive $CD8^+$ T-cell clones.

4.8.2. Tumor-reactive CD8$^+$ T-cell clones release high amounts of XCL1

XCL1 is a member of the γ-class of chemokines (370), initially discovered as chemokine in leukocyte migration (6, 126). Only recently, up-regulation of XCL1 has been described in T cells stimulated with agonist peptide while no significant expression could be observed in unstimulated CD8$^+$ T cells or cells stimulated with irrelevant peptides (238, 239). In line with these observations, the XCL1 mRNA is downregulated in non-tumor-reactive CD8$^+$ T-cell clones as shown in Figure 27. To verify observed reduced mRNA-expression of XCL1 on the protein level, XCL1 was measured in the supernatant of tumor-reactive and non-tumor-reactive CD8$^+$ T-cell clones after stimulation with autologous malignant melanoma cells.

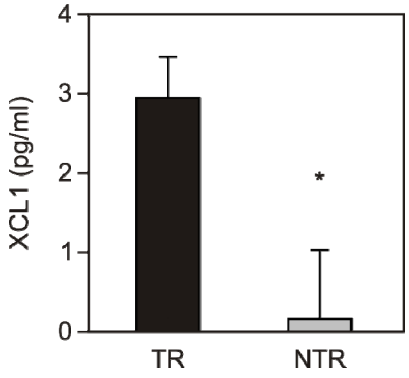

Figure 28 | XCL1 release of non-tumor-reactive and tumor-reactive CD8$^+$ T-cell clones

To test for NY-ESO-1 specific cytokine production of tumor-reactive (TR) and non-tumor-reactive (NTR) CD8$^+$ T-cell clones, T cells were incubated with autologous melanoma cells at a ratio of 1:10 for 24 hours. Supernatants of stimulated T-cell clones were subsequently applied to ELISA to assess XCL1 release into the supernatant. *, $p < 0.05$.

As can be seen in Figure 28, tumor-reactive CD8$^+$ T-cell clones secrete significantly higher amounts of XCL1 in the supernatant than non-tumor-reactive CD8$^+$ T-cell clones. This further confirms the differences in mRNA expression at the protein level.

4.9. Evidence for *in vivo* occurrence of tumor-reactive and non-tumor-reactive CD8$^+$ T-cell clones

4.9.1. Increase of CD8$^+$CD7$^+$CD25$^+$CD69$^+$ T cells in cancer patients

It is well known that vaccination with NY-ESO-1 results in an increase of NY-ESO-1-tetramer stained T cells in the periphery of NY-ESO-1$^+$ cancer patients. T cells that stain with NY-ESO-1-tetramer express T-cell receptors with high avidity towards NY-ESO-1. While this allows for the identification and enumeration of NY-ESO-1 specific tumor-reactive CD8$^+$ T-cell clones, up to now no methodology fo the enumeration of non-tumor-reactive CD8+ T-cell clones exists. As outlined above, in the setting of NY-ESO-1$^+$ malignant melanoma cancer patients, non-tumor-reactive CD8$^+$ T-cell clones can be characterized by their expression of CD7, CD25 and CD69 on the cell surface. We were interested whether this subset, proposed to allegorize the non-tumor-reactive CD8$^+$ T-cell subset, could be detected in cancer patients and healthy controls and assessed the overall frequency of the CD8$^+$CD7$^+$CD25$^+$CD49$^+$ T-cell subset in these patients.

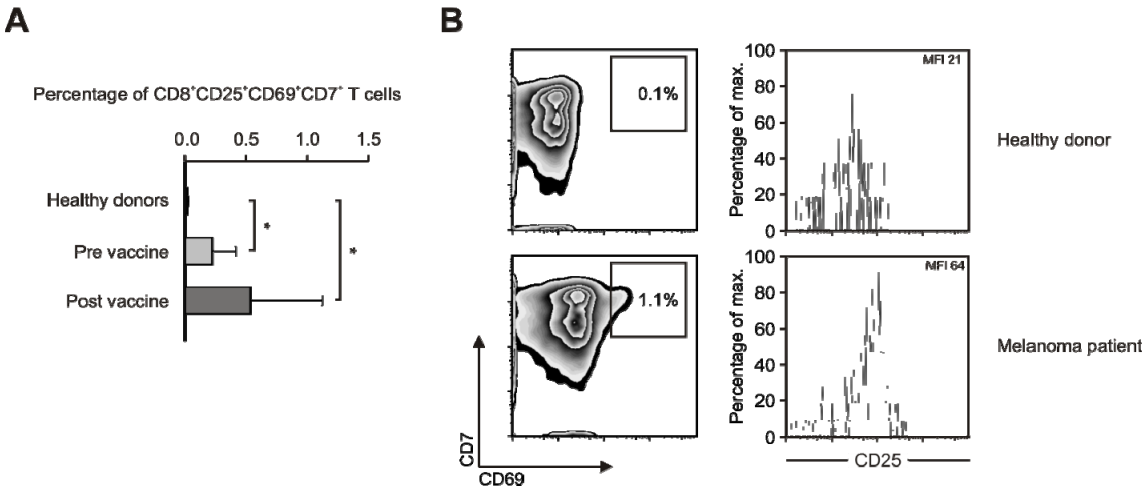

Figure 29 | Frequencies of CD8$^+$CD25$^+$CD69$^+$CD7$^+$ T cells

(A) Frequencies of CD8$^+$CD25$^+$CD69$^+$CD7$^+$ T cells were assessed in the blood of 10 healthy donors and 7 melanoma patients prior to and after vaccination with NY-ESO-1 p157-165 peptide. For that purpose, CD8$^+$ T cells were isolated from peripherally blood as described, stained with the respective fluorescent antibodies and assessed by flow cytometry. Mean expression ± standard deviation. *, $p<0.05$.

(B) Assessment of CD25 expression on the CD8+ CD69+ CD7+ T-cell subpopulation. Representative results for one healthy donor and one melanoma patient after vaccination are shown.

As can be seen in Figure 29a, the $CD8^+CD7^+CD25^+CD49^+$ T-cell subset could barely be detected in healthy individuals. In contrast, 0.23% of $CD8^+$ T cells in NY-ESO-1^+ cancer patients before and 0.54% after vaccination have a phenotype corresponding to the $CD8^+CD7^+CD25^+CD49^+$ T-cell subset both a significant increase over the number of cells in healthy individuals. Although the further expansion after vaccination did not reach statistical significance, it suggests an expansion of non-tumor-reactive $CD8^+$ T-cell clones *in vivo*. Figure 29b further assesses the frequency of $CD25^+$ T cells in the $CD8^+$ $CD69^+$ $CD7^+$ T-cell subset. As can be seen in a representative dotplot from one healthy and one malignant melanoma patient after vaccination, the $CD25^+$ subpopulation is increased in the malignant melanoma patient as compared to a healthy individual.

4.9.2. Kinetic of *in vivo* expansion of NY-ESO-1 specific $CD8^+$ T-Cell clones

During the course of vaccination against tumor antigens, the presence of tumor-reactive $CD8^+$ T cells in malignant melanoma patients has been widely reported (109). In a recent study from the group of *Thierry Boon*, frequencies of Mage-3 specific tumor-reactive $CD8^+$ T-cell clones were reported to be 12-20,000 fold higher than those of non-tumor-reactive but peptide-specific $CD8^+$ T-cell clones (109).

As the subset of $CD8^+CD7^+CD25^+CD69^+$ T cells is proposed to contain the non-tumor-reactive $CD8^+$ T-cell clones and is expanded upon vaccination with NY-ESO-1, we were interested to obtain a kinetic profile of the expansion of both tumor-reactive and non-tumor-reactive $CD8^+$ T-cell clones during vaccination. Thus, a highly concise quantitative PCR-approach was used to detect specific $CD8^+$ T-cell clones during vaccination.

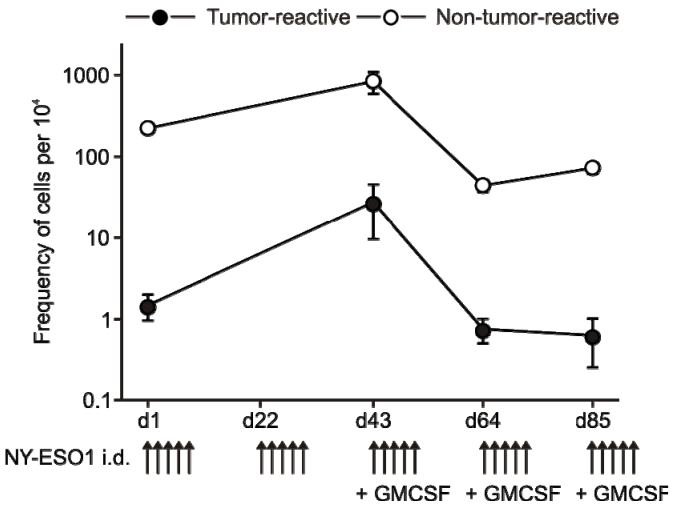

Figure 30 | Quantities of one non-tumor-reactive and one tumor-reactive CD8$^+$ T-cell clone during vaccination.

For patient NW1789, frequencies of one non-tumor-reactive and one tumor-reactive CD8$^+$ T-cell clone were determined using quantitative real-time PCR prior to and during vaccination with NY-ESO-1 peptide. RT-PCR was performed for the corresponding T-cell receptor DNA and normalized to CD8 DNA to determine absolute frequencies. Mean frequencies from at least five independent experiments are shown.

For patient NW1789, primers specific for the CDR3 region in combination with PCR-specific probes could be designed for both tumor-reactive and non-tumor-reactive CD8$^+$ T-cell clones. As can be seen in Figure 30, tumor-reactive and non-tumor-reactive T-cell receptor sequences were already detectable before vaccination, in line with a recent report from *Germeau and colleagues* (109). Furthermore, the frequency of the non-tumor-reactive CD8$^+$ T-cell clone was significantly higher (day 1) compared with the tumor-reactive CD8$^+$ T-cell clone. After the second cycle of vaccination, the frequency of the non-tumor-reactive CD8$^+$ T-cell clone was further increased (4-fold, day 43). However, after addition of GM-CSF to the vaccine formulation, the frequency of the non-tumor-reactive CD8$^+$ T-cell clone declined to a level below the start of vaccination (day 64) and remained steady for another vaccination cycle (day 85). Albeit the base frequency of the tumor-reactive CD8$^+$ T-cell clone was significantly lower on day 1, there was an 18-fold increase after two cycles of NY-ESO-1 peptide vaccination. Similarly to the non-tumor-reactive CD8$^+$ T-cell clone, following this expansion, a contraction occurred during later vaccine cycles.

4.9.3. Existence of non-tumor-reactive CD8$^+$ T-cell clones predicts poor survival

In the above mentioned study from the group of *Thierry Boon*, the level of tumor-reactive CD8$^+$ T-cell clones was not higher in three patients with

regression of tumor load than in two patients with progressive disease (109), implicating that the expansion of tumor-reactive $CD8^+$ T-cell clones is not predictive for anti-tumor response. Consequently, other T-cell subsets are needed to predict response towards peptide vaccination.

Conversely, we assumed that non-tumor-reactive $CD8^+$ T-cell clones would adversely affect survival of vaccinated cancer patients. To test this hypothesis, survival of 17 patients was correlated to the existence or absence of non-tumor-reactive $CD8^+$ T-cell clones. Individuals were divided into three groups based on the existence of tumor-reactive and non-tumor-reactive $CD8^+$ T-cell clones. The "non-reactive" group included all those patients with existence of non-tumor-reactive but not of tumor-reactive $CD8^+$ T-cell clones (n=5). The "non-tumor-reactive" group included (n=6) those with reactive as well as non-tumor-reactive $CD8^+$ T-cell clones. The "tumor-reactive" group included the remainder patients that showed only tumor-reactive $CD8^+$ T-cell clones as a result of vaccination (n=6).

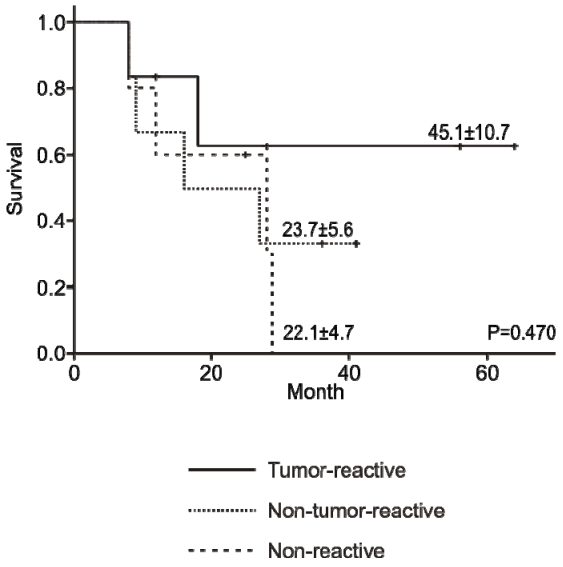

Figure 31 | Kaplan-Meier curves for accessible patients available analysis

Kaplan-Meier curves were calculated for overall survival of 17 cancer patients. According to their T-cell reactivity, patients were divided into three groups as described in the Material and Methods section.

Survival was different for the three groups, although due to the small number of patients included not statistically significant ($p = 0.470$, Fig. 31). Patients with existence of non-tumor-reactive $CD8^+$ T-cell clones experience a higher death hazard as compared to those with existence of tumor-reactive $CD8^+$ T-cell clones. Interestingly, the existence of non-tumor-reactive $CD8^+$ T-cell clones is a predictor of death, independent of the existence of tumor-reactive $CD8^+$ T-cell clones, as both patients with only non-tumor-

reactive $CD8^+$ T-cell clones as response to vaccination (non-reactive group, Fig. 31) as well as patients with both tumor-reactive and non-tumor-reactive (non-tumor-reactive group) $CD8^+$ T-cell clones experience a higher death hazard compared to those patients with only tumor-reactive $CD8^+$ T-cell clones in response to vaccination (tumor-reactive group, Figure 31).

5. Discussion

The existence of circulating T cells specific for malignant melanoma antigens but unresponsive to malignant melanoma cells by means of cytotoxicity has been described and this subset of T cells can represent more than 2% of the total peripheral $CD8^+$ T cells in malignant melanoma patients (175). In parallel, observations indicate that a subset of T cells infiltrates malignant melanoma nodules and shows antigen-specificity, but fails to reduce tumor burden (288). The molecular and functional characteristics of this T-cell subset in the immune response towards malignant melanoma are unknown.

5.1. Phenotypic classification of non-tumor-reactive $CD8^+$ T-Cell Clones

Examination of T cells isolated from malignant melanoma patients has provided evidence connecting T_{EM} and T_{CM} phenotypes to cytotoxicity against malignant melanoma cells. Whereas naïve $CD8^+$ Melan-A-specific T cells show a defective immune response to Melan-A peptide *ex vivo* and terminally differentiated T effector cells are associated with an ineffective clinical antitumor immunity (218), $CD45RA^-CCR7^-$ T_{EM} cells as well as $CD45RA^-CCR7^+$ T_{CM} cells were shown to account for up to 15% and 30% of $CD8^+$ T cells in murine malignant melanoma tissue, respectively (315), and were shown to be effective in antitumor cytotoxicity (366). Despite initially different kinetics in the acquisition of effector function were proposed (272, 314), several recent analyses have shown that central as well as effector $CD8^+$ T cells exhibit only minimal differences in terms of immediate effector functions such as cytotoxicity and cytokine production (257, 316, 348). As both non-tumor-reactive as well as tumor-reactive $CD8^+$ T-cell clones subsets bare a T_{CM} phenotype, merely different designations in terms of effector type classification are unlikely to explain the functional differences we have observed so far. Furthermore, both tumor-reactive and non-tumor-reactive $CD8^+$ T-cell clones do not show terminal differentiation, which has been associated with impaired tumor-cell lysis, and would imply regaining of CD45RA expression (47, 123). Especially in the setting of tumor immunity, terminally differentiated T cells have been described failing to lyse tumor cells. The $CD8^+$ T-cell clones observed here are T_{CM} cells and are not terminally differentiated, as reaquisition of CD45RA expression would be a prerequisite for terminal differentiation. As shown in Figure 12, tumor-reactive

$CD8^+$ T-cell clones are negative for CD7, suggesting that these T cells are fully differentiated. In contrast, non-tumor-reactive $CD8^+$ T-cell clones show high expression of CD7, which recently has been associated with a lack of full effector function (1). Additional cell surface molecules that further describe this T-cell subset are CD25 and CD69. Both CD25 and CD69 are highly expressed in the non-tumor-reactive $CD8^+$ T-cell clones, but not or only slightly in the tumor-reactive $CD8^+$ T-cell clones, respectively, suggesting a functional involvement in the observed T-cell phenotype.

As can be seen in Table 4, the particular tumor-reactive and non-tumor-reactive $CD8^+$ T-cell clones differ considerably in their CDR3 base sequence clearly indicating that these T cells are from different origin. Since CDR3 regions determine the binding avidity of the TCR-peptide-MHC-complex, the observed sequence differences in the CDR3 regions likely lead to functional differences (32, 72, 258). This together with differing CDR1/CDR2 regions might explain the observed reduced binding affinity of the TCR to its cognate pMHC-complex.

Surprisingly when assessing the T-cell receptor signaling pathways, non-tumor-reactive $CD8^+$ T-cell clones showed no defect in phosphorylation of CD3ζ and ZAP-70 on polyclonal stimulation with CD3 and CD28 (see Figure 23). These findings strongly argue against a state of anergy in non-tumor-reactive $CD8^+$ T-cell clones associated with reduced phosphorylation of early T-cell receptor signaling molecules as has been described (280). Additionally, non-tumor-reactive $CD8^+$ T-cell clones showed a significant increase in phosphorylation of ERK upon optimal stimulation, which could also be observed for NF-κB, albeit to a lesser extent, while phosphorylation of p38 was comparable in both subsets. Consequently, the observed partial activation status of non-tumor-reactive $CD8^+$ T-cell clones is unlikely to be linked to impaired T-cell receptor signaling.

5.2. Tolerance maintainance in non-tumor-reactive CD8$^+$ T-cell clones

5.2.1. Current model of ligand discrimination by CD8$^+$ T cells

Several models exist that explain the intrinsic discrimination capacity of T cells towards the pMHC complex.

Structurally, X-ray crystallography of agonist and non-agonist pMHC bound to T-cell receptors show no conformational change specific for agonistic compared to non-agonistic pMHC (78, 107). Additionally, the conformational change of the CDR3 helix upon peptide binding is not exclusively unique to agonistic pMHC complexes. Rather the proximal signaling molecules directly interacting with the T-cell receptor may display such a conformational change, but their structures upon TCR engagement remain to be solved (4, 110, 168).

Functionally, the 'kinetic-proofreading concept' postulates that differences in dissociation rates between T-cell receptor and pMHC determine the signaling strength of the T-cell receptor downstream signaling cascade (191, 209). Slow dissociation rates are typical for agonists, produce stronger T-cell receptor signals and lead to higher T-cell responses, while weak agonists and antagonists display high dissociation rates and result in small T-cell responses. In this model, a lag time exists between initial binding of a pMHC to the T-cell receptor and full activation of the particular T cell. Upon binding, successive phosphorylation steps are fulfilled and quick dissociation of the pMHC from the T-cell receptor – as observed in low affinity ligands – prevents completion of further signaling steps in the cascade that have not yet occurred. This temporal filter limits the ability of low affinity ligands to induce functional responses. A computational study by *Altan-Bonnet* and *Germain* has shown that this model has a significant drawback. When modeling two proofreading steps which would allow sufficient speed of T-cell activation, functional discrimination between agonist and non-agonist is significantly lower than biologically observed. Even by increasing proofreading steps specificity does not reach the values found biologically, and speed and sensitivity of the T-cell response decrease further to values incompatible with the rapidly initiated T-cell response observed macroscopically and functionally by calcium influx (8). In addition, the amplification process allowing full T-cell activation even upon engagement of

many T-cell receptors by a few agonist pMHC (320) is not sufficient in this model suggesting that additional intracellular amplification is necessary. *Altan-Bonnet* and *Germain* propose a 'feedback control model' which describes a negative feedback loop with emphasis on the role of the signal-regulated kinase ERK (8, 294). It reflects the important observation that highlights the modulative capacities of the inner T-cell receptor downstream cascade itself in ligand discrimination. It also better accounts for the fact that potency of a given pMHC to activate a T cell varies during intrathymic differentiation and pMHC's that are non-agonistic in the periphery elicit functional responses in developing thymocytes (131, 132, 193, 245).

Independent from these models which describe regulative motifs intrinsic to the T-cell receptor signaling cascade, each T cell can vary its sensitivity to antigen by comprehension of other signaling pathways. These widely unsolved pathways contribute variable amounts of molecules modulating T-cell sensitivity especially during but not limited to thymic development, including EGR1 and miR-181a, for example (183, 224), the above described mechanism of 'coreceptor tuning' (242), and molecules that render T cells anergic upon forced expression despite high pMHC affinity, as shown with $p27^{kip1}$ (182). Therefore these influencing factors have to be considered when analyzing T-cell responses.

5.2.2. Lck-mediated block in T-cell cytotoxicity and proliferation

CD45 mediated dephosphorylation of Lck tyrosine p505 upon T-cell receptor engagement is critical for the initiation of T-cell receptor signaling and proper T-cell activation. CD45-deficient T-cell clones exhibit a significant increase in Lck p505 phosphorylation, even upon strong polyclonal T-cell receptor engagement by cross-linking CD3 and CD28 mirroring deficient downregulation of Lck-p505 phosphorylation (208, 211, 235). CD45-deficient T-cell clones exhibit a phenotype diminished in its cytolytic capacity by means of decreased maximal lytic capacity and half-maximal effector/target ratio, of particular importance being that residual cytolytic activity remains specific (342). Furthermore, a role of Lck p505 phosphorylation has been suggested in the induction of $p27^{kip1}$ in human $CD4^+$ T cells, resulting in inhibition of T-cell function (48). Concordant to non-tumor-reactive $CD8^+$ T-cell clones, $CD45^{-/-}$T-

cell clones proliferate weakly though reproducibly. The ability to produce cytokines such as IFN-γ in response to T-cell receptor signaling is reduced as well in both $CD45^{-/-}$and non-tumor-reactive T-cell clones. This is in line with experimental data of NY-ESO-1 specific non-tumor-reactive $CD8^+$ T-cell clones.

5.2.3. Block in functionability by CD69 and the TGF-β pathway

It is an interesting but contradictory finding that non-tumor-reactive $CD8^+$ T-cell clones express a higher amount of some activation markers. T-cell activation markers, in particular CD25 and CD69, have been linked to T-cell activation by qualitative means, e.g. expressed versus not expressed, upon antigen encounter. When measuring CD25 and CD69 quantitatively, we could show that the amount of CD25 and CD69 in the non-tumor-reactive $CD8^+$ T-cell clones is inversely correlated to the affinity of TCR-pMHC recognition. With regard to CD8 in the 'co-receptor tuning model' (242), where experimental results have implicated an inverse correlation of TCR affinity/CD5 expression to CD8 expression, it has been shown that surface expression of molecules influencing T-cell responsiveness is modulated upon T-cell receptor triggering.

In a proposed model with inhibited T-cell function upon low affinity antigen exposure, reports concerning the function of CD25 and CD69 in T-cell homeostasis have to be comprised in the assessment. CD69 is generally expressed on activated T cells. When quantitatively measuring CD69 expression upon different strength of T-cell stimulation, e.g. optimal versus suboptimal doses, CD69 expression is strongest at suboptimal stimuli, but declines with signal strength (63).

How is elevated expression of CD69 linked to a T-cell phenotype brought into context with division arrest anergy? $CD69^+$ T cells have been shown to be hypo-responsive, and $CD69^{-/-}$ mice develop an exacerbated form of chronic autoimmune arthritis arguing that CD69 has a silencing role in T-cell activation (128, 276). The mechanism by which CD69 engagement silences T cells have been described to comprise the production of TGF-β, and TGF-β induces $p27^{kip1}$ expression resulting in a phenotype associated with division arrest anergy (246, 276, 285, 312, 352). Hence, down-regulation of CD69 on NK cells leads to enhanced NK cytotoxic activity, reduction in NK-cell TGF-β production and induces antitumor responses *in vivo* (91). Furthermore both CD69 and

CD25 are up-regulated upon stimulation in rapamycin induced T-cell anergy highly resembling ‘division arrest anergy’ as discussed below (249). Precise analysis of CD69 expression in T cells with differing T-cell receptor affinities for a given pMHC has not been described, but its enhanced expression after suboptimal stimulation may reflect a regulatory feature of suboptimal signal strength in these T cells important for keeping the T cells actively inhibited.

Another mechanism which comprises CD69 expression and affects T-cell sensitivity has recently been described. MicroRNA’s, small non-coding RNAs with a length of approximately 22 nucleotides, modulate gene expression post-transcriptionally by binding to target sequences in the 3’ untranslated regions of mRNAs resulting in mRNA degradation and control T-cell development (49). miR-181a is a microRNA with restricted expression in the hematopoetic system. Interestingly, identified target genes include BCL-2, the TCR α-chain, CD69 and EGR1 (224). High expression of miR-181a is associated with enhanced T-cell sensitivity and down-regulation of the four proteins mentioned (183). The amount of mRNA of these exact molecules is elevated, suggesting a potential upstream regulative motif targeting miR-181a, and may lead to dampened reactivity of non-tumor-reactive $CD8^+$ T cells towards malignant melanoma and other tumors (173).

5.2.4. Molecular fingerprint of non-tumor-reactive CD8$^+$ T-cell clones

During T-cell activation, T-cell receptor signaling initiates a genetic program, leading to distinct expression patterns which subsequently result in clonal expansion and differentiation of naïve T cells into different mature subclasses such as effector, regulator or memory T cells. Hence, characteristic expression patterns reveal changes in T-cell activation, signal transduction and cell cycle control varying in different T-cell subsets (9, 54). Non-tumor-reactive CD8$^+$ T-cell clones show a remarkable different set of regulated genes with attributes of T-cell activation and T-cell anergy, with 13 genes down-regulated and 12 genes up-regulated.

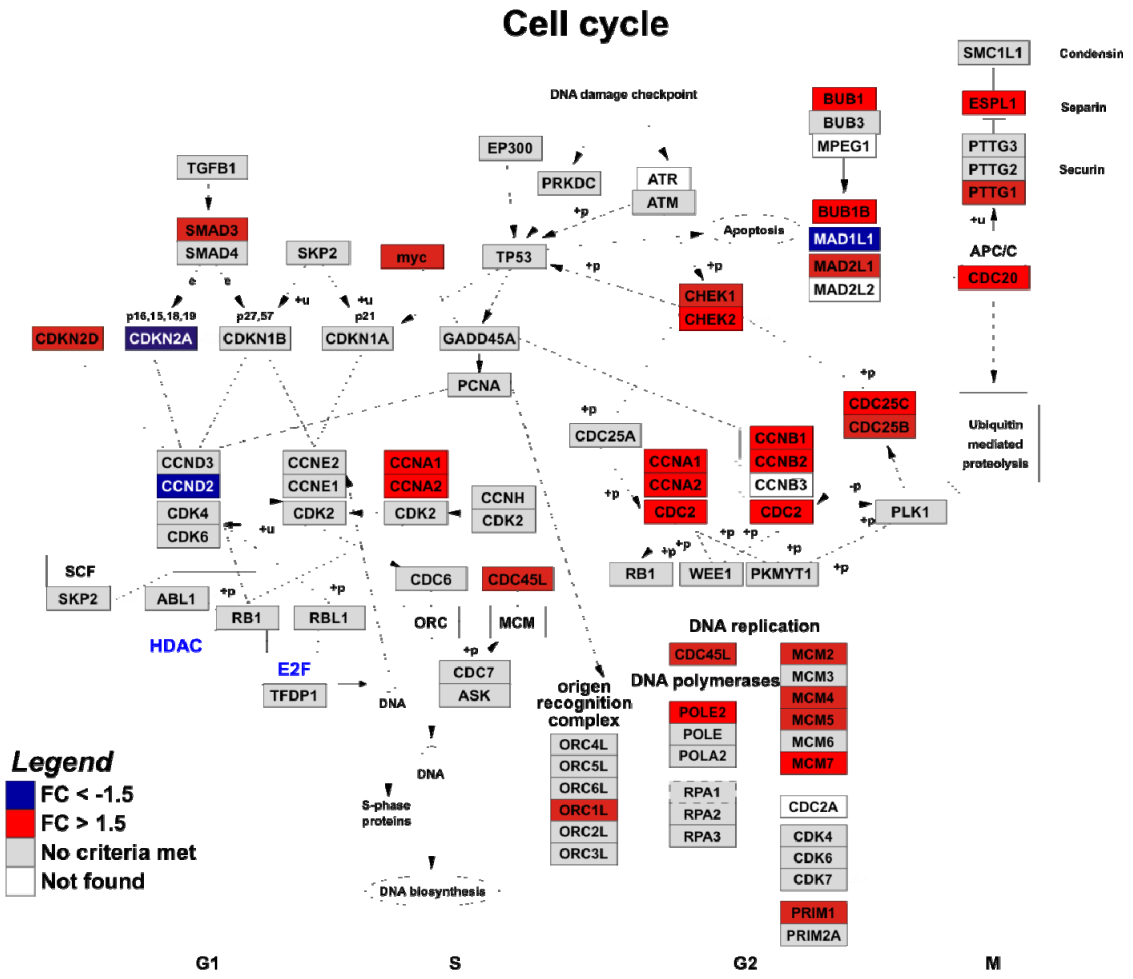

Figure 32 | Gene-expression differences in non-tumor-reactive CD8$^+$ T-cell clones

High-resolution visualization of changes in gene-expression between tumor-reactive and non-tumor-reactive CD8$^+$ T-cell clones within cell-cycle associated genes. Genes with increased expression (fold change (FC) > 1.5, $p < 0.05$) are highlighted in red, genes with decreased expression (FC < -1.5, $p < 0.05$) are highlighted in blue. Mean expression values from 2 tumor-reactive and 2 non-tumor-reactive CD8$^+$ T-cell clones are shown. This figure was generated using GenMAPP 2 software (274).

5.2.4.1. Genes specifically up-regulated in non-tumor-reactive CD8$^+$ T-cell clones

Among the up-regulated genes, KLF2, EGR1, VDR, BCL3, CEBPβ, TIMP1, IFITM2, GZMB, ADAM19, END1, HPGD and SLC27A2 were identified. These genes up-regulated in non-tumor-reactive CD8$^+$ T-cell clones can broadly be grouped into two main groups. At first, genes that are involved in T-cell quiescence and support a T-cell anergy state, which despite insufficient T-cell receptor activation may guarantee survival for future stimuli cognate to the antigen by exerting their anti-apoptotic function. Secondly, genes which hold the T cell in a cell cycle block, in part from G1 to S phase, in part from S to G2 phase. Importantly, although several pathways converge in genes initially defined as pure cell cycle repressors, more and more experimental evidence suggests additional roles beyond cell cycle control in T-cell differentiation, maybe the latter being a consequence of the former function (182).

Molecules involved in signal transduction and immune modulation

Among the signal transduction and immune modulation molecules that are up-regulated in non-tumor-reactive CD8$^+$ T-cell clones, there are several genes brought into context with T-cell anergy.

Krüppel-like factor 2 (KLF2) is a member of zinc-finger transcription factors and is postulated to regulate T-cell homeostasis by promoting T-cell quiescence via up-regulation of cyclin-dependent kinase inhibitor p21WAF1/CIP1. Additionally, KLF2 has been shown to be essential for T-cell trafficking (15, 37, 45, 353).

The Vitamin D receptor (VDR) has potent ability to block antigen specific T-cell responses (26) by inhibiting the NFAT complex formation (301), direct repression of the IL-2 promoter (7) and IFN-γ production (206).

Granzyme B is one of the pivotal proteins in T-cell mediated cytotoxicity. Its major function is the activation of caspases in target cells during cytotoxic lymphocyte granule-induced apoptosis. Although anergic T cells are not cytotoxic they retain the capacity to express IL-2R and granzyme B (298).

Transcription factors

EGR1 is over 9 fold up-regulated in non-tumor-reactive $CD8^+$ T-cell clones. Upregulation of EGR1 in non-tumor-reactive $CD8^+$ T-cell clones is consistent with reports linking high amounts of miR-181a to both reduced expression of its target EGR1 and increased T-cell sensitivity towards pMHC. Interestingly, in the context of 'T-cell division arrest anergy', EGR1 selectively up-regulates $p21^{Cip1}$, beside p27kip1 a factor of cell cycle blockade from G1 to S phase, and down-regulates cdk2 level (255). EGR1 might also partly explain the elevated levels of CD28, as surface expression of CD28 is elevated upon EGR1 expression (44, 187).

The transcription factor BCL3 belongs to the IκB family of proteins and, like other IκB proteins, interacts with the NF-κB transcription factor. Upregulation of BCL3 by mitogenic stimuli represses tumor necrosis factor (TNF)-induced NF-κB transactivation (27, 233) and hence, IL-2 transcription and T-cell activation (259).

The high amounts of c/EBPβ together with EGR1 highlight their combinatory action on a number of gene targets, as an important mechanism of EGR1 in the regulation of target genes is its protein-protein interaction with c/EBPβ (365). c/EBPβ may also have other interactions in the observed anergic phenotype in non-tumor-reactive $CD8^+$ T-cell clones. The c/EBPβ gene encodes a member of the basic leucine zipper family of transcription factors (74). It shows an antiproliferative effect on a multitude of cell types with forced expression arresting the cells at the transition from the G1 to the S state (36, 368). Of particular interest, C/EBPβ-knockout mice display a lymphoproliferative disorder, suggesting an inhibiting role for C/EBPβ in lymphocyte activation and proliferation (283). PGE_2 is another molecule that has been implicated in T-cell unresponsiveness by inducing phosphorylation of Lck p505 and subsequent upregulation of $p27^{kip1}$ (48). Whether this is the only downstream protein by which PGE_2 exerts its repressive function on T cells is not yet fully understood. Interestingly, PGE_2 has been reported to use c/EBPβ to influence gene expression in T cells (87), as c/EBPβ is a downstream molecule of the PGE_2 pathway. There are further strinking interactions with molecules involved in T-cell unresponsiveness by PGE_2, TGF-β and CDK inhibitors.

At first, c/EBPβ is highly similar in its protein sequence to c/EBPα. c/EPBα has two distinct functions. It influences transcription by use of its DNA binding domain and inhibits the kinase activity of cyclin dependent kinases. Hereby, a short region of the c/EBPα polypeptide interacts directly with cdk2 and cdk4 in a manner that prevents cyclin binding and inhibits cell proliferation (335). This cdk2 binding domain consists of 9 aminoacids which are strongly conserved between c/EBPα and c/EBPβ (Figure 33). Especially the proline rich region is necessary to induce cell cycle arrest. These proline rich residues are strongly conserved between c/EBPα and c/EBPβ suggesting similar if not same function in both proteins regarding cdk2 and cdk4 inhibition.

Figure 33 | Conserved amino acids in the cdk2-binding domaine of c/EBPα and c/EBPβ

Figure showing the conserved amino acids in the binding domains for cdk2 of c/EBPα and c/EBPβ. The cdk2 binding domain of c/EBPα constitutes amino acids 174 to 188 (RefSeq NP_004355). The cdk2 binding domain of c/EBPβ constitutes amino acids 156 to 170 (RefSeq NP_005185).

The transcription factor c/EBPα by means of its cdk binding domain therefore mediates growth arrest via a mechanism unrelated to its influence on gene expression (210), but it has yet to be proven directly that c/EBPβ exerts its anti-proliferative effect on non-tumor-reactive $CD8^+$ T-cell clones by the same mechanism.

Second, there is data connecting TGF-β, SMAD3, c/EBPβ and FOXN1 to increased levels of $p21^{cip1}$. Physiologically, upon engagement, the TGF-β receptor complex phosphorylates Smad2 and Smad3 transcription factors. In turn they translocate into the nucleus, bind Smad4, associate with other DNA binding factors and induce specific regulative genes such as $p21^{cip1}$ (205) that mediate cell growth arrest.

A role of the interferon induced transmembrane protein IFITM2 in anergy has not been described, as not much is known about its physiological role.

Cell proliferation

The erythroid potentiating activity (EPA) and tissue inhibitor of metalloproteinases (TIMP) represent two distinct activities of a single protein. Beside its function as a secreted inhibitor of metalloproteinases, TIMP1 promotes cell proliferation in different cell types (125). The description of an influence of TIMP1 on the IL-2 network has so far only been described in mathematical models than in a causal model (61). A direct molecular role in T-cell activation or cytotoxicity has not been described.

5.2.4.2. Genes specifically downregulated in non-tumor-reactive CD8$^+$ T-cell clones

Among the down-regulated genes, XCL1, RORα, CHES1/FOXN3, ASAH1, C6orf111, GNPTAB, GOLGA8B, RBPSUH, SYNE2, TRIM22, XCL2, XIST and ZNF160 were identified. Three of these genes have been previously associated with T-cell activation or T-cell effector function. They function in the transcription of IL-2, the hallmark of sufficient T-cell activation and basis of subsequent transfer from G1 into S and S into G2 phase or have been attributed to T-cell activation by other regulative functions.

Molecules involved in signal transduction and immune modulation

XCL1 is a member of the γ-class of chemokines (370). The production of XCL1 is associated with CD5 expression of CD8$^+$ T cells, questioning a role for T-cell receptor modulation as described for the cytokine IL-7 (242). Beside its function as chemokine in leukocyte migration (6, 126), up-regulation of XCL1 has been described in T cells stimulated with agonist peptide while no significant expression could be observed in unstimulated CD8$^+$ T cells or cells stimulated with irrelevant peptides (238, 239).

Cell cycle

CHES1 is a human forkhead protein. It directly interacts with the C-terminus of SKIP, a nuclear protein involved in regulating cell growth and differentiation through the TGF-β pathway (179, 281). Depending on the cell type, SKIP augments or represses VDR mediated transcription, and deleting SKIP's C-terminus suppresses the protein's ability to augment VDR transcription (21, 180). CHES1's binding to SKIP might occupy its C-terminus

and abolish its effect on VDR mediated transcription, but it is difficult to rule out an opposite function in T-cell cell-cycle. Obviously, the non-tumor-reactive $CD8^+$ T-cell clones are kept in a non-proliferative state, and down-regulation of a cell-cycle suppressor might be the result of a negative feedback loop.

Transcription factors

The retinoid acid-related orphan receptor alpha (RORα) is highly expressed in single-positive $CD8^+$ T cells and downregulated in $CD8^+$ mature T cells. T-cell receptor engagement does not change RORα expression, and it is unlikely that only its expression status can reflect its state of action. It exists in an active and repressive state, dependent on the activation of Ca^{2+}/calmodulin-dependent kinase IV (CaMKIV) (145), and as Calcium influx is part of T-cell activation upon stimulation, activation of CaMKIV likely enhances ROR-mediated transcription of certain genes. Consistently, though it is not essential for the proliferation of T cells upon stimulation, it elevates cytotoxicity during activation (88, 89). Its role in T-cell activation is further supported by *in vivo* models, where targeting its activity with a specific ligand shows antiarthritic activity (216). Although non-tumor-reactive $CD8^+$ T-cell clones show markers of activation, RORα as well as EGR1 are downregulated.

Molecules organizing the cytoskeleton

Syne2 (Nesprin-2) is a component of the outer and inner nuclear membrane and associates directly with lamin A/C and emerin (186). In muscle cells**,** Nesprin-2 associates with myofilaments (367), so it might play a role in leukocyte movement as well, but a specific function in lymphocyte biology has not been described so far.

5.2.5. Control of cell cycle by at least two mechanisms in non-tumor-reactive CD8$^+$ T-cell clones

An important pathway linking cell cycle blockade and T-cell anergy is the "division arrest anergy" first described by *Wells et al.* (344). After this initial report, the importance of the cell cycle inhibitor p27^{kip1} has been delineated in various settings of immune regulation with p27^{kip1} linked to a general pathway of T-cell tolerance different than that described for adaptive tolerance or clonal anergy.

Upregulation of p27^{kip1} usually occurs in the growth arrest phase of cellular differentiation. Forced expression of p27^{kip1} blocks cell proliferation (246, 247, 312) and inhibition of p27^{kip1} both inhibits down-regulation of cdk activity and exit from cell cycle (58, 261). With respect to T cells, p27^{kip1} can be induced by starvation from mitogens and consecutively binds to the cyclin E-cdk2 complex inhibiting its effect on cell cycle progression (59). Upregulation of other factors has been shown to compensate for or to cooperate with p27^{kip1} in respect to cell cycle inhibition, as p130 (59) and c/EBPα (335), for example.

Various studies characterizing anergic/tolerized T cells have proposed that the central gap is the failure to activate mediators of the cell cycle progression from G1 to S phase (33, 120, 249, 270, 345). Pharmaceutical blockade at the G1 phase by rapamycin despite sufficient co-stimulation and IL-2 induces T-cell tolerance, whereas blockade at the S phase by hydroxyurea does not, suggesting a causative role for G1-S phase block in this type of T-cell tolerance (249). In 2006, *Li et al.* systematically assessed the requirement for G1 phase block and the involvement of p27^{kip1} in tolerance induction of CD8$^+$ T cells (182). They found that mice lacking the cdk-binding domain of p27^{kip1} are resistant to tolerance induction and progress from G-to S-phase despite tolerizing treatment, a result in line with previous suggestions. In 2006, *Rudd* published a model (see Figure 34) connecting the role of p27^{kip1} and IL-2 in the blockade of T-cell function (270).

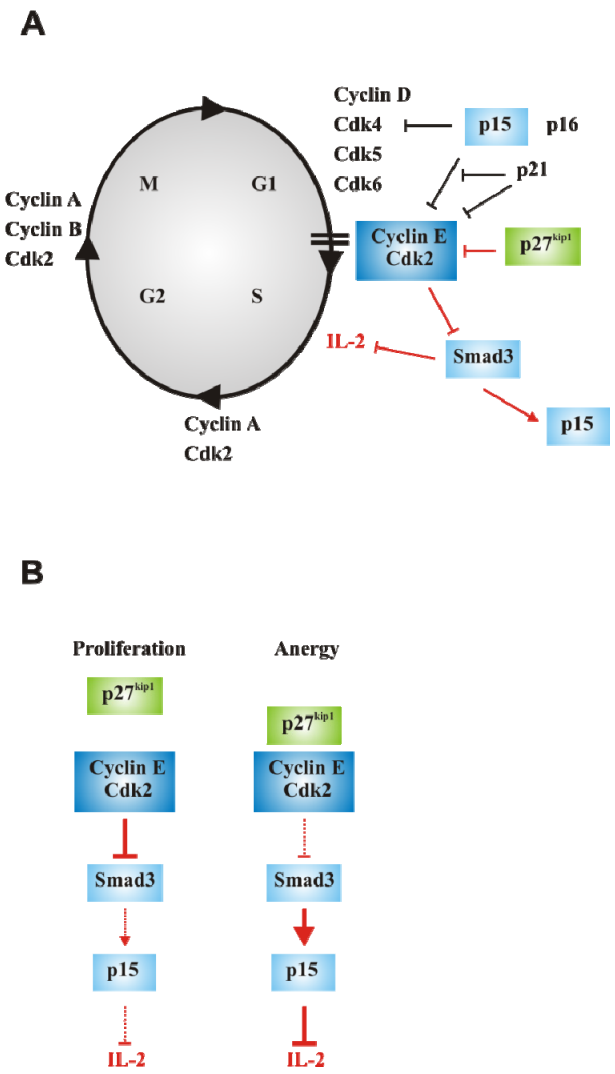

Figure 34 | Model of CD8$^+$ T-cell division arrest anergy

A. Cell cycle regulation. In order to transit from one cell cycle phase to another, expression of particular cyclin-cdk complexes is required. Cyclin E-cdk2 complex drives the transition from G1 to S phase, whereas cyclin A-cdk2 and cyclin A-cyclin B-cdk2 complexes force transition from S to G2 and from G2 to M phase, respectively. p27^{kip1} binds and inhibits the cyclin E-cdk2 complex. Cdk2 itself phosphorylates Smad3 and inhibits therefore its increasing function towards p15 (Cdk inhibitor 2B) and its inhibiting function towards IL-2. Independently from p27^{kip1}, p21^{Cip1} and p15^{Ink4B} inhibit cdk4, which is needed for G1 progression. Adapted from Rudd et al. (270).

B. Model of p27^{kip1} influence on T-cell function. p27^{kip1} binding leads to inhibition of cyclin E-cdk2 complex and inhibitory phosphorylation of Smad3 is reduced. Smad3 activity and consecutive p15^{Ink4B} expression are increased, which leads to inhibition of IL-2. Conversely, upon proliferative stimuli, p27^{kip1} expression or its binding to cyclin-E-cdk2 complex are reduced, resulting in increased phosphorylation of the inhibitory residue 212 of Smad3, reduction in p15 and IL-2 transcription. Adapted from Rudd et al. (270).

Integration of the molecular changes observed in non-tumor-reactive CD8$^+$ T-cell clones allows an integrated model of T-cell inhibition adapted from the one proposed by Rudd et al. as proposed in (Figure 35).

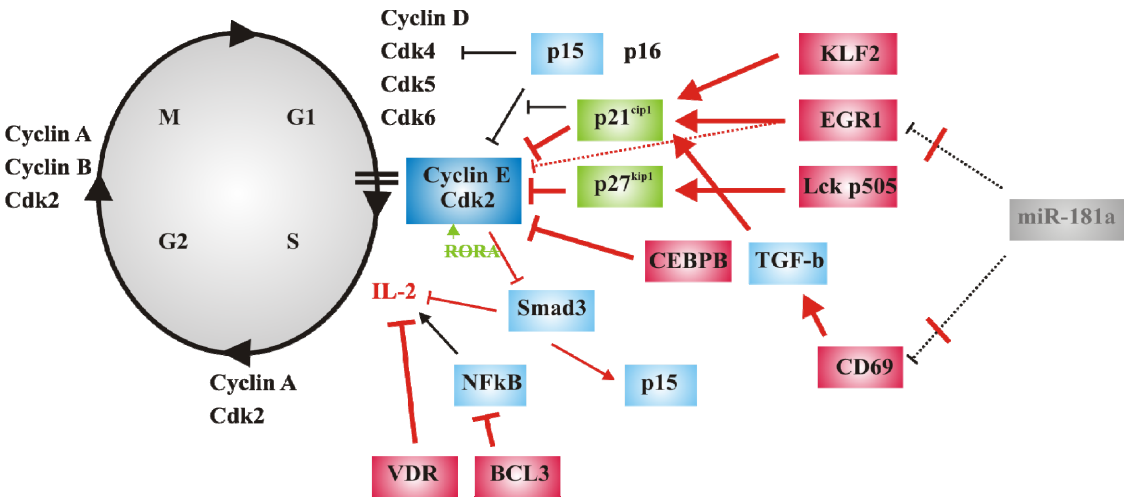

Figure 35 | Replenished model of CD8$^+$ T-cell division arrest anergy

Model of tumor associated division arrest anergy integrating cell surface expression, intracellular protein content and genomic data of non-tumor-reactive CD8$^+$ T-cell clones. This model shows the two main contact points at which the anergic phenotype is controlled. Association of cdk2 with p27^{kip1} is likely to be the primary mechanism by which cdk2 is inactivated, but additional molecules can regulate cdk2 in the absence of p27^{kip1} as well. p21^{cip1} (induced by EGR1 and KLF2), EGR1 directly and c/EBPβ directly inhibit the cyclinE-cdk2 complex. High levels of p27^{kip1} are maintained by Lck p505. IL-2 transcription is concertedly inhibited by VDR and BCL3. Adapted from Rudd et al. (270).

One puzzling observation reported in experiments with forced expression of p27^{kip1} (182) and the basis for us to generate clones from a single anergic T cell is the ability to expand these cells despite high amount of p27^{kip1}. In the context of these pathways, p27^{kip1} was initially reported to be involved in cell cycle control, and p27^{kip1} expression should result in blockade of the cell cycle in T cells primed in tolerizing conditions and allow at best minimal expansion of this tolerized subset of T cells. Interestingly, *Li et al.* reported equal numbers of cell divisions in both tolerized T cells and T cells with p27^{kip1} mutants that lacked the cdk-binding domain with >50% of cells undergoing four or five rounds of cell cycle division. This at least in part explains the elevated levels of non-tumor-reactive CD8$^+$ T-cell clones despite the existence of a cell cycle block associated with expression of p27^{kip1}. The observed changes in gene expression may further explain the synchronous existence of an anergic phenotype with the observed expansion of anergic T cells despite high amounts of p27^{kip1} with recently published work able to reconcile this discrepancy. Spatial segregation of p27^{kip1} from its targets in the nucleus seems to allow p27^{kip1} to exert functions accessory to its cell cycle blocking influence. High expression of EGR1 induces expression of cyclin D2, which translokates p27^{kip1} out of the

nucleus (299). This might allow the highly expressed cdc2, cdc20 and cyclin B1 to drive the anergic T cells through the cell cycle whereas the high amounts of $p27^{kip1}$ outside the nucleus render the T cells anergic through cell cycle independent mechanisms.

5.3. Correlation of non-tumor-reactive CD8$^+$ T-cell phenotype with T-cell phenotypes in T-cell tolerance

As mentioned above, T-cell tolerance is associated with several distinct T-cell phenotypes. In general, tolerant T cells as well as T cells endowed by other functions than cytotoxicity could present as non-tumor-reactive T cells. Consequently, several T-cell types with impaired effector function have to be considered.

One T-cell subset showing an anergic phenotyp with respect to cytotoxicity but with distinct other functional properties is the CD8$^+$CD28$^-$ suppressor T-cell subset. Instead of inhibiting other T cells directly, $T_{suppressor}$ cells recognize peptides on APC and lead to downregulation of co-stimulatory molecules on their surface. These cells do not proliferate upon restimulation (146, 189). Like non-tumor-reactive CD8$^+$ T-cell clones, they express CD45RA and GITR upon stimulation, but neither express CD28, CD45RO, CD27 nor CCR7, all expressed on non-tumor-reactive CD8$^+$ T-cell clones, and are also negative for OX40, CD103, 4-1BB, which are also expressed on non-tumor-reactive CD8$^+$ T-cell clones (282).

T-cell phenotypes associated with anergy in a more narrow sense can be divided in several distinct molecular pathway blocks which result in an anergic phenotype.

The prototype of anergy is clonal anergy in T cells. These cells present distinct biochemical alterations upon activation with an early block in T-cell receptor activation with phosphorylation of LAT and ZAP-70, while Phospholipase Cγ1 is decreased (280). At the same time the MAPK pathway is inhibited with a reduced activation of ERK and JNK and a defect in phospho-p38 formation (306).

In ‘adaptive T-cell tolerance’, also called ‘*in vivo* anergy’ (244, 280), T cells are generated in the setting of repeated stimulation with strong or even superantigen. This results in an initially rapid expansion after antigen exposure, suggesting T-cell receptor affinity for pMHC to be rather strong. A hallmark of adaptive tolerance is the requirement for antigen persistence to maintain this status (153, 266). Elimination of stimulus enables these cells to regain lytic

functions (265). Thus this status rather reflects a transient defense mechanism against activation induced cell death or a mechanism to prevent overt immune responses.

Comparison of non-tumor-reactive $CD8^+$ T-cell clones defined in this work to different subsets of T cells with impaired or absent effector functions clearly distinguishes them from the subsets described before, with the exception of a small subset recently described as “Division arrest T cells”. It has been noticed that a significant percentage of T cells partially fail to divide following stimulation with anti-CD3 and APC although all cells become ”activated“ as delineated by the expression of the early activation marker CD69. Following restimulation, these T cells only proliferate slightly and exogenous addition of IL-2 confirmed the failure of division not simply to be due to a lack of IL-2. Comparable to non-tumor-reactive $CD8^+$ T-cell clones, it was found that lack of expression of the IL-2α, the IL-2β and the IL-2γ receptor chains are not responsible for this block of proliferation, as they are sufficiently expressed on the surface of these “division arrest” anergic T cells (112, 344). Rather than IL-2 depletion, a profound block in the cell cycle is responsible for the observed phenotype. Under normal circumstances, IL-2 is released in consequence of T-cell activation and leads to downregulation of $p27^{kip1}$, allowing the release of cdk2 from its binding with $p27^{kip1}$ and entry in the transition from G1-to S-phase. In division arrest T cells there exists an intrinsic failure to downregulate $p27^{kip1}$ the exact cause of which has not been delineated so far. This results in an intrinsic block to undergo transition from G1 to S phase (112, 344, 352). In previous reports, the proximal signaling cascade was unaffected with ZAP-70 und lck showing normal phosphorylation. Importantly, these cells show strong CD69 expression upon stimulation and massively impaired IFN-γ production upon stimulation (112).

Non-tumor-reactive $CD8^+$ T-cell clones display the hallmark of ‘division arrest T cells’, high amounts of $p27^{kip1}$. Additionally, genes whose analogy is the down-regulation and/or inhibition of IL-2, e.g. VDR, XCL1, BCL3, and c/EBPβ, are up-regulated suggesting a bimodal cell cycle block at the level of CyclinE-cdk2 and IL-2. Additionally, c/EBPβ leads to the block in cell cycle progression similarly to $p27^{kip1}$.

5.4. CD8$^+$ T cells with low affinity T-cell receptors are actively inhibited rather than solely suboptimal stimulated

Most analyses of T-cell responses, whether directed towards self or non-self antigens, concentrate on overall population responses (82). In this context, assays with bulk population of T cells after antigen exposure have the drawback to solely estimate the overall activation/cytokine production of responding T cells regardless of clonal characteristics. In a model where different T-cell receptor avidities lead to distinct T-cell phenotypes as response to antigen, T-cell receptor avidity is decisive to guide the particular T-cell response to a cytotoxic, memory, cytokine productive or anergic phenotype. As has been shown for T-cell responses of influenza-virus-specific T cells with variable TCR-pMHC avidity, a hierarchy of the T-cell cytokine response pattern can be postulated dependent on T-cell receptor avidity towards pMHC(172).

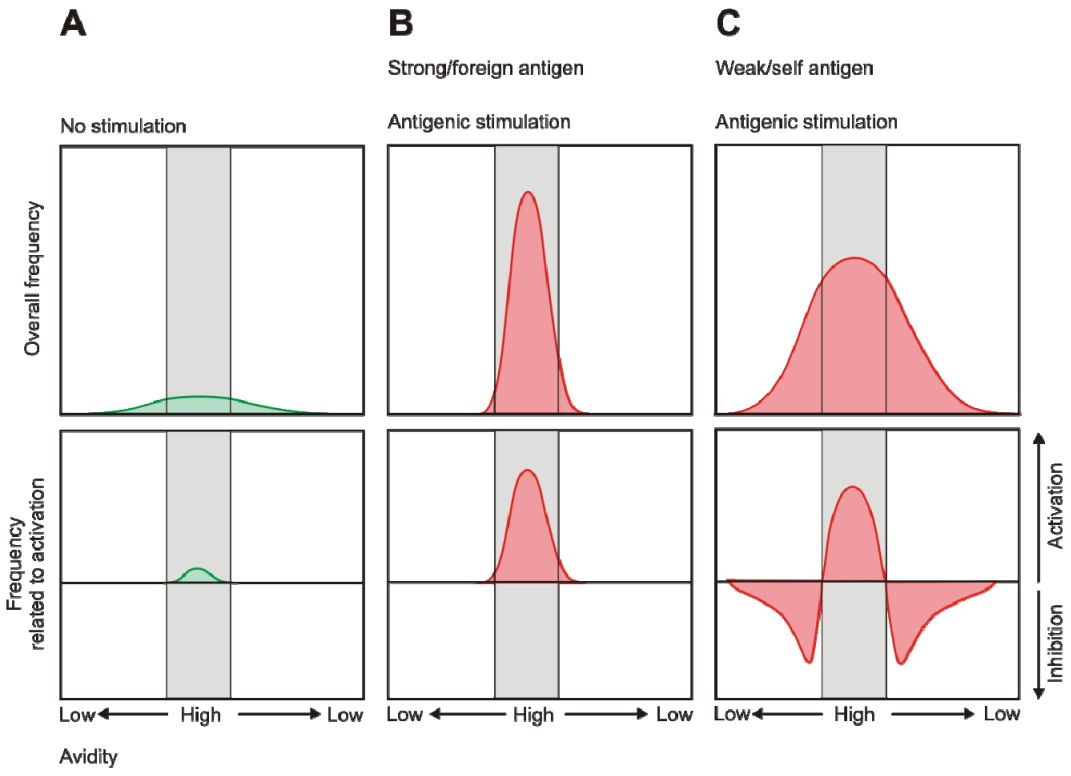

Figure 36 | Model for the outcome after antigenic stimulation of CD8$^+$ T cells

(A) In the absence of an antigenic challenge, T cells are kept alive through recognition of self antigens and common-γ-chain cytokine signals.

(B) Stimulation with a foreign antigen induces strong activation and results in an expansion of T cells with high avidity T-cell receptors for the target antigen.

(C) In the context of tumor-antigens and vaccination, non-tumor-reactive CD8$^+$ T cells with low-avidity T-cell receptors are expanded but actively and antigen-specifically inhibited by mechanisms related to anergy resulting in a population of T cells with unresponsiveness related to division arrest anergy.

Induction of the observed phenotype in non-tumor-reactive $CD8^+$ T-cell clones argues for an alternative outcome of antigenic stimulation, at least for antigens such as NY-ESO-1 (25). It could be shown that T cells with lower affinity for the antigenic peptide are neither deleted nor only sub-optimally activated. Instead, the obtained results argue for an avidity-controlled active inhibitory T-cell feedback loop in the response of T cells, characterized on the clonal level to be in line with a $CD8^+$ T-cell division arrest anergy phenotype. This observation and a proposed inhibitory feedback align with results from T cells expressing two T-cell receptors where binding of an antagonist to one T-cell receptor affects signaling to agonist binding of the other T-cell receptor (79, 263). One such feedback loop has been shown to involve the tyrosine phosphatase SHP-I (294). These $CD8^+$ T cells are not classically "tolerant" since they proliferate, lyse, and produce cytokines *in vitro* upon stimulation with antigen presented by T2 cells.

The T-cell phenotype established here for non-tumor-reactive $CD8^+$ T cells adds another level of complexity to T-cell biology. Other models of T-cell activation have suggested that the low affinity signal “expires” somewhere in the T-cell receptor downstream cascade. The opposite might be true. In the area of a certain (for example +1) standard deviation of the mean towards low affinity with regard to optimal T-cell receptor avidity, it appears that T cells are hold actively inactive by the use of CD69, CD25, and c/EBPβ upregulation converging in p27kip1 expression and expression of “survival molecules” in a state that allows survival despite low stimulation. To bring back in mind: usually, antigen deprived T cells die within short time after a first stimulus when not rescued. This raises the question, why such unresponsive or anergic $CD8^+$ T cells are induced in context of self-antigen stimulation and whether this anergic phenotype is reversible and antigen-specific (25). Since there is a certain promiscuity of any given T-cell receptor for different antigens, the observed inhibitory mechanisms might indeed be antigen-specific and therefore determined by the avidity of the respective TCR/pMHC complex interaction. Non-tumor-reactive $CD8^+$ T cells might result from stimulation with the “wrong” peptide leading to the observed unresponsiveness, a status that is maintained by the molecular profile described here. Consequently, their function might be quickly recovered in response to an unrelated peptide antigen – as simulated

using polyclonal stimulation – where avidity of the TCR/pMHC interaction is significantly higher subsequently leading to productive immunity (25).

5.5. Correlation of non-tumor-reactive phenotype with functional impaired T cells in the setting of malignant melanoma/ tumor immunity

Importantly, it could be shown that antigen-specific T cells can lack effector activity and display tolerance upon antigen exposure despite sufficient growth potential. These T cells lack reactivity with MHC tetramers. During viral infection, it has been observed that only fractions of activated $CD8^+$ T cells ranging from 1-5% (3, 81, 369) up to the major fraction of 50-70% are antigen specific (219). In these experiments, T cells were termed “activated” by means of activation molecules on the cell surface but not termed “antigen-specific” when pMHC-tetramer staining was used. Monitoring T-cell responses by a single technique therefore leads to misconceptions of the nature of an ongoing T-cell response, and other methods have to be included when estimating immune responses toward tumors as well as infections (346).

Only recently, the existence of a subset of T cells has been described, which is generated during tumor vaccination and recognizes peptide-pulsed target cells but not malignant melanoma cells (62, 360). The prevalence of these malignant melanoma antigen-reactive, but non-tumor-reactive $CD8^+$ T cells in malignant melanoma can reach up to 2% (236). Comparison of maturation phenotypes of T cells specific for malignant melanoma antigen provided immunhistochemic evidence for the distribution of tumor specific T cells with different properties in tumor infiltrated lymph-nodes. Here, high granzyme B expression, as in non-tumor-reactive $CD8^+$ T-cell clones, was observed mainly in cells surrounding the tumor rather than in T cells infiltrating the tumor (218).

Other groups have mainly concentrated on describing the tumor-reactive MHC-tetramer-positive $CD8^+$ T-cell subsets, as only those are believed to mediate tumor regression. Consistently, the data presented here illustrates that the immune response towards a self peptide, which is not expressed in the thymus, can generate tumor-reactive cytotoxic T cells. Most importantly, this immune response generates both a tumor-reactive and a non-tumor-reactive $CD8^+$ T-cell pool *in vivo.* In the setting of adoptive T-cell therapy, both the

tumor-reactive and the non-tumor-reactive $CD8^+$ T-cell subset are expanded by repetitive stimulation with the cognate antigen NY-ESO-1 *in vitro* and *in vivo* (25).

This observation is of direct importance for the effectiveness of a T-cell response in the tumor microenvironment. In settings of autoimmunity, the numerical dominance of auto-reactive T cells outcompetes the protective function of accumulating T-regulatory cells (163). Although infusion of malignant melanoma antigen specific $CD8^+$ T cells into patients with metastatic malignant melanoma has indeed shown to result in infiltration in both skin and tumor tissue (361), and levels of antigen specific $CD8^+$ T cells in the blood after adoptive T-cell therapy are increased as has been measured by tetramer staining (198), the observed clinical antitumor response is often insufficient, and this fact cannot be explained solely by antigen escape mechanisms (203). Hints linking insufficient clinical response to distinct T-cell subsets are histological observations of tumor samples, which link distinct populations of T cells within the tumor to survival (57, 214, 277, 337). In a recent study, *Lurquin et al.* showed that both tumor-reactive as well as non-tumor-reactive $CD8^+$ T-cell clones are present inside malignant melanoma metastasis with tumor-reactive $CD8^+$ T-cell clones representing the majority of cells (195). Nonetheless, also antigen-specific, but non-tumor-reactive $CD8^+$ T-cell clones were modestly enriched in metastasis, and survival of patients did not correspond to the level of tumor-reactive $CD8^+$ T-cell clones (109, 195), in line with other reports, which have shown that occurrence of antigen-specific T cells in terms of tetramer-staining often does not correspond to a better prognosis (329).

Once more, the importance of low avidity TCR-pMHC interaction for the outcome of an antigen-directed immune response might be drawn from *in vitro* assays titrating high affinity and low affinity pMHC-tetramers onto T cells (134). As can be shown in these assays, high numbers of low affinity tetramer, figuratively representing low affinity T cells, can compete for a given number of pMHC presented on tumor cells. Similar to the *in vitro* experiments, one could argue for a shift in the equilibrium of the reaction, allowing high numbers of low-affinity T cells (with high CD8 co-expression adding binding energy to the apparent affinity of the low affinity TCR-pMHC complex) to decrease the overall antitumor response of high-affinity T cells to a clinically insufficient level.

Furthermore, non-tumor-reactive $CD8^+$ T-cell clones could block sufficient activation of tumor-reactive $CD8^+$ T-cell clones by depriving the microenvironment of soluble stimulatory molecules, e.g. IL-2.

It is consistently enunciated by *Thierry Boon et al.* that therapeutic success following vaccination may not depend on the overall number of T cells produced by the vaccine but rather on the production of a $CD8^+$ T-cell clone with functional properties that enable it to migrate to the tumor and resist the local immunosuppressive environment to initiate a regression process (31).

Complementing this statement with the observation of the occurrence, biology and importance of non-tumor-reactive $CD8^+$ T-cell clones in the setting of tumor vaccination generates an image, which implicates that indeed the occurrence of non-tumor-reactive $CD8^+$ T-cell clones could be predictive for the clinical response to tumor-peptide vaccination. This $CD8^+CD7^+CD25^+CD69^+$ T-cell subset is characterized by a distinct expression of surface molecules that allows its differentiation from tumor-reactive $CD8^+$ T cells. Furthermore it could be shown that this T-cell subset has distinct functional properties in terms of T-cell receptor responsiveness due to T-cell receptor signaling alterations resulting in phosphorylation of lck p505 with consecutive upregulation of $p27^{kip1}$. This leads to a phenotype described as “T-cell division arrest anergy”, whose characteristic features could be expanded by substantial functional and genomic data. The importance of this T-cell subset in the setting of immunotherapy is supported by survival data, which shows that indeed patients with occurrence of non-tumor-reactive $CD8^+$ T cell-clones experience a higher death hazard compared to those patients with only tumor-reactive $CD8^+$ T-cell clones. In conclusion, the more we learn about the relationship between immune system and tumor we will be able to develop even more effective methods to advance tumor vaccination strategies to manipulate those responses for successful immunotherapy.

6. Summary

Immune-mediated tumor rejection relies on fully functional T-cell responses and neutralization of an adverse tumor microenvironment. Vaccination with tumor-specific antigens induces peptide-specific, but non-tumor-reactive and therefore not fully functional $CD8^+$ T cells. Understanding of the molecular mechanisms behind non-tumor-reactivity is a prerequisite to overcome this $CD8^+$ T-cell deviation. Currently discussed molecular mechanisms of insufficient T-cell responses in the setting of tumor immunotherapy comprise mechanisms ranging from T-cell anergy to induction of classical peripheral T-cell tolerance.

In this work the phenotype of non-tumor-reactive $CD8^+$ T cells specific for NY-ESO-1, a melanoma expressed antigen, were investigated. Sequence analysis of the CDR3 region of $CD8^+$ T-cell clones revealed that the particular tumor-reactive and non-tumor-reactive $CD8^+$ T-cell clones differ considerably in their CDR3 base sequence stressing that these T cells are from different origin. Non-tumor-reactive $CD8^+$ T cells are characterized by low to middle T-cell receptor-pMHC avidity and missing binding of the NY-ESO-1-MHC-tetramer. Non-tumor-reactive $CD8^+$ T-cell clones express CD7, CD25, and CD69, as well as elevated levels of lck^{p505} and $p27^{kip1}$, a molecular program associated with hallmarks of 'division arrest anergy'. This molecular profile was completed with gene expression profiles which were validated using RT-PCR.

To show relevance of this cell population in patients with malign melanoma, blood samples of healthy individuals and patients with malign melanoma were assessed for prevalence of $CD8^+CD69^+CD25^+CD7^+$ T cells. This subset of $CD8^+$ T cells could be detected in patients with malign melanoma, but not in healthy individuals. *In vivo* quantification using a highly concise PCR approach revealed high prevalence of non-tumor-reactive T cells with increased levels during cancer vaccination.

Furthermore, the clinical importance of this cell population is underlined by survival curves, where presence of $CD8^+CD69^+CD25^+CD7^+$ T cells is associated with a shorter survival. The difficult detection of these non-tumor-reactive $CD8^+$ T cells requiring a combination of classical T-cell cloning and quantitative PCR increases the complexity to determine interaction between

tumor and patient. Dynamics and frequencies of non-target-reactive T cells need to be further addressed in context of therapeutic vaccine development in cancer. Detection of this T-cell subset might be important in the future to determine the effectiveness of a vaccine and to early conduct patients with detectable non-tumor-reactive $CD8^+$ T cells to other more effective therapies.

7. Zusammenfassung

Vakzinierung von Krebspatienten mit Tumor-spezifischen Antigenen induziert peptid-spezifische, aber nicht-tumor-reaktive $CD8^+$ T Zellen. Die Erkenntnisse über die molekularen Ursachen für unzureichende T Zell Antworten im Rahmen der Tumorimmuntherapie reichen derzeit von T Zell Anergie durch T Zell Erschöpfung bis zur Induktion von klassischer peripherer T Zell Toleranz.

In dieser Arbeit wurden $CD8^+$ T Zellen spezifisch für das von Zellen des malignen Melanoms exprimierte Peptid NY-ESO-1 untersucht. Durch Sequenzanalyse der CDR3 Region der T Zell Klone konnte gezeigt werden, dass sich bei Vakzinierung entstehende tumor-reaktive und nicht-tumor-reaktive T Zellen – trotz gleicher Spezifität – aus unterschiedlichen T Zell Progenitoren ableiten. Nicht-tumor-reaktive T Zellen sind weiterhin charakterisiert durch niedrig bis mittelstarke Avidität des T Zell Rezeptors zu dem NY-ESO-1-MHC-Komplex und fehlende Bindung an das NY-ESO-1-MHC-Tetramer. Nicht-tumor-reaktive T Zellen exprimieren erhöhte Level von CD69, CD25 und CD7, Zeichen der T Zell „division arrest“ Anergie. Dazu passend konnten erhöhte Werte für den Zellzyklusregulator $p27^{kip1}$ und das mit T Zell Rezeptor-Signalblockade assoziierte lck^{p505} gemessen werden, die in $CD4^+$ T Zellen mit ähnlichem Phänotyp assoziiert sind. Das Genexpressionsprofil dieser nicht-tumor-reaktiven T Zellen wurde mittels globaler Geneexpressionsanalysen bestimmt und validiert durch RT-PCR.

Um die Relevanz dieser Zellen in Patienten mit Tumoren aufzuzeigen, wurden Blutproben von gesunden Individuen und Melanompatienten auf dieses Subpopulation in $CD8^+$ T Zellen ($CD8^+CD69^+CD25^+CD7^+$) hin untersucht. Diese Zellen konnten in Melanompatienten nachgewiesen werden, nicht aber in gesunden Individuen. Unter Verwendung einer für tumor-reaktive und nicht-tumor-reaktive T Zell Klone spezifischen PCR konnte die Prävalenz dieser Klone unter Immuntherapie *in vivo* beobachtet werden. Dabei nahm – anders als erwartet – die Prävalenz dieser Zellen unter Immuntherapie zu.

Die klinische Bedeutung dieser T Zell Population in der Tumorimmuntherapie wird unterstrichen durch Überlebenskurven, in denen die Prävalenz dieser Zellen gleichbedeutend ist mit kürzerem Überleben. Die

Tatsache, dass Expansion dieser nicht-tumor-reaktiven T Zellen nur durch Kombination von klassischer T Zell Klonierung und quantitativer PCR nachweisbar ist, erhöht die Komplexizität der Untersuchung der Tumor-Patient-Interaktion. Der Nachweis dieser Zellen könnte in Zukunft bei der Analyse der Effektivität einer Vakzine wichtig sein, um Patienten mit Existenz dieser T Zell Population frühzeitig einer anderen Therapie zuzuführen.

8. References

1. Aandahl, E.M., Sandberg, J.K., Beckerman, K.P., Tasken, K., Moretto, W.J. and Nixon, D.F.: CD7 is a differentiation marker that identifies multiple CD8 T cell effector subsets. J Immunol. 170, 2349 (2003).

2. Adorini, L., Appella, E., Doria, G. and Nagy, Z.A.: Mechanisms influencing the immunodominance of T cell determinants. J Exp Med. 168, 2091 (1988).

3. Ahmed, R. and Gray, D.: Immunological memory and protective immunity: understanding their relation. Science. 272, 54 (1996).

4. Aivazian, D. and Stern, L.J.: Phosphorylation of T cell receptor zeta is regulated by a lipid dependent folding transition. Nat Struct Biol. 7, 1023 (2000).

5. Alexander-Miller, M.A., Leggatt, G.R. and Berzofsky, J.A.: Selective expansion of high- or low-avidity cytotoxic T lymphocytes and efficacy for adoptive immunotherapy. Proc Natl Acad Sci U S A. 93, 4102 (1996).

6. Allavena, P., Bianchi, G., Giardina, P., Polentarutti, N., Zhou, D., Introna, M., Sozzani, S. and Mantovani, A.: Migratory Response of Human NK Cells to Monocyte-Chemotactic Proteins. Methods. 10, 145 (1996).

7. Alroy, I., Towers, T.L. and Freedman, L.P.: Transcriptional repression of the interleukin-2 gene by vitamin D3: direct inhibition of NFATp/AP-1 complex formation by a nuclear hormone receptor. Mol Cell Biol. 15, 5789 (1995).

8. Altan-Bonnet, G. and Germain, R.N.: Modeling T cell antigen discrimination based on feedback control of digital ERK responses. PLoS Biol. 3, e356 (2005).

9. Anderson, P.O., Manzo, B.A., Sundstedt, A., Minaee, S., Symonds, A., Khalid, S., Rodriguez-Cabezas, M.E., Nicolson, K., Li, S., Wraith, D.C. and Wang, P.: Persistent antigenic stimulation alters the transcription program in T cells, resulting in antigen-specific tolerance. Eur J Immunol. 36, 1374 (2006).

10. Andrew, D.P., Ruffing, N., Kim, C.H., Miao, W., Heath, H., Li, Y., Murphy, K., Campbell, J.J., Butcher, E.C. and Wu, L.: C-C chemokine receptor 4 expression defines a major subset of circulating nonintestinal memory T cells of both Th1 and Th2 potential. J Immunol. 166, 103 (2001).

11. Anichini, A., Maccalli, C., Mortarini, R., Salvi, S., Mazzocchi, A., Squarcina, P., Herlyn, M. and Parmiani, G.: Melanoma cells and normal melanocytes share antigens recognized by HLA-A2-restricted cytotoxic T cell clones from melanoma patients. J Exp Med. 177, 989 (1993).

12. Appay, V., Bosio, A., Lokan, S., Wiencek, Y., Biervert, C., Kusters, D., Devevre, E., Speiser, D., Romero, P., Rufer, N. and Leyvraz, S.: Sensitive Gene Expression Profiling of Human T Cell Subsets Reveals Parallel Post-Thymic Differentiation for CD4+ and CD8+ Lineages. J Immunol. 179, 7406 (2007).

13. Arstila, T.P., Casrouge, A., Baron, V., eacute, ronique, Even, J., Kanellopoulos, J. and Kourilsky, P.: A Direct Estimate of the Human T Cell Receptor Diversity. Science. 286, 958 (1999).

14. Azuma, M., Phillips, J.H. and Lanier, L.L.: CD28- T lymphocytes. Antigenic and functional properties. J Immunol. 150, 1147 (1993).

15. Bai, A., Hu, H., Yeung, M. and Chen, J.: Kruppel-like factor 2 controls T cell trafficking by activating L-selectin (CD62L) and sphingosine-1-phosphate receptor 1 transcription. J Immunol. 178, 7632 (2007).

16. Baksh, S. and Burakoff, S.J.: The role of calcineurin in lymphocyte activation. Semin Immunol. 12, 405 (2000).

17. Balch, C.M., Buzaid, A.C., Soong, S.J., Atkins, M.B., Cascinelli, N., Coit, D.G., Fleming, I.D., Gershenwald, J.E., Houghton, A., Jr., Kirkwood, J.M., McMasters, K.M., Mihm, M.F., Morton, D.L., Reintgen, D.S., Ross, M.I., Sober, A., Thompson, J.A. and Thompson, J.F.: Final version of the American Joint Committee on Cancer staging system for cutaneous melanoma. J Clin Oncol. 19, 3635 (2001).

18. Balch, C.M., Soong, S.J., Gershenwald, J.E., Thompson, J.F., Reintgen, D.S., Cascinelli, N., Urist, M., McMasters, K.M., Ross, M.I., Kirkwood, J.M., Atkins, M.B., Thompson, J.A., Coit, D.G., Byrd, D., Desmond, R., Zhang, Y., Liu, P.Y., Lyman, G.H. and Morabito, A.: Prognostic factors analysis of 17,600 melanoma patients: validation of the American Joint Committee on Cancer melanoma staging system. J Clin Oncol. 19, 3622 (2001).

19. Baldwin, R.W.: Immunity to methylcholanthrene-induced tumours in inbred rats following atrophy and regression of the implanted tumours. Br J Cancer. 9, 652 (1955).

20. Barrett, T., Troup, D.B., Wilhite, S.E., Ledoux, P., Rudnev, D., Evangelista, C., Kim, I.F., Soboleva, A., Tomashevsky, M. and Edgar, R.: NCBI GEO: mining tens of millions of expression profiles--database and tools update. Nucleic Acids Res. 35, D760 (2007).

21. Baudino, T.A., Kraichely, D.M., Jefcoat, S.C., Jr., Winchester, S.K., Partridge, N.C. and MacDonald, P.N.: Isolation and characterization of a novel coactivator protein, NCoA-62, involved in vitamin D-mediated transcription. J Biol Chem. 273, 16434 (1998).

22. Bender, A., Karbach, J., Neumann, A., Jager, D., Al-Batran, S.E., Atmaca, A., Weidmann, E., Biskamp, M., Gnjatic, S., Pan, L., Hoffman, E., Old, L.J., Knuth, A. and Jager, E.: LUD 00-009: phase 1 study of intensive course immunization with NY-ESO-1 peptides in HLA-A2 positive patients with NY-ESO-1-expressing cancer. Cancer Immun. 7, 16 (2007).

23. Bettini, M., Xi, H. and Kersh, G.J.: T cell stimulation in the absence of exogenous antigen: a T cell signal is induced by both MHC-dependent and -independent mechanisms. Eur J Immunol. 33, 3109 (2003).

24. Beverley, P.C.: Is T-cell memory maintained by crossreactive stimulation? Immunol Today. 11, 203 (1990).

25. Beyer, M., Karbach, J., Mallmann, M.R., Zander, T., Eggle, D., Classen, S., Debey-Pascher, S., Famulok, M., Jager, E. and Schultze, J.L.: Cancer vaccine enhanced, non-tumor-reactive CD8(+) T cells exhibit a distinct molecular program associated with "division arrest anergy". Cancer Res. 69, 4346 (2009).

26. Bhalla, A.K., Amento, E.P., Serog, B. and Glimcher, L.H.: 1,25-Dihydroxyvitamin D3 inhibits antigen-induced T cell activation. J Immunol. 133, 1748 (1984).

27. Bhatia, K., Huppi, K., McKeithan, T., Siwarski, D., Mushinski, J.F. and Magrath, I.: Mouse bcl-3: cDNA structure, mapping and stage-dependent expression in B lymphocytes. Oncogene. 6, 1569 (1991).

28. Bioley, G., Guillaume, P., Luescher, I., Bhardwaj, N., Mears, G., Old, L., Valmori, D. and Ayyoub, M.: Vaccination with a recombinant protein encoding the tumor-specific antigen NY-ESO-1 elicits an A2/157-165-specific CTL repertoire structurally distinct and of reduced tumor reactivity than that elicited by spontaneous immune responses to NY-ESO-1-expressing Tumors. J Immunother. 32, 161 (2009).

29. Blaschke, V., Reich, K., Blaschke, S., Zipprich, S. and Neumann, C.: Rapid quantitation of proinflammatory and chemoattractant cytokine expression in small tissue samples and monocyte-derived dendritic cells: validation of a new real-time RT-PCR technology. J Immunol Methods. 246, 79 (2000).

30. Boasberg, P.D., Hoon, D.S., Piro, L.D., Martin, M.A., Fujimoto, A., Kristedja, T.S., Bhachu, S., Ye, X., Deck, R.R. and O'Day, S.J.: Enhanced survival associated with vitiligo expression during maintenance biotherapy for metastatic melanoma. J Invest Dermatol. 126, 2658 (2006).

31. Boon, T., Coulie, P.G., Van den Eynde, B.J. and van der Bruggen, P.: Human T cell responses against melanoma. Annu Rev Immunol. 24, 175 (2006).

32. Borg, N.A., Ely, L.K., Beddoe, T., Macdonald, W.A., Reid, H.H., Clements, C.S., Purcell, A.W., Kjer-Nielsen, L., Miles, J.J., Burrows, S.R., McCluskey, J. and Rossjohn, J.: The CDR3 regions of an immunodominant T cell receptor dictate the 'energetic landscape' of peptide-MHC recognition. Nat Immunol. 6, 171 (2005).

33. Boussiotis, V.A., Freeman, G.J., Taylor, P.A., Berezovskaya, A., Grass, I., Blazar, B.R. and Nadler, L.M.: p27kip1 functions as an anergy factor inhibiting interleukin 2 transcription and clonal expansion of alloreactive human and mouse helper T lymphocytes. Nat Med. 6, 290 (2000).

34. Brichard, V., Van Pel, A., Wolfel, T., Wolfel, C., De Plaen, E., Lethe, B., Coulie, P. and Boon, T.: The tyrosinase gene codes for an antigen recognized by autologous cytolytic T lymphocytes on HLA-A2 melanomas. J Exp Med. 178, 489 (1993).

35. Bubenik, J.: Tumour MHC class I downregulation and immunotherapy (Review). Oncol Rep. 10, 2005 (2003).

36. Buck, M., Turler, H. and Chojkier, M.: LAP (NF-IL-6), a tissue-specific transcriptional activator, is an inhibitor of hepatoma cell proliferation. Embo J. 13, 851 (1994).

37. Buckley, A.F., Kuo, C.T. and Leiden, J.M.: Transcription factor LKLF is sufficient to program T cell quiescence via a c-Myc--dependent pathway. Nat Immunol. 2, 698 (2001).

38. Burnet, F.M.: The concept of immunological surveillance. Prog Exp Tumor Res. 13, 1 (1970).

39. Busygina, V., Kottemann, M.C., Scott, K.L., Plon, S.E. and Bale, A.E.: Multiple endocrine neoplasia type 1 interacts with forkhead transcription factor CHES1 in DNA damage response. Cancer Res. 66, 8397 (2006).

40. Cabaniols, J.P., Fazilleau, N., Casrouge, A., Kourilsky, P. and Kanellopoulos, J.M.: Most alpha/beta T cell receptor diversity is due to terminal deoxynucleotidyl transferase. J Exp Med. 194, 1385 (2001).

41. Cai, Z., Kishimoto, H., Brunmark, A., Jackson, M.R., Peterson, P.A. and Sprent, J.: Requirements for Peptide-induced T Cell Receptor Downregulation on Naive CD8+ T Cells. J. Exp. Med. 185, 641 (1997).

42. Call, M.E., Pyrdol, J., Wiedmann, M. and Wucherpfennig, K.W.: The organizing principle in the formation of the T cell receptor-CD3 complex. Cell. 111, 967 (2002).

43. Cantrell, D.: T cell antigen receptor signal transduction pathways. Annu Rev Immunol. 14, 259 (1996).

44. Carleton, M., Haks, M.C., Smeele, S.A.A., Jones, A., Belkowski, S.M., Berger, M.A., Linsley, P., Kruisbeek, A.M. and Wiest, D.L.: Early Growth Response Transcription Factors Are Required for Development of CD4-CD8- Thymocytes to the CD4+CD8+ Stage. J Immunol. 168, 1649 (2002).

45. Carlson, C.M., Endrizzi, B.T., Wu, J., Ding, X., Weinreich, M.A., Walsh, E.R., Wani, M.A., Lingrel, J.B., Hogquist, K.A. and Jameson, S.C.: Kruppel-like factor 2 regulates thymocyte and T-cell migration. Nature. 442, 299 (2006).

46. Caux, C., Dezutter-Dambuyant, C., Schmitt, D. and Banchereau, J.: GM-CSF and TNF-alpha cooperate in the generation of dendritic Langerhans cells. Nature. 360, 258 (1992).

47. Champagne, P., Ogg, G.S., King, A.S., Knabenhans, C., Ellefsen, K., Nobile, M., Appay, V., Rizzardi, G.P., Fleury, S., Lipp, M., Forster, R., Rowland-Jones, S., Sekaly, R.P., McMichael, A.J. and Pantaleo, G.: Skewed maturation of memory HIV-specific CD8 T lymphocytes. Nature. 410, 106 (2001).

48. Chemnitz, J.M., Driesen, J., Classen, S., Riley, J.L., Debey, S., Beyer, M., Popov, A., Zander, T. and Schultze, J.L.: Prostaglandin E2 Impairs CD4+ T Cell Activation by Inhibition of lck: Implications in Hodgkin's Lymphoma. Cancer Res. 66, 1114 (2006).

49. Chen, C.Z., Li, L., Lodish, H.F. and Bartel, D.P.: MicroRNAs modulate hematopoietic lineage differentiation. Science. 303, 83 (2004).

50. Chen, D.S., Soen, Y., Stuge, T.B., Lee, P.P., Weber, J.S., Brown, P.O. and Davis, M.M.: Marked differences in human melanoma antigen-specific T cell responsiveness after vaccination using a functional microarray. PLoS Med. 2, e265 (2005).

51. Chen, J.L., Stewart-Jones, G., Bossi, G., Lissin, N.M., Wooldridge, L., Choi, E.M., Held, G., Dunbar, P.R., Esnouf, R.M., Sami, M., Boulter, J.M., Rizkallah, P., Renner, C., Sewell, A., van der Merwe, P.A., Jakobsen, B.K., Griffiths, G., Jones, E.Y. and Cerundolo, V.: Structural and kinetic basis for heightened immunogenicity of T cell vaccines. J Exp Med. 201, 1243 (2005).

52. Chen, Y.T., Gure, A.O., Tsang, S., Stockert, E., Jager, E., Knuth, A. and Old, L.J.: Identification of multiple cancer/testis antigens by allogeneic antibody screening of a melanoma cell line library. Proc Natl Acad Sci U S A. 95, 6919 (1998).

53. Chiodetti, L., Choi, S., Barber, D.L. and Schwartz, R.H.: Adaptive tolerance and clonal anergy are distinct biochemical states. J Immunol. 176, 2279 (2006).

54. Chtanova, T., Newton, R., Liu, S.M., Weininger, L., Young, T.R., Silva, D.G., Bertoni, F., Rinaldi, A., Chappaz, S., Sallusto, F., Rolph, M.S. and Mackay, C.R.: Identification of T cell-restricted genes, and signatures for different T cell responses, using a comprehensive collection of microarray datasets. J Immunol. 175, 7837 (2005).

55. Ciubotariu, R., Colovai, A.I., Pennesi, G., Liu, Z., Smith, D., Berlocco, P., Cortesini, R. and Suciu-Foca, N.: Specific suppression of human CD4+ Th cell responses to pig MHC antigens by CD8+CD28- regulatory T cells. J Immunol. 161, 5193 (1998).

56. Clark, D.R., de Boer, R.J., Wolthers, K.C. and Miedema, F.: T cell dynamics in HIV-1 infection. Adv Immunol. 73, 301 (1999).

57. Clemente, C.G., Mihm, M.C., Jr., Bufalino, R., Zurrida, S., Collini, P. and Cascinelli, N.: Prognostic value of tumor infiltrating lymphocytes in the vertical growth phase of primary cutaneous melanoma. Cancer. 77, 1303 (1996).

58. Coats, S., Flanagan, W.M., Nourse, J. and Roberts, J.M.: Requirement of p27Kip1 for restriction point control of the fibroblast cell cycle. Science. 272, 877 (1996).

59. Coats, S., Whyte, P., Fero, M.L., Lacy, S., Chung, G., Randel, E., Firpo, E. and Roberts, J.M.: A new pathway for mitogen-dependent cdk2 regulation uncovered in p27(Kip1)-deficient cells. Curr Biol. 9, 163 (1999).

60. Connor, S.J., Paraskevopoulos, N., Newman, R., Cuan, N., Hampartzoumian, T., Lloyd, A.R. and Grimm, M.C.: CCR2 expressing CD4+ T lymphocytes are preferentially recruited to the ileum in Crohn's disease. Gut. 53, 1287 (2004).

61. Contasta, I., Berghella, A.M., Pellegrini, P., Del Beato, T., Casciani, C.A. and Adorno, D.: Relationships between the activity of MMP1/TIMP1 enzymes and the TH1/TH2 cytokine network. Cancer Biother Radiopharm. 14, 465 (1999).

62. Cordaro, T.A., de Visser, K.E., Tirion, F.H., Schumacher, T.N. and Kruisbeek, A.M.: Can the low-avidity self-specific T cell repertoire be exploited for tumor rejection? J Immunol. 168, 651 (2002).

63. Cosulich, M.E., Rubartelli, A., Risso, A., Cozzolino, F. and Bargellesi, A.: Functional characterization of an antigen involved in an early step of T-cell activation. Proc Natl Acad Sci U S A. 84, 4205 (1987).

64. Coudronniere, N., Villalba, M., Englund, N. and Altman, A.: NF-kappa B activation induced by T cell receptor/CD28 costimulation is mediated by protein kinase C-theta. Proc Natl Acad Sci U S A. 97, 3394 (2000).

65. Crabtree, G.R.: Contingent genetic regulatory events in T lymphocyte activation. Science. 243, 355 (1989).

66. Critchley-Thorne, R.J., Yan, N., Nacu, S., Weber, J., Holmes, S.P. and Lee, P.P.: Down-regulation of the interferon signaling pathway in T lymphocytes from patients with metastatic melanoma. PLoS Med. 4, e176 (2007).

67. Croft, M.: Costimulation of T cells by OX40, 4-1BB, and CD27. Cytokine Growth Factor Rev. 14, 265 (2003).

68. Davey, G.M., Schober, S.L., Endrizzi, B.T., Dutcher, A.K., Jameson, S.C. and Hogquist, K.A.: Preselection Thymocytes Are More Sensitive to T Cell Receptor Stimulation Than Mature T Cells. J. Exp. Med. 188, 1867 (1998).

69. Davis, M.M. and Bjorkman, P.J.: T-cell antigen receptor genes and T-cell recognition. Nature. 334, 395 (1988).

70. DeBenedette, M.A., Wen, T., Bachmann, M.F., Ohashi, P.S., Barber, B.H., Stocking, K.L., Peschon, J.J. and Watts, T.H.: Analysis of 4-1BB ligand (4-1BBL)-deficient mice and of mice lacking both 4-1BBL and CD28 reveals a role for 4-1BBL in skin allograft rejection and in the cytotoxic T cell response to influenza virus. J Immunol. 163, 4833 (1999).

71. Debey, S., Schoenbeck, U., Hellmich, M., Gathof, B.S., Pillai, R., Zander, T. and Schultze, J.L.: Comparison of different isolation techniques prior gene expression profiling of blood derived cells: impact on physiological responses, on overall expression and the role of different cell types. Pharmacogenomics J. 4, 193 (2004).

72. Degano, M., Garcia, K.C., Apostolopoulos, V., Rudolph, M.G., Teyton, L. and Wilson, I.A.: A functional hot spot for antigen recognition in a superagonist TCR/MHC complex. Immunity. 12, 251 (2000).

73. Derre, L., Bruyninx, M., Baumgaertner, P., Ferber, M., Schmid, D., Leimgruber, A., Zoete, V., Romero, P., Michielin, O., Speiser, D.E. and Rufer, N.: Distinct sets of alphabeta TCRs confer similar recognition of tumor antigen NY-ESO-1157-165 by interacting with its central Met/Trp residues. Proc Natl Acad Sci U S A. 105, 15010 (2008).

74. Descombes, P., Chojkier, M., Lichtsteiner, S., Falvey, E. and Schibler, U.: LAP, a novel member of the C/EBP gene family, encodes a liver-enriched transcriptional activator protein. Genes Dev. 4, 1541 (1990).

75. DeSilva, D.R., Jones, E.A., Feeser, W.S., Manos, E.J. and Scherle, P.A.: The p38 mitogen-activated protein kinase pathway in activated and anergic Th1 cells. Cell Immunol. 180, 116 (1997).

76. DiDonato, J.A., Hayakawa, M., Rothwarf, D.M., Zandi, E. and Karin, M.: A cytokine-responsive IkappaB kinase that activates the transcription factor NF-kappaB. Nature. 388, 548 (1997).

77. Dietrich, P.Y., Walker, P.R., Quiquerez, A.L., Perrin, G., Dutoit, V., Lienard, D., Guillaume, P., Cerottini, J.C., Romero, P. and Valmori, D.: Melanoma patients respond to a cytotoxic T lymphocyte-defined self-peptide with diverse and nonoverlapping T-cell receptor repertoires. Cancer Res. 61, 2047 (2001).

78. Ding, Y.H., Baker, B.M., Garboczi, D.N., Biddison, W.E. and Wiley, D.C.: Four A6-TCR/peptide/HLA-A2 structures that generate very different T cell signals are nearly identical. Immunity. 11, 45 (1999).

79. Dittel, B.N., Stefanova, I., Germain, R.N. and Janeway, C.A., Jr.: Cross-antagonism of a T cell clone expressing two distinct T cell receptors. Immunity. 11, 289 (1999).

80. Dobrzanski, M.J., Reome, J.B. and Dutton, R.W.: Therapeutic Effects of Tumor-Reactive Type 1 and Type 2 CD8+ T Cell Subpopulations in Established Pulmonary Metastases. J Immunol. 162, 6671 (1999).

81. Doherty, P.C., Allan, W., Eichelberger, M. and Carding, S.R.: Roles of alpha beta and gamma delta T cell subsets in viral immunity. Annu Rev Immunol. 10, 123 (1992).

82. Doherty, P.C. and Christensen, J.P.: Accessing complexity: the dynamics of virus-specific T cell responses. Annu Rev Immunol. 18, 561 (2000).

83. Dong, C., Yang, D.D., Wysk, M., Whitmarsh, A.J., Davis, R.J. and Flavell, R.A.: Defective T cell differentiation in the absence of Jnk1. Science. 282, 2092 (1998).

84. Dreno, B., Nguyen, J.M., Khammari, A., Pandolfino, M.C., Tessier, M.H., Bercegeay, S., Cassidanius, A., Lemarre, P., Billaudel, S., Labarriere, N. and Jotereau, F.: Randomized trial of adoptive transfer of melanoma tumor-infiltrating lymphocytes as adjuvant therapy for stage III melanoma. Cancer Immunol Immunother. 51, 539 (2002).

85. Dubey, P., Hendrickson, R.C., Meredith, S.C., Siegel, C.T., Shabanowitz, J., Skipper, J.C., Engelhard, V.H., Hunt, D.F. and Schreiber, H.: The immunodominant antigen of an ultraviolet-induced regressor tumor is generated by a somatic point mutation in the DEAD box helicase p68. J Exp Med. 185, 695 (1997).

86. Dudda, J.C., Simon, J.C. and Martin, S.: Dendritic cell immunization route determines CD8+ T cell trafficking to inflamed skin: role for tissue microenvironment and dendritic cells in establishment of T cell-homing subsets. J Immunol. 172, 857 (2004).

87. Dumais, N., Bounou, S., Olivier, M. and Tremblay, M.J.: Prostaglandin E2-Mediated Activation of HIV-1 Long Terminal Repeat Transcription in Human T Cells Necessitates CCAAT/Enhancer Binding Protein (C/EBP) Binding Sites in Addition to Cooperative Interactions Between C/EBP{beta} and Cyclic Adenosine 5'-Monophosphate Response Element Binding Protein. J Immunol. 168, 274 (2002).

88. Dzhagalov, I., Giguere, V. and He, Y.W.: Lymphocyte development and function in the absence of retinoic acid-related orphan receptor alpha. J Immunol. 173, 2952 (2004).

89. Dzhagalov, I., Zhang, N. and He, Y.W.: The roles of orphan nuclear receptors in the development and function of the immune system. Cell Mol Immunol. 1, 401 (2004).

90. Eagar, T.N., Karandikar, N.J., Bluestone, J.A. and Miller, S.D.: The role of CTLA-4 in induction and maintenance of peripheral T cell tolerance. Eur J Immunol. 32, 972 (2002).

91. Esplugues, E., Vega-Ramos, J., Cartoixa, D., Vazquez, B.N., Salaet, I., Engel, P. and Lauzurica, P.: Induction of tumor NK-cell immunity by anti-CD69 antibody therapy. Blood. 105, 4399 (2005).

92. Eton, O., Legha, S.S., Bedikian, A.Y., Lee, J.J., Buzaid, A.C., Hodges, C., Ring, S.E., Papadopoulos, N.E., Plager, C., East, M.J., Zhan, F. and Benjamin, R.S.: Sequential biochemotherapy versus chemotherapy for metastatic melanoma: results from a phase III randomized trial. J Clin Oncol. 20, 2045 (2002).

93. Ferrone, S. and Marincola, F.M.: Loss of HLA class I antigens by melanoma cells: molecular mechanisms, functional significance and clinical relevance. Immunol Today. 16, 487 (1995).

94. Fields, P.E., Gajewski, T.F. and Fitch, F.W.: Blocked Ras activation in anergic CD4+ T cells. Science. 271, 1276 (1996).

95. Filaci, G., Fravega, M., Negrini, S., Procopio, F., Fenoglio, D., Rizzi, M., Brenci, S., Contini, P., Olive, D., Ghio, M., Setti, M., Accolla, R.S., Puppo, F. and Indiveri, F.: Nonantigen specific CD8+ T suppressor lymphocytes originate from CD8+CD28- T cells and inhibit both T-cell proliferation and CTL function. Hum Immunol. 65, 142 (2004).

96. Foley, E.J.: Antigenic properties of methylcholanthrene-induced tumors in mice of the strain of origin. Cancer Res. 13, 835 (1953).

97. Foley, E.J.: Attempts to induce immunity against mammary adenocarcinoma in inbred mice. Cancer Res. 13, 578 (1953).

98. Fujimaki, W., Iwashima, M., Yagi, J., Zhang, H., Yagi, H., Seo, K., Imai, Y., Imanishi, K. and Uchiyama, T.: Functional uncoupling of T-cell receptor engagement and Lck activation in anergic human thymic CD4+ T cells. J Biol Chem. 276, 17455 (2001).

99. Fukui, Y., Oono, T., Cabaniols, J.P., Nakao, K., Hirokawa, K., Inayoshi, A., Sanui, T., Kanellopoulos, J., Iwata, E., Noda, M., Katsuki, M., Kourilsky, P. and Sasazuki, T.: Diversity of T cell repertoire shaped by a single peptide ligand is critically affected by its amino acid residue at a T cell receptor contact. Proc Natl Acad Sci U S A. 97, 13760 (2000).

100. Gajewski, T.F., Meng, Y., Blank, C., Brown, I., Kacha, A., Kline, J. and Harlin, H.: Immune resistance orchestrated by the tumor microenvironment. Immunol Rev. 213, 131 (2006).

101. Gajewski, T.F., Meng, Y. and Harlin, H.: Immune suppression in the tumor microenvironment. J Immunother. 29, 233 (2006).

102. Gajewski, T.F., Qian, D., Fields, P. and Fitch, F.W.: Anergic T-lymphocyte clones have altered inositol phosphate, calcium, and tyrosine kinase signaling pathways. Proc Natl Acad Sci U S A. 91, 38 (1994).

103. Gallimore, A., Dumrese, T., Hengartner, H., Zinkernagel, R.M. and Rammensee, H.G.: Protective immunity does not correlate with the hierarchy of virus-specific cytotoxic T cell responses to naturally processed peptides. J Exp Med. 187, 1647 (1998).

104. Garbe, C., Radny, P., Linse, R., Dummer, R., Gutzmer, R., Ulrich, J., Stadler, R., Weichenthal, M., Eigentler, T., Ellwanger, U. and Hauschild, A.: Adjuvant low-dose interferon {alpha}2a with or without dacarbazine compared with surgery alone: a prospective-randomized phase III DeCOG trial in melanoma patients with regional lymph node metastasis. Ann Oncol. 19, 1195 (2008).

105. Garboczi, D.N., Ghosh, P., Utz, U., Fan, Q.R., Biddison, W.E. and Wiley, D.C.: Structure of the complex between human T-cell receptor, viral peptide and HLA-A2. Nature. 384, 134 (1996).

106. Garcia, K.C., Degano, M., Stanfield, R.L., Brunmark, A., Jackson, M.R., Peterson, P.A., Teyton, L. and Wilson, I.A.: An alphabeta T cell receptor

structure at 2.5 A and its orientation in the TCR-MHC complex. Science. 274, 209 (1996).

107. Garcia, K.C., Teyton, L. and Wilson, I.A.: Structural basis of T cell recognition. Annu Rev Immunol. 17, 369 (1999).

108. Genevee, C., Diu, A., Nierat, J., Caignard, A., Dietrich, P.Y., Ferradini, L., Roman-Roman, S., Triebel, F. and Hercend, T.: An experimentally validated panel of subfamily-specific oligonucleotide primers (V alpha 1-w29/V beta 1-w24) for the study of human T cell receptor variable V gene segment usage by polymerase chain reaction. Eur J Immunol. 22, 1261 (1992).

109. Germeau, C., Ma, W., Schiavetti, F., Lurquin, C., Henry, E., Vigneron, N., Brasseur, F., Lethe, B., De Plaen, E., Velu, T., Boon, T. and Coulie, P.G.: High frequency of antitumor T cells in the blood of melanoma patients before and after vaccination with tumor antigens. J Exp Med. 201, 241 (2005).

110. Gil, D., Schamel, W.W., Montoya, M., Sanchez-Madrid, F. and Alarcon, B.: Recruitment of Nck by CD3 epsilon reveals a ligand-induced conformational change essential for T cell receptor signaling and synapse formation. Cell. 109, 901 (2002).

111. Giudicelli, V., Duroux, P., Ginestoux, C., Folch, G., Jabado-Michaloud, J., Chaume, D. and Lefranc, M.P.: IMGT/LIGM-DB, the IMGT comprehensive database of immunoglobulin and T cell receptor nucleotide sequences. Nucleic Acids Res. 34, D781 (2006).

112. Glennie, S., Soeiro, I., Dyson, P.J., Lam, E.W. and Dazzi, F.: Bone marrow mesenchymal stem cells induce division arrest anergy of activated T cells. Blood. 105, 2821 (2005).

113. Gnjatic, S., Atanackovic, D., Jager, E., Matsuo, M., Selvakumar, A., Altorki, N.K., Maki, R.G., Dupont, B., Ritter, G., Chen, Y.T., Knuth, A. and Old, L.J.: Survey of naturally occurring CD4+ T cell responses against NY-ESO-1 in cancer patients: correlation with antibody responses. Proc Natl Acad Sci U S A. 100, 8862 (2003).

114. Godfrey, W.R., Fagnoni, F.F., Harara, M.A., Buck, D. and Engleman, E.G.: Identification of a human OX-40 ligand, a costimulator of CD4+ T cells with homology to tumor necrosis factor. J. Exp. Med. 180, 757 (1994).

115. Goodall, J.C., Henwood, J., Bacon, P.A. and Gaston, J.S.: Marked conservation of complementarity-determining region 3 of the beta-chain of TCRs recognizing a mycobacterial heat shock protein 60-derived peptide with strong sequence similarity to human heat shock protein 60. J Immunol. 155, 2329 (1995).

116. Gorski, J., Yassai, M., Zhu, X., Kissela, B., Kissella, B., Keever, C. and Flomenberg, N.: Circulating T cell repertoire complexity in normal individuals and bone marrow recipients analyzed by CDR3 size spectratyping. Correlation with immune status. J Immunol. 152, 5109 (1994).

117. Grakoui, A., Bromley, S.K., Sumen, C., Davis, M.M., Shaw, A.S., Allen, P.M. and Dustin, M.L.: The Immunological Synapse: A Molecular Machine Controlling T Cell Activation. Science. 285, 221 (1999).

118. Gramaglia, I., Jember, A., Pippig, S.D., Weinberg, A.D., Killeen, N. and Croft, M.: The OX40 costimulatory receptor determines the development of CD4 memory by regulating primary clonal expansion. J Immunol. 165, 3043 (2000).

119. Gramaglia, I., Weinberg, A.D., Lemon, M. and Croft, M.: Ox-40 Ligand: A Potent Costimulatory Molecule for Sustaining Primary CD4 T Cell Responses. J Immunol. 161, 6510 (1998).

120. Greenwald, R.J., Boussiotis, V.A., Lorsbach, R.B., Abbas, A.K. and Sharpe, A.H.: CTLA-4 regulates induction of anergy in vivo. Immunity. 14, 145 (2001).

121. Grob, J.J. and Bonerandi, J.J.: The 'ugly duckling' sign: identification of the common characteristics of nevi in an individual as a basis for melanoma screening. Arch Dermatol. 134, 103 (1998).

122. Gross, L.: Intradermal Immunization of C3H Mice against a Sarcoma That Originated in an Animal of the Same Line. Cancer Res. 3, 326 (1943).

123. Hamann, D., Baars, P.A., Rep, M.H., Hooibrink, B., Kerkhof-Garde, S.R., Klein, M.R. and van Lier, R.A.: Phenotypic and functional separation of memory and effector human CD8+ T cells. J Exp Med. 186, 1407 (1997).

124. Harlin, H., Kuna, T.V., Peterson, A.C., Meng, Y. and Gajewski, T.F.: Tumor progression despite massive influx of activated CD8(+) T cells in a patient with malignant melanoma ascites. Cancer Immunol Immunother. 55, 1185 (2006).

125. Hayakawa, T., Yamashita, K., Kishi, J. and Harigaya, K.: Tissue inhibitor of metalloproteinases from human bone marrow stromal cell line KM 102 has erythroid-potentiating activity, suggesting its possibly bifunctional role in the hematopoietic microenvironment. FEBS Lett. 268, 125 (1990).

126. Hedrick, J.A., Saylor, V., Figueroa, D., Mizoue, L., Xu, Y., Menon, S., Abrams, J., Handel, T. and Zlotnik, A.: Lymphotactin is produced by NK cells and attracts both NK cells and T cells in vivo. J Immunol. 158, 1533 (1997).

127. Herlyn, M. and Koprowski, H.: Melanoma antigens: immunological and biological characterization and clinical significance. Annu Rev Immunol. 6, 283 (1988).

128. Hernández-García, C., Fernández-Gutiérrez , B., Morado, I.C., Bañares, A.A. and Jover, J.A.: The CD69 activation pathway in rheumatoid arthritis synovial fluid t cells. Arthritis & Rheumatism. 39, 1277 (1996).

129. Hewitt, H.B., Blake, E.R. and Walder, A.S.: A critique of the evidence for active host defence against cancer, based on personal studies of 27 murine tumours of spontaneous origin. Br J Cancer. 33, 241 (1976).

130. Hickman, S.P., Yang, J., Thomas, R.M., Wells, A.D. and Turka, L.A.: Defective activation of protein kinase C and Ras-ERK pathways limits IL-2 production and proliferation by CD4+CD25+ regulatory T cells. J Immunol. 177, 2186 (2006).

131. Hogquist, K.A., Jameson, S.C., Heath, W.R., Howard, J.L., Bevan, M.J. and Carbone, F.R.: T cell receptor antagonist peptides induce positive selection. Cell. 76, 17 (1994).

132. Hogquist, K.A., Tomlinson, A.J., Kieper, W.C., McGargill, M.A., Hart, M.C., Naylor, S. and Jameson, S.C.: Identification of a naturally occurring ligand for thymic positive selection. Immunity. 6, 389 (1997).

133. Holdorf, A.D., Lee, K.-H., Burack, W.R., Allen, P.M. and Shaw, A.S.: Regulation of Lck activity by CD4 and CD28 in the immunological synapse. Nat Immunol. 3, 259 (2002).

134. Holmberg, K., Mariathasan, S., Ohteki, T., Ohashi, P.S. and Gascoigne, N.R.: TCR binding kinetics measured with MHC class I tetramers reveal a positive selecting peptide with relatively high affinity for TCR. J Immunol. 171, 2427 (2003).

135. Houghton, A.N. and Guevara-Patino, J.A.: Immune recognition of self in immunity against cancer. J Clin Invest. 114, 468 (2004).

136. Isakov, N., Wange, R.L., Burgess, W.H., Watts, J.D., Aebersold, R. and Samelson, L.E.: ZAP-70 binding specificity to T cell receptor tyrosine-based activation motifs: the tandem SH2 domains of ZAP-70 bind distinct tyrosine-based activation motifs with varying affinity. J Exp Med. 181, 375 (1995).

137. Jager, E., Chen, Y.T., Drijfhout, J.W., Karbach, J., Ringhoffer, M., Jager, D., Arand, M., Wada, H., Noguchi, Y., Stockert, E., Old, L.J. and Knuth, A.: Simultaneous humoral and cellular immune response against cancer-testis antigen NY-ESO-1: definition of human histocompatibility leukocyte antigen (HLA)-A2-binding peptide epitopes. J Exp Med. 187, 265 (1998).

138. Jager, E., Gnjatic, S., Nagata, Y., Stockert, E., Jager, D., Karbach, J., Neumann, A., Rieckenberg, J., Chen, Y.T., Ritter, G., Hoffman, E., Arand, M., Old, L.J. and Knuth, A.: Induction of primary NY-ESO-1 immunity: CD8+ T lymphocyte and antibody responses in peptide-vaccinated patients with NY-ESO-1+ cancers. Proc Natl Acad Sci U S A. 97, 12198 (2000).

139. Jager, E., Ringhoffer, M., Dienes, H.P., Arand, M., Karbach, J., Jager, D., Ilsemann, C., Hagedorn, M., Oesch, F. and Knuth, A.: Granulocyte-macrophage-colony-stimulating factor enhances immune responses to melanoma-associated peptides in vivo. Int J Cancer. 67, 54 (1996).

140. Jager, E., Stockert, E., Zidianakis, Z., Chen, Y.T., Karbach, J., Jager, D., Arand, M., Ritter, G., Old, L.J. and Knuth, A.: Humoral immune responses of cancer patients against "Cancer-Testis" antigen NY-ESO-1: correlation with clinical events. Int J Cancer. 84, 506 (1999).

141. Jain, J., Loh, C. and Rao, A.: Transcriptional regulation of the IL-2 gene. Curr Opin Immunol. 7, 333 (1995).

142. Janeway, C.A. and Medzhitov, R.: INNATE IMMUNE RECOGNITION. Annual Review of Immunology. 20, 197 (2002).

143. Jemal, A., Siegel, R., Ward, E., Murray, T., Xu, J., Smigal, C. and Thun, M.J.: Cancer statistics, 2006. CA Cancer J Clin. 56, 106 (2006).

144. Jemal, A., Ward, E., Hao, Y. and Thun, M.: Trends in the leading causes of death in the United States, 1970-2002. Jama. 294, 1255 (2005).

145. Jetten, A.M., Kurebayashi, S. and Ueda, E.: The ROR nuclear orphan receptor subfamily: critical regulators of multiple biological processes. Prog Nucleic Acid Res Mol Biol. 69, 205 (2001).

146. Jiang, S., Tugulea, S., Pennesi, G., Liu, Z., Mulder, A., Lederman, S., Harris, P., Cortesini, R. and Suciu-Foca, N.: Induction of MHC-class I restricted human suppressor T cells by peptide priming in vitro. Hum Immunol. 59, 690 (1998).

147. Josephy, P.D., Eling, T. and Mason, R.P.: The horseradish peroxidase-catalyzed oxidation of 3,5,3',5'-tetramethylbenzidine. Free radical and charge-transfer complex intermediates. J Biol Chem. 257, 3669 (1982).

148. June, C.H.: Adoptive T cell therapy for cancer in the clinic. J Clin Invest. 117, 1466 (2007).

149. Jungbluth, A.A., Chen, Y.T., Stockert, E., Busam, K.J., Kolb, D., Iversen, K., Coplan, K., Williamson, B., Altorki, N. and Old, L.J.: Immunohistochemical analysis of NY-ESO-1 antigen expression in normal and malignant human tissues. Int J Cancer. 92, 856 (2001).

150. Kanamaru, F., Youngnak, P., Hashiguchi, M., Nishioka, T., Takahashi, T., Sakaguchi, S., Ishikawa, I. and Azuma, M.: Costimulation via glucocorticoid-induced TNF receptor in both conventional and CD25+ regulatory CD4+ T cells. J Immunol. 172, 7306 (2004).

151. Kappler, J.W., Roehm, N. and Marrack, P.: T cell tolerance by clonal elimination in the thymus. Cell. 49, 273 (1987).

152. Karbach, J., Gnjatic, S., Pauligk, C., Bender, A., Maeurer, M., Schultze, J.L., Nadler, K., Wahle, C., Knuth, A., Old, L.J. and Jager, E.: Tumor-reactive CD8+ T-cell clones in patients after NY-ESO-1 peptide vaccination. Int J Cancer. 121, 2042 (2007).

153. Kearney, E.R., Pape, K.A., Loh, D.Y. and Jenkins, M.K.: Visualization of peptide-specific T cell immunity and peripheral tolerance induction in vivo. Immunity. 1, 327 (1994).

154. Keino, H., Masli, S., Sasaki, S., Streilein, J.W. and Stein-Streilein, J.: CD8+ T regulatory cells use a novel genetic program that includes CD103 to suppress Th1 immunity in eye-derived tolerance. Invest Ophthalmol Vis Sci. 47, 1533 (2006).

155. Kemp, R.A. and Ronchese, F.: Tumor-Specific Tc1, But Not Tc2, Cells Deliver Protective Antitumor Immunity. J Immunol. 167, 6497 (2001).

156. Khoshnan, A., Kempiak, S.J., Bennett, B.L., Bae, D., Xu, W., Manning, A.M., June, C.H. and Nel, A.E.: Primary human CD4+ T cells contain heterogeneous I kappa B kinase complexes: role in activation of the IL-2 promoter. J Immunol. 163, 5444 (1999).

157. Kim, R., Emi, M. and Tanabe, K.: Cancer immunosuppression and autoimmune disease: beyond immunosuppressive networks for tumour immunity. Immunology. 119, 254 (2006).

158. Kirkwood, J.M., Ibrahim, J.G., Sondak, V.K., Richards, J., Flaherty, L.E., Ernstoff, M.S., Smith, T.J., Rao, U., Steele, M. and Blum, R.H.: High- and low-dose interferon alfa-2b in high-risk melanoma: first analysis of intergroup trial E1690/S9111/C9190. J Clin Oncol. 18, 2444 (2000).

159. Kirkwood, J.M., Ibrahim, J.G., Sosman, J.A., Sondak, V.K., Agarwala, S.S., Ernstoff, M.S. and Rao, U.: High-dose interferon alfa-2b significantly prolongs relapse-free and overall survival compared with the GM2-KLH/QS-21 vaccine in

patients with resected stage IIB-III melanoma: results of intergroup trial E1694/S9512/C509801. J Clin Oncol. 19, 2370 (2001).

160. Kirkwood, J.M., Strawderman, M.H., Ernstoff, M.S., Smith, T.J., Borden, E.C. and Blum, R.H.: Interferon alfa-2b adjuvant therapy of high-risk resected cutaneous melanoma: the Eastern Cooperative Oncology Group Trial EST 1684. J Clin Oncol. 14, 7 (1996).

161. Koebel, C.M., Vermi, W., Swann, J.B., Zerafa, N., Rodig, S.J., Old, L.J., Smyth, M.J. and Schreiber, R.D.: Adaptive immunity maintains occult cancer in an equilibrium state. Nature. 450, 903 (2007).

162. Kohm, A.P., Williams, J.S. and Miller, S.D.: Cutting edge: ligation of the glucocorticoid-induced TNF receptor enhances autoreactive CD4+ T cell activation and experimental autoimmune encephalomyelitis. J Immunol. 172, 4686 (2004).

163. Korn, T., Reddy, J., Gao, W., Bettelli, E., Awasthi, A., Petersen, T.R., Backstrom, B.T., Sobel, R.A., Wucherpfennig, K.W., Strom, T.B., Oukka, M. and Kuchroo, V.K.: Myelin-specific regulatory T cells accumulate in the CNS but fail to control autoimmune inflammation. Nat Med. 13, 423 (2007).

164. Krieg, A.M.: CpG motifs in bacterial DNA and their immune effects. Annu Rev Immunol. 20, 709 (2002).

165. Krieg, A.M.: CpG motifs: the active ingredient in bacterial extracts? Nat Med. 9, 831 (2003).

166. Kroczek, R.A., Mages, H.W. and Hutloff, A.: Emerging paradigms of T-cell co-stimulation. Current Opinion in Immunology. 16, 321 (2004).

167. Kroger, C.J. and Alexander-Miller, M.A.: Cutting edge: CD8+ T cell clones possess the potential to differentiate into both high- and low-avidity effector cells. J Immunol. 179, 748 (2007).

168. Krogsgaard, M., Prado, N., Adams, E.J., He, X.L., Chow, D.C., Wilson, D.B., Garcia, K.C. and Davis, M.M.: Evidence that structural rearrangements and/or flexibility during TCR binding can contribute to T cell activation. Mol Cell. 12, 1367 (2003).

169. Kruit, W.H., van Ojik, H.H., Brichard, V.G., Escudier, B., Dorval, T., Dreno, B., Patel, P., van Baren, N., Avril, M.F., Piperno, S., Khammari, A., Stas, M., Ritter, G., Lethe, B., Godelaine, D., Brasseur, F., Zhang, Y., van der Bruggen, P., Boon, T., Eggermont, A.M. and Marchand, M.: Phase 1/2 study of subcutaneous and intradermal immunization with a recombinant MAGE-3 protein in patients with detectable metastatic melanoma. Int J Cancer. 117, 596 (2005).

170. Kubsch, S., Graulich, E., Knop, J. and Steinbrink, K.: Suppressor activity of anergic T cells induced by IL-10-treated human dendritic cells: association with IL-2- and CTLA-4-dependent G1 arrest of the cell cycle regulated by p27Kip1. Eur J Immunol. 33, 1988 (2003).

171. Kumar, S., Jones, T.R., Oakley, M.S., Zheng, H., Kuppusamy, S.P., Taye, A., Krieg, A.M., Stowers, A.W., Kaslow, D.C. and Hoffman, S.L.: CpG oligodeoxynucleotide and Montanide ISA 51 adjuvant combination enhanced the protective efficacy of a subunit malaria vaccine. Infect Immun. 72, 949 (2004).

172. La Gruta, N.L., Turner, S.J. and Doherty, P.C.: Hierarchies in cytokine expression profiles for acute and resolving influenza virus-specific CD8+ T cell responses: correlation of cytokine profile and TCR avidity. J Immunol. 172, 5553 (2004).

173. Laufer, T.M.: T-cell sensitivity: a microRNA regulates the sensitivity of the T-cell receptor. Immunol Cell Biol. 85, 346 (2007).

174. Lee, N.A., Loh, D.Y. and Lacy, E.: CD8 surface levels alter the fate of alpha/beta T cell receptor-expressing thymocytes in transgenic mice. J Exp Med. 175, 1013 (1992).

175. Lee, P.P., Yee, C., Savage, P.A., Fong, L., Brockstedt, D., Weber, J.S., Johnson, D., Swetter, S., Thompson, J., Greenberg, P.D., Roederer, M. and Davis, M.M.: Characterization of circulating T cells specific for tumor-associated antigens in melanoma patients. Nat Med. 5, 677 (1999).

176. Lee, P.U., Churchill, H.R., Daniels, M., Jameson, S.C. and Kranz, D.M.: Role of 2CT cell receptor residues in the binding of self- and allo-major histocompatibility complexes. J Exp Med. 191, 1355 (2000).

177. Leen, A.M., Rooney, C.M. and Foster, A.E.: Improving T cell therapy for cancer. Annu Rev Immunol. 25, 243 (2007).

178. Lefranc, M.P., Giudicelli, V., Kaas, Q., Duprat, E., Jabado-Michaloud, J., Scaviner, D., Ginestoux, C., Clement, O., Chaume, D. and Lefranc, G.: IMGT, the international ImMunoGeneTics information system. Nucleic Acids Res. 33, D593 (2005).

179. Leong, G.M., Subramaniam, N., Figueroa, J., Flanagan, J.L., Hayman, M.J., Eisman, J.A. and Kouzmenko, A.P.: Ski-interacting protein interacts with Smad proteins to augment transforming growth factor-beta-dependent transcription. J Biol Chem. 276, 18243 (2001).

180. Leong, G.M., Subramaniam, N., Issa, L.L., Barry, J.B., Kino, T., Driggers, P.H., Hayman, M.J., Eisman, J.A. and Gardiner, E.M.: Ski-interacting protein, a bifunctional nuclear receptor coregulator that interacts with N-CoR/SMRT and p300. Biochem Biophys Res Commun. 315, 1070 (2004).

181. Li, H., Jiang, H.J., Ma, M.Q., Wei, F., An, X.M. and Ren, X.B.: Vaccination with allogeneic GM-CSF gene-modified lung cancer cells: antitumor activity comparing with that induced by autologous vaccine. Cancer Biother Radiopharm. 22, 790 (2007).

182. Li, L., Iwamoto, Y., Berezovskaya, A. and Boussiotis, V.A.: A pathway regulated by cell cycle inhibitor p27Kip1 and checkpoint inhibitor Smad3 is involved in the induction of T cell tolerance. Nat Immunol. 7, 1157 (2006).

183. Li, Q.J., Chau, J., Ebert, P.J., Sylvester, G., Min, H., Liu, G., Braich, R., Manoharan, M., Soutschek, J., Skare, P., Klein, L.O., Davis, M.M. and Chen, C.Z.: miR-181a is an intrinsic modulator of T cell sensitivity and selection. Cell. 129, 147 (2007).

184. Li, W., Whaley, C.D., Mondino, A. and Mueller, D.L.: Blocked signal transduction to the ERK and JNK protein kinases in anergic CD4+ T cells. Science. 271, 1272 (1996).

185. Li, W.F., Fan, M.D., Pan, C.B. and Lai, M.Z.: T cell epitope selection: dominance may be determined by both affinity for major histocompatibility complex and stoichiometry of epitope. Eur J Immunol. 22, 943 (1992).

186. Libotte, T., Zaim, H., Abraham, S., Padmakumar, V.C., Schneider, M., Lu, W., Munck, M., Hutchison, C., Wehnert, M., Fahrenkrog, B., Sauder, U., Aebi, U., Noegel, A.A. and Karakesisoglou, I.: Lamin A/C-dependent localization of Nesprin-2, a giant scaffolder at the nuclear envelope. Mol Biol Cell. 16, 3411 (2005).

187. Lin, C.J. and Tam, R.C.: Transcriptional Regulation of CD28 Expression by CD28GR, a Novel Promoter Element Located in Exon 1 of the CD28 Gene. J Immunol. 166, 6134 (2001).

188. Lin, X., O'Mahony, A., Mu, Y., Geleziunas, R. and Greene, W.C.: Protein kinase C-theta participates in NF-kappaB activation induced by CD3-CD28 costimulation through selective activation of IkappaB kinase beta. Mol Cell Biol. 20, 2933 (2000).

189. Liu, Z., Tugulea, S., Cortesini, R. and Suciu-Foca, N.: Specific suppression of T helper alloreactivity by allo-MHC class I-restricted CD8+CD28- T cells. Int Immunol. 10, 775 (1998).

190. Lo-Man, R., Langeveld, J.P., Martineau, P., Hofnung, M., Meloen, R.H. and Leclerc, C.: Immunodominance does not result from peptide competition for MHC class II presentation. J Immunol. 160, 1759 (1998).

191. Lord, G.M., Lechler, R.I. and George, A.J.: A kinetic differentiation model for the action of altered TCR ligands. Immunol Today. 20, 33 (1999).

192. Love, P.E. and Shores, E.W.: ITAM multiplicity and thymocyte selection: how low can you go? Immunity. 12, 591 (2000).

193. Lucas, B., Stefanova, I., Yasutomo, K., Dautigny, N. and Germain, R.N.: Divergent changes in the sensitivity of maturing T cells to structurally related ligands underlies formation of a useful T cell repertoire. Immunity. 10, 367 (1999).

194. Luescher, I.F., Vivier, E., Layer, A., Mahiou, J., Godeau, F., Malissen, B. and Romero, P.: CD8 modulation of T-cell antigen receptor-ligand interactions on living cytotoxic T lymphocytes. Nature. 373, 353 (1995).

195. Lurquin, C., Lethe, B., De Plaen, E., Corbiere, V., Theate, I., van Baren, N., Coulie, P.G. and Boon, T.: Contrasting frequencies of antitumor and anti-vaccine T cells in metastases of a melanoma patient vaccinated with a MAGE tumor antigen. J Exp Med. 201, 249 (2005).

196. Lurquin, C., Van Pel, A., Mariame, B., De Plaen, E., Szikora, J.P., Janssens, C., Reddehase, M.J., Lejeune, J. and Boon, T.: Structure of the gene of tum- transplantation antigen P91A: the mutated exon encodes a peptide recognized with Ld by cytolytic T cells. Cell. 58, 293 (1989).

197. Macian, F., Garcia-Cozar, F., Im, S.H., Horton, H.F., Byrne, M.C. and Rao, A.: Transcriptional mechanisms underlying lymphocyte tolerance. Cell. 109, 719 (2002).

198. Mackensen, A., Meidenbauer, N., Vogl, S., Laumer, M., Berger, J. and Andreesen, R.: Phase I study of adoptive T-cell therapy using antigen-specific

CD8+ T cells for the treatment of patients with metastatic melanoma. J Clin Oncol. 24, 5060 (2006).

199. Madrenas, J., Wange, R.L., Wang, J.L., Isakov, N., Samelson, L.E. and Germain, R.N.: Zeta phosphorylation without ZAP-70 activation induced by TCR antagonists or partial agonists. Science. 267, 515 (1995).

200. Manning, T.C., Schlueter, C.J., Brodnicki, T.C., Parke, E.A., Speir, J.A., Garcia, K.C., Teyton, L., Wilson, I.A. and Kranz, D.M.: Alanine scanning mutagenesis of an alphabeta T cell receptor: mapping the energy of antigen recognition. Immunity. 8, 413 (1998).

201. Marchand, M., Punt, C.J., Aamdal, S., Escudier, B., Kruit, W.H., Keilholz, U., Hakansson, L., van Baren, N., Humblet, Y., Mulders, P., Avril, M.F., Eggermont, A.M., Scheibenbogen, C., Uiters, J., Wanders, J., Delire, M., Boon, T. and Stoter, G.: Immunisation of metastatic cancer patients with MAGE-3 protein combined with adjuvant SBAS-2: a clinical report. Eur J Cancer. 39, 70 (2003).

202. Marchand, M., van Baren, N., Weynants, P., Brichard, V., Dreno, B., Tessier, M.H., Rankin, E., Parmiani, G., Arienti, F., Humblet, Y., Bourlond, A., Vanwijck, R., Lienard, D., Beauduin, M., Dietrich, P.Y., Russo, V., Kerger, J., Masucci, G., Jager, E., De Greve, J., Atzpodien, J., Brasseur, F., Coulie, P.G., van der Bruggen, P. and Boon, T.: Tumor regressions observed in patients with metastatic melanoma treated with an antigenic peptide encoded by gene MAGE-3 and presented by HLA-A1. Int J Cancer. 80, 219 (1999).

203. Marincola, F.M., Jaffee, E.M., Hicklin, D.J. and Ferrone, S.: Escape of human solid tumors from T-cell recognition: molecular mechanisms and functional significance. Adv Immunol. 74, 181 (2000).

204. Marshall, D.R., Olivas, E., Andreansky, S., La Gruta, N.L., Neale, G.A., Gutierrez, A., Wichlan, D.G., Wingo, S., Cheng, C., Doherty, P.C. and Turner, S.J.: Effector CD8+ T cells recovered from an influenza pneumonia differentiate to a state of focused gene expression. Proc Natl Acad Sci U S A. 102, 6074 (2005).

205. Massague, J., Seoane, J. and Wotton, D.: Smad transcription factors. Genes Dev. 19, 2783 (2005).

206. Matsui, T., Takahashi, R., Nakao, Y., Koizumi, T., Katakami, Y., Mihara, K., Sugiyama, T. and Fujita, T.: 1,25-Dihydroxyvitamin D3-regulated expression of genes involved in human T-lymphocyte proliferation and differentiation. Cancer Res. 46, 5827 (1986).

207. Matzinger, P.: Immunology. Memories are made of this? Nature. 369, 605 (1994).

208. McFarland, E.D.C., Hurley, T.R., Pingel, J.T., Sefton, B.M., Shaw, A. and Thomas, M.L.: Correlation Between Src Family Member Regulation by the Protein-Tyrosine- Phosphatase CD45 and Transmembrane Signaling Through the T-Cell Receptor. Proceedings of the National Academy of Sciences. 90, 1402 (1993).

209. McKeithan, T.W.: Kinetic proofreading in T-cell receptor signal transduction. Proc Natl Acad Sci U S A. 92, 5042 (1995).

210. McKnight, S.L.: McBindall--a better name for CCAAT/enhancer binding proteins? Cell. 107, 259 (2001).

211. McNeill, L., Salmond, R.J., Cooper, J.C., Carret, C.K., Cassady-Cain, R.L., Roche-Molina, M., Tandon, P., Holmes, N. and Alexander, D.R.: The Differential Regulation of Lck Kinase Phosphorylation Sites by CD45 Is Critical for T Cell Receptor Signaling Responses. Immunity. 27, 425 (2007).

212. Melero, I., Shuford, W.W., Newby, S.A., Aruffo, A., Ledbetter, J.A., Hellstrom, K.E., Mittler, R.S. and Chen, L.: Monoclonal antibodies against the 4-1BB T-cell activation molecule eradicate established tumors. Nat Med. 3, 682 (1997).

213. Michie, C.A., McLean, A., Alcock, C. and Beverley, P.C.: Lifespan of human lymphocyte subsets defined by CD45 isoforms. Nature. 360, 264 (1992).

214. Mihm, M.C., Jr., Clemente, C.G. and Cascinelli, N.: Tumor infiltrating lymphocytes in lymph node melanoma metastases: a histopathologic prognostic indicator and an expression of local immune response. Lab Invest. 74, 43 (1996).

215. Miller, A.J. and Mihm, M.C., Jr.: Melanoma. N Engl J Med. 355, 51 (2006).

216. Missbach, M., Jagher, B., Sigg, I., Nayeri, S., Carlberg, C. and Wiesenberg, I.: Thiazolidine diones, specific ligands of the nuclear receptor retinoid Z receptor/retinoid acid receptor-related orphan receptor alpha with potent antiarthritic activity. J Biol Chem. 271, 13515 (1996).

217. Monks, C.R., Freiberg, B.A., Kupfer, H., Sciaky, N. and Kupfer, A.: Three-dimensional segregation of supramolecular activation clusters in T cells. Nature. 395, 82 (1998).

218. Mortarini, R., Piris, A., Maurichi, A., Molla, A., Bersani, I., Bono, A., Bartoli, C., Santinami, M., Lombardo, C., Ravagnani, F., Cascinelli, N., Parmiani, G. and Anichini, A.: Lack of terminally differentiated tumor-specific CD8+ T cells at tumor site in spite of antitumor immunity to self-antigens in human metastatic melanoma. Cancer Res. 63, 2535 (2003).

219. Murali-Krishna, K., Altman, J.D., Suresh, M., Sourdive, D., Zajac, A. and Ahmed, R.: In vivo dynamics of anti-viral CD8 T cell responses to different epitopes. An evaluation of bystander activation in primary and secondary responses to viral infection. Adv Exp Med Biol. 452, 123 (1998).

220. Naeher, D., Daniels, M.A., Hausmann, B., Guillaume, P., Luescher, I. and Palmer, E.: A constant affinity threshold for T cell tolerance. J Exp Med. 204, 2553 (2007).

221. Nagata, S. and Golstein, P.: The Fas death factor. Science. 267, 1449 (1995).

222. Natali, P.G., Cavaliere, R., Bigotti, A., Nicotra, M.R., Russo, C., Ng, A.K., Giacomini, P. and Ferrone, S.: Antigenic heterogeneity of surgically removed primary and autologous metastatic human melanoma lesions. J Immunol. 130, 1462 (1983).

223. Natali, P.G., Nicotra, M.R., Bigotti, A., Venturo, I., Marcenaro, L., Giacomini, P. and Russo, C.: Selective changes in expression of HLA class I polymorphic determinants in human solid tumors. Proc Natl Acad Sci U S A. 86, 6719 (1989).

224. Neilson, J.R., Zheng, G.X., Burge, C.B. and Sharp, P.A.: Dynamic regulation of miRNA expression in ordered stages of cellular development. Genes Dev. 21, 578 (2007).

225. Nel, A.E.: T-cell activation through the antigen receptor. Part 1: signaling components, signaling pathways, and signal integration at the T-cell antigen receptor synapse. J Allergy Clin Immunol. 109, 758 (2002).

226. Newcom, S.R. and Gu, L.: Transforming growth factor beta 1 messenger RNA in Reed-Sternberg cells in nodular sclerosing Hodgkin's disease. J Clin Pathol. 48, 160 (1995).

227. Newcom, S.R., Kadin, M.E., Ansari, A.A. and Diehl, V.: L-428 nodular sclerosing Hodgkin's cell secretes a unique transforming growth factor-beta active at physiologic pH. J Clin Invest. 82, 1915 (1988).

228. Niehans, G.A., Brunner, T., Frizelle, S.P., Liston, J.C., Salerno, C.T., Knapp, D.J., Green, D.R. and Kratzke, R.A.: Human lung carcinomas express Fas ligand. Cancer Res. 57, 1007 (1997).

229. Nocentini, G., Giunchi, L., Ronchetti, S., Krausz, L.T., Bartoli, A., Moraca, R., Migliorati, G. and Riccardi, C.: A new member of the tumor necrosis factor/nerve growth factor receptor family inhibits T cell receptor-induced apoptosis. Proc Natl Acad Sci U S A. 94, 6216 (1997).

230. Norment, A.M., Salter, R.D., Parham, P., Engelhard, V.H. and Littman, D.R.: Cell-cell adhesion mediated by CD8 and MHC class I molecules. Nature. 336, 79 (1988).

231. Novellino, L., Castelli, C. and Parmiani, G.: A listing of human tumor antigens recognized by T cells: March 2004 update. Cancer Immunol Immunother. 54, 187 (2005).

232. Ohlen, C., Kalos, M., Cheng, L.E., Shur, A.C., Hong, D.J., Carson, B.D., Kokot, N.C., Lerner, C.G., Sather, B.D., Huseby, E.S. and Greenberg, P.D.: CD8(+) T cell tolerance to a tumor-associated antigen is maintained at the level of expansion rather than effector function. J Exp Med. 195, 1407 (2002).

233. Ohno, H., Takimoto, G. and McKeithan, T.W.: The candidate proto-oncogene bcl-3 is related to genes implicated in cell lineage determination and cell cycle control. Cell. 60, 991 (1990).

234. Ostergaard, H.L. and Lysechko, T.L.: Focal adhesion kinase-related protein tyrosine kinase Pyk2 in T-cell activation and function. Immunol Res. 31, 267 (2005).

235. Ostergaard, H.L., Shackelford, D.A., Hurley, T.R., Johnson, P., Hyman, R., Sefton, B.M. and Trowbridge, I.S.: Expression of CD45 Alters Phosphorylation of the lck-Encoded Tyrosine Protein Kinase in Murine Lymphoma T-Cell Lines. Proceedings of the National Academy of Sciences. 86, 8959 (1989).

236. Ostrand-Rosenberg, S. and Sinha, P.: Myeloid-derived suppressor cells: linking inflammation and cancer. J Immunol. 182, 4499 (2009).

237. Overwijk, W.W., Tsung, A., Irvine, K.R., Parkhurst, M.R., Goletz, T.J., Tsung, K., Carroll, M.W., Liu, C., Moss, B., Rosenberg, S.A. and Restifo, N.P.: gp100/pmel 17 is a murine tumor rejection antigen: induction of "self"-reactive, tumoricidal T cells using high-affinity, altered peptide ligand. J Exp Med. 188, 277 (1998).

238. Palena, C., Arlen, P., Zeytin, H., Greiner, J.W., Schlom, J. and Tsang, K.Y.: Enhanced expression of lymphotactin by CD8+ T cells is selectively induced by enhancer agonist peptides of tumor-associated antigens. Cytokine. 24, 128 (2003).

239. Palena, C., Schlom, J. and Tsang, K.Y.: Differential gene expression profiles in a human T-cell line stimulated with a tumor-associated self-peptide versus an enhancer agonist peptide. Clin Cancer Res. 9, 1616 (2003).

240. Pannetier, C., Cochet, M., Darche, S., Casrouge, A., Zoller, M. and Kourilsky, P.: The sizes of the CDR3 hypervariable regions of the murine T-cell receptor beta chains vary as a function of the recombined germ-line segments. Proc Natl Acad Sci U S A. 90, 4319 (1993).

241. Pardoll, D.: Does the immune system see tumors as foreign or self? Annu Rev Immunol. 21, 807 (2003).

242. Park, J.H., Adoro, S., Lucas, P.J., Sarafova, S.D., Alag, A.S., Doan, L.L., Erman, B., Liu, X., Ellmeier, W., Bosselut, R., Feigenbaum, L. and Singer, A.: 'Coreceptor tuning': cytokine signals transcriptionally tailor CD8 coreceptor expression to the self-specificity of the TCR. Nat Immunol. 8, 1049 (2007).

243. Pectasides, D., Dafni, U., Bafaloukos, D., Skarlos, D., Polyzos, A., Tsoutsos, D., Kalofonos, H., Fountzilas, G., Panagiotou, P., Kokkalis, G., Papadopoulos, O., Castana, O., Papadopoulos, S., Stavrinidis, E., Vourli, G., Ioannovich, J. and Gogas, H.: Randomized Phase III Study of 1 Month Versus 1 Year of Adjuvant High-Dose Interferon Alfa-2b in Patients With Resected High-Risk Melanoma. J Clin Oncol. (2009).

244. Perez, V.L., Van Parijs, L., Biuckians, A., Zheng, X.X., Strom, T.B. and Abbas, A.K.: Induction of peripheral T cell tolerance in vivo requires CTLA-4 engagement. Immunity. 6, 411 (1997).

245. Pircher, H., Rohrer, U.H., Moskophidis, D., Zinkernagel, R.M. and Hengartner, H.: Lower receptor avidity required for thymic clonal deletion than for effector T-cell function. Nature. 351, 482 (1991).

246. Polyak, K., Kato, J.Y., Solomon, M.J., Sherr, C.J., Massague, J., Roberts, J.M. and Koff, A.: p27Kip1, a cyclin-Cdk inhibitor, links transforming growth factor-beta and contact inhibition to cell cycle arrest. Genes Dev. 8, 9 (1994).

247. Polyak, K., Lee, M.H., Erdjument-Bromage, H., Koff, A., Roberts, J.M., Tempst, P. and Massague, J.: Cloning of p27Kip1, a cyclin-dependent kinase inhibitor and a potential mediator of extracellular antimitogenic signals. Cell. 78, 59 (1994).

248. Potter, T.A., Grebe, K., Freiberg, B. and Kupfer, A.: Formation of supramolecular activation clusters on fresh ex vivo CD8+ T cells after engagement of the T cell antigen receptor and CD8 by antigen-presenting cells. Proceedings of the National Academy of Sciences of the United States of America. 98, 12624 (2001).

249. Powell, J.D., Lerner, C.G. and Schwartz, R.H.: Inhibition of cell cycle progression by rapamycin induces T cell clonal anergy even in the presence of costimulation. J Immunol. 162, 2775 (1999).

250. Prehn, R.T. and Main, J.M.: Immunity to methylcholanthrene-induced sarcomas. J Natl Cancer Inst. 18, 769 (1957).

251. Price, D.A., Brenchley, J.M., Ruff, L.E., Betts, M.R., Hill, B.J., Roederer, M., Koup, R.A., Migueles, S.A., Gostick, E., Wooldridge, L., Sewell, A.K., Connors, M. and Douek, D.C.: Avidity for antigen shapes clonal dominance in CD8+ T cell populations specific for persistent DNA viruses. J Exp Med. 202, 1349 (2005).

252. Qi, Q. and August, A.: Keeping the (kinase) party going: SLP-76 and ITK dance to the beat. Sci STKE. 2007, pe39 (2007).

253. Rabinovich, G.A., Gabrilovich, D. and Sotomayor, E.M.: Immunosuppressive strategies that are mediated by tumor cells. Annu Rev Immunol. 25, 267 (2007).

254. Ragazzo, J.L., Ozaki, M.E., Karlsson, L., Peterson, P.A. and Webb, S.R.: Costimulation via lymphocyte function-associated antigen 1 in the absence of CD28 ligation promotes anergy of naive CD4+ T cells. Proc Natl Acad Sci U S A. 98, 241 (2001).

255. Ragione, F.D., Cucciolla, V., Criniti, V., Indaco, S., Borriello, A. and Zappia, V.: p21Cip1 gene expression is modulated by Egr1: a novel regulatory mechanism involved in the resveratrol antiproliferative effect. J Biol Chem. 278, 23360 (2003).

256. Rao, A., Luo, C. and Hogan, P.G.: Transcription factors of the NFAT family: regulation and function. Annu Rev Immunol. 15, 707 (1997).

257. Ravkov, E.V., Myrick, C.M. and Altman, J.D.: Immediate early effector functions of virus-specific CD8+CCR7+ memory cells in humans defined by HLA and CC chemokine ligand 19 tetramers. J Immunol. 170, 2461 (2003).

258. Reiser, J.B., Darnault, C., Gregoire, C., Mosser, T., Mazza, G., Kearney, A., van der Merwe, P.A., Fontecilla-Camps, J.C., Housset, D. and Malissen, B.: CDR3 loop flexibility contributes to the degeneracy of TCR recognition. Nat Immunol. 4, 241 (2003).

259. Richard, M., Louahed, J., Demoulin, J.B. and Renauld, J.C.: Interleukin-9 regulates NF-kappaB activity through BCL3 gene induction. Blood. 93, 4318 (1999).

260. Rincon, M., Conze, D., Weiss, L., Diehl, N.L., Fortner, K.A., Yang, D., Flavell, R.A., Enslen, H., Whitmarsh, A. and Davis, R.J.: Conference highlight: do T cells care about the mitogen-activated protein kinase signalling pathways? Immunol Cell Biol. 78, 166 (2000).

261. Rivard, N., L'Allemain, G., Bartek, J. and Pouyssegur, J.: Abrogation of p27Kip1 by cDNA antisense suppresses quiescence (G0 state) in fibroblasts. J Biol Chem. 271, 18337 (1996).

262. Robbins, P.F., Li, Y.F., El-Gamil, M., Zhao, Y., Wargo, J.A., Zheng, Z., Xu, H., Morgan, R.A., Feldman, S.A., Johnson, L.A., Bennett, A.D., Dunn, S.M., Mahon, T.M., Jakobsen, B.K. and Rosenberg, S.A.: Single and dual amino acid substitutions in TCR CDRs can enhance antigen-specific T cell functions. J Immunol. 180, 6116 (2008).

263. Robertson, J.M. and Evavold, B.D.: Cutting edge: dueling TCRs: peptide antagonism of CD4+ T cells with dual antigen specificities. J Immunol. 163, 1750 (1999).

264. Robey, E.A., Ramsdell, F., Kioussis, D., Sha, W., Loh, D., Axel, R. and Fowlkes, B.J.: The level of CD8 expression can determine the outcome of thymic selection. Cell. 69, 1089 (1992).

265. Rocha, B., Tanchot, C. and Von Boehmer, H.: Clonal anergy blocks in vivo growth of mature T cells and can be reversed in the absence of antigen. J Exp Med. 177, 1517 (1993).

266. Rocha, B. and von Boehmer, H.: Peripheral selection of the T cell repertoire. Science. 251, 1225 (1991).

267. Ronchetti, S., Nocentini, G., Riccardi, C. and Pandolfi, P.P.: Role of GITR in activation response of T lymphocytes. Blood. 100, 350 (2002).

268. Ronchetti, S., Zollo, O., Bruscoli, S., Agostini, M., Bianchini, R., Nocentini, G., Ayroldi, E. and Riccardi, C.: GITR, a member of the TNF receptor superfamily, is costimulatory to mouse T lymphocyte subpopulations. Eur J Immunol. 34, 613 (2004).

269. Rooney, C.M., Smith, C.A., Ng, C.Y., Loftin, S., Li, C., Krance, R.A., Brenner, M.K. and Heslop, H.E.: Use of gene-modified virus-specific T lymphocytes to control Epstein-Barr-virus-related lymphoproliferation. Lancet. 345, 9 (1995).

270. Rudd, C.E.: Cell cycle 'check points' T cell anergy. Nat Immunol. 7, 1130 (2006).

271. Sahin, U., Tureci, O. and Pfreundschuh, M.: Serological identification of human tumor antigens. Curr Opin Immunol. 9, 709 (1997).

272. Sallusto, F., Lenig, D., Forster, R., Lipp, M. and Lanzavecchia, A.: Two subsets of memory T lymphocytes with distinct homing potentials and effector functions. Nature. 401, 708 (1999).

273. Sallusto, F., Lenig, D., Mackay, C.R. and Lanzavecchia, A.: Flexible programs of chemokine receptor expression on human polarized T helper 1 and 2 lymphocytes. J Exp Med. 187, 875 (1998).

274. Salomonis, N., Hanspers, K., Zambon, A.C., Vranizan, K., Lawlor, S.C., Dahlquist, K.D., Doniger, S.W., Stuart, J., Conklin, B.R. and Pico, A.R.: GenMAPP 2: new features and resources for pathway analysis. BMC Bioinformatics. 8, 217 (2007).

275. Samelson, L.E.: Signal transduction mediated by the T cell antigen receptor: the role of adapter proteins. Annu Rev Immunol. 20, 371 (2002).

276. Sancho, D., Gomez, M., Viedma, F., Esplugues, E., Gordon-Alonso, M., Garcia-Lopez, M.A., de la Fuente, H., Martinez, A.C., Lauzurica, P. and Sanchez-Madrid, F.: CD69 downregulates autoimmune reactivity through active transforming growth factor-beta production in collagen-induced arthritis. J Clin Invest. 112, 872 (2003).

277. Sato, E., Olson, S.H., Ahn, J., Bundy, B., Nishikawa, H., Qian, F., Jungbluth, A.A., Frosina, D., Gnjatic, S., Ambrosone, C., Kepner, J., Odunsi, T., Ritter, G., Lele, S., Chen, Y.T., Ohtani, H., Old, L.J. and Odunsi, K.: Intraepithelial CD8+ tumor-infiltrating lymphocytes and a high CD8+/regulatory T cell ratio are associated with favorable prognosis in ovarian cancer. Proc Natl Acad Sci U S A. 102, 18538 (2005).

278. Savage, P.A. and Davis, M.M.: A Kinetic Window Constricts the T Cell Receptor Repertoire in the Thymus. Immunity. 14, 243 (2001).

279. Schneider, H., Valk, E., Leung, R. and Rudd, C.E.: CTLA-4 activation of phosphatidylinositol 3-kinase (PI 3-K) and protein kinase B (PKB/AKT) sustains T-cell anergy without cell death. PLoS ONE. 3, e3842 (2008).

280. Schwartz, R.H.: T cell anergy. Annu Rev Immunol. 21, 305 (2003).

281. Scott, K.L. and Plon, S.E.: CHES1/FOXN3 interacts with Ski-interacting protein and acts as a transcriptional repressor. Gene. 359, 119 (2005).

282. Scotto, L., Naiyer, A.J., Galluzzo, S., Rossi, P., Manavalan, J.S., Kim-Schulze, S., Fang, J., Favera, R.D., Cortesini, R. and Suciu-Foca, N.: Overlap between molecular markers expressed by naturally occurring CD4+CD25+ regulatory T cells and antigen specific CD4+CD25+ and CD8+CD28- T suppressor cells. Hum Immunol. 65, 1297 (2004).

283. Screpanti, I., Romani, L., Musiani, P., Modesti, A., Fattori, E., Lazzaro, D., Sellitto, C., Scarpa, S., Bellavia, D., Lattanzio, G. and et al.: Lymphoproliferative disorder and imbalanced T-helper response in C/EBP beta-deficient mice. Embo J. 14, 1932 (1995).

284. Sefton, B.M. and Campbell, M.A.: The role of tyrosine protein phosphorylation in lymphocyte activation. Annu Rev Cell Biol. 7, 257 (1991).

285. Sherr, C.J. and Roberts, J.M.: Inhibitors of mammalian G1 cyclin-dependent kinases. Genes Dev. 9, 1149 (1995).

286. Shimizu, J., Yamazaki, S., Takahashi, T., Ishida, Y. and Sakaguchi, S.: Stimulation of CD25(+)CD4(+) regulatory T cells through GITR breaks immunological self-tolerance. Nat Immunol. 3, 135 (2002).

287. Singh, A., Svaren, J., Grayson, J. and Suresh, M.: CD8 T cell responses to lymphocytic choriomeningitis virus in early growth response gene 1-deficient mice. J Immunol. 173, 3855 (2004).

288. Singh, V., Ji, Q., Feigenbaum, L., Leighty, R.M. and Hurwitz, A.A.: Melanoma progression despite infiltration by in vivo-primed TRP-2-specific T cells. J Immunother. 32, 129 (2009).

289. Slifka, M.K. and Whitton, J.L.: Functional avidity maturation of CD8(+) T cells without selection of higher affinity TCR. Nat Immunol. 2, 711 (2001).

290. Sloan-Lancaster, J., Shaw, A.S., Rothbard, J.B. and Allen, P.M.: Partial T cell signaling: altered phospho-zeta and lack of zap70 recruitment in APL-induced T cell anergy. Cell. 79, 913 (1994).

291. Soler, D., Humphreys, T.L., Spinola, S.M. and Campbell, J.J.: CCR4 versus CCR10 in human cutaneous TH lymphocyte trafficking. Blood. 101, 1677 (2003).

292. Song, E., Chen, J., Ouyang, N., Su, F., Wang, M. and Heemann, U.: Soluble Fas ligand released by colon adenocarcinoma cells induces host lymphocyte apoptosis: an active mode of immune evasion in colon cancer. Br J Cancer. 85, 1047 (2001).

293. Starr, T.K., Jameson, S.C. and Hogquist, K.A.: Positive and negative selection of T cells. Annu Rev Immunol. 21, 139 (2003).

294. Stefanova, I., Hemmer, B., Vergelli, M., Martin, R., Biddison, W.E. and Germain, R.N.: TCR ligand discrimination is enforced by competing ERK positive and SHP-1 negative feedback pathways. Nat Immunol. 4, 248 (2003).

295. Stockert, E., Jager, E., Chen, Y.T., Scanlan, M.J., Gout, I., Karbach, J., Arand, M., Knuth, A. and Old, L.J.: A survey of the humoral immune response of cancer patients to a panel of human tumor antigens. J Exp Med. 187, 1349 (1998).

296. Stuber, E. and Strober, W.: The T cell-B cell interaction via OX40-OX40L is necessary for the T cell-dependent humoral immune response. J Exp Med. 183, 979 (1996).

297. Sugita, Y., Wada, H., Fujita, S., Nakata, T., Sato, S., Noguchi, Y., Jungbluth, A.A., Yamaguchi, M., Chen, Y.T., Stockert, E., Gnjatic, S., Williamson, B., Scanlan, M.J., Ono, T., Sakita, I., Yasui, M., Miyoshi, Y., Tamaki, Y., Matsuura, N., Noguchi, S., Old, L.J., Nakayama, E. and Monden, M.: NY-ESO-1 expression and immunogenicity in malignant and benign breast tumors. Cancer Res. 64, 2199 (2004).

298. Sundstedt, A., Hoiden, I., Hansson, J., Hedlund, G., Kalland, T. and Dohlsten, M.: Superantigen-induced anergy in cytotoxic CD8+ T cells. J Immunol. 154, 6306 (1995).

299. Susaki, E., Nakayama, K. and Nakayama, K.I.: Cyclin D2 translocates p27 out of the nucleus and promotes its degradation at the G0-G1 transition. Mol Cell Biol. 27, 4626 (2007).

300. Suzuki, T., Tahara, H., Narula, S., Moore, K.W., Robbins, P.D. and Lotze, M.T.: Viral interleukin 10 (IL-10), the human herpes virus 4 cellular IL-10 homologue, induces local anergy to allogeneic and syngeneic tumors. J Exp Med. 182, 477 (1995).

301. Takeuchi, A., Reddy, G.S., Kobayashi, T., Okano, T., Park, J. and Sharma, S.: Nuclear factor of activated T cells (NFAT) as a molecular target for 1alpha,25-dihydroxyvitamin D3-mediated effects. J Immunol. 160, 209 (1998).

302. Tan, J.T., Whitmire, J.K., Ahmed, R., Pearson, T.C. and Larsen, C.P.: 4-1BB ligand, a member of the TNF family, is important for the generation of antiviral CD8 T cell responses. J Immunol. 163, 4859 (1999).

303. Tan, J.T., Whitmire, J.K., Murali-Krishna, K., Ahmed, R., Altman, J.D., Mittler, R.S., Sette, A., Pearson, T.C. and Larsen, C.P.: 4-1BB costimulation is required for protective anti-viral immunity after peptide vaccination. J Immunol. 164, 2320 (2000).

304. Tanchot, C., Guillaume, S., Delon, J., Bourgeois, C., Franzke, A., Sarukhan, A., Trautmann, A. and Rocha, B.: Modifications of CD8+ T cell function during in vivo memory or tolerance induction. Immunity. 8, 581 (1998).

305. Tavano, R., Gri, G., Molon, B., Marinari, B., Rudd, C.E., Tuosto, L. and Viola, A.: CD28 and Lipid Rafts Coordinate Recruitment of Lck to the Immunological Synapse of Human T Lymphocytes. J Immunol. 173, 5392 (2004).

306. Tham, E.L., Shrikant, P. and Mescher, M.F.: Activation-induced nonresponsiveness: a Th-dependent regulatory checkpoint in the CTL response. J Immunol. 168, 1190 (2002).

307. Thomas, M.L.: Cellular and Humoral Aspects of the Hypersensitive States. Journal. 667 pp. (1959).

308. Tian, S., Maile, R., Collins, E.J. and Frelinger, J.A.: CD8+ T Cell Activation Is Governed by TCR-Peptide/MHC Affinity, Not Dissociation Rate. J Immunol. 179, 2952 (2007).

309. Tone, M., Tone, Y., Adams, E., Yates, S.F., Frewin, M.R., Cobbold, S.P. and Waldmann, H.: Mouse glucocorticoid-induced tumor necrosis factor receptor ligand is costimulatory for T cells. Proc Natl Acad Sci U S A. 100, 15059 (2003).

310. Tough, D.F., Borrow, P. and Sprent, J.: Induction of bystander T cell proliferation by viruses and type I interferon in vivo. Science. 272, 1947 (1996).

311. Tough, D.F. and Sprent, J.: Viruses and T cell turnover: evidence for bystander proliferation. Immunol Rev. 150, 129 (1996).

312. Toyoshima, H. and Hunter, T.: p27, a novel inhibitor of G1 cyclin-Cdk protein kinase activity, is related to p21. Cell. 78, 67 (1994).

313. Tsao, H., Atkins, M.B. and Sober, A.J.: Management of cutaneous melanoma. N Engl J Med. 351, 998 (2004).

314. Tussey, L., Speller, S., Gallimore, A. and Vessey, R.: Functionally distinct CD8+ memory T cell subsets in persistent EBV infection are differentiated by migratory receptor expression. Eur J Immunol. 30, 1823 (2000).

315. Umansky, V., Abschuetz, O., Osen, W., Ramacher, M., Zhao, F., Kato, M. and Schadendorf, D.: Melanoma-specific memory T cells are functionally active in Ret transgenic mice without macroscopic tumors. Cancer Res. 68, 9451 (2008).

316. Unsoeld, H., Krautwald, S., Voehringer, D., Kunzendorf, U. and Pircher, H.: Cutting edge: CCR7+ and CCR7- memory T cells do not differ in immediate effector cell function. J Immunol. 169, 638 (2002).

317. Unutmaz, D., Pileri, P. and Abrignani, S.: Antigen-independent activation of naive and memory resting T cells by a cytokine combination. J Exp Med. 180, 1159 (1994).

318. Utting, O., Teh, S.J. and Teh, H.S.: A population of in vivo anergized T cells with a lower activation threshold for the induction of CD25 exhibit differential requirements in mobilization of intracellular calcium and mitogen-activated protein kinase activation. J Immunol. 164, 2881 (2000).

319. Uyttenhove, C., Pilotte, L., Theate, I., Stroobant, V., Colau, D., Parmentier, N., Boon, T. and Van den Eynde, B.J.: Evidence for a tumoral immune resistance mechanism based on tryptophan degradation by indoleamine 2,3-dioxygenase. Nat Med. 9, 1269 (2003).

320. Valitutti, S., Muller, S., Cella, M., Padovan, E. and Lanzavecchia, A.: Serial triggering of many T-cell receptors by a few peptide-MHC complexes. Nature. 375, 148 (1995).

321. Valitutti, S., Muller, S., Dessing, M. and Lanzavecchia, A.: Signal extinction and T cell repolarization in T helper cell-antigen-presenting cell conjugates. Eur J Immunol. 26, 2012 (1996).

322. Valitutti, S., Muller, S., Salio, M. and Lanzavecchia, A.: Degradation of T Cell Receptor (TCR)-CD3-zeta Complexes after Antigenic Stimulation. J. Exp. Med. 185, 1859 (1997).

323. Valmori, D., Dutoit, V., Lienard, D., Rimoldi, D., Pittet, M.J., Champagne, P., Ellefsen, K., Sahin, U., Speiser, D., Lejeune, F., Cerottini, J.C. and Romero, P.: Naturally occurring human lymphocyte antigen-A2 restricted CD8+ T-cell response to the cancer testis antigen NY-ESO-1 in melanoma patients. Cancer Res. 60, 4499 (2000).

324. Valmori, D., Dutoit, V., Schnuriger, V., Quiquerez, A.L., Pittet, M.J., Guillaume, P., Rubio-Godoy, V., Walker, P.R., Rimoldi, D., Lienard, D., Cerottini, J.C., Romero, P. and Dietrich, P.Y.: Vaccination with a Melan-A peptide selects an oligoclonal T cell population with increased functional avidity and tumor reactivity. J Immunol. 168, 4231 (2002).

325. van Baren, N., Bonnet, M.-C., Dreno, B., Khammari, A., Dorval, T., Piperno-Neumann, S., Lienard, D., Speiser, D., Marchand, M., Brichard, V.G., Escudier, B., Negrier, S., Dietrich, P.-Y., Maraninchi, D., Osanto, S., Meyer, R.G., Ritter, G., Moingeon, P., Tartaglia, J., van der Bruggen, P., Coulie, P.G. and Boon, T.: Tumoral and Immunologic Response After Vaccination of Melanoma Patients With an ALVAC Virus Encoding MAGE Antigens Recognized by T Cells. J Clin Oncol. 23, 9008 (2005).

326. van der Bruggen, P., Traversari, C., Chomez, P., Lurquin, C., De Plaen, E., Van den Eynde, B., Knuth, A. and Boon, T.: A gene encoding an antigen recognized by cytolytic T lymphocytes on a human melanoma. Science. 254, 1643 (1991).

327. van der Merwe, P.A. and Davis, S.J.: Molecular interactions mediating T cell antigen recognition. Annu Rev Immunol. 21, 659 (2003).

328. van Oers, N.S.C.: T cell receptor-mediated signs and signals governing T cell development. Seminars in Immunology. 11, 227 (1999).

329. van Oijen, M., Bins, A., Elias, S., Sein, J., Weder, P., de Gast, G., Mallo, H., Gallee, M., Van Tinteren, H., Schumacher, T. and Haanen, J.: On the role of melanoma-specific CD8+ T-cell immunity in disease progression of advanced-stage melanoma patients. Clin Cancer Res. 10, 4754 (2004).

330. van Olffen, R.W., Koning, N., van Gisbergen, K.P.J.M., Wensveen, F.M., Hoek, R.M., Boon, L., Hamann, J., van Lier, R.A.W. and Nolte, M.A.: GITR Triggering Induces Expansion of Both Effector and Regulatory CD4+ T Cells In Vivo. J Immunol. 182, 7490 (2009).

331. Verdeil, G., Puthier, D., Nguyen, C., Schmitt-Verhulst, A.M. and Auphan-Anezin, N.: Gene profiling approach to establish the molecular bases for partial versus full activation of naive CD8 T lymphocytes. Ann N Y Acad Sci. 975, 68 (2002).

332. Villalba, M., Coudronniere, N., Deckert, M., Teixeiro, E., Mas, P. and Altman, A.: A novel functional interaction between Vav and PKCtheta is required for TCR-induced T cell activation. Immunity. 12, 151 (2000).

333. Viola, A. and Lanzavecchia, A.: T cell activation determined by T cell receptor number and tunable thresholds. Science. 273, 104 (1996).

334. Walunas, T.L., Bakker, C.Y. and Bluestone, J.A.: CTLA-4 ligation blocks CD28-dependent T cell activation. J Exp Med. 183, 2541 (1996).

335. Wang, H., Iakova, P., Wilde, M., Welm, A., Goode, T., Roesler, W.J. and Timchenko, N.A.: C/EBP[alpha] Arrests Cell Proliferation through Direct Inhibition of Cdk2 and Cdk4. Molecular Cell. 8, 817 (2001).

336. Wang, H.C., Zhou, Q., Dragoo, J. and Klein, J.R.: Most murine CD8+ intestinal intraepithelial lymphocytes are partially but not fully activated T cells. J Immunol. 169, 4717 (2002).

337. Wang, H.Y., Lee, D.A., Peng, G., Guo, Z., Li, Y., Kiniwa, Y., Shevach, E.M. and Wang, R.F.: Tumor-specific human CD4+ regulatory T cells and their ligands: implications for immunotherapy. Immunity. 20, 107 (2004).

338. Wang, L., Goillot, E. and Tepper, R.I.: IL-10 inhibits alloreactive cytotoxic T lymphocyte generation in vivo. Cell Immunol. 159, 152 (1994).

339. Wang, Y., Wu, X.J., Zhao, A.L., Yuan, Y.H., Chen, Y.T., Jungbluth, A.A., Gnjatic, S., Santiago, D., Ritter, G., Chen, W.F., Old, L.J. and Ji, J.F.: Cancer/testis antigen expression and autologous humoral immunity to NY-ESO-1 in gastric cancer. Cancer Immun. 4, 11 (2004).

340. Wasserman, H.A., Beal, C.D., Zhang, Y., Jiang, N., Zhu, C. and Evavold, B.D.: MHC variant peptide-mediated anergy of encephalitogenic T cells requires SHP-1. J Immunol. 181, 6843 (2008).

341. Watts, T.H.: TNF/TNFR family members in costimulation of T cell responses. Annu Rev Immunol. 23, 23 (2005).

342. Weaver, C.T., Pingel, J.T., Nelson, J.O. and Thomas, M.L.: CD8+ T-cell clones deficient in the expression of the CD45 protein tyrosine phosphatase have impaired responses to T-cell receptor stimuli. Mol. Cell. Biol. 11, 4415 (1991).

343. Weekes, M.P., Carmichael, A.J., Wills, M.R., Mynard, K. and Sissons, J.G.: Human CD28-CD8+ T cells contain greatly expanded functional virus-specific memory CTL clones. J Immunol. 162, 7569 (1999).

344. Wells, A.D., Walsh, M.C., Bluestone, J.A. and Turka, L.A.: Signaling through CD28 and CTLA-4 controls two distinct forms of T cell anergy. J Clin Invest. 108, 895 (2001).

345. Wells, A.D., Walsh, M.C., Sankaran, D. and Turka, L.A.: T cell effector function and anergy avoidance are quantitatively linked to cell division. J Immunol. 165, 2432 (2000).

346. Welsh, R.M.: Assessing CD8 T Cell Number and Dysfunction in the Presence of Antigen. J. Exp. Med. 193, 19F (2001).

347. Wherry, E.J., Ha, S.J., Kaech, S.M., Haining, W.N., Sarkar, S., Kalia, V., Subramaniam, S., Blattman, J.N., Barber, D.L. and Ahmed, R.: Molecular signature of CD8+ T cell exhaustion during chronic viral infection. Immunity. 27, 670 (2007).

348. Wherry, E.J., Teichgraber, V., Becker, T.C., Masopust, D., Kaech, S.M., Antia, R., von Andrian, U.H. and Ahmed, R.: Lineage relationship and protective immunity of memory CD8 T cell subsets. Nat Immunol. 4, 225 (2003).

349. WHO: Mortality statistics 2006. http://www.who.int/healthinfo/morttables/en/.

350. Wiedemann, A., Muller, S., Favier, B., Penna, D., Guiraud, M., Delmas, C., Champagne, E. and Valitutti, S.: T-cell activation is accompanied by an ubiquitination process occurring at the immunological synapse. Immunol Lett. 98, 57 (2005).

351. Wills, M.R., Okecha, G., Weekes, M.P., Gandhi, M.K., Sissons, P.J. and Carmichael, A.J.: Identification of naive or antigen-experienced human CD8(+) T cells by expression of costimulation and chemokine receptors: analysis of the human cytomegalovirus-specific CD8(+) T cell response. J Immunol. 168, 5455 (2002).

352. Wolfraim, L.A., Walz, T.M., James, Z., Fernandez, T. and Letterio, J.J.: p21Cip1 and p27Kip1 act in synergy to alter the sensitivity of naive T cells to TGF-beta-mediated G1 arrest through modulation of IL-2 responsiveness. J Immunol. 173, 3093 (2004).

353. Wu, J. and Lingrel, J.B.: KLF2 inhibits Jurkat T leukemia cell growth via upregulation of cyclin-dependent kinase inhibitor p21WAF1/CIP1. Oncogene. 23, 8088 (2004).

354. Wu, L.C., Tuot, D.S., Lyons, D.S., Garcia, K.C. and Davis, M.M.: Two-step binding mechanism for T-cell receptor recognition of peptide MHC. Nature. 418, 552 (2002).

355. Xiao, Z., Mescher, M.F. and Jameson, S.C.: Detuning CD8 T cells: down-regulation of CD8 expression, tetramer binding, and response during CTL activation. J Exp Med. 204, 2667 (2007).

356. Xu, C., Gagnon, E., Call, M.E., Schnell, J.R., Schwieters, C.D., Carman, C.V., Chou, J.J. and Wucherpfennig, K.W.: Regulation of T cell receptor activation by dynamic membrane binding of the CD3epsilon cytoplasmic tyrosine-based motif. Cell. 135, 702 (2008).

357. Xu, T., Shu, C.T., Purdom, E., Dang, D., Ilsley, D., Guo, Y., Weber, J., Holmes, S.P. and Lee, P.P.: Microarray analysis reveals differences in gene expression of circulating CD8(+) T cells in melanoma patients and healthy donors. Cancer Res. 64, 3661 (2004).

358. Yang, D.D., Conze, D., Whitmarsh, A.J., Barrett, T., Davis, R.J., Rincon, M. and Flavell, R.A.: Differentiation of CD4+ T cells to Th1 cells requires MAP kinase JNK2. Immunity. 9, 575 (1998).

359. Yang, L. and Carbone, D.P.: Tumor-host immune interactions and dendritic cell dysfunction. Adv Cancer Res. 92, 13 (2004).

360. Yee, C., Thompson, J.A., Byrd, D., Riddell, S.R., Roche, P., Celis, E. and Greenberg, P.D.: Adoptive T cell therapy using antigen-specific CD8+ T cell clones for the treatment of patients with metastatic melanoma: in vivo persistence, migration, and antitumor effect of transferred T cells. Proc Natl Acad Sci U S A. 99, 16168 (2002).

361. Yee, C., Thompson, J.A., Roche, P., Byrd, D.R., Lee, P.P., Piepkorn, M., Kenyon, K., Davis, M.M., Riddell, S.R. and Greenberg, P.D.: Melanocyte destruction after antigen-specific immunotherapy of melanoma: direct evidence of t cell-mediated vitiligo. J Exp Med. 192, 1637 (2000).

362. Yu, Z., Theoret, M.R., Touloukian, C.E., Surman, D.R., Garman, S.C., Feigenbaum, L., Baxter, T.K., Baker, B.M. and Restifo, N.P.: Poor immunogenicity of a self/tumor antigen derives from peptide-MHC-I instability and is independent of tolerance. J Clin Invest. 114, 551 (2004).

363. Zal, T., Zal, M.A. and Gascoigne, N.R.: Inhibition of T cell receptor-coreceptor interactions by antagonist ligands visualized by live FRET imaging of the T-hybridoma immunological synapse. Immunity. 16, 521 (2002).

364. Zamoyska, R.: CD4 and CD8: modulators of T-cell receptor recognition of antigen and of immune responses? Curr Opin Immunol. 10, 82 (1998).

365. Zhang, F., Lin, M., Abidi, P., Thiel, G. and Liu, J.: Specific interaction of Egr1 and c/EBPbeta leads to the transcriptional activation of the human low density lipoprotein receptor gene. J Biol Chem. 278, 44246 (2003).

366. Zhang, P., Cote, A.L., de Vries, V.C., Usherwood, E.J. and Turk, M.J.: Induction of postsurgical tumor immunity and T-cell memory by a poorly immunogenic tumor. Cancer Res. 67, 6468 (2007).

367. Zhang, Q., Ragnauth, C.D., Skepper, J.N., Worth, N.F., Warren, D.T., Roberts, R.G., Weissberg, P.L., Ellis, J.A. and Shanahan, C.M.: Nesprin-2 is a multi-isomeric protein that binds lamin and emerin at the nuclear envelope and forms a subcellular network in skeletal muscle. J Cell Sci. 118, 673 (2005).

368. Zhu, S., Oh, H.S., Shim, M., Sterneck, E., Johnson, P.F. and Smart, R.C.: C/EBPbeta modulates the early events of keratinocyte differentiation involving growth arrest and keratin 1 and keratin 10 expression. Mol Cell Biol. 19, 7181 (1999).

369. Zinkernagel, R.M., Bachmann, M.F., Kundig, T.M., Oehen, S., Pirchet, H. and Hengartner, H.: On immunological memory. Annu Rev Immunol. 14, 333 (1996).

370. Zlotnik, A. and Yoshie, O.: Chemokines: a new classification system and their role in immunity. Immunity. 12, 121 (2000).

371. Zou, W.: Immunosuppressive networks in the tumour environment and their therapeutic relevance. Nat Rev Cancer. 5, 263 (2005).

9. Preliminary publications

A part of this work is based on the following publication which is reproduced with the kind permission of the respective publishers:

(1) Marc Beyer*, Julia Karbach*, **Michael R. Mallmann***, Thomas Zander, Daniela Eggle, Sabine Classen, Svenja Debey-Pascher, Michael Famulok, Elke Jäger and Joachim L. Schultze: Cancer Vaccine Enhanced, Non-Tumor-Reactive $CD8^+$ T Cells Exhibit a Distinct Molecular Program Associated with "Division Arrest Anergy".
Cancer Research 69, 4346, May 15, 2009

*authors contributed equally to this work

Parts of this work have been presented at the following scientific meetings & congresses:

(1) 95th Annual Meeting of the American Association of Immunologists, San Diego 2008: Beyer M, Karbach J, **Mallmann MR**, Zander T, Eggle D, Classen S, Debey-Pascher S, Jäger E, Schultze JL: Cancer vaccine enhanced, non-tumor-reactive $CD8^+$ T cells exhibit a distinct molecular program associated with 'division arrest anergy'.

(2) World Immune Regulation Meeting II, Davos 2008: **Mallmann MR**, Beyer M, Karbach J, Zander T, Eggle D, Classen S, Debey-Pascher S, Jäger E, Schultze JL: Cancer vaccine enhanced, non-tumor-reactive $CD8^+$ T cells exhibit a distinct molecular program associated with 'division arrest anergy'.

(3) Jahrestagung der Deutschen Gesellschaft für Immunologie, Berlin 2008: Beyer M, Karbach J, **Mallmann MR**, Zander T, Eggle D, Classen S, Debey-Pascher S, Jäger E, Schultze JL: Cancer vaccine enhanced, non-tumor-reactive $CD8^+$ T cells exhibit a distinct molecular program associated with 'division arrest anergy'.

10. Supplement

10.1. Chemicals

Acrylamide	Bio-Rad, Hercules, CA, USA
APS	Carl Roth GmbH + Co. KG, Karlsruhe, Germany
Boric Acid	Sigma, Steinheim, Germany
Bromphenolblue	Carl Roth GmbH + Co. KG, Karlsruhe, Germany
BSA	Perbio Science GmbH, Bonn, Germany
Complet Mini Protease Inhibitor	Roche Diagnostics, Mannheim, Germany
CFSE	Molecular Probes, Leiden, The Netherlands
DMEM	Invitrogen, Karlsruhe, Germany
FCS	Invitrogen, Karlsruhe, Germany
0,22 µm Filter	Millipore, Schwalbach, Germany
Glycerol	Sigma, Steinheim, Germany
HCl	Merck, Darmstadt, Germany
Hepes buffer	Invitrogen, Karlsruhe, Germany
H_2O	Fresenius Kabi AG, Bad Homburg, Germany
IL-2	Proimmune, Bradenton, FL, USA

KCl	Carl Roth GmbH + Co. KG, Karlsruhe, Germany
KH_2PO_4	Carl Roth GmbH + Co. KG, Karlsruhe, Germany
L-Glutamine	Invitrogen, Karlsruhe, Germany
Milk powder	Carl Roth GmbH + Co. KG, Karlsruhe, Germany
Na_2-EDTA	Carl Roth GmbH + Co. KG, Karlsruhe, Germany
Na_2HPO_4	Carl Roth GmbH + Co. KG, Karlsruhe, Germany
Na_3VO_4	Sigma, Steinheim, Germany
Nonessential amino acids	Invitrogen, Karlsruhe, Germany
NaCl	Sigma, Steinheim, Germany
NaF	Sigma, Steinheim, Germany
NaN_3	Sigma, Steinheim, Germany
NP40	Sigma, Steinheim, Germany
Paraformaldehyde	Sigma, Steinheim, Germany
Penicilline	Invitrogen, Karlsruhe, Germany
Phosphatase Inhibitor Cocktail 1	Sigma, Steinheim, Germany
Phosphatase Inhibitor Cocktail 2	Sigma, Steinheim, Germany
PMSF	Roche Diagnostics, Mannheim, Germany

RPMI 1640	Invitrogen, Karlsruhe, Germany
SDS	Carl Roth GmbH + Co. KG, Karlsruhe, Germany
SeeBlue® Plus2 Pre-Stained Stand.	Invitrogen, Karlsruhe, Germany
Streptomycin	Invitrogen, Karlsruhe, Germany
TEMED	Carl Roth GmbH + Co. KG, Karlsruhe
TFA	Thermo Fisher Scientific, Rockford, IL, USA
Triton X	Promega, Mannheim, Germany
Trypan Blue Solution (0.4%)	Sigma, Steinheim, Germany
Tris Base	Sigma, Steinheim, Germany
Tris-HCl	Sigma, Steinheim, Germany

10.2. Instruments/ hardware

Thermoblock Tb1	Biometra, Goettingen, Germany
Hera safe HS 12/2 Laminar-Flow-Box	Heraeus Instruments, Haunau, Germany
Microscope Televal 31	Carl Zeiss MicroImaging GmbH, Goettingen, Germany
BD FACSCanto™ flow cytometer	BD Biosciences, Heidelberg, Germany
Heatable Warmbath	Koettermann GmbH & Co KG, Uetze/ Haenigsen, Germany
Incubator shaker	New Brunswick Scientific GmbH, Nuertingen, Germany
Scale EW600-2M	Gottl. Kern & Sohn GmbH, Albstadt, Germany
Megafuge 1.0R	Kendro, Langenselbold, Germany
Incubator Type 5060 EK/CO 2	Heraeus Instruments, Haunau, Germany
Ice machine	Scotsman Ice Systems, Vernon Hills, IL, USA
Powerpac 300	Bio-Rad, Hercules, CA, USA
Shaker PS-M3D	Grant-bio, Shepreth, UK
Roller Mixer SRT1	Stuart Scientific, Stone, UK
Vortex Genie 2	Bender & Hobein AG, Zurich, Switzerland
Cooling Centrifuge 5402	Eppendorf, Hamburg, Germany

Electroporesis EPS 601 Power Supply	GE Healthcare, Munich, Germany
Microwave M/W 232C	Continent, Germany
Ultraspec 2100pro	GE Healthcare, Munich, Germany
UV-Transilluminator	MWG Biotech, Ebersberg, Germany
UV-Transilluminator	Stratagene, La Jolla, CA, USA
Electrophoresis Chamber	Kenner GmbH, Dannstadt, Germany
Rotator SB3	Stuart Scientific, Staffordshire, UK
Biophotometer RS 232 C	Eppendorf, Hamburg, Germany
Thermal Printer DPU-414	Seiko Instruments GmbH, Neu-Isenburg, Germany
Quartz cuvette	Eppendorf, Hamburg, Germany
LightCycler 1.3 instrument	Roche Diagnostics, Penzberg, Germany

10.3. Cell culture equipment/ expendables

Tissue Culture Plate 24-Well	Sarstedt, Newton, NC, USA
Tissue Culture Plate 48-Well	Corning Incorporated, Corning, NY, USA
Tissue Culture Plate 96-Well	Sarstedt, Newton, NC, USA
Serological Pipette 2ml	Sarstedt, Nuembrecht, Germany
Serological Pipette 5ml	Sarstedt, Nuembrecht, Germany
Serological Pipette 10ml	Sarstedt, Nuembrecht, Germany
Serological Pipette 25ml	Sarstedt, Nuembrecht, Germany
Falcon® 15ml	BD Labware, Le Pont de Claix, France
Falcon® 50ml	BD Labware, Le Pont de Claix, France
FACS tube, 5ml	BD Falcon, Germany

10.4. RT-PCR primer

All primers were obtained from Sigma-Aldrich Chemie GmbH, Taufkirchen, Germany

Gene	Direction	Primer-Sequence
GAPDH	forward	5'-TGA TGA CAT CAA GAA GGT GGT GAA-3'
	reverse	5'-TCC TTG GAG GCC ATG TGG GCC AT-3'
TIMP1	forward	5'-AGA CAC CAG AGA ACC CAC CAT-3'
	reverse	5'-CGC TGG TAT AAG GTG GTC TGG-3'
XCL1	forward	5'-ATC CAG TCT TCA CTG GGT TCC-3'
	reverse	TTG TCC AAT TCA AAG GGT ATT GA-3'
GZMB	forward	5'-CCT TCC TGA GAA GAT GCA ACC-3'
	reverse	5'-TTA TGG AGC TTC CCC AAC AGT-3'
XCL2	forward	5'-TGA AGT CTC ACA TAG GAG GAC C-3'
	reverse	5'-GAG TAT AAT CTC AGT CCA TGA GG-3'
VDR	forward	5'-GAG TTT TTA TGG GGC TGA ACG-3'
	reverse	5'-CAC ACA TTC CTG CCT TCT CTG-3'
RORα	forward	5'-ATA ACG TGG CAG ACC T-3'
	reverse	5'-GGG GCT GGC ATA CTT C-3'
ASAH1	forward	5'-GCT TCA AGC TTT GCT GGC TAT-3'
	reverse	5'-ATA AAG TAG GCT GGG GCC AAT-3'
EGR1	forward	5'-TCT TGG TGC CTT TTG TGT GA-3'
	reverse	5'-TCT GGA GAA CCG AAG CTC AG-3'
BCL3	forward	5'-TAC TAC CCC GGA GCC TTA CTG-3'
	reverse	5'-GCA CCA CAG CAA TAT GGA GAG-3'
IFITM2	forward	5'-TCC CAA CTA CGA GAT GCT CAA-3'
	reverse	5'-GCA TTC ATG AAG AGG GTG TTG-3'
c/EBPβ	forward	5'-GGC CCT GAG TAA TCG CTT AAA-3'
	reverse	5'-CCC AAA AGG CTT TGT AAC CAT-3'
CHES1	forward	5'-CCC CTG AGA TAC AAG CAG GTT-3'
	reverse	5'-TTG GCA CTG CTG TAG TTG TGA-3'
SYNE2	forward	5'-CAA TCA GCT GGC AAT TTT GAG-3'
	reverse	5'-TCA AGT CGG TAG TTT GGC ATT-3'
ZNF160	forward	5'-AAT CAC ATT CTT TCT GCC AAC A-3'
	reverse	5'-TCA AGC ACA AAA TGC GGT TAT-3'

Supplemental Table 1 | RT-PCR primer

10.5. T-Cell receptor specific PCR-primer

Specificity	Sequence
C_β	5'-CGG GCT GCT CCT TGA GGG GCT GCG-3'
$V_\beta 1$	5'-CCG CAC AAC AGT TCC CTG ACT TGC-3'
$V_\beta 2$	5'-GGC CAC ATA CGA GCA AGG CGT CGA-3'
$V_\beta 3$	5'-CGC TTC TCC CGG ATT CTG GAG TCC-3'
$V_\beta 4$	5'-TTC CCA TCA GCC GCC CAA ACC TAA-3'
$V_\beta 5$	5'-AGC TCT GAG CTG AAT GTG AAC GCC-3'
$V_\beta 6$	5'-TCT CAG GTG TGA TCC AAA TTC GGG-3'
$V_\beta 7$	5'-CCT GAA TGC CCC AAC AGC TCT CTC-3'
$V_\beta 8$	5'-CCA TGA TGC GGG GAC TGG AGT TGC-3'
$V_\beta 9$	5'-TTC CCT GGA GCT TGG TGA CTC TGC-3'
$V_\beta 10$	5'-CCA CGG AGT CAG GGG ACA CAG CAC-3'
$V_\beta 11$	5'-TGC CAG GCC CTC ACA TAC CTC TCA-3'
$V_\beta 12$	5'-TGT CAC CAG ACT GGG AAC CAC CAC-3'
$V_\beta 13$	5'-CAC TGC GGT GTA CCC AGG ATA TGA-3'
$V_\beta 14$	5'-GGG CTC GGC TTA AGG CAG ACC TAC-3'
$V_\beta 15$	5'-CAG GCA CAG GCT AAA TTC TCC CTG-3'
$V_\beta 16$	5'-GCC TGC AGA ACT GGA GGA TTC TGG-3'
$V_\beta 17$	5'-CTG CTG AAT TTC CCA AAG AGG GCC-3'
$V_\beta 18$	5'-TGC CCC AGA ATC TCT CAG CCT CCA-3'
$V_\beta 19$	5'-TCC TCT CAC TGT GAC ATC GGC CCA-3'
$V_\beta 20$	5'-TCT CAA TGC CCC AAG AAC GCA CCC-3'
V_β w21	5'-TCC AAC CTG CAA GGC TTG ACG ACT-3'
V_β w22	5'-AAG TGA TCT TGC GCT GTG TCC CCA-3'
V_β w23	5'-GCA GGG TCC AGG TCA GGA CCC CCA-3'
V_β w24	5'-CCC AGT TTG GAA AGC CAG TGA CCC-3'

Supplemental Table 2 | T-cell Receptor specific PCR-primer

10.6. Flow cytometry antibodies – staining of surface proteins

The following antibodies were used:

Antibody	Color	Clone	Manufacturer
CCR2	APC	48607	R&D Systems
CCR4	PE	1G1	BD PharMingen
CD3	PerCP	SK7	BD PharMingen
CD5	FITC	L17F12	BD Biosciences
CD7	PE-Cy-5	M-T701	BD PharMingen
CD8	APC-Cy-7	SK1	BD PharMingen
CD25	PE-Cy-7	2A3	BD Biosciences
CD28	FITC	YTH913.12	MorphoSys UK Ltd.
CD38	PE	HIT2	BD PharMingen
CD45RA	PE-Cy-5	HI100	BD PharMingen
CD62L (L-selectin)	FITC	DREG-56	BD PharMingen
CD69	APC	FN50	BD PharMingen
CD69	PerCP	L78	BD Biosciences
CD95 (Fas/APO-1)	FITC	DX2	BD PharMingen
CD103	FITC	Ber-ACT8	BD PharMingen
CD122 (IL-2Rβ)	PE	Mik-β2	BD PharMingen
CD134 (OX40)	FITC	ACT35	BD PharMingen
CD137 (4-1BB)	PE	4B4-1	BD PharMingen
CD154 (CD40L)	PE	89-76	BD Biosciences
CD183 (CXCR3)	APC	1C6/CXR3	BD PharMingen
CD197 (CCR7)	Alexa647	3D12	BD PharMingen
GITR/TNFRSF18	APC	110416	R&D Systems
HLA-DR	PerCP	L243	BD Biosciences
TCR α/β	FITC	T10B9.1A-3	BD PharMingen
TCR γ/δ	PE	B1	BD PharMingen

Supplemental Table 3 | Flow cytometry antibodies

The following isotype controls were used:

Isotype	Color	Clone	Manufacturer
Mouse IgG_1	APC	MOPC-21	BD PharMingen
Mouse IgG_1	APC-Cy-7	MOPC-21	BD PharMingen
Mouse IgG_1	FITC	X40	BD Biosciences
Mouse IgG_{2a}	PE	X39	BD Biosciences
Mouse IgG_1	PE-Cy-5	MOPC-21	BD PharMingen
Mouse IgG_1	PE-Cy-7	MOPC-21	BD PharMingen

Supplemental Table 4 | Flow cytometry isotype control antibodies

10.7. Flow cytometry antibodies – detection of signaling molecule-phosphorylation

The following antibodies were used:

Antibody	Color	Clone	Manufacturer
CD3ζ (pY142)	Alexa Fluor® 647	K25-407.69	BD™ Phosflow
ERK1/2 (pT202/pY204)	Alexa Fluor® 647	20A	BD™ Phosflow
Lck (pY505)	PE	4/Lck-Y505	BD™ Phosflow
NF-κB p65 (pS529)	Alexa Fluor® 647	K10-895.12.50	BD™ Phosflow
p38 MAPK (pT180/pY182)	Alexa Fluor® 647	36/p38	BD™ Phosflow
Zap-70 (pY319)/Syk (pY352)	Alexa Fluor® 647	17a/P-ZAP70	BD™ Phosflow

Supplemental Table 5 | Phosphorylation specific flow cytometry antibodies

The following isotype controls were used:

Isotype	Color	Clone	Manufacturer
Mouse IgG_1	PE	MOPC-21	BD™ Pharmingen
Mouse IgG_1	Alexa Fluor® 647	MOPC-21	BD™ Phosflow
Mouse IgG_{2b}	Alexa Fluor® 647	clone 27-35	BD™ Pharmingen

Supplemental Table 6 | Flow cytometry isotype control antibodies

10.8. Detailed tables of significantly regulated genes in non-tumor-reactive CD8$^+$ T-cell clones

10.8.1. Genes significantly upregulated in non-tumor-reactive CD8$^+$ T-cell clones

GeneID	Accession	Gene Symbol	tumor reactive – mean	non tumor reactive – mean	Fold change	paired p value	AFFY HG U133 probe set ID
1958	NM_001964	*EGR1*	127.04	2283.59	17.98	0.034318	201694_s_at
7076	NM_003254	*TIMP1*	216.54	1572.29	7.26	0.020906	201666_at
10365	NM_016270	*KLF2*	54.69	282.70	5.17	0.04204	219371_s_at
602	NM_005178	*BCL3*	73.23	281.05	3.84	0.033404	204908_s_at
8523	NM_003645	*SLC27A2*	143.57	497.35	3.46	0.048569	205769_at
3002	J03189	*GZMB*	2303.73	6133.65	2.66	0.036333	210164_at
7421	NM_000376	*VDR*	120.6	297.06	2.46	0.049616	204254_s_at
1051	AL564683	*c/EBP/β*	336.77	744.97	2.21	0.042375	212501_at
10581	NM_006435	*IFITM2*	1372.7	2974.66	2.17	0.034248	201315_x_at
8728	Y13786	*ADAM19*	447.27	908.58	2.03	0.020424	209765_at
3248	J05594	*HPGD*	347.39	662.82	1.91	0.045606	211548_s_at
2023	U88968	*ENO1*	226.29	381.75	1.69	0.020415	217294_s_at

Supplemental Table 7 | Significantly upregulated genes

10.8.2. Genes significantly downregulated in non-tumor-reactive CD8$^+$ T-cell clones

GeneID	Accession	Gene Symbol	Tumor-reactive – mean	Non-tumor reactive – mean	Fold change	Paired p value	AFFY HG U133 probe set
6846	NM_003175	*XCL2*	424.64	48.57	-8.74	0.049122	214567_s_at
6375	U23772	*XCL1*	674.12	80.27	-8.4	0.041017	206366_x_at
10346	AA083478	*TRIM22*	747.64	199.24	-3.75	0.03398	213293_s_at
55918	AK001821	*GNPTAB*	893.92	280.82	-3.18	0.044094	212959_s_at
427	AI934569	*ASAH1*	395.95	156.56	-2.53	0.023795	213702_x_at
6095	U04897 L14611	*RORA*	558.05 527.53	220.13 211.32	-2.54 -2.5	0.049176 0.036602	210426_x_at 210479_s_at
3516	AL513759	*RBPSUH*	1708.81	644.51	-2.65	0.049027	211974_x_at
23224	NM_015180	*SYNE2*	203.97	97.73	-2.09	0.040098	202761_s_at
25957	NM_015491	*C6orf111*	138.58	68.79	-2.01	0.048566	212177_at
23015	AW006438	*GOLGA8B*	1207.82	623.99	-1.94	0.046437	213650_at
7503	NR_001564	*XIST*	451.71	258.02	-1.75	0.04904	214218_s_at
90338	AK024789	*ZNF160*	161.51	97.86	-1.65	0.047555	214715_x_at
1112	NM_005197	*FOXN3*	440.65	284.47	-1.55	0.0464	205022_s_at

Supplemental Table 8 | Significantly downregulated genes

11. Curriculum Vitae

Mein Lebenslauf wird aus Gründen des Datenschutzes in der elektronischen Fassung meiner Arbeit nicht veröffentlicht.